



HAL
open science

Analyzing the role of SoxC genes in murine kidney development

Vladimir Kozlov

► **To cite this version:**

Vladimir Kozlov. Analyzing the role of SoxC genes in murine kidney development. Molecular biology. Université Côte d'Azur, 2020. English. NNT : 2020COAZ6010 . tel-03122693

HAL Id: tel-03122693

<https://theses.hal.science/tel-03122693>

Submitted on 27 Jan 2021

HAL is a multi-disciplinary open access archive for the deposit and dissemination of scientific research documents, whether they are published or not. The documents may come from teaching and research institutions in France or abroad, or from public or private research centers.

L'archive ouverte pluridisciplinaire **HAL**, est destinée au dépôt et à la diffusion de documents scientifiques de niveau recherche, publiés ou non, émanant des établissements d'enseignement et de recherche français ou étrangers, des laboratoires publics ou privés.

THÈSE DE DOCTORAT

Etude du rôle des gènes *SoxC* au cours
du développement du rein de souris

Vladimir KOZLOV

Institut de Biologie Valrose (iBV)

**Présentée en vue de l'obtention
du grade de docteur en** Sciences de la vie
et de la santé

d'Université Côte d'Azur

Dirigée par : Andreas Schedl

Soutenue le : 31 Août 2020

Devant le jury, composé de :

Thomas Lamonerie, professeur, Université
Côte d'Azur

Andreas Schedl, directeur de recherche,
Institut de Biologie Valrose

Muriel Umbhauer, professeur, Université
Pierre-et-Marie-Curie

Seppo Vainio, professeur, Université d'Oulu

Etude du rôle des gènes SoxC au cours du développement du rein de souris

Jury :

Président du jury

Thomas Lamonerie, professeur, Université Côte d'Azur

Rapporteurs

Muriel Umbhauer, professeur, Université Pierre-et-Marie-Curie

Seppo Vainio, professeur, Université d'Oulu

Directeur de thèse

Andreas Schedl, directeur de recherche, Institut de Biologie Valrose

Etude du rôle des gènes *SoxC* au cours du développement du rein de souris

Résumé

Les anomalies congénitales des reins et des voies urinaires (CAKUT) sont un groupe de malformations fréquemment trouvées chez les patients humains qui résultent de défauts dans le programme de développement de ces organes. *Sox11* fait partie de la famille des facteurs de transcription *SoxC*, qui joue un rôle important dans le développement de divers organes chez les vertébrés. Les souris *Sox11*^{-/-} meurent juste après la naissance et présentent une grande variété de CAKUT. Alors que les reins duplex sont une anomalie courante du développement rénal, le mécanisme moléculaire qui amène les mutants *Sox11* à développer cette malformation reste incertain. Dans ce projet, j'ai analysé le phénotype rénal des souris *Sox11*^{-/-} et montré que les reins duplex sont causés par l'expansion du mésenchyme métanéphrique (MM). D'autres expériences ont été réalisées pour déterminer si l'origine de cette expansion résidait dans une apoptose insuffisante ou dans l'absence de migration des cellules du MM. Une analyse tridimensionnelle par microscopie confocale des cellules apoptotiques a révélé que chez les embryons *Sox11*^{-/-} le MM subissait une apoptose dans la région d'intérêt similaire à celles des embryons de type sauvage. Un test *in vitro* de cicatrisation des plaies a démontré que les gènes *SoxC* sont nécessaires pour la migration des cellules du MM. La délétion de ces gènes à un stade tardif du développement conduit à une hypoplasie rénale et à une diminution du nombre de néphrons due à l'arrêt de la néphrogenèse. Pour étudier le rôle des gènes *SoxC* au cours de la formation des reins, j'ai établi une culture de cellules progénitrices rénales permettant l'inactivation de ces gènes en présence de 4OH-Tamoxifène. L'analyse de l'expression génique a confirmé la suppression efficace des gènes *SoxC*, tout en maintenant l'identité des cellules progénitrices du néphron. Après induction de la délétion, ces cellules sont incapables de s'épithélialiser, du fait d'une activité accrue de la voie Wnt/ β -caténine. Afin de valider ces résultats et d'identifier les cibles en aval des gènes *SoxC*, j'ai effectué une analyse ARN-seq d'organoïdes rénaux subissant une transition mésenchymateuse-épithéliale. Les données acquises par ces expériences révèlent que de nombreuses voies de signalisation sont affectées. En particulier, l'insuffisance du gène *Ezh2* codant pour une protéine du groupe Polycomb, pourrait être à l'origine de changements transcriptomiques généralisés empêchant les cellules progénitrices déficientes en *SoxC* de se différencier. L'ensemble de ces données démontre l'importance des gènes de la famille *SoxC* dans le développement précoce et tardif du rein, dont l'analyse moléculaire conduira à des orientations possibles pour les recherches et les traitements futurs.

Mots clés : Développement rénal, duplication des voies urinaires, transition mésenchymateuse-épithéliale, cellules progénitrices

Analyzing the role of SoxC genes in murine kidney development

Abstract

Congenital Anomalies of Kidneys and Urinary Tract (CAKUT) are a group of birth defects that arise from defects in the developmental program of organ development and are frequently found in human patients. *Sox11* is a member of *SoxC* family of transcription factors, which plays an important role in the development of various organs in vertebrates. *Sox11* knockout mice die soon after birth and display a wide variety of CAKUT, including duplex kidneys and nephrogenesis defects. While duplex kidneys are a common renal development anomaly, the molecular mechanism causing *Sox11* mutants to develop duplex kidneys remains unclear. In this project, I analyzed the renal phenotype of *Sox11* knockout mice and discovered that the duplex kidneys are caused by the expansion of metanephric mesenchyme (MM). Further experiments were performed to determine whether the origin of this expansion lies in insufficient apoptosis of MM cells or lack of MM cell migration. Three-dimensional confocal microscopy analysis with LysoTracker Red staining of apoptotic cells revealed that MM undergoes apoptosis in the region of interest in wildtype embryos, however the apoptosis seems to persist in *Sox11*^{-/-} embryos as well. However, *in vitro* scratch wound assay provided evidence that *SoxC* genes are necessary for migration of MM cells. In the late kidney development, *SoxC* deletion is leading to renal hypoplasia and reduced nephron number due to cessation of nephrogenesis. To study the role of *SoxC* in nephrogenesis, I set up an *in vitro* renal progenitor cell culture which allows for the timed deletion of *SoxC* genes by a 4OH-tamoxifen induced knockout. Gene expression analysis confirmed efficient deletion of *SoxC* genes, while maintaining nephron progenitor cell identity. After deletion, renal progenitor cells were found to be unable to epithelialize, linked with increased activity of Wnt/ β -catenin pathway. To validate these findings and discover the downstream targets of *SoxC* genes, I developed a system for an RNA-seq analysis of renal organoids undergoing mesenchymal-to-epithelial transition. Data acquired in these experiments reveal numerous regulatory pathways affected in *SoxC*-knockout renal progenitor cells, with the deficiency of Polycomb group gene *Ezh2* as a likely origin of widespread transcription changes leading to the inability of *SoxC*-deficient progenitor cells to differentiate. Taken together these data demonstrate the importance of *Sox11* and other *SoxC* genes in early and late kidney development, with molecular analysis providing plausible directions for future research and interventions.

Keywords : Kidney development, duplicated collecting system, mesenchymal-epithelial transition, progenitor cells

Table of Contents

Acknowledgments	2
Introduction.....	3
The kidney	3
Renal anatomy and function in mammals.....	3
Early renal differentiation	5
Nephrogenesis and nephron maturation.....	12
Sox genes.....	20
Sox gene structure and function	20
Sox genes functions in development	25
Congenital anomalies of kidney and urinary tract	29
Article 1: Duplex kidney formation: developmental mechanisms and genetic predisposition	31
Aims of the project.....	44
Results and Discussion	44
Role of <i>Sox11</i> in CAKUT	44
Article 2: <i>Sox11</i> gene disruption causes congenital anomalies of the kidney and urinary tract (CAKUT)	44
Role of <i>SoxC</i> in MET.....	80
Conclusions and perspectives	112
<i>Sox11</i> role during ureteric bud emergence.....	112
<i>SoxC</i> genes in nephrogenesis	113
Materials and methods	115
Bibliography.....	120

Acknowledgments

First, I would like to thank Dr Seppo Vainio and Dr Muriel Umbhauer for having kindly accepted to participate in my thesis defence as reviewers, as well as Dr Thomas Lamonerie for taking the role of the president of the committee. It's an honour to be a part of kidney research community.

Of course, none of this would be possible without Andreas accepting me as his student, directing my research and managing my stay in the lab, for which I am incredibly thankful. It's immensely valuable to have a director who's always available for discussion and advice, and who can turn my mistakes into valuable lessons about good research practices. The members of Schedl lab provided me with their invaluable help: Filippo with cloning and sequencing, Fariba with microscopy and cell culture, and Valerie with mouse work. I appreciate that Filippo, as my supervisor, has spent a colossal amount of his time and patience helping me with my experimental setup, evaluating my results and providing feedback on my manuscript. Fariba is very kind for hosting events at her private place, which is a valuable opportunity to socialize the French way for a foreign student like me. And I'm grateful to Valerie for bringing snacks to the office, making sure none of us students work while hungry.

I want to thank Yasmine and Haroun as my predecessors on this research project, for being available for discussion. Anaëlle, Fabio, Ioannis, Chamara and Rodanthi provided their support and suggestions to me, and I hope I was helpful in return. And though research work can be challenging, Amèlie, Clara and Aurelie were instrumental in keeping it not irritating, for which I'm grateful.

The institut de Biologie Valrose was a great place to work at, not just for the scenic location, but for wonderful people as well. I'm thankful to Collombat lab, Studer lab and especially Chaboissier lab for sharing their suggestions and their equipment. Thanks to PhD pizza club participants and organizers, it was a good place to practice giving presentations. And thanks to mouse facility group for their special attention to my mice.

I'm grateful to have a wonderful support network outside of the institute building, with 11 other students from the Renaltract group it was much easier to make our way in science together. I want to thank Aryuna and Artyom for providing an inspiring work environment while writing this manuscript. And finally, thank you my family for believing I can endure this journey.

Introduction

The kidney

Renal anatomy and function in mammals

The kidneys are two bean-shaped organs situated in the back of the abdominal cavity in the retroperitoneal space between the dorsal wall and the peritoneum. They filter blood before sending it back to the heart and produce urine which is then excreted. Kidneys are complex organs that morphologically can be divided into three layers: the cortex that represent the outermost layer and contains the blood filtrating glomeruli, the medulla that consists of Henle's loop and collecting ducts, and the renal pelvis that collects the concentrated urine and connects via the ureter to the bladder. Kidneys receive blood flow through the renal arteries, which direct blood into capillaries passing through the filtering apparatus of the kidney. Filtering is occurring inside the microscopical structures called nephrons, starting with a structure called glomerulus, continuing through a long epithelial tube passing from cortex to medulla and back, ending in a collecting duct.

The process of filtration occurs in three stages: filtration, secretion and reabsorption. Blood filtration involves a selective barrier that is compose of fenestrated endothelial cells, a negatively charged basement membrane and an ultrastructural molecular filter, the slit diaphragm. This glomerular filter allows fluids and small molecules such as waste products, nutrients and ions to pass from the blood into the Bowman's space of the glomerulus, while larger molecules, such as proteins, are retained in the blood and exit through the peritubular capillaries called vasa recta. The fluid collected by the glomerulus passes into proximal tubules, where most of the water and nutrients are reabsorbed from the primary filtrate. Water and electrolytes are reabsorbed by the loop of Henle and the water content of urine is fine-tuned in the distal tubules and collecting ducts. The filtered blood is carried by the efferent arteriole, while the urine is transported via the ureter to the bladder (Figure 1). (Scott and Quaggin, 2015)

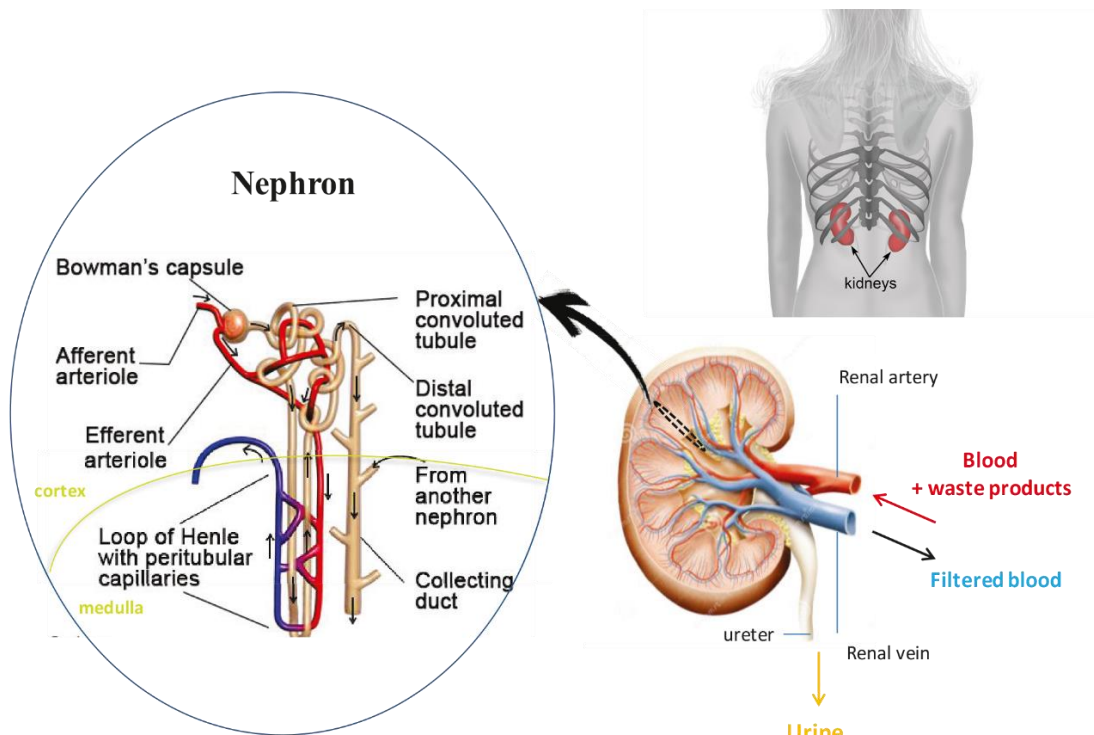


Figure 1: The anatomy of adult mammalian kidney and a structure of the nephron.

An adult human kidney contains approximately 1 million nephrons that filter around 180 litres of plasma per day. The initially produced pre-urine is processed all along the convoluted tubule and involves active tubular excretion and resorption. Concentration of the urine within the loop of Henle involves an osmotic gradient. It does this by actively transporting out salts from the ascending limb, which creates increased salt concentration in the interstitial fluid of the medulla. This results in the passive flow of water from the descending loop into the interstitial space. This water gets absorbed into blood, keeping the conditions inside the interstitial space constant (Figure 2).

Disposal of metabolic waste products while retaining electrolytes is one of the main functions of the kidney. This way, the kidney maintains homeostasis and water balance, and regulates acid-base balance by reabsorbing the filtered bicarbonate and excreting the fixed acids. Moreover, the kidney regulates the blood pressure by controlling electrolyte homeostasis, as well as by secreting renin, a crucial component of the renin-angiotensin-aldosterone system. The kidney also regulates the production of red blood cells in the bone marrow via the secretion of erythropoietin. Moreover, kidneys maintain bone density by converting

vitamin D into the biologically active calcitriol which in turn regulates calcium balance. The kidney also plays an important role in glucose balance by reabsorbing the filtered glucose using sodium-glucose cotransporters on proximal tubules (Vander's Renal Physiology, 2013).

Early renal differentiation

In the early embryo, gastrulation leads to the development of the mesoderm that can be subdivided into paraxial, intermediate and lateral mesoderm, according to their position. All kidney tissue in vertebrates arises from the intermediate mesoderm (IM) (Grobstein 1967; Fleming et al., 2013). Apart from kidneys, the IM also contributes to the development of the gonads and adrenal gland. Intermediate mesoderm forms paired elevations called urogenital ridges, which later on give rise to the nephrogenic cords (NC) and the the gonadal ridges that will form the kidneys and gonads, respectively.

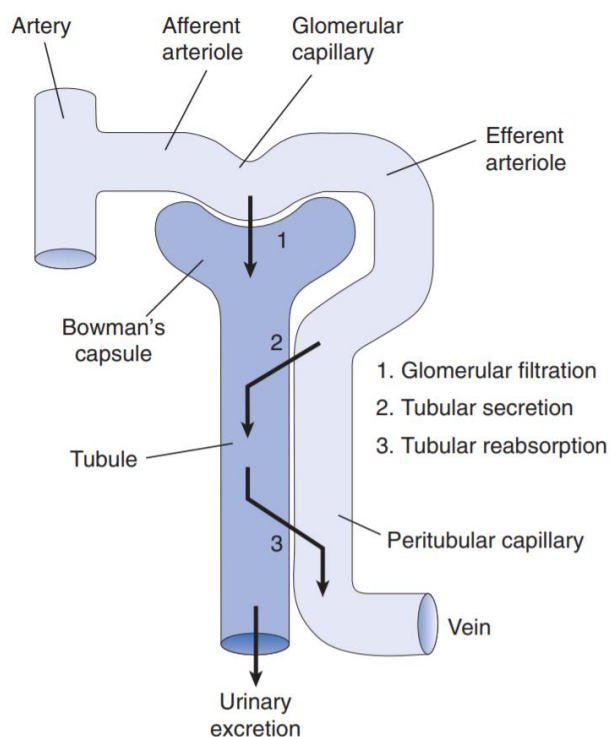


Figure 2: Fundamental elements of renal function – glomerular filtration, tubular secretion and tubular reabsorption – and the association between the tubule and vasculature in the cortex. (From Vander's Renal Physiology, 2013)

Along the anterior-posterior axis of the NC, three distinct types of kidney are developing in higher vertebrates: pronephros, mesonephros, and metanephros (Saxén 1987, Vize et al., 1997) (Figure 3). In mammals, pronephros and mesonephros are only transiently present during early embryonic life. The pronephros appears to be functional only in lower vertebrates. (Brändli 1999). The mesonephros develops caudally and degenerates or becomes part of the male reproductive system in mammals (Burns, 1955; Balinsky, 1972). The metanephros gives rise to the adult mammalian kidney.

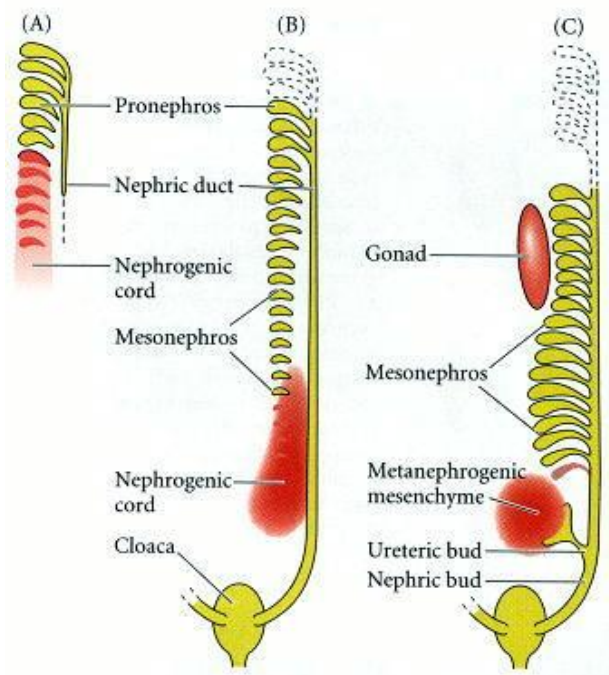


Figure 3: Three embryonic kidneys: pronephros (a), mesonephros (b) and metanephros (c). (Saxen, 1987)

The nephric (or wolffian) duct (ND) is the first epithelial structure formed within the IM. Active migration and proliferation of ND cells results in caudal extension of ND and in induction of mesonephric tubules within the NC (Carroll et al., 2005). By embryonic day (E) 10.5 in the mouse, the ND reaches the Metanephric Mesenchyme (MM), a distinct zone of the NC (Figure 4). The MM cell population are nephron progenitor cells. Inductive signals produced by the MM cause ND to form an outgrowth, called the Ureteric Bud (UB), which makes contact with the adjacent MM and both the UB and the MM undergo extensive morphogenesis to form up to 20,000 nephrons and collecting ducts in mouse, forming a kidney (Murawski et al., 2010).

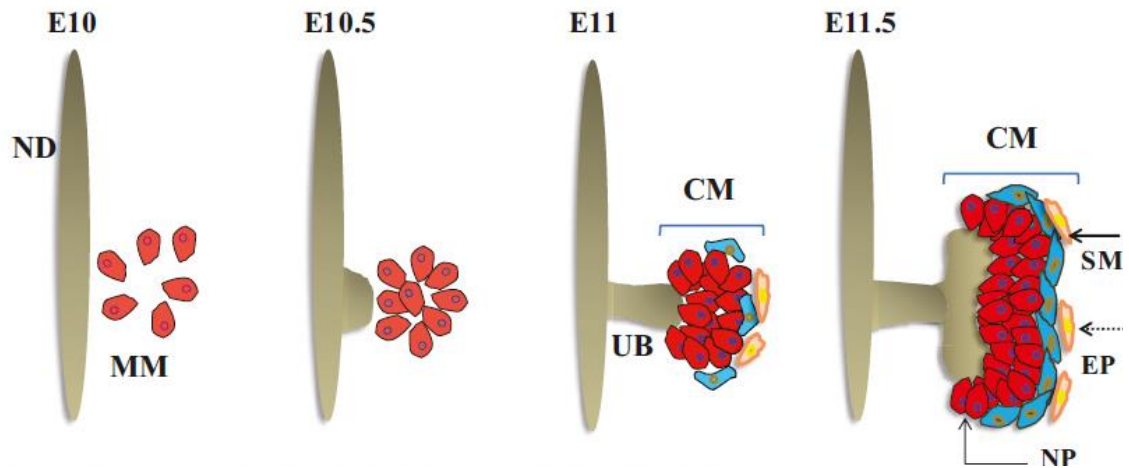


Figure 4: Schematic representation of early kidney development. ND – nephric duct, MM – metanephric mesenchyme, UB – ureteric bud, CM – cap mesenchyme, NP - nephron progenitors, SM - stromal cells, EP - endothelial precursors. At the start of metanephric development, MM is specified adjacent to the ND. Later, at E10.5, ND stratification leads to UB outgrowth. This triggers proliferation of the MM. The growing UB invades MM niche, inducing condensation of MM around UB tips, forming CM. This niche is composed of several types of cells: NP, EP and SM. (Motamedi, 2015)

The contact of renal progenitor cells with the UB is a critical event for metanephric development. Metanephric Mesenchyme (MM) gives rise to nephrons, stroma and potentially also some of the vasculature (Munro et al, 2017). Once the MM cells get in proximity of the UB, these cells are rapidly compartmentalized to form a region referred to as Cap Mesenchyme (CM). The first CM cells appear at E11 during MM condensation around the original UB tip (Figure 4). In the rest of the kidney development, CM cells make up a niche of nephron progenitor cells around each single UB tip of the branching ureteric tree. This cell population is exhausted by the second to third day after birth (Rumballe et al., 2011), after which nephrogenesis stops. No stem cell population which can form new nephrons in adult life has been identified.

Transcription factor ODD1, also known as OSR1, is the earliest known marker of the IM (James et al., 2006) (Mugford et al., 2008). The *Osr1*⁺ cell population gives rise to the ND, the MM and its epithelial derivatives (nephrons) (Grobstein, 1953, 1955). The ND is the first epithelial tubule to differentiate from the IM that is essential for all further urogenital development. PAX2, LIM1, and OSR1 are DNA-binding proteins that are required to specify the IM. (Patel et al., 2007; Dressler 1990). The *Pax2* and *Pax8* genes are redundant for the initiation of the specification of the ND lineage at E9.5. *Pax2* is expressed during formation and differentiation of all epithelial structures derived from the IM. In *Pax2* mutants, the mesonephric tubules fail to form. The ND appears normal but fails to extend caudally and degenerates. Mice

heterozygous for *Pax2* mutations frequently exhibit a hypoplastic kidney (Dressler et al., 1990; Torres et al., 1995). Surprisingly, the *Pax8* mutants do not display renal defects (Mansouri et al., 1998) suggesting that *Pax2* might compensate for the loss of *Pax8* in kidney development. (Bouchard et al, 2000; Grote et al., 2006). *Pax2/Pax8* activate *Lim1*, also known as *Lhx1*, which is involved in the caudal extension and development of the ND (Pedersen et al. 2005; Tsang et al., 2000). *Pax2/Pax8* also activate the expression of the transcription factor *Gata3* and receptor *c-Ret*. *Gata3* expression commences in ND precursors at E8.5 and appears to control ND extension (Grote et al., 2006). In contrast, *Ret* mutant mice develop a ND indicating that *Gata3* function during ND extension is *Ret* independent. (Grote et al., 2008)

Wolffian duct and metanephric mesenchyme

Specification of the MM is the earliest step of the metanephric kidney development. This event occurs at around E10 in the caudal part of the ND (Figure 4). The induction of the MM is regulated by a variety of transcription factors including *Osr1* (James et al., 2006; Mugford et al., 2008), *Pax2/8* (Bouchard et al., 2000), *Lim1* (Shawlot, and Behringer, 1995), *Sall1* (Nishinakamura et al., 2001; Kiefer et al., 2010), *Six1* (Xu et al., 2003), *Six2* (Self et al., 2006), *Wt1* (Kreidberg et al., 1993), *Hox11* paralogues (Wellik, 2002, Davis et al., 1994) or transcriptional coactivator *Eya1* (Xu et al., 1999; Sajithlal et al., 2005). Interestingly, specification of the MM doesn't require the caudal extension of the ND, such as in the case of the conditional deletion of *Gata3* in the ND (*HoxB7-Cre; Gata3^{fl/fl}*). In these embryos, in the absence of the caudal part of the ND, the PAX2⁺ MM cells are still detected at E11.5 (Grote et al., 2008).

Osr1 is one of the upstream components in the network of transcription factors regulating the initiation of kidney development. *Osr1* orchestrates the specification of the mesonephric and metanephric mesenchyme. Mice lacking *Osr1* do not form the MM and fail to express *Lim1*, *Eya1*, *Pax2*, *Six2*, *Sall1* or *Gdnf* (Mugford et al., 2006). *Osr1* expression was found to be highly restricted to the non-differentiated subpopulation of the CM (Xu et al. 2014).

Pax2 is expressed in both the UB and the MM. In *Pax2* knockouts, a morphologically distinct MM cell population forms but metanephric development does not occur due to the failure of UB outgrowth (Torres et al., 1995). The absence of UB induction is caused by the lack of the *Ret* ligand GDNF, which is required for UB outgrowth (Moore et al., 1996). *Pax2* protein can

bind to upstream regulatory elements within the GDNF promoter region and can transactivate expression of reporter genes (Brophy et al., 2011). The double *Pax2/Pax8* mutants exhibit complete absence of the ND and the MM never differentiates. (Bouchard et al., 2002)

Lim1 (also known as *Lhx1*) is expressed in the tubule-forming tissue in pronephros, mesonephros and metanephros (Kobayashi 2005). Deletion of *Lim1* leads to a disorganization of the IM and a total absence of the MM (Tsang et al., 2000) suggesting that *Lim1* is involved in the specification of the MM. In addition to its role in early kidney development, the conditional deletion of *Lim1* at E11.5 in MM has demonstrated that its expression is also required for nephrogenesis and nephron patterning (Kobayashi et al., 2005). (Figure 5).

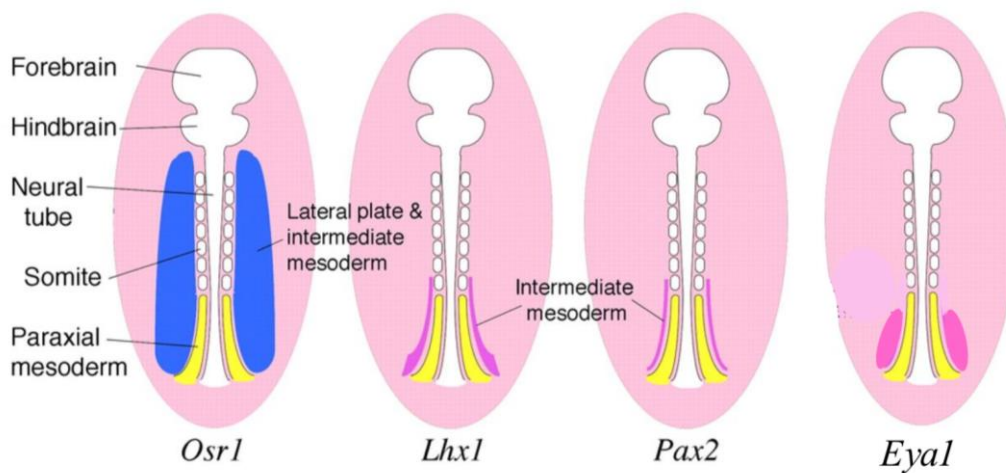


Figure 5: A posterior cross-section of the mouse embryo at E8.5. The expression of transcription factor *Osr1* is shown in blue, *Lhx1*, *Pax2*, *Eya1* are shown in purple. *Osr1* is expressed anterior compared to other genes. (Dressler, 2009; Sajithlal, 2005)

Eya1 is expressed early within the IM (Figure 5) becoming progressively restricted to the caudal end where the UB grows out. At E11.5, *Eya1* expression is localized to the MM. *Eya1* is the transcriptional coactivator that has a specific role in determining metanephric cell fate within the nephrogenic mesoderm. The absence of MM specification in *Eya1* mutants is not caused by a lack of signalling emanating from the UB, but due to a cell autonomous defect owing to the lack of *Eya1*. (Sajithlal et al., 2005)

Sall1 is expressed in multiple tissues including the brain, limbs, heart, ear, and kidney. *Sall1*^{-/-} mice display a lack of kidney development. *Sall1* has a major role in UB invasion that appears to be independent of GDNF/RET signaling. At E10.5, *Sall1* is expressed in the ND and MM. By E11.5, its expression is restricted to the CM surrounding the UB tip. In these mutants, the specification of the MM occurs, but the UB fails to invade the MM. MM cells isolated from

Sall1^{-/-} embryos are capable of epithelialization. In *Sall1* mutants, *Gdnf* is expressed normally at first, but its expression drops off at E11.5 due to the lack of a feedback loop with the UB (Nishinakamura et al., 2001).

Six1 is expressed in the MM starting from E10.5 and is maintained in CM until birth. *Six1*^{-/-} mice display smaller kidneys with a variable penetrance of phenotype. In *Six1* mutants, the UB fails to invade the MM and the MM cells rapidly undergo apoptosis (Li et al., 2003). SIX1 was found to form a transcriptional complex with PAX2 and EYA1. (Xu et al. 2003). *Six4*, a gene in the same gene family, expresses in many of the same regions as *Six1*. *Six4* and *Six1*, are necessary for development of the MM by regulating the level of *Pax2-Gdnf* expression. *Six1/Six4*-deficient mice exhibit a more severe kidney phenotype than the *Six1*-deficient mice with a complete absence of *Pax2*, *Pax8*, and *Gdnf*. (Brophy et al., 2001). (Kobayashi et al., 2007).

While it was found that ND forms by migration of the cells of the pronephric duct along an anterioposterior axis to give rise to the ND (Drawbridge et al., 2003; Kopan et al., 2014), the origin of MM remains uncertain. In the classical view the MM stems from the anterior IM. However, fate mapping and in vitro nephrogenesis experiments provided evidence that while the UB emerges from the descending pronephric duct, the metanephric anlagen arise from posteriorly located mesoderm (Taguchi et al., 2014)

Ureteric bud formation

By E10, the ND and MM have been specified at the caudal end of the NC. Later, at around E10.5, the induction of the UB occurs. The UB emerges from the ND and invades the adjacent MM. The formation of the UB is a crucial event in kidney development, with absence of UB leading to renal agenesis.

The initial outgrowth of the UB and its branching are both controlled by the GDNF/RET receptor-tyrosine kinase pathway (RTK). While c-Ret is located on the surface of the UB, GDNF is secreted by the MM (Pichel et al., 1996; Costantini, 2010). From E9 to E10 *Gdnf* expression is found along the ND before becoming restricted to the caudal end of the ND where the UB appears at E10.5.

Genetic deletion of *Gdnf* (Sanchez et al., 1996; Pichel et al., 1996; Sainio et al., 1997), its receptor *c-Ret* (Durbec et al., 1996), or its co-factor *GdnfR- α 1* (Jing et al., 1996) leads to UB outgrowth failure and subsequent kidney agenesis. However, in these mutants, the MM undergoes specification, which demonstrates that GDNF/RET signaling is not directly involved

in MM specification. The GDNF/RET signaling pathway acts through ETV4/ETV5 effectors and mice lacking both *Etv4* and *Etv5* fail to develop kidneys (Lu et al., 2009).

GDNF and c-Ret action is fine-tuned by many upstream genes such as *Eya1*, *Gata3*, *Pax2*, and *Sall1*. Further description of molecular pathways regulating the UB formation can be found in Article 1 below.

Branching

When the UB emerges from the ND and invades the MM, a repetitive dichotomous branching is initiated that is maintained until birth. This process includes the branching and elongation of the UB, which forms the ureteric tree of the kidney. Molecular analysis identifies at least two types of UB cells: 1) Tip cells that express *Sox9*, *Wnt11* and *Ret*, and are highly proliferative forming new branches. 2) Stalk cells that have lost tip markers and show less proliferation that will form the collecting duct (CD). (Figure 6) Disruption in the morphogenetic program at this stage leads to renal malformation. Growth and branching of the ureteric tree is regulated through feedback loops primarily involving the signalling molecules WNT11 and GDNF by promoting cell migration and proliferation. (Majumdar et al., 2003) (Reginensi et al., 2011). The branching pattern is largely bifid, with occasional trifid and lateral branches (Blake, Rosenblum, 2014).

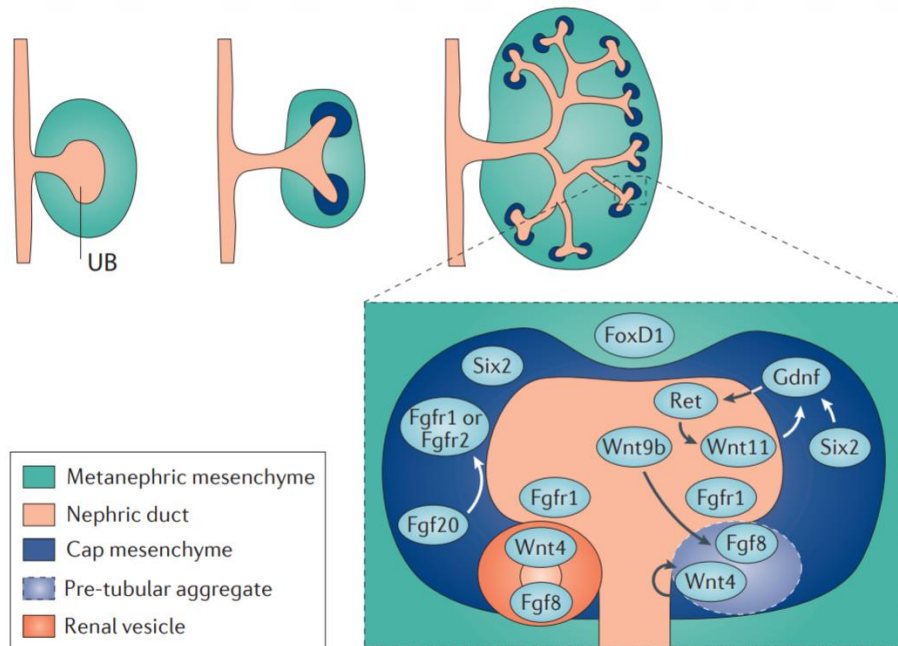


Figure 6: The process of ureteric tree branching is driven by a network of genetic and protein interactions principally controlled by Gdnf/Ret, Wnt and Fgf signalling networks. (Short, Smyth, 2016)

Nephrogenesis and nephron maturation

Cap mesenchyme

The cap mesenchyme of the forming metanephros is composed of nephron progenitor cells surrounding the UB tips on the periphery of the kidney. In the mouse, CM is emerging at E11.5 and persists until postnatal day 2 (Mugford et al., 2009). While individual CM cells undergo migration in accordance to their stage of differentiation, the CM as a whole stays just below the kidney capsule, under the layer of stromal cells. The CM can be

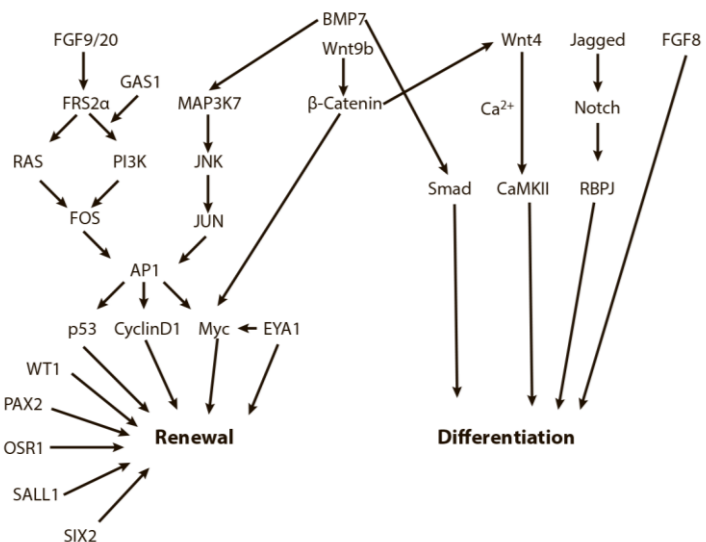


Figure 7: Schematic representation of important regulators of the balance between NPC renewal and differentiation. Arrows represent information flow between pathway nodes, and many of the complex molecular interactions have been simplified to allow for an overview of the major factors that balance the renewal-differentiation axis. (Oxburgh, 2018)

divided in two compartments corresponding to the expression of two expression factors: *Cited1* (Boyle et al., 2007) and *Six2* (Self et al., 2006). *Cited1* expression is restricted to the unique subpopulation of CM cells. Fate-mapping approaches using *Cited1-CreERT2* have shown that the CITED1⁺ cells develop exclusively into the epithelial structures of the nephron, apart from the CD (Boyle et al., 2008). *Six2* is also expressed in CITED1⁺ cells, and the deletion of *Six2* leads to the exhaustion of progenitor cell population due to premature differentiation (Self et al., 2006). *Six2*^{-/-} mice develop smaller kidneys as a consequence of the decrease in the number of nephrons. In addition, cell fate analysis demonstrates the role of SIX2⁺ cells as the progenitors of the nephron lineage (Kobayashi et al., 2008). The importance of *Six2* as a key transcription factor in nephron development leads to the conclusion that the CITED1⁺/SIX2⁺ subpopulation functions as a pool of non-committed progenitor cells during the nephrogenesis. As the differentiation starts, cells reach the CITED1⁻/SIX2⁺ subdomain of CM. These cells undergo pSMAD activation which leads to higher levels of β-catenin signalling resulting in the formation of a fully-formed nephron. (Brown et al., 2013)

SIX2 was found to act synergistically with OSR1 to maintain progenitor identity of the CM population. SIX2 is required to maintain the expression of OSR1 to prevent premature differentiation of the CM (Xu et al., 2014). In *Osr1* mutants, *Six2* expression was not affected, however the embryos displayed reduced kidney size. On the other hand, in *Six2*^{-/-} mutants a reduction of *Osr1* expression was observed. Co-immunoprecipitation experiments confirmed the formation of a SIX2-OSR1 complex. OSR1 protects the progenitor pool identity by enhancing TCF interaction with the Groucho family transcription co-repressors, thereby repressing the Wnt/β-catenin pathway. These results suggest that the early differentiation of CM starts with CITED1⁺/OSR1⁺/SIX2⁺ progenitor stage, progresses through CITED1⁻/OSR1⁺/SIX2⁺ and finally to CITED1⁻/OSR1⁻/SIX2⁺.

WT1 is an essential transcription factor for the regulation of NPCs. In *Wt1* knockout mice, the MM undergoes apoptosis and as a consequence the UB never forms. (Kreidberg et al., 1993). MM lacking *Wt1* fails to undergo epithelialization when paired with wild-type UBs, despite preserved GDNF expression (Donovan et al., 1999). ChIP experiments demonstrate the binding of WT1 to genes which function as regulators of kidney development, such as *Bmper*, *Bmp7*, *Pax2*, *Sall1* and *Fgf20*, which is consistent with a role of WT1 as a crucial factor in kidney development (Hartwig et al., 2010; Motamedi et al., 2014). (Figure 8) It was found that the elevation of BMP/SMAD pathway is directly responsible for the dysfunction of the WT1 mutant MM, as activation of this signalling pathway in organ cultures leads to apoptosis;

however, addition of FGF20 to the cultures rescues cell death, suggesting a deeper interplay of factors promoting MM survival. (Motamedi et al., 2014). WT1 was found to control expression of the membrane protein GAS1 in the CM; the inactivation of *Gas1* leads to premature depletion of CM pool, suggesting a role in maintenance of progenitor population. GAS1 amplifies the PI3K signalling response in the CM, which results in overall function of WT1 promoting proliferation of CM through directing the response to FGF9/20 to the PI3K response (Kann et al., 2015).

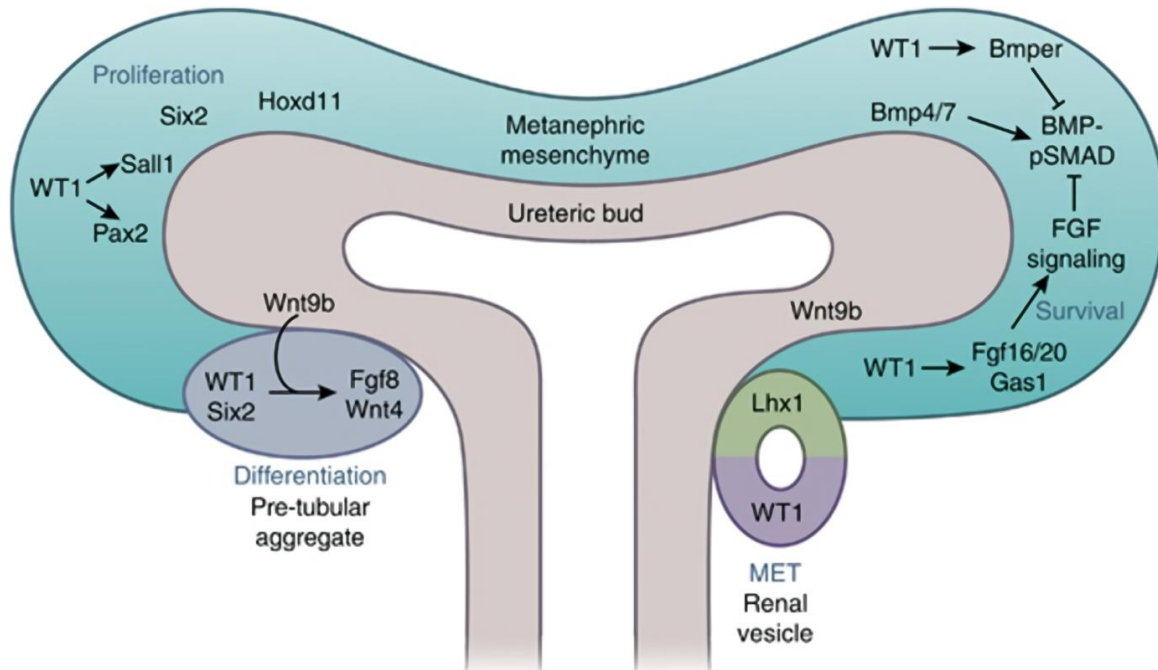


Figure 8: *WT1*, *Six2*, and *Hoxd11* are individually required for survival and self-renewal of MM. SALL1 and PAX2 transcription factors lie downstream of WT1. BMP4 induces the apoptosis of MM; however, BMP7 promotes the MM differentiation. WT1 directly regulates BMPER, a BMP-pSMAD inhibitor, and activates the FGF signaling pathway via regulating *Fgf20/Fgf16* and *Gas1* expression to antagonize BMP-pSMAD signaling for the survival and self-renewal of MM. High expression level of *Wnt9b* in the ureteric tip increases the Wnt signaling activity near the MM; there, the β -catenin-LEF/TCF complex works together with SIX2 and WT1 activating the critical differentiation factors, FGF8 and WNT4, to form PTA. Signals produced by PTA promote the MET to form renal vesicles. The proximal part of the renal vesicle expressing *Wt1* will develop into the epithelial cells of the glomerulus and the distal part of the renal vesicle expressing *Lhx1* will develop into the epithelial cells of the nephron tubule. (Dong, Pietsch, Englert, 2015)

PAX2 is a transcription factor that activates *Gdnf*, which orchestrates the recruitment of UB to MM (Brophy et al., 2001, Ranghini & Dressler, 2015) In the progenitor cell niche, PAX2 maintains the identity of the nephron lineage, preventing transdifferentiation to other cell types. Pax2 conditional inactivation in CM leads to the nephron progenitor cells differentiating to various stromal cell types (Naiman et al., 2017).

SALL1 is expressed in the MM, with knockouts suffering from renal hypoplasia due to the defects in UB recruitment to MM. (Nishinakamura et al., 2001) Conditional inactivation of *Sall1* in CM leads to premature depletion of renal progenitors (Kanda et al., 2014). *Sall1* null CM exhibit decreased expression of genes important for nephron progenitor maintenance, such as *Eya1*, *Myc*, *Six2*, *Fgf20*, which is consistent with the role of SALL1 as a broad regulator of NPC self-renewal (Basta et al., 2017). However, that finding is unexpected in the context of SALL1 function as a transcriptional co-repressor by associating with NuRD complex, suggesting another explanation of gene expression decrease in *Sall1* knockouts. One possible mechanism is synergy between SIX2 and SALL1, where the two act as transcriptional activators in the co-occupied loci. This was confirmed by observing co-occupation of self-renewal gene loci by SIX2 and SALL1 using CHIP (Kanda et al., 2014).

Eya1 mutants lack expression of *Six2*, with defects in early kidney development (Xu et al., 1999) as well as premature differentiation of CM in conditional CM knockouts (Xu et al., 2014b). EYA1 is also interacting with SIX2 with the formation of the protein-protein complex, which increases the stability of MYC, promoting NPC proliferation on the cell cycle level, in addition to the transcriptional control (Xu et al., 2014b).

A multitude of signaling pathways play an important role in regulation of nephrogenesis. FGF2, a member of FGF signaling pathway, was revealed to promote mesenchyme survival without inducing MET (Perantoni et al., 1995; Dudley et al., 1999; Barasch, 1997). Inactivation of FGF receptors FGFR1 and FGFR2 in the MM leads to a decrease in MM growth and subsequent renal aplasia (Celli et al., 1998; Poladia et al., 2006). FGF2 and FGF9, generated by the UB, promote survival and proliferation of NPCs, and removal of the UB leads to death of MM (Brown et al., 2011). *Fgf9* is also expressed in NPC themselves (Barak et al., 2012). However inactivation experiments demonstrate that this expression acts redundantly with *Fgf20* (Ortega et al., 1998; Zhou et al., 1998; Dono et al., 1998; Colvin et al., 2001). *Fgf20* is expressed solely in NPCs, and together with *Fgf9* is essential for the maintenance of NPC proliferation. (Barak et al., 2012). Indeed, compound inactivation of *Fgf9* and *Fgf20* leads to apoptosis of NPC and loss of MM (Barak et al., 2012). *Fgf* expression in the MM is however not sufficient for the survival of NPCs in culture, indicating that additional factors from the UB or stroma are required.

WNT9B, a pro-differentiation factor expressed in the UB and promoting expression of *Wnt4* and *Fgf8* in PTA, is acting as a proliferation factor in CM, indicating a bimodal role of UB in nephrogenesis (Carroll et al., 2005; Karner et al., 2011) The switch between two functions of

WNT9B could be determined by the relative intensity of WNT9B signal to *Six2* expression, and by activation of the BMP-SMAD signaling pathway (Brown et al., 2013; Karner et al., 2011). Cortical interstitium may play a role in modulating the response to WNT9B, keeping the balance between the proliferation and differentiation, by regulating nuclear versus cytoplasmic localization of the transcriptional regulator YAP. YAP cooperates with β -catenin to regulate expression of WNT9B targets in NPC such as *Cited1*.(Das et al., 2013) The *Six2*-mediated deletion of *Yap* in the CM (*Yap*^{CM-/-}) leads to an impaired transition of the renal vesicle to the S-shaped body structure resulting in hypoplastic kidneys. The conditional inactivation of Rho GTPase *Cdc42* in CM compartment leads to a similar phenotype. In addition, lack of *Cdc42* leads to reduced nuclear localization of YAP and also loss of *Yap*-dependent gene expression suggesting a role for *Cdc42* to regulate the *Yap* activity (Reginensi et al., 2013).

BMP ligands are capable of activating both SMAD and MAPK signaling pathways. *Bmp7* is expressed in the CM as well as in the CD (Dudley et al., 1997). The collecting duct provides a WNT9B signal which is required to maintain *Bmp7* expression in the MM.(Park et al., 2012; Godin et al., 1998) NPC require BMP7 for proliferation and survival, and inactivation of *Bmp7* leads to depletion and death of CM (Dudley et al., 1995; Luo et al., 1995). This requirement is present even at later stages of nephrogenesis, as conditional inactivation of *Bmp7* at E12.5 after the onset of nephrogenesis recapitulated the *Bmp7* null phenotype (Tomita et al., 2013) Downstream of BMP ligands and receptors, SMAD and MAPK signaling is activated. Activation of MAP3K7 promotes NPC proliferation, which explains the premature exhaustion of NPC in *Bmp7* null mutant. The same lack of proliferation can be observed by inactivating JNK or activating Jun and ATF2, indicating that the proliferative signal is transduced through the BMP7-JNK-pJUN/pATF2 pathway (Blank et al., 2009).

Although *Bmp7* null CM displays lack of proliferation, there are still CITED1+ cells retained within the compartment, though these NPC don't progress to the epithelialized state, indicating additional functions of BMP7 in regulating MET (Brown et al., 2013; Dudley et al., 1997). Indeed, CM cells require BMP7-SMAD1/5 signaling to transform from CITED1-expressing state to the next compartment which is receptive to β -catenin activation (Brown et al., 2013). CITED1+ cells maintain low levels of activated SMAD1/5, and they increase as cells exit the CITED1+ compartment (Blank et al., 2008). This demonstrates a bimodal role of BMP7, a factor responsible both for maintenance and differentiation of CM.

Mesenchymal to epithelial transition in kidney

The process of the Mesenchyme to Epithelial Transition (MET) is a critical step during nephron progenitor differentiation. This process is initiated at E11.5 in murine kidneys, and is regulated through the crosstalk of multiple signalling pathways helping to maintain the proper balance between differentiation and self-renewal of the progenitor pool. The initiation of MET is mediated by the canonical WNT/ β -catenin signalling, as demonstrated by a number of loss- and gain-of-function studies (Park et al., 2007; Dressler, 2009; Little, Mc Mahon 2012). The first inductive signal initiating the MET process is *Wnt9b*, expressed in the UB tips. (Carroll et al., 2005). A subpopulation of *CITED1*⁻/*OSR1*⁻/*SIX2*⁺ progenitor cells starts to aggregate below the UB tip, following the reduction in the expression of *Bmp4* (Michos et al., 2007; Schedl 2007). These progenitor cells differentiate into pre-tubular aggregates (PTA) and start to express early epithelial markers after the loss of *Six2* expression and under the influence of *Wnt9b* inductive signal. These markers include *Lef1*, *Jag1*, *Cdh4/6*, *Wnt4*, *Fgf8*, *Pax8*, *Lim1* (Kobayashi et al., 2008). Inductive signal of *Wnt9b* may be substituted by sustained genetic activation of β -catenin in CM, however full epithelialization is not achieved in these conditions, indicating possible mechanisms of inhibition of β -catenin signal in the course of epithelialization (Park et al., 2007).

Positional identity of progenitor cells during aggregation was identified as an important factor in the process of nephrogenesis. The timing of NPC recruitment dictates the spatial positioning of each cell and the subsequent fate of cells along the proximal-distal axis of the nephron. This process of cell-streaming continues from PTA to late RV stage, when podocyte precursors become the last cells to be incorporated into the proximal RV. This finding forms a basis of Time-dependent Cell-fate Acquisition (TCA) model of nephron patterning. (Lindström et al., 2018)

Wnt4, expressed in the PTA, CSB and the distal part of SSB, is a central component of the nephron induction pathway (Perantoni et al., 2005). Its expression is regulated by *Wt1* (Essafi et al., 2011), *Pax2* (Torban et al., 2006) and *Fgf8* (Perantoni et al., 2005). *Wnt4* expression in CM is suppressed by the synergistic action of *SIX2* and *OSR1* proteins to prevent premature exhaustion of the progenitor cell population (Xu et al., 2014). Positive feedback loops increase the *Wnt4* expression to reach the critical threshold when a PTA is transformed into a RV. Embryos lacking *Wnt4* expression demonstrate inability to form any epithelial nephron structures and the lack of expression of *Pax8*, *Fgf8* and *Lim1* differentiation markers (Stark et

al., 1994). WNT4 is thought to induce nephrogenesis through its canonical direct target, β -catenin (Park, Valerius & McMahon, 2007). However, *Wnt4* induction has been suggested to act through the non-canonical Wnt-Calcium-NFAT pathway as well (Tanigawa et al., 2011; Burn et al., 2011). *Wnt4* induces calcium influx in primary MM, which causes epithelialization and can be mimicked by treatment with ionomycin (Tanigawa et al., 2011)

The role of WT1 in MET was studied using a conditional allele inactivated by Nestin-Cre. Nestin is expressed in CM cells in a WT1-dependent manner (Wagner et al., 2006), which allows to bypass the MM loss-of-function phenotype. Reduction in nephron numbers at later stages of development reveals the role of *Wt1* throughout the renal differentiation process (Berry et al., 2015). The explanation for this is the role WT1 plays in controlling the transcription of *Wnt4* (Essafi et al., 2011). Similar loss of CM differentiation was observed after inducible expression of a short hairpin RNA directed against *Wt1* (Kann et al., 2015).

ChIP analysis was used to study the regulation of differentiation of NPCs, leading to a model where WNT/ β -catenin and SIX2 regulate a number of genes, such as *Bmp7*, *Wnt4*, *Fgf8*, therefore influencing the balance between self-renewal and differentiation in the progenitor cell population. (Park et al., 2012) There is a remarkable overlap between regulatory targets of SIX2 and WT1, with SIX2-binding sites found on the *Wt1* locus, and some of the SIX2 target genes containing WT1-binding motif (O'Brien et al., 2016) Notch was determined to be a negative regulator of *Six2*, with overactivation of Notch in the CM leading to the loss of SIX2 expression and further NPC differentiation, while inactivation causes loss of nephron differentiation (Boyle et al., 2011; Chung et al., 2017).

Anatomically, compartmentalization of cap mesenchyme reflects different stages of the differentiation process, as defined by sequential growth factor signaling. WNT9B induction mediated by UB activates the expression of *Wnt4* and *Fgf8* in the pre-tubular aggregate, which are required for the formation of the renal vesicle. (Park et al., 2012; Stark et al., 1994; Grieshammer et al., 2005). FGF8 is required for *Wnt4* expression and for other components of the MET process, as evidenced by the lack of MET in the absence of *Fgf8* even with *Wnt4* ectopically induced (Perantoni et al., 2005).

Nephron patterning

Following MET, the renal vesicle forms a lumen, starts to pattern along the proximal-distal axis and undergoes complex transformation to form a “comma-shape” and then a “S- shape” body before developing into a mature nephron (Figure 9). This dynamic process is regulated by various signalling pathways, which give rise to multiple distinct cell sub-populations. These, in turn, form the distal tubule, Henle’s loop, proximal tubule and glomerulus. In the process of nephron formation, each cell sub-population expresses different segment-specific genes controlling their fate (Desgrange, Sereghini, 2015).

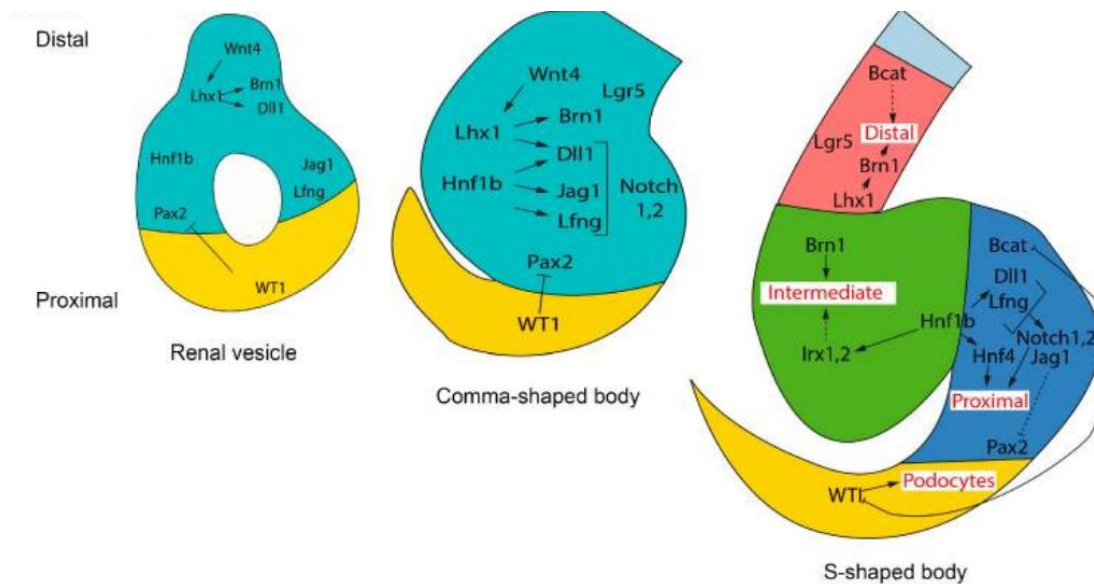


Figure 9: Genetic pathways of nephron segmentation in mouse. (Desgrange, Sereghini, 2015)

One of the major pathways involved in nephron segmentation is *Notch* signaling. NOTCH proteins are transmembrane molecules, which activate their downstream effectors after binding to Delta-like and Jagged ligands (Mukherjee et al., 2019). While *Notch* signaling is required for medial and proximal development (Cheng et al., 2007), *Lim1* regulates the development of distal structures, which also express *Jag1*, *Wnt4*, *Lef1* and *Dkk1* (Perantoni et al., 2005; Dressler et al., 2006; Kopan et al., 2007; Schedl 2007; Little and McMahon 2012). *Pax* genes play a crucial role in nephron patterning, as evidenced by *Pax2/Pax8* heterozygous embryos displaying abnormal segmentation in distal tubules (Narlis et al., 2007).

A gradient of β -catenin activity along the proximal-distal axis controls the differentiation of segment-specific cell fates through interactions with the PTEN/PI3K, and Notch pathways. Conversely, BMP/pSmad and PI3K signalling are negatively modulating β -catenin activity (Lindström et al., 2015).

Wt1 is expressed in the proximal part of the comma-shaped body and its expression becomes restricted to the presumptive podocyte layer of the S-shaped body. *Wt1* is required for glomerulus podocyte layer specification, structure, function and maintenance (Kreidberg et al., 1993) (Hastie, 2017). *Hnf1b* was found to control proximal-intermediate nephron identity by regulating *Irx1/2* and Notch pathway components *Lfng*, *Dll1* and *Jag1*. HNF1B is recruited to regulatory regions of these genes. *Hnf1b*^{-/-} mutants display lack of proliferation in CSB followed by apoptosis in late SSB. However, glomerulogenesis was weakly affected. (Heliot et al, 2013) (Massa et al., 2013)

Brn1, also known as *Pou3f3*, appears to be involved in the development of multiple nephron segments, including thick ascending limb of Henle's loop, Macula Densa and distal tubule (Nakai et al., 2003). *Brn1* is also important in nephron induction, the determination of nephron numbers, and in nephron size in the murine kidney (Rieger et al., 2016).

Sox genes

Sox is a family of 20 genes, that encode important transcriptional regulators that are involved in a variety of developmental and pathological processes. The prototypical member of the group is *Sry* (*Sex-determining region Y*), located on the Y chromosome and responsible for sex determination in most mammals (Gubbay et al., 1990; Sinclair et al., 1990). Following the discovery, a number of genes were identified that share homology with the originally identified DNA-binding domain of *Sry*, dubbed *Sry* box or *Sox* genes. *Sox* genes are subdivided into 9 groups (A to H) on the basis of the homology of their DNA-binding domain. Genes in the same group share at least 80% homology inside their *Sry* box region, as well as substantial homology regions outside. (Wegner, 1999)

Sox gene structure and function

Multiple types of functional domains were identified in *Sox* genes. These include a DNA-binding domain of the HMG (High Mobility Group) type, a dimerization domain on the N-terminal side of the HMG box, and a trans-activation or trans-repression domain on the C-terminal side of the HMG box (Lefebvre et al., 2007)

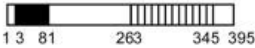
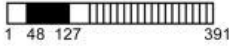
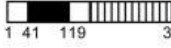
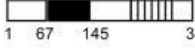
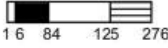
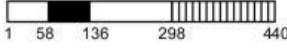
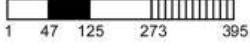
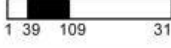
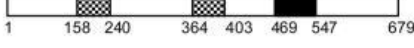
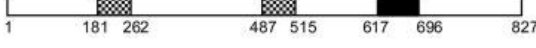
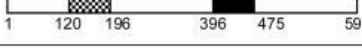
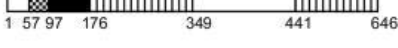
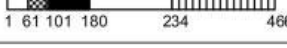
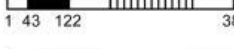
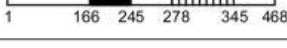
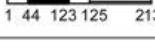
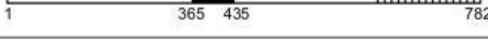
Group	Gene	Locus	Schematic	References
A	<i>Sry</i>	YC3		Gubbay et al., 1992 Dubin et al., 1995
B1	<i>Sox1</i>	8 A1-A2		Collignon et al., 1996 Kamachi et al., 1999
	<i>Sox2</i>	3 A2-B		
	<i>Sox3</i>	X A7.3-B		
B2	<i>Sox14</i>	9 E3.3		Hargrave et al., 2000
	<i>Sox21</i>	14 E4		Uchikawa et al., 1999
C	<i>Sox4</i>	13 A3-A5		van de Wetering et al., 1993 Kuhlbrodt et al., 1998 NCBI - CAM23207
	<i>Sox11</i>	12 A3		
	<i>Sox12</i>	2 G3		
D	<i>Sox5</i>	6 G3		Denny et al., 1992 Lefebvre et al., 1998 Lefebvre et al., 1998 Hiroaka et al., 1998 Lefebvre et al., 1998 Takamatsu et al. 1995 Connor et al., 1995 Kido et al., 1998
	<i>L-Sox5</i>	6 G3		
	<i>Sox6</i>	7 F1		
	<i>Sox13</i>	1 E4		
E	<i>Sox8</i>	17 A3		Schepers et al., 2000 Sudbeck et al., 1996 Wright et al., 1995 Pusch et al., 1998 Kuhlbrodt et al., 1998
	<i>Sox9</i>	11 E2		
	<i>Sox10</i>	15 E1		
F	<i>Sox7</i>	14 C3		Taniguchi et al., 1999 Takash et al., 2001 Kanai et al., 1996 Dunn et al., 1995 Hosking et al., 2001
	<i>Sox17</i>	1 A1		
	<i>Sox18</i>	2 H4		
G	<i>Sox15</i>	11 B3		Beranger et al., 2000
H	<i>Sox30</i>	11 B1.1		Osaki et al., 1999

Figure 10: Classification and structure of murine SOX proteins (Lefebvre et al., 2007)

Different *Sox* members expressed within the same cell type can target different genes, as well as the same *Sox* gene within different cell types. This points towards other factors that can determine targets of *Sox* genes, including DNA-binding motif, protein interactions, post-translational modifications and nucleus shuttling.

HMG box conformation is responsible for binding the minor groove of DNA and bending it in an L shape (Ferrari et al., 1992; Connor et al., 1994) with the consensus motif 5'-(A/T)(A/T)CAA(A/T)-3' *in vitro* (Harley et al., 1994). *Sox* genes vary in their binding affinity depending on their subgroup, such as the preference of hSOX9 (human SOX9) to bind to the 5'-AACAAAT-3' motif, and hSOX4 to bind to the 5'-AACAAA-3' motif (Mertin et al., 1999; Scharer et al., 2009). Nucleotides adjacent to the consensus motif are also responsible for the difference in specificity between *Sox* genes of different subgroups. For example, hSOX9 binds predominantly the 5'-AGAACAATGG-3' sequence *in vitro*, while hSRY preferentially binds to 5'-(T/A)(T/A)AACAAATAG-3' (Mertin et al., 1999, Harley et al., 1994)

An identical consensus sequence can be bound by SOX proteins of different groups, and this interaction can regulate gene expression differently depending on the cellular context. For example, co-binding of SOX-D and SOX-E on the same enhancer sequence of the *Col2a1* (*Collagen, type II, Alpha I*) gene promotes its expression and subsequent cartilage development, while in oligodendrocyte development, SOX-E and SOX-D compete to bind this enhancer and have opposite roles (Lefebvre et al., 1998; Stolt et al., 2006). The different action of different SOX factors, is thought to be brought about by their association with different interaction partners.

The HMG domain was also discovered to be responsible for the interaction with other transcription factors such as PAX proteins, POU factors and Zinc-finger proteins. A SOX protein can form heterodimers with different partners. For instance, SOX2 can synergize with BRN2 in neural primordium, with OCT2/3 in stem cells, and PAX6 in lens cells (Lefebvre et al., 2007).

TAD and TRD

TADs and TRDs were identified with the help of reporter assays in which isoforms of SOX proteins are truncated, but the HMG box is left intact. Truncated proteins lacking TAD/TRD domains are not able to activate or repress the reporter plasmid despite the HMG box retaining

its DNA-binding capability, indicating the critical role of TADs and TRDs in *Sox* transcriptional regulation function (Kamachi et al., 1999)..

TAD and TRD are located at the C-terminal side of the HMG box. Their protein sequences have a high variability between Sox members of different subgroups, providing specificity in regard to target gene regulation between Sox members. For example, chimeric proteins made of the chSOX9 (chicken SOX9) and chSOX1 revealed that the TAD of chSOX1 activates the DC5 enhancer of the Delta1 crystallin gene, although the 2 different HMG boxes can be interchangeable and display similar properties for DC5 enhancer's binding and bending (Kamachi et al., 1999).

The SOX proteins contain 2 distinct TADs in SOX-E (SOX8/9/10) and SOX-F (SOX7/17/18) members. Which TAD displays the strongest functional relevance depends of the cellular context and can differ between SOX proteins of the same subgroup (Wegner, 2010), which means a gene's target specificity exists even between the closest related Sox members. For example, Sox10 is an important regulator of neural crest lineage development. Early in development, it is required for the maintenance and survival of neural crest stem cells (Kim et al., 2003) and later for terminal differentiation of their derivatives (Stolt et al., 2002). Experiments using different Sox10 alleles lacking either one of the TADs showed that they were specifically required at 2 distinct stages of neural crest derivative differentiation, while early events were only slightly affected in both mutants (Schreiner et al., 2007)

Dimerization domains

Homodimerization domains, found only in SOX-D (SOX5/6/13) and SOX-E (SOX8/9/10), are responsible for the physical interaction with the same SOX protein or with a SOX member of the same subgroup. The existence for homodimerization implies the possibility of existence of two adjacent binding sites on DNA. Such a dimeric binding site is contained at the promoter of the *Mpz* (Myelin protein zero) gene, whose expression is controlled by SOX10 in neural crest derivatives. Reporter experiments demonstrated that removal of one of these binding sites severely decreased *Mpz* promoter activation by SOX10 (Schlierf et al., 2002). Therefore, protein dimerization ability is essential for this specific type of regulation.

Mutations of SOX9 in humans cause campomelic dysplasia syndrome, displaying skeletal malformations frequently associated with male sex reversal. Identification of mutation in hSox9

dimerization domain revealed the importance of this mechanism for gene regulation in cartilage development, but not for sex-determination genes. This was consistent with the patient's phenotype, which didn't show sex-reversal. (Bernard et al., 2003). This demonstrates that SOX homodimerization requirement for gene regulation is cell context-dependent.

Heterodimers can also form with other transcription factors through non-HMG domains. A short motif on N-terminal portion of SOX6 recruits the co-repressor CtBP2 (C-terminal binding protein 2) on the *Fgf3* promoter to repress its transcription (Murakami et al., 2001)

Nuclear-cytoplasmic shuttling

The HMG box comprises 2 distinct nuclear localization signal motifs (NLS). These motifs are highly conserved among the different Sox members, but were functionally characterized only in SRY, SOX9 and SOX2. Nuclear import mediated by the N-terminal NLS motif was found to be dependent on the interaction with activated CALMODULIN, intracellular mediator of the Calcium pathway, and the transporting protein EXPORTIN4. The C-terminal NLS motif was shown to interact with IMPORTIN-B. In sex-reversal patients, mutations in both NLS motifs of hSox9 were described, pointing towards the functional relevance for the Sox nuclear import mechanism.

The HMG box also contains a Nuclear Export Signal motif (NES), described in SOX9 and SOX10, and requires EXPORTIN1 for the process of nuclear export. Although this NES motif is found among all Sox genes, there is a specific amino-acid consensus of the NES of Sox-E members, suggesting a specific nuclear export regulation for Sox8, Sox9 and Sox10. (Malki et al., 2010)

Post-translational modifications

Sox activity is influenced by phosphorylation, acetylation and sumoylation. Acetylation of the HMG domain of hSRY promotes NLS motif binding to Importin- β *in vitro*, and triggers the subsequent nuclear localization, while deacetylation triggers its cytoplasmic subcellular relocation (Thevenet et al., 2004).

Phosphorylation of several SOX members was shown to promote their activity, such as phosphorylation of *Sox2* in induced pluripotent stem cell reprogramming (Jeong et al., 2010), phosphorylation of *Sox9* in chondrocytespecific gene activation (Huang et al., 2000), or phosphorylation of *chSox9* in neural crest cell delamination in a and canonical *Wnt*- and BMP-dependent manner (Liu et al., 2013).

SOX3, SOX4, SOX6 and Sox-E were discovered to be modified by sumoylation, resulting in a decreased transactivation potential, decreased synergism with protein partners or increased nuclear localization and subsequent transactivation (Fernández-Lloris et al., 2006) (Girard et al., 2006) (Hattoriet al., 2006) (Savare et al., 2005).

Sox genes functions in development

Sox and WNT signalling

WNT growth factors facilitate essential embryogenesis processes through canonical and non-canonical WNT pathways. As discussed above, canonical WNT/ β -CATENIN, WNT/CALCIUM and PCP pathways must be tightly controlled during kidney development to allow proper morphogenesis. *In vitro* studies showed that several SOX proteins could modulate WNT/ β -CATENIN activity reporter through physical interaction with β -CATENIN, promoting its degradation or stabilization (Sinner et al., 2007). The *in vivo* functional relevance of this mechanism was demonstrated in the process of skeletogenesis, where WNT/ β CATENIN is tightly controlled and its silencing is crucial for chondrocyte differentiation. This inhibition takes place with the binding of SOX9 to β -CATENIN leading to its proteosomal degradation. Gene targeting in mice revealed similar skeletal phenotypes between *β -catenin* stabilization and *Sox9* deletion, or *β -catenin* deletion and *Sox9* overexpression (Akiyama et al., 2004). In summary, WNT and SOX9 crosstalk is an essential mechanism of bone formation. *Sox*-WNT interaction was also found to be occurring during pancreas formation, T-cell development, sex determination and neural development (Kormish et al., 2010) (Tang et al., 2020). In addition, there is evidence for a WNT signalling role in regulation of the *Sox* genes through a feedback loop mechanism (Kormish et al., 2010)

Sox and Notch signalling

The NOTCH signaling pathway is a pro-artery cell fate modulator during arterio-venous differentiation of endothelial cells (Lawson et al., 2001). Activation of the artery-specific gene *Dll4* requires binding of SOX-F (SOX7 and SOX18) to the NOTCH effectors NCID/RBPJ (Notch intracellular domain/Recombination signal binding protein for immunoglobulin kappa J region), while the triple knock-down of *Sox7*, *Sox18* and *Rbjp* abolishes arterial marker expression (Sacilotto et al., 2013). Thus, NOTCH and *Sox-F* cooperate in vascular development. In mouse retina development, the expression of *Sox8* and *Sox9*, and subsequent Müller glial cells development, is induced by activated NOTCH signaling (Muto et al., 2009). In this context, NOTCH signalling is an upstream regulator for *Sox* function.

Sox and FGF-BMP signalling

Neural induction in *Xenopus* is triggered by endogenous BMP4 antagonists or by activation of FGF signalling. *Sox2* is an early neural gene induced upon BMP inhibition, which stimulated responsiveness to FGF-neuralizing signal. Consequently, FGF treatment of *Sox2*-injected individuals triggered neural and neuronal differentiation in standard medium (Mizuseki et al., 1998). As a result, BMP signalling represses *Sox*-FGF interaction.

Sox and SMAD signalling

Adult epithelial cells of the mouse lung can be reprogrammed and re-specified into several airway epithelia cell types, in a reversible manner. *Sox17* controls this plasticity at least at two levels: by direct binding and activation of the pro-proliferative *CyclinD1* gene, and by repression of the anti-proliferative TGF β /SMAD signalling pathway through physical interaction with SMAD3 (Lange et al., 2009). While adult lung cell plasticity relies on antagonistic effects driven by SOX17 and SMAD, SOX4-mediated inhibition of lymphocyte TH2 differentiation requires activated TGF β signalling and subsequent binding of SMAD2/3 to the *Sox4* promoter (Kawahara et al., 2012). This way, SOX/SMAD crosstalk can be antagonistic or cooperative.

Sox genes in kidney development

Little is known about the roles of *Sox* genes during kidney formation. Campomelic dysplasia patients occasionally display renal malformations, such as renal hypoplasia, hydronephrosis, hydroureter, and rarely renal cysts (Houston et al., 1983). *SOX9* is a gene causing campomelic dysplasia syndrome, thus it might also play important roles during kidney development. Expression analysis in mice supported this conclusion by discovering expression of several *Sox* members in embryonic kidneys: *Sox8* and *Sox9* which belong to the *Sox-E* subgroup, and the 3 *Sox-C* members *Sox4*, *Sox11* and *Sox12* (Kent et al., 1996)(Schepers et al., 2000) (Hoser et al., 2008).

SoxE and ureter development

Sox9 was demonstrated to be transiently expressed in the ureteric mesenchyme where it is required for its differentiation into ureter smooth muscle cells (SMC), and *Sox9* removal in this compartment resulted in hydroureter (Airik et al., 2010). Another study further characterized the mechanism by which *SOX9* regulates SMC differentiation (Martin et al., 2013). Martin et al., showed that *SOX9* physically interacts with the transcription factor *TSHZ3* (Teashirt3), also required for SMC differentiation. In contrast to *Sox9*, *Tshz3* is expressed at every differentiation step in the differentiation of precursors into SMC. They proposed a model in which the *SOX9/TSHZ3* complex inhibits the function of *MYCOD* (Myocardin), a master transcriptional activator of the smooth muscle program, and *Sox9* downregulation removes this inhibition, concomitant with *MYCOD*-driven transcriptional program. Interestingly, *Sox9* and *Tshz3* are both required independently for *Mycod* expression at the time of SMC induction. Thus, *Sox9* appears to act as a “buffering” factor of SMC differentiation program, by orchestrating the molecular steps driving progression through the myogenic program.

Both *Sox8* and *Sox9* were implicated in regulation of ureter branching and collecting duct development. *Sox8/Sox9* double mutant mice maintained *Ret* expression but failed to initiate branching of the UB. *SOX8/9* were found to be required, but not sufficient, for *GDNF/RET* signalling by controlling the expression of its major effector genes. In later development, *Sox9* mutant mice displayed abnormal induction of nephrogenesis in the outermost layer of the

embryonic kidney. In this case, loss of ureteric tip identity leads to expansion of *Wnt9b* expression domain, causing the formation of ectopic aggregates (Reginensi et al., 2011).

Sox17 and human CAKUT

Sox17 has been shown to negatively regulate β -CATENIN transcriptional activity *in vitro* (Sinner et al., 2007). To further analyze WNT/ β CATENIN signalling during kidney development, a sequence analysis of the *SOX17* gene in a human CAKUT cohort was performed and 3 mutations were identified in 8 patients (Gimelli et al., 2010). All of them displayed vesico-ureteral reflux with one patient suffering from a duplicated collecting system. Two of these mutations resulted in a single amino-acid change and one led to a two amino acid frame-shift insertion. Interestingly, the *p.Y259N* mutation was found in 2 unrelated sporadic cases and 4 familial cases derived from 2 families, in which the mutation segregated with the CAKUT phenotype. *In vitro* experiments demonstrated higher protein levels correlating with the stronger inhibition of the WNT/ β -CATENIN reporter by the mutant protein compared to wildtype, despite having similar transcript levels. Therefore, the *p.Y259N* mutation renders SOX17 protein more stable with subsequent renal developmental defects due to inappropriate inhibition of WNT signalling, which makes *Sox17* a CAKUT-causing gene

Cooperation between SOXC and WT1 in kidney development

Wt1 is a key gene for kidney formation. It is required for MM survival (Kreidberg et al., 1993) (Motamedi et al., 2014), nephron formation (Essafi et al., 2011) (Murugan et al., 2012), and glomerulus maintenance (Hammes et al., 2001). Murugan et al. found that WT1 positively regulates *Wtn4*, a master gene for mesenchyme-to-epithelial transition of nephron precursors. Using the *Xenopus* pronephros as a model, the authors identified a 4 kb region upstream of the *Wtn4* translation start that was synergistically activated by WT1 and SOX11 *in vitro*, and knockdown of each of these genes resulted in a downregulation of *Wnt4* expression *in vivo*. They further demonstrated that SOX11 physically interacts with WT1 in mouse embryonic kidneys (Murugan et al., 2012), suggesting that their cooperation might be a critical event for nephrogenesis in mammals. Likewise, interaction between WT1 and SOX4 was found to be important for renal development (Huang et al., 2013) Conditional ablation of *Sox4* in nephron

progenitors results in significant reduction in nephron endowment, with loss of WT1+ podocytes and resulting renal failure. These observations are consistent with a specific role of SOX4 in podocyte lineage.

Congenital anomalies of kidney and urinary tract

Congenital anomalies of kidney and urinary tract (CAKUT) are developmental malformations that can have dramatic consequences in early and adult life. CAKUT are responsible for 30-50% cases of end-stage renal diseases in children (Seikaly et al., 2003). When asymptomatic, kidney malformations predispose to renal deficiency in adult life, promoting diseases such as hypertension or cardiovascular diseases. Kidney malformations in humans are found in 1 out of 500 newborns. They are often found in the prenatal development, representing approximately 20 to 30 % of all anomalies identified (Pichel et al., 1996). The *in utero* environment can be a contributing risk factor when issues such as maternal diabetes, diet or drug uptake are involved (Aisa et al., 2019) (Lee et al., 2018) (Boubred et al., 2006). In addition, familial clustering of kidney abnormalities is found only in 20% of patients, suggesting non-hereditary factors for predisposition to these diseases (Satko & Freedman, 2005)

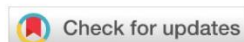
Types of CAKUT include: renal agenesis (complete absence of kidney), renal hypoplasia (reduced size of the kidney), renal dysplasia (incomplete or abnormal development of the kidney), Wilms' tumor (pediatric renal tumor), duplex kidney (duplication of kidney and collecting system), hydronephrosis and hydroureter (abnormal dilation of renal pelvis and ureter), vesicoureteral reflux (retrograde flow of urine), polycystic kidney disease (progressively expanding cystic structures in the kidney) and horseshoe kidney (two kidneys are fused at their lower pole). (Song & Yosypiv, 2011)

Since CAKUT were found to be inherited in some cases, a genetic basis for inheritance was proposed. The development of DNA sequencing capabilities that allowed human whole-genome analysis, coupled with genetic modification tools allowing targeted gene alteration in animal models, provided powerful tools to reproduce and follow CAKUT progression, allowing a better characterization of the mechanisms leading to human diseases. Based on the observation of human duplex kidneys samples, Mackie and Stephens proposed the ureteric bud (UB) theory (Mackie & Stephens, 1975). They found a strong correlation between the mispositioned ureter-bladder orifice and the hydronephrosis/hydroureter features displayed by

the corresponding kidney and ureter. They proposed a model in which the initial position of the UB (the future ureter) at the onset of kidney development dictates the final position of ureter orifice into the bladder, with an ectopic budding site leading to duplex kidneys. This hypothesis was confirmed using a mouse model (*Foxc1* (Forkhead box C1) knock-out) (Kume et al., 2000). Later, a mutation of the *FOXC1* gene was found in a cohort of CAKUT patients (Nakano et al., 2003). Currently, more than 180 monogenic causes of murine CAKUT have been described, with many of the 40 identified human CAKUT genes first described in a mouse model (van der Ven et al., 2018) including *PAX2* (Paired box gene 2), *EYAI* (Eyes absent homolog 1), *SALL1* (Spalt-like transcription factor 1), *HNF1B* (HNF1 homeobox B) and *SIX1* (SIX homeobox 1). While these genes were found mutated in a significant proportion of CAKUT patients (Yosypiv, 2012), their role as disease-causing factors is debated.

Treatments for CAKUT are limited in effectiveness. In the best cases renal failure can be treated with surgery and/or dialysis but the patients often fail recover full renal function. Kidney transplantation can cure the disease; however, patients face the obstacles of the low number of compatible donors and graft rejection issues. Regenerative medicine or cell therapy approaches that involve the *in vitro* production of renal structures or particular cell types could be the basis of future renal failure treatments. Extensive research has led to the identification of organ culture conditions that can mimic some of the renal development processes, however so far the *in vitro* generation of a functional kidney has not been achieved. In addition, a high proportion of human CAKUT cases escape genetic testing and remain without genetic or environmental explanation. To further the development of therapies and CAKUT diagnosis and etiology, it is important to understand how the kidneys develop in the normal situation and to characterize the molecular mechanisms controlling their morphogenesis.

Article 1: Duplex kidney formation: developmental mechanisms and genetic predisposition



REVIEW

Duplex kidney formation: developmental mechanisms and genetic predisposition [version 1; peer review: 2 approved]

Vladimir M. Kozlov, Andreas Schedl 

iBV, Institut de Biologie Valrose, Equipe Labellisée Ligue Contre le Cancer, Université Cote d'Azur, Centre de Biochimie, UFR Sciences, Parc Valrose, Nice Cedex 2, 06108, France

v1 First published: 06 Jan 2020, 9(F1000 Faculty Rev):2 (<https://doi.org/10.12688/f1000research.19826.1>)Latest published: 06 Jan 2020, 9(F1000 Faculty Rev):2 (<https://doi.org/10.12688/f1000research.19826.1>)**Abstract**

Congenital abnormalities of the kidney and urinary tract (CAKUT) are a highly diverse group of diseases that together belong to the most common abnormalities detected in the new-born child. Consistent with this diversity, CAKUT are caused by mutations in a large number of genes and present a wide spectrum of phenotypes. In this review, we will focus on duplex kidneys, a relatively frequent form of CAKUT that is often asymptomatic but predisposes to vesicoureteral reflux and hydronephrosis. We will summarise the molecular programs responsible for ureter induction, review the genes that have been identified as risk factors in duplex kidney formation and discuss molecular and cellular mechanisms that may lead to this malformation.

Keywords

CAKUT, kidney development, duplex systems, ureter budding

Open Peer ReviewReviewer Status  

	Invited Reviewers	
	1	2
version 1 published 06 Jan 2020		

F1000 Faculty Reviews are written by members of the prestigious F1000 Faculty. They are commissioned and are peer reviewed before publication to ensure that the final, published version is comprehensive and accessible. The reviewers who approved the final version are listed with their names and affiliations.

- Norman D Rosenblum**, The Hospital for Sick Children, Toronto, Canada
- Satu Kuure**, University of Helsinki, Helsinki, Finland

Any comments on the article can be found at the end of the article.

Corresponding author: Andreas Schedl (schedl@unice.fr)

Author roles: Kozlov VM: Visualization, Writing – Original Draft Preparation, Writing – Review & Editing; Schedl A: Writing – Original Draft Preparation, Writing – Review & Editing

Competing interests: No competing interests were disclosed.

Grant information: This work was supported by the La Ligue Contre le Cancer.

The funders had no role in study design, data collection and analysis, decision to publish, or preparation of the manuscript.

Copyright: © 2020 Kozlov VM and Schedl A. This is an open access article distributed under the terms of the [Creative Commons Attribution License](#), which permits unrestricted use, distribution, and reproduction in any medium, provided the original work is properly cited.

How to cite this article: Kozlov VM and Schedl A. **Duplex kidney formation: developmental mechanisms and genetic predisposition [version 1; peer review: 2 approved]** F1000Research 2020, 9(F1000 Faculty Rev):2 (<https://doi.org/10.12688/f1000research.19826.1>)

First published: 06 Jan 2020, 9(F1000 Faculty Rev):2 (<https://doi.org/10.12688/f1000research.19826.1>)

Introduction

The urinary tract, composed of the kidneys, ureters, bladder and urethra, represents the main excretory system of the mammalian organism. Development of the urinary system, made up of more than 40 different cell types, needs to proceed in a highly organised manner. Given this complexity, it is not surprising that mutations in developmental genes can lead to a wide variety of abnormalities that are usually grouped together as congenital abnormalities of the kidneys and urinary tract (CAKUT). Defects affecting the kidneys range from renal agenesis (a complete lack of kidney development) to hypoplasia (reduced size), dysplasia (abnormally developed tissue), cystic dysplasia, and terminal differentiation defects. Lower urinary tract malformations include vesicoureteral reflux (VUR), hypospadias (opening of the urethra at the lower side of the penis) and posterior urethral valves that often lead to outflow obstructions. Although individual malformations are considered rare diseases, CAKUT, taken together, have an incidence of about 3 to 6 in 1000 live births and thus belong to the most frequent abnormalities detected in the new-born child¹. An in-depth presentation of all subclasses and their aetiology would be far beyond the scope of this review and therefore interested readers are referred to other publications that present an overview of CAKUT phenotypes and the genetics underlying them²⁻⁶. Here, we will instead concentrate on duplex (or multiplex) kidneys, a very frequent subclass of CAKUT, which is often neglected in the literature.

Development of the urinary system

To understand the aetiology of duplex kidneys, it is important to consider how the urinary system forms. From a developmental point of view, the urogenital tract derives from two independent germ layers with kidneys and ureters arising from the intermediate mesoderm (IM) and the bladder and urethra developing from cloacal endoderm⁷. Accordingly, malformations of the urinary system can be further classified into congenital abnormalities of the upper and lower urinary tract (and the latter are sometimes abbreviated as CALUT). Despite this developmental distinction, it should be noted that some authors group malformations of the ureter as part of congenital abnormalities of the lower urinary tract.

Kidney development in mammals commences with the formation of the nephric duct (ND) at the anterior (rostral) pole of the IM. As development proceeds, epithelial cells of the ND proliferate and actively migrate towards the caudal end of the nephrogenic cord⁸⁻¹⁰. Eventually, the ND fuses with the cloaca, a process that involves dedicated apoptosis and requires GATA3 and LHX1 as well as retinoic acid and RET and FGF signalling⁹⁻¹³.

As the ND elongates caudally, a series of tubules forms within the nephrogenic cord. The most anteriorly positioned pronephric tubules are considered an evolutionary remnant and are non-functional in mammals. Subsequently, a wave of mesonephric tubules develop that fall into two groups. While rostrally positioned tubules are connected to the ND and serve as an embryonic kidney, more caudally located tubules do not drain into the ND and are non-functional^{14,15}. Both pronephros

and mesonephros are transitory structures in the mammalian embryo and disappear (pronephros) or are remodelled (mesonephros) at later stages of development.

The metanephros represents the permanent kidney in mammals and develops at the most caudal position of the IM. Metanephros development is first detectable as a population of slightly condensed mesenchymal cells within the nephrogenic cord which express a set of molecular markers (*HOX11*, *SIX2*, *GDNF*, *EYAI*)^{15,16}. In normal development, signalling from the metanephric mesenchyme (MM) induces the formation and outgrowth of a single ureteric bud (UB) from the ND, which will invade the MM and undergo a first stereotypic dichotomous branching event (T-shaped ureter). The collecting duct system (ureteric tree) forms through further rounds of branching that often include tri-tips, which, however, eventually resolve into ureter bifurcations^{17,18}. In return, signals released from the ureter will induce the MM to differentiate into nephrons, the functional units of the kidney. For further details on this process, we refer the reader to recent reviews¹⁹⁻²².

Development of the urinary system is not restricted to kidney formation but also involves extensive developmental remodelling of the lower tract. An excellent and detailed description of this complex process can be found in 7. In brief, the emerging UB is initially connected to the cloaca via the distal part of the ND, also termed the common nephric duct (CND). Downgrowth of the urorectal septum leads to a separation of the cloaca into a ventrally located urogenital sinus and a dorsally positioned anorectal sinus^{7,23-25}. The cranial urogenital sinus will further elongate to develop into the bladder, whereas its posterior portion will form the urethra. As development proceeds, apoptosis eliminates the CND, leading to the fusion of the ureter with the future bladder, thus creating the ureterovesical junction²⁶.

Classification and epidemiology of duplex kidneys

Duplex systems can have a variety of phenotypes, and multiple classification systems have been proposed to categorise this pathology (Figure 1)²⁷. In incomplete duplication, the two poles of a duplex kidney share the same ureteral orifice of the bladder. Such duplex kidneys with a bifid pelvis or ureter arise when an initially single UB bifurcates before it reaches the ampulla. This is likely caused by a premature first branching event that occurred before the ureter has reached the MM. Much more frequent are complete duplications, which occur when two UBs emerge from the ND. In most cases, the lower pole of the kidney is normal and the upper pole is abnormal^{28,29}, an observation explained by the fact that the ectopic UB frequently emerges anteriorly to the position of the normal UB and drives the formation of the upper pole of a duplex kidney. Inverted Y-ureteral duplication is a rare condition in which two ureteral orifices drain from a single normal kidney. Inverted Y-ureteral duplication is believed to be caused by the merging of two independent UBs just before or as they reach the kidney anlagen³⁰. A very rare H-shaped ureter has also been reported³¹. Although the vast majority of cases involve a simple duplication, multiplex ureters with up to six independent buds have also been

described^{32–37}. In some cases, the additional ureter or ureters are ectopic and fail to connect to the bladder or the kidney (blind ending ureter)³³.

The aetiology of most duplex kidneys can be traced back to the very first induction steps of the ureter. In the majority of cases, an additional UB emerges in a rostral position to the normal outgrowth. By contrast, in adults, the upper (abnormal) kidney pole drains into the bladder at a site distal to the orifice of the lower kidney pole³⁸. This paradoxical phenomenon, known as the Weigert–Meyer rule²⁹, can be explained by the significant amount of remodelling occurring at the future ureter–bladder junction during development. Indeed, as apoptosis eliminates the CND, the ureter inserts into the developing bladder and moves upwards (Figure 2)^{7,39–41}. An initially anteriorly positioned ureter thus ends up with a more distal insertion site in the bladder, a model that has been proposed by

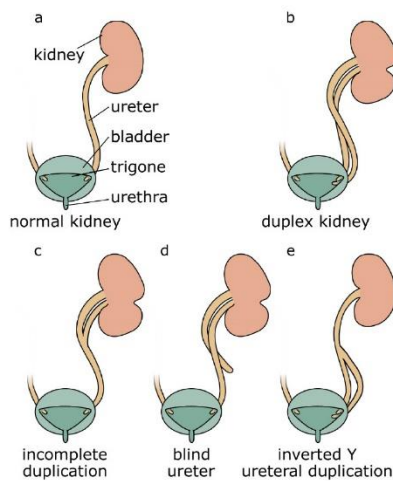


Figure 1. Classification of duplex kidney anatomy. Compared with a normal kidney (a), complete duplication produces a duplex kidney with two poles that drain into two ureters (b). Incomplete duplication leads to a Y-shaped ureter (c). Blind ureters do not drain into the bladder (d). In the rare case of inverted Y-ureteral duplication, two ureters fuse before entering the kidney (e).

Mackie and Stephens⁴². Correct positioning of the ureter into the bladder is important to allow formation of a normal trigone (the triangle formed by the two ureter orifices and the urethra) and prevent ureter reflux caused by a malfunctioning valve or a too-short ureter tunnel. Because the vast majority of duplex kidneys arise from an ectopic bud in a rostral position, it is usually the upper pole of the kidney that is affected by VUR and hydronephrosis.

Estimates suggest a prevalence of duplex kidneys of between 0.2 and 2% in the general population, and females are affected twice as frequently as males^{38,43}. The reasons for this sex bias are unknown. About 40% of patients with duplex kidneys have been reported to exhibit pathological manifestations⁴³. However, because duplex kidneys are frequently asymptomatic and therefore predominantly detected in patients who seek medical assistance, the actual percentage of patients with symptoms is likely to be lower. Symptoms associated with duplex kidneys can include pain, haematuria, dysuria and difficulty or abnormal frequency of micturition^{38,43}. Specific manifestation of the pathology depends on the anatomy of each duplication event⁴⁴. Furthermore, duplex kidneys are linked to a number of renal disorders, including pelvi-calyceal dilatation, cortical scarring, VUR, hydronephrosis, ureteroceles on the non-duplex side, calculi or yo-yo reflux (in the incomplete duplication cases)^{38,43}.

Molecular pathways controlling ureter induction

If duplex kidney formation is rooted in the formation of two ureteric tips, how can we explain the outgrowth of supernumerary buds on a molecular level? Interactions between MM and the ND are crucial to ensure the induction of the ureter from the ND, and a key pathway controlling this process is the GDNF/RET signalling axis (Figure 3)⁴⁵. GDNF, a distant member of the transforming growth factor beta (TGF β) superfamily of signalling molecules, is specifically expressed within the MM, whereas its cognate receptor RET is expressed along the entire length of the ND. Binding of GDNF to RET is greatly facilitated by the co-receptor GFR α 1. The requirement for these genes in ureter outgrowth has been extensively demonstrated by using gene targeting in mice, and homozygous mutations in either of these genes leads to a failure of ureter induction and consequently renal agenesis^{46–50}. Binding of GDNF to the receptor tyrosine kinase RET induces autophosphorylation and recruitment of the

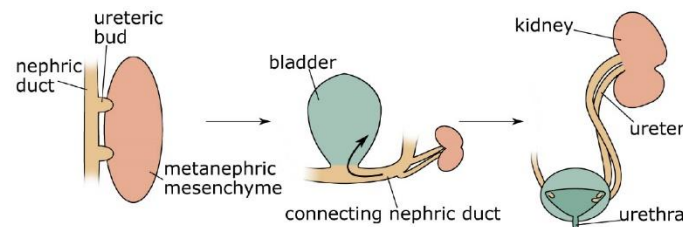


Figure 2. Morphogenesis of duplex kidney. Duplex kidneys form through the induction of two ureteric buds from the nephric duct that will invade the metanephric mesenchyme. Subsequently, apoptosis of the common nephric duct (CND) leads to the insertion of both ureters into the developing bladder with the orifice of the initially posteriorly positioned ureteric bud ending up in a superior position.

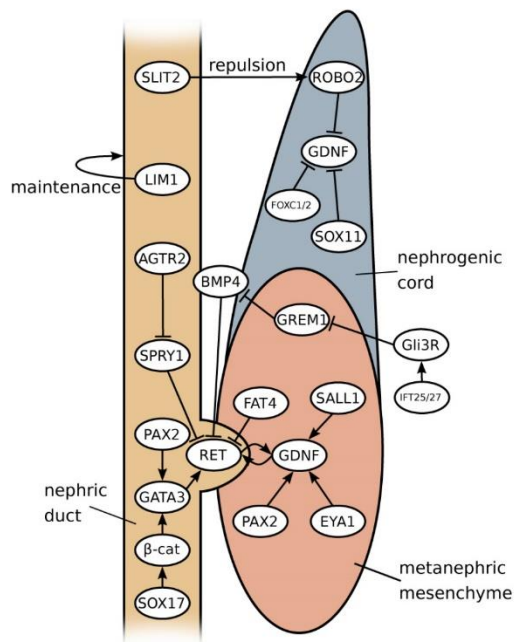


Figure 3. Molecular interactions during kidney development. GDNF-RET signalling is at the core of the signalling network in kidney development and is responsible for ureteric bud (UB) emergence. GDNF expression is positively modulated by factors expressed in metanephric mesenchyme (PAX2, EYA1 and SALL1) and negatively (probably in an indirect manner) by SOX11, FOXC1, FOXC2 and ROBO2 in anterior domains of the nephrogenic cord. Ectopic formation of the UB is prevented by the factors expressed in nephric duct (SLIT2, SPRY1 and GATA3) and in the enveloping mesenchyme (BMP4 and FAT4). Influence from other upstream factors leads to the formation of a complex regulatory landscape.

tyrosine phosphatase SHP2^{51,52}, which results in the activation of several intracellular signalling cascades, including RAS/MAPK, PLC γ /Ca²⁺, PI3K-AKT⁵³, and culminates in the transcriptional activation of a set of downstream target genes⁵⁴. Ureter branching appears to involve, in particular, the ERK/MAPK pathway, and mice lacking the kinases *Mek1* and *Mek2* fail to form a properly branched ureteric tree⁵⁵. Activated RET signalling induces not only proliferation but also cellular motility. Indeed, experiments in chimeric mice demonstrated that wild-type cells move towards the tip of the UB but that *Ret* mutant cells are left behind⁵⁶. This cellular sorting mechanism ensures a strong and directed response that, under normal circumstances, results in the outgrowth of a single UB.

Factors regulating Gdnf expression

Given the crucial function of *Gdnf* in ureter induction, we need to consider how the expression of this gene is regulated. Activation of *Gdnf* in the mesenchyme relies on a set of transcription factors, including SALL1, PAX2 and EYA1. Deletion of either of these factors in mice leads to a lack of ureter induction and consequently to renal agenesis^{57–59}. Heterozygous mutations in each

of these genes have been shown to be involved in CAKUT^{5,6}, and SALL1, in particular, has also been linked to duplex kidney formation⁶⁰. In addition, *Gdnf* mRNA levels appear to be regulated post-transcriptionally via its 3' untranslated region (UTR). Indeed, replacement with a heterologous UTR sequence resulted in increased *Gdnf* expression levels that were associated with ND remodelling defects independent of apoptosis⁶¹.

In the mouse, *Gdnf* expression commences in rostral domains of the nephrogenic cord at embryonic day 9.5 (E9.5), about 1 day before ureter induction. The ND, however, does not respond to the GDNF signal in those anterior regions and this is likely to be due to two reasons: First, the anterior IM has relatively high levels of BMP signalling, which is known to suppress ureter branching (see the 'Restricting Ret activation' section below). Second, SLIT/ROBO signalling, a pathway that is known for its role in axon repulsion⁶², appears to repulse *Gdnf*-expressing cells from the ND, thus causing a physical separation of these two structures in anterior regions⁶³. *Robo2* knockout mice lack this separation and show ectopic buds along the entire length of the ND⁶⁴. The physical separation of ND and *Gdnf*-expressing cells may explain why in *Foxc1*, *Foxc2* and *Sox11* mouse mutants, which all display a dramatic expansion of *Gdnf* expression, the ND does not respond in the anterior domain^{64–66}. Instead, only the region just rostrally to the normal site of induction responds by forming a second ureter. Mutations in *ROBO2*, *SLIT2* and its associated GTPase-activating protein *SRGAP2* are found in patients with VUR and duplex systems^{67,68}.

By the time of ureter induction (E10.5 in mice), mesenchymal cells that express *Gdnf* become restricted to the caudal part of the MM (Figure 4). Three possible mechanisms for this restriction could be envisaged: (1) Active suppression of *Gdnf* expression in more rostral domains could occur. Since the expression of *Foxc1* and *Sox11* overlaps with the *Gdnf* domain, active suppression of the latter seems unlikely. (2) *Gdnf*-positive cells at the rostral end could undergo cell death. The pro- and mesonephros are known to be subject to massive apoptosis, although this seems to affect, in particular, the epithelial cells of tubules. However, preliminary data from our lab suggest that mesenchymal cells positioned just rostrally of the *Gdnf*-expressing domain also undergo apoptosis. (3) Finally, rostrally positioned *Gdnf*-positive cells may undergo directed migration towards the caudal end. The proposed distinct origin of ND and MM from the anterior and posterior IM, respectively, would argue against this possibility¹⁶. However, *Slit/Robo* signalling and members of the *SoxC* class genes have been implicated in cell migration^{62,69}. Perhaps *Gdnf* restriction is a combination of several mechanisms, including cell clearance through apoptosis and directed cell migration of anteriorly positioned *Gdnf*-positive cells. A careful analysis of mouse mutants showing an expansion of the *Gdnf* expression domain, perhaps coupled with live imaging in explant cultures, may help to address this open question.

Pathways in nephric duct-specific activation

PAX2 not only is involved in the activation of *GDNF* but also is required for the expression of ND-specific genes. A key target appears to be the transcription factor GATA3, which in

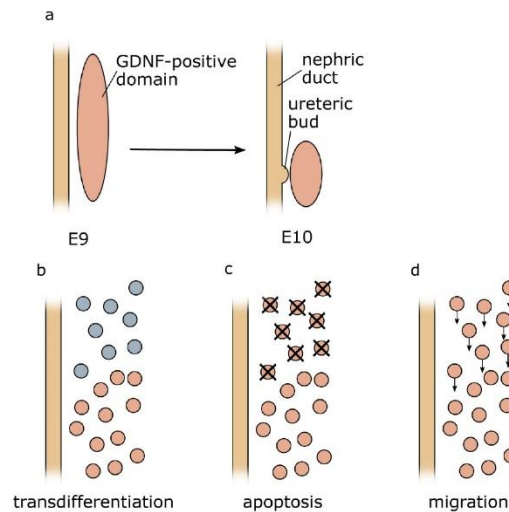


Figure 4. Possible causes of caudal *Gdnf* domain restriction. (a) At early stages during development, *Gdnf* expression can be found in rostral domains of the intermediate mesoderm but over time becomes caudally restricted. Three mechanisms could explain this observation: (b) active suppression of *Gdnf* expression in more rostral domains (c), apoptosis of *Gdnf*-expressing cells (d), or migration of the cells towards the caudal end of the intermediate mesoderm. E, embryonic day.

turn transcriptionally activates *Ret*. Tissue-specific knockout mice that lack *Gata3* within the ND show an altered response to local growth factors (GDNF and FGF) and display premature cell differentiation and differential cell adhesion properties. As a result, cells with sufficient levels of GATA3 and RET segregate from GATA3-deficient cells and expand, forming ectopic buds and kidneys⁷⁰.

Beta-catenin, a multifunctional protein involved in cell–cell adhesion and transcriptional regulation, appears to be one of the factors involved in this growth. Conditional inactivation of β -catenin in the ND leads to a range of kidney defects, including duplex kidney formation⁷¹. Molecular markers affected in these mutants were the transcription factors EMX2 and SOX9, both of which are known to be involved in ureter budding^{72,73}. However, ectopic budding was observed only in cases where loss of β -catenin expression was mosaic⁷⁴. Hypoxia-induced reduction of β -catenin has also been shown to cause duplex kidneys amongst other CAKUT phenotypes⁷⁵. Beta-catenin action during kidney induction is mediated at least partly through the transcription factor GATA3⁷⁰.

Sox17 mutations have been identified in a cohort of human patients with CAKUT, including a duplicated pyeloureteral system. The authors demonstrated that the mutation influenced protein stability and reduced β -catenin activity⁷⁶. It is therefore possible that the mutated SOX17 protein leads to lower β -catenin and, in turn, reduced GATA3 levels.

In parallel to GATA3, LHX1 (LIM1) appears to be essential in permitting normal budding⁷⁷. Tissue-specific deletion of LIM1 in ND derivatives leads to renal hypoplasia and hydronephrosis

and an impaired extension of the ND. Some conditional mutants of *Lim1* also display incomplete duplication of kidney ureters where both poles of a duplex kidney merge before entering the bladder. This form of duplex kidney was traced back to the first UB branching event, where defective UB forms a Y-shaped rather than a T-shaped structure⁹.

Restricting Ret activation

To limit ureter outgrowth to a single site, a series of negative regulators that suppress the RET signalling cascade are in place. BMP signalling, in particular, seems to be a suppressor of ureter outgrowth and branching, and heterozygous *Bmp4* mutations in mice lead to a wide range of CAKUT phenotypes, including duplex kidneys⁷⁸. BMP and FGF signalling are known antagonists in epithelial branching of the lung⁷⁹ but also kidney development⁸⁰. Since FGF and RET receptors are receptor tyrosine kinases that use similar intracellular signal transduction pathways, we can reason that the antagonistic action of BMP acts in analogous fashion on RET signalling. To permit ureter outgrowth specifically at the site of the future kidney, MM cells express the BMP inhibitor Gremlin (*Grem1*), which counteracts the BMP function⁸¹. Heterozygous *BMP4* and *GREM1* mutations have both been identified in human patients with CAKUT^{82,83}, although it is not clear whether variants in these genes also predispose to duplex kidney formation.

A number of other genes involved in duplex kidney formation appear to affect the BMP/Gremlin axis. Mutants for the intra-flagellar transport proteins IFT25 or IFT27, which are believed to increase GLI3R, a repressor of SHH signalling, show a high penetrance of duplex kidney formation (~50%)⁸⁴. Similarly, constitutive expression of a truncation mutation in *Gli3* (*Gli3* ^{Δ 699}),

which is found in Pallister–Hall syndrome and is likely to sensitise tissue for SHH signalling, causes CAKUT with duplex kidneys⁸⁵. The phenotype has been linked to an increased sensitivity of the ND by lowering BMP4 signalling.

Of interest, several genes that are implicated in the formation of cilia (for example, *Cep290*, *Dync2h1*, *Tbc1d32* and *Tmem67*) have also been implicated in duplex kidney formation⁸⁶. The primary cilia is an organelle that has a key function in cellular signalling⁸⁷, and SHH signalling, in particular, is directly linked to this organelle. Because SHH signalling has been proposed to be involved in duplex kidney formation (88 and above), it is tempting to speculate that the above cilia-related genes also influence this pathway.

In addition to extracellular modulators, cytoplasmic antagonists exist to suppress ureter outgrowth. Most notably, Sprouty (*Spry1*) suppresses MAPK signalling in the absence of GDNF, and inactivation in mice results in the formation of multiple UBs⁸⁹. Signalling through the angiotensin receptor appears to be important in suppressing *Spry1* expression⁹⁰ but also in activating *Ret* expression, and *Agtr2* knockout mice show a range of CAKUT phenotypes, including a duplex system⁹¹. To date, no pathogenetic *SPRY1* mutations have been identified in patients with CAKUT, and it is currently unclear to what extent this gene contributes to duplex kidney formation in human patients. Interestingly, in the absence of *Spry1*, GDNF signalling

is no longer required for ureter induction, and *Spry1*^{-/-}/*Gdnf*^{-/-} double knockout mice develop normal kidneys. In this context, FGF10, which normally plays only a minor role in kidney development, becomes indispensable for kidney induction, and triple mutants (*Fgf10*^{-/-}/*Spry1*^{-/-}/*Gdnf*^{-/-}) display renal agenesis⁹². FGF signalling thus can be considered a reinforcing signal that contributes to enhanced epithelial growth and budding. FGF signalling serves as the main pathway in branching morphogenesis of other organs such as the lung⁹³, and we can speculate that GDNF/RET signalling has taken over the ancestral function of FGF in epithelial branching of the kidney.

Finally, tissue-specific knockout of *Fat4* within the nephrogenic cord results in a duplex kidney phenotype that can be rescued by reducing the dose of GDNF (*Gdnf*^{fl/fl}). Recent molecular experiments demonstrated that FAT4 directly binds to RET and restricts its activity in the ND/UB by disrupting the formation of RET-GFRA1-GDNF complex^{94,95}.

There are a number of other genes which have been shown to be implicated in duplex kidney formation but for which the molecular events leading to supernumerary buds are not well defined. Because in these cases the causative nature of mutations for duplex kidney formation is less established, we refrain from a mere listing of genes at this place. The interested reader is referred to Table 1 of genes involved, the associated phenotypes and corresponding references.

Table 1. Genes involved in duplex kidney formation.

Group	Genotype	Mechanism	Reference
GDNF domain	<i>Robo2</i> ^{-/-}	Abnormal <i>Gdnf</i> expression domain MM fails to separate from WD	Grieshammer <i>et al.</i> ⁶⁴ Wainwright <i>et al.</i> ⁶³
	<i>Slit2</i> ^{-/-}	Abnormal <i>Gdnf</i> expression domain	Grieshammer <i>et al.</i> ⁶⁴
	<i>Foxc1</i> ^{-/-}	MM fails to reduce in size	Kume <i>et al.</i> ⁶⁵ Komaki <i>et al.</i> ⁹⁶
	<i>Sox11</i> ^{-/-}	MM fails to reduce in size	Neirijnck <i>et al.</i> ⁶⁶
	Increased sensitivity of WD	<i>Bmp4</i> ^{-/-}	Lack of inhibition of WNT11, a target of GDNF
<i>lft25</i> ^{-/-} , <i>lft27</i> ^{-/-}		Increased sensitivity of WD through Gremlin-BMP4 cascade	Desai <i>et al.</i> ⁸⁴
<i>Gli3</i> ^{Δ699/Δ699}		Increased sensitivity of WD through Gremlin-BMP4 cascade	Blake <i>et al.</i> ⁸⁵
<i>Agtr2</i> ^Y		Disrupted renin-angiotensin signalling leads to aberrant UB morphogenesis	Nishimura <i>et al.</i> ⁹¹ Yosypiv <i>et al.</i> ⁹⁰
<i>p53</i> ^{-/-} , <i>p53</i> ^{UB-/-}		Increased response of WD to GDNF signal. Two ureters fuse in the later development and resemble a bifurcation	Saifudeen <i>et al.</i> ⁹⁷ El-dahr <i>et al.</i> ⁹⁸
<i>Fat4</i> ^{-/-} <i>Fjx1</i> ^{-/-}		Premature branching with incomplete duplication due to overactive GDNF-RET signalling	Saburi <i>et al.</i> ⁹⁴ Zhang <i>et al.</i> ⁹⁵

Group	Genotype	Mechanism	Reference
	<i>Hoxb7-Cre</i> <i>β-catenin^{fl/c}</i>	Ectopic activation of UB branching pathway in WD	Marose <i>et al.</i> ⁷⁴
	<i>Spry1^{-/-}</i>	Increased sensitivity of WD to GDNF-RET signalling	Basson <i>et al.</i> ⁹⁹
	<i>Gata3^{ND/-}</i>	The entire length on WD is covered by ectopic UBs, most of which subsequently regress	Grote <i>et al.</i> ⁷⁰
Cell polarity defect			
	<i>T-Cre Wnt5a^{flΔ}</i>	Double UB, abnormal morphology of posterior WD, defects in IM morphogenesis	Yun <i>et al.</i> ⁹⁹
	<i>Ror2^{-/-}</i>	Similar to <i>Wnt5a</i> phenotype	Yun <i>et al.</i> ⁹⁹
Cell adhesion defect			
	<i>L1^{-Y}</i>	Either incomplete or complete duplication. Double UB on WD or accessory budding from the main ureter	Debiec <i>et al.</i> ¹⁰⁰
Unknown			
	<i>Pax2^{+/-}</i>	Premature branching with incomplete duplication, linked with inactivation of GDNF expression	Brophy <i>et al.</i> ¹⁰¹
	<i>Pax2-Cre Lim1^{ΔΔ}</i>	WD fails to extend caudally; UB is absent or Y-shaped	Pedersen <i>et al.</i> ⁹
	<i>Cc2d2a, Mks1, Cep290, Dync2h1, Tbc1d32, Tmem67</i>	Duplex kidney as a part of a ciliopathy phenotype	San agustin <i>et al.</i> ⁸⁶
	<i>Sox17^{259N/+}</i>	Duplicated pyeloureteral collecting system	Gimelli <i>et al.</i> ⁷⁶
	<i>Nfia^{-/-}</i>	Partial ureteral duplication	Lu <i>et al.</i> ¹⁰²
	<i>Adamts18^{-/-}</i>	Complete ureteral duplication, increased nephron endowment	Rutledge <i>et al.</i> ¹⁰³

Conclusions and perspectives

As we have seen, the seemingly simple event of ureteric budding is a highly complicated and stringently controlled process that employs both positive and negative feedback loops. As such, the fact that a large number of genes are involved in duplex kidney formation is not surprising, and future analyses are likely to identify many more factors involved in these abnormalities. However, the incomplete penetrance of phenotypes and the multigenic basis of this malformation make the confirmation of mutations as being disease-causing increasingly difficult. Indeed, our own unpublished data suggest that duplex kidney phenotypes can be highly genetic background-dependent, indicating the presence of modifier genes. Moreover, intergenic/regulatory mutations or epigenetic mechanisms that

affect gene expression levels rather than protein function are likely to contribute to disease. Finally, we should keep in mind that, despite a large degree of conservation, mice and humans show significant differences on a developmental and molecular level^{104–106}. Findings in knockout mice are therefore only indicative and should not be directly extrapolated to human patients. Future research should also address the disparity in the frequency of duplex kidneys occurring in men and women. In the long run, the integration of a large amount of whole genome sequencing data coupled with a better understanding of how gene regulation is achieved will be required to corroborate the involvement of genomic changes and predict the phenotypic outcome in duplex kidneys.

References



1. Queisser-Luft A, Stolz G, Wiesel A, *et al.*: **Malformations in newborn: results based on 30,940 infants and fetuses from the Mainz congenital birth defect monitoring system (1990-1998).** *Arch Gynecol Obstet.* 2002; 266(3): 163–7. [PubMed Abstract](#) | [Publisher Full Text](#)
2. Capone VP, Morello W, Taroni F, *et al.*: **Genetics of Congenital Anomalies of the Kidney and Urinary Tract: The Current State of Play.** *Int J Mol Sci.* 2017; 18(4): pii: E796. [PubMed Abstract](#) | [Publisher Full Text](#) | [Free Full Text](#) | [F1000 Recommendation](#)

3. **F** Jain S, Chen F: **Developmental pathology of congenital kidney and urinary tract anomalies.** *Clin Kidney J.* 2018; **12**(3): 382–99.
[PubMed Abstract](#) | [Publisher Full Text](#) | [Free Full Text](#) | [F1000 Recommendation](#)
4. Schedl A: **Renal abnormalities and their developmental origin.** *Nat Rev Genet.* 2007; **8**(10): 791–802.
[PubMed Abstract](#) | [Publisher Full Text](#)
5. Nicolaou N, Renkema KY, Bongers EM, et al.: **Genetic, environmental, and epigenetic factors involved in CAKUT.** *Nat Rev Nephrol.* 2015; **11**(12): 720–31.
[PubMed Abstract](#) | [Publisher Full Text](#)
6. **F** van der Ven AT, Vivante A, Hildebrandt F: **Novel Insights into the Pathogenesis of Monogenic Congenital Anomalies of the Kidney and Urinary Tract.** *J Am Soc Nephrol.* 2018; **29**(1): 36–50.
[PubMed Abstract](#) | [Publisher Full Text](#) | [Free Full Text](#) | [F1000 Recommendation](#)
7. **F** Georgas KM, Armstrong J, Keast JR, et al.: **An Illustrated anatomical ontology of the developing mouse lower urogenital tract.** *Development.* 2015; **142**(10): 1893–908.
[PubMed Abstract](#) | [Publisher Full Text](#) | [Free Full Text](#) | [F1000 Recommendation](#)
8. **F** Grote D, Souabni A, Busslinger M, et al.: **Pax 2/9-regulated Gata 3 expression is necessary for morphogenesis and guidance of the nephric duct in the developing kidney.** *Development.* 2006; **133**(1): 53–61.
[PubMed Abstract](#) | [Publisher Full Text](#) | [F1000 Recommendation](#)
9. Pedersen A, Skjong C, Shawlot W: **Lim 1 is required for nephric duct extension and ureteric bud morphogenesis.** *Dev Biol.* 2005; **288**(2): 571–81.
[PubMed Abstract](#) | [Publisher Full Text](#)
10. Attia L, Schneider J, Yelin R, et al.: **Collective cell migration of the nephric duct requires FGF signaling.** *Dev Dyn.* 2015; **244**(2): 157–67.
[PubMed Abstract](#) | [Publisher Full Text](#)
11. Walker KA, Sims-Lucas S, Di Giovanni VE, et al.: **Deletion of fibroblast growth factor receptor 2 from the peri-wolffian duct stroma leads to ureteric induction abnormalities and vesicoureteral reflux.** *PLoS One.* 2013; **8**(2): e56062.
[PubMed Abstract](#) | [Publisher Full Text](#) | [Free Full Text](#)
12. Chia I, Grote D, Marotte M, et al.: **Nephric duct insertion is a crucial step in urinary tract maturation that is regulated by a Gata3-Raldh2-Ret molecular network in mice.** *Development.* 2011; **138**(10): 2089–97.
[PubMed Abstract](#) | [Publisher Full Text](#) | [Free Full Text](#)
13. **F** Hoshi M, Reginhensi A, Joens MS, et al.: **Reciprocal Spatiotemporally Controlled Apoptosis Regulates Wolffian Duct Cloaca Fusion.** *J Am Soc Nephrol.* 2018; **29**(3): 775–783.
[PubMed Abstract](#) | [Publisher Full Text](#) | [Free Full Text](#) | [F1000 Recommendation](#)
14. Sainio K, Hellstedt P, Kreidberg JA, et al.: **Differential regulation of two sets of mesonephric tubules by WT-1.** *Development.* 1997; **124**(7): 1293–9.
[PubMed Abstract](#)
15. Mugford JW, Sipilä P, Kobayashi A, et al.: **Hoxd11 specifies a program of metanephric kidney development within the intermediate mesoderm of the mouse embryo.** *Dev Biol.* 2008; **319**(2): 396–405.
[PubMed Abstract](#) | [Publisher Full Text](#) | [Free Full Text](#)
16. **F** Taguchi A, Kaku Y, Ohmori T, et al.: **Redefining the in vivo origin of metanephric nephron progenitors enables generation of complex kidney structures from pluripotent stem cells.** *Cell Stem Cell.* 2014; **14**(1): 53–67.
[PubMed Abstract](#) | [Publisher Full Text](#) | [F1000 Recommendation](#)
17. **F** Lefevre JG, Short KM, Lamberton TO, et al.: **Branching morphogenesis in the developing kidney is governed by rules that pattern the ureteric tree.** *Development.* 2017; **144**(23): 4377–85.
[PubMed Abstract](#) | [Publisher Full Text](#) | [F1000 Recommendation](#)
18. Short KM, Combes AN, Lefevre J, et al.: **Global quantification of tissue dynamics in the developing mouse kidney.** *Dev Cell.* 2014; **29**(2): 188–202.
[PubMed Abstract](#) | [Publisher Full Text](#)
19. McMahon AP: **Development of the Mammalian Kidney.** *Curr Top Dev Biol.* 2016; **117**: 31–64.
[PubMed Abstract](#) | [Publisher Full Text](#) | [Free Full Text](#)
20. **F** O'Brien LL: **Nephron progenitor cell commitment: Striking the right balance.** *Semin Cell Dev Biol.* 2019; **91**: 94–103.
[PubMed Abstract](#) | [Publisher Full Text](#) | [F1000 Recommendation](#)
21. **F** Kurtzeborn K, Cebrian C, Kuure S: **Regulation of Renal Differentiation by Trophic Factors.** *Front Physiol.* 2018; **9**: 1588.
[PubMed Abstract](#) | [Publisher Full Text](#) | [Free Full Text](#) | [F1000 Recommendation](#)
22. **F** Oxburgh L: **Kidney Nephron Determination.** *Annu Rev Cell Dev Biol.* 2018; **34**: 427–50.
[PubMed Abstract](#) | [Publisher Full Text](#) | [F1000 Recommendation](#)
23. Huang YC, Chen F, Li X: **Clarification of mammalian cloacal morphogenesis using high-resolution episcopic microscopy.** *Dev Biol.* 2016; **409**(1): 106–13.
[PubMed Abstract](#) | [Publisher Full Text](#) | [Free Full Text](#)
24. Matsumaru D, Murashima A, Fukushima J, et al.: **Systematic stereoscopic analyses for cloacal development: The origin of anorectal malformations.** *Sci Rep.* 2015; **5**: 13943.
[PubMed Abstract](#) | [Publisher Full Text](#) | [Free Full Text](#)
25. **F** Kruepunga N, Hiksloops JPM, Mekonen HK, et al.: **The development of the cloaca in the human embryo.** *J Anat.* 2018; **233**(6): 724–39.
[PubMed Abstract](#) | [Publisher Full Text](#) | [Free Full Text](#) | [F1000 Recommendation](#)
26. **F** Liaw A, Cunha GR, Shen J, et al.: **Development of the human bladder and ureterovesical junction.** *Differentiation.* 2018; **103**: 66–73.
[PubMed Abstract](#) | [Publisher Full Text](#) | [F1000 Recommendation](#)
27. Glassberg KI, Braren V, Duckett JW, et al.: **Suggested Terminology for Duplex Systems, Ectopic Ureters and Ureterocele.** *J Urol.* 1984; **132**(6): 1153–4.
[PubMed Abstract](#) | [Publisher Full Text](#)
28. Zissin R, Apter S, Yaffe D, et al.: **Renal duplication with associated complications in adults: CT findings in 26 cases.** *Clin Radiol.* 2001; **56**(1): 58–63.
[PubMed Abstract](#) | [Publisher Full Text](#)
29. Weigert C: **Ueber einige Bildungsfehler der Ureteren.** *Virchows Arch.* 1877; **70**(4): 490–501.
[Publisher Full Text](#)
30. Britt DB, Borden TA, Woodhead DM: **Inverted Y Ureteral Duplication with a Blind-Ending Branch.** *J Urol.* 1972; **108**(3): 387–8.
[PubMed Abstract](#) | [Publisher Full Text](#)
31. Akbulut F, Savun M, Ucpinar B, et al.: **Duplicated Renal System with H Shaped Ureter: An Extraordinary Anomaly.** *Case Rep Urol.* 2016; **2016**: 4062515.
[PubMed Abstract](#) | [Publisher Full Text](#) | [Free Full Text](#)
32. Begg RC: **Sextuplitas Renum: A Case of Six Functioning Kidneys and Ureters in an Adult Female.** *J Urol.* 1953; **70**(5): 686–93.
[PubMed Abstract](#) | [Publisher Full Text](#)
33. Senel U, Tanriverdi HI, Ozmen Z, et al.: **Ectopic Ureter Accompanied by Duplicated Ureter: Three Cases.** *J Clin Diagn Res.* 2015; **9**(9): PD10–2.
[PubMed Abstract](#) | [Publisher Full Text](#) | [Free Full Text](#)
34. Lopes RI, Lopes RN, Filho CMB: **Ureteral quadruplication with contralateral triplicate ureter.** *J Urol.* 2001; **166**(3): 979–80.
[PubMed Abstract](#) | [Publisher Full Text](#)
35. Kudela G, Koszutski T, Mikosinski M, et al.: **Ureteral triplication—report of four cases.** *Eur J Pediatr Surg.* 2006; **16**(4): 279–81.
[PubMed Abstract](#) | [Publisher Full Text](#)
36. Bolker M, Moskovitz B, Ginesin Y, et al.: **Incomplete quadruplication of urinary tract with contralateral agenesis of the kidney.** *Eur Urol.* 1991; **19**(3): 267–8.
[PubMed Abstract](#) | [Publisher Full Text](#)
37. Jurkiewicz B, Zabkowski T, Shevchuk D: **Ureteral quintuplication with renal atrophy in an infant after the 1986 Chernobyl nuclear disaster.** *Urology.* 2014; **83**(1): 211–3.
[PubMed Abstract](#) | [Publisher Full Text](#)
38. Privett JTJ, Jeans WD, Roylance J: **The incidence and importance of renal duplication.** *Clin Radiol.* 1976; **27**(4): 521–30.
[PubMed Abstract](#) | [Publisher Full Text](#)
39. **F** Batourina E, Chol C, Paragas N, et al.: **Distal ureter morphogenesis depends on epithelial cell remodeling mediated by vitamin A and Ret.** *Nat Genet.* 2002; **32**(1): 109–15.
[PubMed Abstract](#) | [Publisher Full Text](#) | [F1000 Recommendation](#)
40. **F** Uetani N, Bertozzi K, Chagnon MJ, et al.: **Maturation of ureter-bladder connection in mice is controlled by LAR family receptor protein tyrosine phosphatases.** *J Clin Invest.* 2009; **119**(4): 924–35.
[PubMed Abstract](#) | [Publisher Full Text](#) | [Free Full Text](#) | [F1000 Recommendation](#)
41. **F** Batourina E, Tsai S, Lambert S, et al.: **Apoptosis induced by vitamin A signaling is crucial for connecting the ureters to the bladder.** *Nat Genet.* 2005; **37**(10): 1082–9.
[PubMed Abstract](#) | [Publisher Full Text](#) | [F1000 Recommendation](#)
42. Mackie GG, Stephens FD: **Duplex kidneys: a correlation of renal dysplasia with position of the ureteral orifice.** *J Urol.* 1975; **114**(2): 274–80.
[PubMed Abstract](#) | [Publisher Full Text](#)
43. Doery AJ, Ang E, Ditchfield MR: **Duplex kidney: not just a drooping lilly.** *J Med Imaging Radiat Oncol.* 2015; **59**(2): 149–53.
[PubMed Abstract](#) | [Publisher Full Text](#)
44. **F** Didier RA, Chow JS, Kwatra NS, et al.: **The duplicated collecting system of the urinary tract: embryology, imaging appearances and clinical considerations.** *Pediatr Radiol.* 2017; **47**(11): 1526–38.
[PubMed Abstract](#) | [Publisher Full Text](#) | [F1000 Recommendation](#)
45. Davis TK, Hoshi M, Jain S: **To bud or not to bud: the RET perspective in CAKUT.** *Pediatr Nephrol.* 2014; **29**(4): 597–608.
[PubMed Abstract](#) | [Publisher Full Text](#) | [Free Full Text](#)
46. Schuchardt A, D'Agati V, Larsson-Blomberg L, et al.: **Defects in the kidney and enteric nervous system of mice lacking the tyrosine kinase receptor Ret.** *Nature.* 1994; **367**(6461): 380–3.
[PubMed Abstract](#) | [Publisher Full Text](#)
47. Sánchez MP, Silos-Santiago I, Frisén J, et al.: **Renal agenesis and the absence of enteric neurons in mice lacking GDNF.** *Nature.* 1996; **382**(6586): 70–3.
[PubMed Abstract](#) | [Publisher Full Text](#)
48. Pichel JG, Shen L, Sheng HZ, et al.: **Defects in enteric innervation and kidney development in mice lacking GDNF.** *Nature.* 1996; **382**(6586): 73–6.
[PubMed Abstract](#) | [Publisher Full Text](#)
49. Moore MW, Klein RD, Fariñas I, et al.: **Renal and neuronal abnormalities in mice lacking GDNF.** *Nature.* 1996; **382**(6586): 76–9.
[PubMed Abstract](#) | [Publisher Full Text](#)

50. Cacalano G, Fariñas I, Wang LC, *et al.*: **GFRalpha1 is an essential receptor component for GDNF in the developing nervous system and kidney.** *Neuron*. 1998; 21(1): 53–62.
[PubMed Abstract](#) | [Publisher Full Text](#) | [Free Full Text](#)
51. Willecke R, Heuberger J, Grossmann K, *et al.*: **The tyrosine phosphatase Shp2 acts downstream of GDNF/Ret in branching morphogenesis of the developing mouse kidney.** *Dev Biol*. 2011; 360(2): 310–7.
[PubMed Abstract](#) | [Publisher Full Text](#)
52. Perrinquet M, Vilar M, Ibáñez CF: **Protein-tyrosine phosphatase SHP2 contributes to GDNF neurotrophic activity through direct binding to phospho-Tyr⁶⁸⁷ in the RET receptor tyrosine kinase.** *J Biol Chem*. 2010; 285(41): 31867–75.
[PubMed Abstract](#) | [Publisher Full Text](#) | [Free Full Text](#)
53. Takahashi M: **The GDNF/RET signaling pathway and human diseases.** *Cytokine Growth Factor Rev*. 2001; 12(4): 361–73.
[PubMed Abstract](#) | [Publisher Full Text](#)
54. Lu BC, Cebrían C, Chi X, *et al.*: **Etv4 and Etv5 are required downstream of GDNF and Ret for kidney branching morphogenesis.** *Nat Genet*. 2009; 41(12): 1295–302.
[PubMed Abstract](#) | [Publisher Full Text](#) | [Free Full Text](#) | [F1000 Recommendation](#)
55. Ihermann-Hella A, Lume M, Miinalainen J, *et al.*: **Mitogen-activated protein kinase (MAPK) pathway regulates branching by remodeling epithelial cell adhesion.** *PLoS Genet*. 2014; 10(3): e1004193.
[PubMed Abstract](#) | [Publisher Full Text](#) | [Free Full Text](#)
56. Chi X, Michos O, Shakya R, *et al.*: **Ret-dependent cell rearrangements in the Wolffian duct epithelium initiate ureteric bud morphogenesis.** *Dev Cell*. 2009; 17(2): 199–209.
[PubMed Abstract](#) | [Publisher Full Text](#) | [Free Full Text](#) | [F1000 Recommendation](#)
57. Torres M, Gómez-Pardo E, Dressler GR, *et al.*: **Pax-2 controls multiple steps of urogenital development.** *Development*. 1995; 121(12): 4057–65.
[PubMed Abstract](#)
58. Kiefer SM, Robbins L, Stumpff KM, *et al.*: **Sall1-dependent signals affect Wnt signaling and ureter tip fate to initiate kidney development.** *Development*. 2010; 137(18): 3099–106.
[PubMed Abstract](#) | [Publisher Full Text](#) | [Free Full Text](#)
59. Xu PX, Adams J, Peters H, *et al.*: **Eya1-deficient mice lack ears and kidneys and show abnormal apoptosis of organ primordia.** *Nat Genet*. 1999; 23(1): 113–7.
[PubMed Abstract](#) | [Publisher Full Text](#)
60. Hwang DY, Dworschak GC, Kohl S, *et al.*: **Mutations in 12 known dominant disease-causing genes clarify many congenital anomalies of the kidney and urinary tract.** *Kidney Int*. 2014; 85(6): 1429–33.
[PubMed Abstract](#) | [Publisher Full Text](#) | [Free Full Text](#)
61. Li H, Jakobson M, Ola R, *et al.*: **Development of the urogenital system is regulated via the 3'UTR of GDNF.** *Sci Rep*. 2019; 9(1): 5302.
[PubMed Abstract](#) | [Publisher Full Text](#) | [Free Full Text](#) | [F1000 Recommendation](#)
62. Blockus H, Chédotal A: **Slit-Robo signaling.** *Development*. 2016; 143(17): 3037–44.
[PubMed Abstract](#) | [Publisher Full Text](#)
63. Wainwright EN, Wilhelm D, Combes AN, *et al.*: **ROBO2 restricts the nephrogenic field and regulates Wolffian duct-nephrogenic cord separation.** *Dev Biol*. 2015; 404(2): 88–102.
[PubMed Abstract](#) | [Publisher Full Text](#)
64. Grieshammer U, Le Ma, Plump AS, *et al.*: **SLIT2-mediated ROBO2 signaling restricts kidney induction to a single site.** *Dev Cell*. 2004; 6(5): 709–17.
[PubMed Abstract](#) | [Publisher Full Text](#)
65. Kume T, Deng K, Hogan BL: **Murine forkhead/winged helix genes Foxc1 (Mf1) and Foxc2 (Mfh1) are required for the early organogenesis of the kidney and urinary tract.** *Development*. 2000; 127(7): 1387–95.
[PubMed Abstract](#)
66. Neirijnck Y, Reginensi A, Renkema KY, *et al.*: **Sox11 gene disruption causes congenital anomalies of the kidney and urinary tract (CAKUT).** *Kidney Int*. 2018; 93(5): 1142–53.
[PubMed Abstract](#) | [Publisher Full Text](#)
67. Lu W, van Eerde AM, Fan X, *et al.*: **Disruption of ROBO2 is associated with urinary tract anomalies and confers risk of vesicoureteral reflux.** *Am J Hum Genet*. 2007; 80(4): 616–32.
[PubMed Abstract](#) | [Publisher Full Text](#) | [Free Full Text](#)
68. Hwang DY, Kohl S, Fan X, *et al.*: **Mutations of the SLIT2-ROBO2 pathway genes SLIT2 and SRGAP1 confer risk for congenital anomalies of the kidney and urinary tract.** *Hum Genet*. 2015; 134(8): 905–16.
[PubMed Abstract](#) | [Publisher Full Text](#) | [Free Full Text](#)
69. Cheng Q, Wu J, Zhang Y, *et al.*: **SOX4 promotes melanoma cell migration and invasion through the activation of the NF- κ B signaling pathway.** *Int J Mol Med*. 2017; 40(2): 447–53.
[PubMed Abstract](#) | [Publisher Full Text](#) | [Free Full Text](#) | [F1000 Recommendation](#)
70. Grole D, Bouallia SK, Souabni A, *et al.*: **Gata3 acts downstream of beta-catenin signaling to prevent ectopic metanephric kidney induction.** *PLoS Genet*. 2008; 4(12): e1000316.
[PubMed Abstract](#) | [Publisher Full Text](#) | [Free Full Text](#)
71. Bridgewater D, Cox B, Cain J, *et al.*: **Canonical WNT/beta-catenin signaling is required for ureteric branching.** *Dev Biol*. 2008; 317(1): 83–94.
[PubMed Abstract](#) | [Publisher Full Text](#)
72. Miyamoto N, Yoshida M, Kuratani S, *et al.*: **Defects of urogenital development in mice lacking Emx2.** *Development*. 1997; 124(9): 1653–64.
[PubMed Abstract](#)
73. Reginensi A, Clarkson M, Neirijnck Y, *et al.*: **SOX9 controls epithelial branching by activating RET effector genes during kidney development.** *Hum Mol Genet*. 2011; 20(6): 1143–53.
[PubMed Abstract](#) | [Publisher Full Text](#) | [Free Full Text](#) | [F1000 Recommendation](#)
74. Marose TD, Merkel CE, McMahon AP, *et al.*: **Beta-catenin is necessary to keep cells of ureteric bud/Wolffian duct epithelium in a precursor state.** *Dev Biol*. 2008; 314(1): 112–26.
[PubMed Abstract](#) | [Publisher Full Text](#) | [Free Full Text](#)
75. Wilkinson LJ, Neal CS, Singh RR, *et al.*: **Renal developmental defects resulting from in utero hypoxia are associated with suppression of ureteric β -catenin signaling.** *Kidney Int*. 2015; 87(5): 975–83.
[PubMed Abstract](#) | [Publisher Full Text](#)
76. Gimelli S, Caridi G, Beri S, *et al.*: **Mutations in SOX17 are associated with congenital anomalies of the kidney and the urinary tract.** *Hum Mutat*. 2010; 31(12): 1352–9.
[PubMed Abstract](#) | [Publisher Full Text](#) | [Free Full Text](#)
77. Kobayashi A, Kwan KM, Carroll TJ, *et al.*: **Distinct and sequential tissue-specific activities of the LIM-class homeobox gene *Lim1* for tubular morphogenesis during kidney development.** *Development*. 2005; 132(12): 2809–23.
[PubMed Abstract](#) | [Publisher Full Text](#) | [F1000 Recommendation](#)
78. Miyazaki Y, Oshima K, Fogo A, *et al.*: **Bone morphogenetic protein 4 regulates the budding site and elongation of the mouse ureter.** *J Clin Invest*. 2000; 105(7): 863–73.
[PubMed Abstract](#) | [Publisher Full Text](#) | [Free Full Text](#)
79. Weaver M, Dunn NR, Hogan BL: **Bmp4 and Fgf10 play opposing roles during lung bud morphogenesis.** *Development*. 2000; 127(12): 2695–704.
[PubMed Abstract](#)
80. Motamedi FJ, Badro DA, Clarkson M, *et al.*: **WT1 controls antagonistic FGF and BMP-pSMAD pathways in early renal progenitors.** *Nat Commun*. 2014; 5: 4444.
[PubMed Abstract](#) | [Publisher Full Text](#)
81. Michos O, Gonçalves A, Lopez-Rilos J, *et al.*: **Reduction of BMP4 activity by gremlin 1 enables ureteric bud outgrowth and GDNF/WNT11 feedback signalling during kidney branching morphogenesis.** *Development*. 2007; 134(13): 2397–405.
[PubMed Abstract](#) | [Publisher Full Text](#)
82. Weber S, Taylor JC, Winyard P, *et al.*: **SIX2 and BMP4 Mutations Associate With Anomalous Kidney Development.** *J Am Soc Nephrol*. 2008; 19(5): 891–903.
[PubMed Abstract](#) | [Publisher Full Text](#) | [Free Full Text](#)
83. van Eerde AM, Duran K, van Riel E, *et al.*: **Genes in the Ureteric Budding Pathway: Association Study on Vesico-Ureteral Reflux Patients.** *PLoS One*. 2012; 7(4): e31327.
[PubMed Abstract](#) | [Publisher Full Text](#) | [Free Full Text](#)
84. Desai PB, San Agustín JT, Stuck MW, *et al.*: **Itf25 is not a cystic kidney disease gene but is required for early steps of kidney development.** *Mech Dev*. 2018; 151: 10–7.
[PubMed Abstract](#) | [Publisher Full Text](#) | [Free Full Text](#) | [F1000 Recommendation](#)
85. Blake J, Di Hu, Cain JE, *et al.*: **Urogenital development in Pallister-Hall syndrome is disrupted in a cell-lineage-specific manner by constitutive expression of GLI3 repressor.** *Hum Mol Genet*. 2016; 25(3): 437–47.
[PubMed Abstract](#) | [Publisher Full Text](#) | [Free Full Text](#) | [F1000 Recommendation](#)
86. San Agustín JT, Klona N, Granath K, *et al.*: **Genetic link between renal birth defects and congenital heart disease.** *Nat Commun*. 2016; 7: 11103.
[PubMed Abstract](#) | [Publisher Full Text](#) | [Free Full Text](#) | [F1000 Recommendation](#)
87. Elliott KH, Bruggmann SA: **Sending mixed signals: Cilia-dependent signaling during development and disease.** *Dev Biol*. 2019; 447(1): 28–41.
[PubMed Abstract](#) | [Publisher Full Text](#) | [Free Full Text](#)
88. Weber S, Landwehr C, Renkert M, *et al.*: **Mapping candidate regions and genes for congenital anomalies of the kidneys and urinary tract (CAKUT) by array-based comparative genomic hybridization.** *Nephrol Dial Transplant*. 2011; 26(1): 136–43.
[PubMed Abstract](#) | [Publisher Full Text](#)
89. Basson MA, Akbulut S, Watson-Johnson J, *et al.*: **Sprouty1 is a Critical Regulator of GDNF/RET-Mediated Kidney Induction.** *Dev Cell*. 2005; 8(2): 229–39.
[PubMed Abstract](#) | [Publisher Full Text](#) | [F1000 Recommendation](#)
90. Yosypiv IV, Boh MK, Spera MA, *et al.*: **Downregulation of Spry-1, an inhibitor of GDNF/Ret, causes angiotensin II-induced ureteric bud branching.** *Kidney Int*. 2008; 74(10): 1287–93.
[PubMed Abstract](#) | [Publisher Full Text](#) | [Free Full Text](#)
91. Nishimura H, Yerkes E, Hohenfellner K, *et al.*: **Role of the Angiotensin Type 2 Receptor Gene in Congenital Anomalies of the Kidney and Urinary Tract, CAKUT, of Mice and Men.** *Mol Cell*. 1999; 3(1): 1–10.
[PubMed Abstract](#) | [Publisher Full Text](#)
92. Michos O, Cebrían C, Hyink D, *et al.*: **Kidney development in the absence of *Gdnf* and *Spry1* requires *Fgf10*.** *PLoS Genet*. 2010; 6(1): e1000809.
[PubMed Abstract](#) | [Publisher Full Text](#) | [Free Full Text](#) | [F1000 Recommendation](#)
93. Morrisey EE, Hogan BLM: **Preparing for the First Breath: Genetic and Cellular Mechanisms in Lung Development.** *Dev Cell*. 2010; 18(1): 8–23.
[PubMed Abstract](#) | [Publisher Full Text](#) | [Free Full Text](#)

94. **F** Saburi S, Hester I, Fischer E, *et al.*: **Loss of Fat4 disrupts PCP signaling and oriented cell division and leads to cystic kidney disease.** *Nat Genet.* 2008; **40**(8): 1010–5.
[PubMed Abstract](#) | [Publisher Full Text](#) | [F1000 Recommendation](#)
95. **F** Zhang H, Bagherie-Lachidan M, Badouel C, *et al.*: **FAT4 Fine-Tunes Kidney Development by Regulating RET Signaling.** *Dev Cell.* 2019; **48**(6): 780–792.e4.
[PubMed Abstract](#) | [Publisher Full Text](#) | [Free Full Text](#) | [F1000 Recommendation](#)
96. Komaki F, Miyazaki Y, Niimura F, *et al.*: **Foxc1 gene null mutation causes ectopic budding and kidney hypoplasia but not dysplasia.** *Cells Tissues Organs.* 2013; **198**(1): 22–7.
[PubMed Abstract](#) | [Publisher Full Text](#)
97. Saifudeen Z, Dipp S, Stefkova J, *et al.*: **p53 regulates metanephric development.** *J Am Soc Nephrol.* 2009; **20**(11): 2328–37.
[PubMed Abstract](#) | [Publisher Full Text](#) | [Free Full Text](#)
98. El-Dahr S, Hilliard S, Aboudehen K, *et al.*: **The MDM2-p53 pathway: Multiple roles in kidney development.** *Pediatr Nephrol.* 2014; **29**(4): 621–7.
[PubMed Abstract](#) | [Publisher Full Text](#) | [Free Full Text](#)
99. Yun K, Ajima R, Sharma N, *et al.*: **Non-canonical Wnt5a/Ror2 signaling regulates kidney morphogenesis by controlling intermediate mesoderm extension.** *Hum Mol Genet.* 2014; **23**(25): 6807–14.
[PubMed Abstract](#) | [Publisher Full Text](#) | [Free Full Text](#)
100. Debiec H, Kutsche M, Schachner M, *et al.*: **Abnormal renal phenotype in L1 knockout mice: A novel cause of CAKUT.** *Nephrol Dial Transplant.* 2002; **17** Suppl 9: 42–4.
[PubMed Abstract](#) | [Publisher Full Text](#)
101. **F** Brophy PD, Ostrom L, Lang KM, *et al.*: **Regulation of ureteric bud outgrowth by Pax2-dependent activation of the glial derived neurotrophic factor gene.** *Development.* 2001; **128**(23): 4747–56.
[PubMed Abstract](#) | [F1000 Recommendation](#)
102. Lu W, Quintero-Rivera F, Fan Y, *et al.*: **NFIA haploinsufficiency is associated with a CNS malformation syndrome and urinary tract defects.** *PLoS Genet.* 2007; **3**(5): e80.
[PubMed Abstract](#) | [Publisher Full Text](#) | [Free Full Text](#)
103. **F** Rutledge EA, Parvez RK, Short KM, *et al.*: **Morphogenesis of the kidney and lung requires branch-tip directed activity of the Adamts18 metalloprotease.** *Dev Biol.* 2019; **454**(2): 156–69.
[PubMed Abstract](#) | [Publisher Full Text](#) | [Free Full Text](#) | [F1000 Recommendation](#)
104. **F** Lindström NO, Guo J, Kim AD, *et al.*: **Conserved and Divergent Features of Mesenchymal Progenitor Cell Types within the Cortical Nephrogenic Niche of the Human and Mouse Kidney.** *J Am Soc Nephrol.* 2018; **29**(3): 806–824.
[PubMed Abstract](#) | [Publisher Full Text](#) | [Free Full Text](#) | [F1000 Recommendation](#)
105. **F** Lindström NO, McMahon JA, Guo J, *et al.*: **Conserved and Divergent Features of Human and Mouse Kidney Organogenesis.** *J Am Soc Nephrol.* 2018; **29**(3): 785–805.
[PubMed Abstract](#) | [Publisher Full Text](#) | [Free Full Text](#) | [F1000 Recommendation](#)
106. **F** Lindström NO, Tran T, Guo J, *et al.*: **Conserved and Divergent Molecular and Anatomic Features of Human and Mouse Nephron Patterning.** *J Am Soc Nephrol.* 2018; **29**(3): 825–840.
[PubMed Abstract](#) | [Publisher Full Text](#) | [Free Full Text](#) | [F1000 Recommendation](#)

Open Peer Review

Current Peer Review Status:  

Editorial Note on the Review Process

F1000 Faculty Reviews are written by members of the prestigious F1000 Faculty. They are commissioned and are peer reviewed before publication to ensure that the final, published version is comprehensive and accessible. The reviewers who approved the final version are listed with their names and affiliations.

The reviewers who approved this article are:

Version 1

- Satu Kuure**
Helsinki Institute of Life Science / STEMM Research Program, Faculty of Medicine, University of Helsinki, Helsinki, Finland
Competing Interests: No competing interests were disclosed.
- Norman D Rosenblum**
Department of Paediatrics, The Hospital for Sick Children, Toronto, Canada
Competing Interests: No competing interests were disclosed.

The benefits of publishing with F1000Research:

- Your article is published within days, with no editorial bias
- You can publish traditional articles, null/negative results, case reports, data notes and more
- The peer review process is transparent and collaborative
- Your article is indexed in PubMed after passing peer review
- Dedicated customer support at every stage

For pre-submission enquiries, contact research@f1000.com

F1000Research

Aims of the project

As outlined above, SOX transcription factors are a protein family highly important in the process of development of multiple organs. One of the most striking phenotypes of *Sox11*^{-/-} embryos is the duplication of their collecting system. Importantly, only one ectopic UB is formed, which sets this phenotype apart from many other multiplex kidney mutations, indicating it occurs through a separate molecular mechanism. Previous analysis in our laboratory demonstrated a rostral extension of *Gdnf* expression domain. I employed a variety of microscopic methods to study this phenotype *in vivo* and uncover a mechanism leading to its emergence. As *Sox11* variants were identified in a cohort of human CAKUT patients, elucidating the cause for this phenotype is important for finding avenues to prevent developmental abnormalities.

A second goal of this project was to examine the role of *SoxC* genes (*Sox4*, *Sox11*, *Sox12*) in the nephrogenesis. *SoxC* mutant embryos were found to exhibit anomalies in their nephron patterning, such as shortened Henle's loops. To gain insight into the function of *SoxC* genes in nephrogenesis, I focused on the *in vitro* approach using nephron progenitor cells isolated from *SoxC* conditional knockout mouse embryos. After conditional deletion of *SoxC* using Cre-Lox recombination, I induced the cells to undergo mesenchymal-to-epithelial transition. I performed molecular analysis to uncover the changes in cellular differentiation brought by the absence of *SoxC*, which allowed me to propose a model for their action in nephrogenesis.

Results and Discussion

Role of *Sox11* in CAKUT

Article 2: Sox11 gene disruption causes congenital anomalies of the kidney and urinary tract (CAKUT)

Sox11 gene disruption causes congenital anomalies of the kidney and urinary tract (CAKUT)



Yasmine Neirijnck^{1,10}, Antoine Reginensi^{1,10}, Kirsten Y. Renkema², Filippo Massa¹, Vladimir M. Kozlov¹, Haroun Dhib¹, Ernie M.H.F. Bongers³, Wout F. Feitz⁴, Albertien M. van Eerde², Veronique Lefebvre⁵, Nine V.A.M. Knoers², Mansoureh Tabatabaei⁶, Herbert Schulz⁷, Helen McNeill⁸, Franz Schaefer⁶, Michael Wegner⁹, Elisabeth Sock⁹ and Andreas Schedl¹

¹Université Nice Sophia Antipolis, Inserm, CNRS, iBV, Nice, France; ²Department of Genetics, Center for Molecular Medicine, University Medical Center Utrecht, Utrecht, The Netherlands; ³Department of Human Genetics, Radboud University Medical Center, Nijmegen, The Netherlands; ⁴Department of Urology, Radboudumc Amalia Children's Hospital, Radboud University Medical Center, Nijmegen, The Netherlands; ⁵Department of Cellular and Molecular Medicine, Cleveland Clinic–Lerner Research Institute, Cleveland, Ohio, USA; ⁶Division of Pediatric Nephrology, Heidelberg University Center for Pediatrics and Adolescent Medicine, Heidelberg, Germany; ⁷University of Cologne, Cologne Center for Genomics, Cologne, Germany; ⁸Lunenfeld-Tanenbaum Research Institute, Mount Sinai Hospital, Toronto, Ontario, Canada; and ⁹Institute of Biochemistry, Friedrich-Alexander University Erlangen-Nürnberg, Germany

Congenital abnormalities of the kidney and the urinary tract (CAKUT) belong to the most common birth defects in human, but the molecular basis for the majority of CAKUT patients remains unknown. Here we show that the transcription factor SOX11 is a crucial regulator of kidney development. SOX11 is expressed in both mesenchymal and epithelial components of the early kidney anlagen. Deletion of Sox11 in mice causes an extension of the domain expressing Gdnf within rostral regions of the nephrogenic cord and results in duplex kidney formation. On the molecular level SOX11 directly binds and regulates a locus control region of the protocadherin B cluster. At later stages of kidney development, SOX11 becomes restricted to the intermediate segment of the developing nephron where it is required for the elongation of Henle's loop. Finally, mutation analysis in a cohort of patients suffering from CAKUT identified a series of rare SOX11 variants, one of which interferes with the transactivation capacity of the SOX11 protein. Taken together these data demonstrate a key role for SOX11 in normal kidney development and may suggest that variants in this gene predispose to CAKUT in humans.

Kidney International (2018) **93**, 1142–1153; <https://doi.org/10.1016/j.kint.2017.11.026>

KEYWORDS: CAKUT; duplex kidneys; kidney induction; nephron; Sox11
Copyright © 2017, International Society of Nephrology. Published by Elsevier Inc. All rights reserved.

Correspondence: Andreas Schedl, Inserm UMR1091, Centre de Biochimie, Parc Valrose, 06108 Nice, France. E-mail: Schedl@unice.fr

¹⁰YN and AR contributed equally to this work.

Received 3 February 2017; revised 26 November 2017; accepted 20 November 2017; published online 17 February 2018

With an incidence of 1 in 500, congenital abnormalities of the kidney and urinary tract (CAKUT) belong to the most common defects in the unborn child. CAKUT unites a diverse group of disease entities including renal agenesis, hypoplasia and dysplasia, as well as defects affecting the ureter.¹ Despite its importance as the major cause of renal failure in children, the molecular basis of CAKUT is unknown in as many as 80% of cases.²

CAKUT is rooted in defective kidney development. In the mouse embryo, metanephric development commences at around embryonic day (E)10 with the specification of the metanephric mesenchyme (MM) at the caudal end of the nephrogenic cord.³ MM cells release the glial-derived neurotrophic factor (GDNF), which serves as an inductive signal that initiates ureteric budding from the Wolffian duct. At the molecular level, GDNF binds at the surface of Wolffian duct cells to its tyrosine kinase receptor RET and induces ureteric bud (UB) growth and branching.⁴ The UB subsequently invades the MM to undergo a series of dichotomous branching events giving rise to the ureteric tree. Induction of the UB outgrowth must be tightly controlled, as failure of UB induction leads to renal agenesis.⁵ Conversely, ectopic signaling causes supernumerary UBs that can lead to duplex kidneys, a condition that is frequently associated with hydronephrosis and hydroureter.^{6,7}

Signals released from the ureter induce mesenchymal cells to epithelialize through the mesenchymal to epithelial transition,⁸ and the resulting renal vesicle undergoes further patterning events and morphogenetic movements to form the differentiated nephron, the functional unit of the kidney. Nephrons are highly segmented, with the glomerulus, proximal tubule, Henle's loop, and distal tubule serving distinct functions and expressing a specific set of marker genes.

The Sox family comprises 20 genes that encode transcription factors involved in a diverse range of developmental and pathologic processes.⁹ Based on the phylogenetic homology of their HMG box DNA-binding domain, Sox genes are categorized into 8 groups.¹⁰ We previously reported

an important function of *Sox8* and *Sox9* in kidney development¹¹ and renal repair.¹² Members of the *SoxC* group, *Sox4*, *Sox11*, and *Sox12*, are also expressed in kidney development, and *Sox4* has been suggested to play a role in nephron endowment.¹³ *Sox11* knockout analysis has revealed its requirement for the development of a variety of organs,^{14,15} but potential involvement of this gene in kidney development has not yet been reported.

Here we show that SOX11 fulfills essential regulatory functions during early kidney induction, as well as nephron maturation in mice. Moreover, the identification and characterization of rare human SOX11 gene variants in CAKUT patients further suggest that this gene may also contribute to human kidney disease.

RESULTS

SOX11 is required for normal development of the urogenital tract

Although previous studies have already reported *Sox11* to be expressed in kidney development,^{13,14,16} a detailed analysis, in particular at early stages of kidney induction, has been missing. Immunostaining at E11 revealed relatively broad SOX11 expression in the mesenchyme of the nephrogenic cord, the UB, and the Wolffian duct (Figure 1a and Supplementary Figure S1). At later stages, SOX11 expression was maintained in the epithelial and mesenchymal compartments (ureter, UB, and cap mesenchyme, respectively) of the developing kidney (Figure 1a), but was absent in FoxD1-positive stromal cells (Figure 1b). Upon mesenchymal to epithelial transition, robust staining was observed throughout the newly formed renal vesicle, which, by the S-shaped body stage, was strongest within the intermediate segment (future Henle's loop) (Figure 1c). Upon differentiation, expression persisted at low levels in elongating nephron tubules (Figure 1a, right panel), but no signal was detected in fully differentiated cells or adult kidneys (Figure 1d). Similar to kidney development, *Sox11* was found broadly expressed at early stages (E12.5) of urethra development, but was no longer detectable from E14.5 onward (Figure 1e and data not shown).

To analyze a potential role of SOX11 in urogenital development, we used a previously reported knockout allele that in the homozygous state results in perinatal death due to heart failure.¹⁴ Analysis of dissected urinary tracts in E18.5 embryos revealed a range of defects including unilateral and bilateral duplex kidneys, hydronephrosis, hydroureter, and abnormally positioned ureters (Figure 2, Table 1, and data not shown). Interestingly, duplex kidneys were also seen in a small proportion of heterozygous mutants (5.1%), indicating *Sox11* haploinsufficiency (Figure 2b, e, i and Table 1). Histologic analysis revealed that duplex kidneys were associated with an ectopic ureter that connects to the bladder in a position caudal to that of the normal site (Figure 2h). In addition to kidney and ureter defects, a proportion of *Sox11* null mutants also displayed genital tract defects, including misplaced ovaries and undescended testes (Supplementary Figure S2).

When present, these defects were always found in association with duplex kidneys, suggesting that the abnormal position of the gonads might be linked to renal abnormalities.

Sox11 restricts ureter budding to a single site

The occurrence of duplex kidneys in *Sox11* mutants suggested an early developmental defect. Indeed, dissection of kidney rudiments at E11.5 revealed 2 UBs that, when cultured, developed into 2 kidneys (Supplementary Figure S3). Ureteric budding is primarily regulated by GDNF/Ret signaling.³ To test whether ectopic budding may be caused by a disruption of this signaling pathway, we performed quantitative polymerase chain reaction (PCR) and whole-mount *in situ* hybridization (ISH) analysis on E10.5 and 11.5 embryos. qPCR analysis of *Ret* and *Gdnf* expression did not reveal any significant change in expression levels in wild-type and mutant embryos (Supplementary Figure S4A and B). As expected, *Ret* expression was found within the mesonephric duct and the T-shaped branched ureter in wild-type embryos (Figure 3a). In homozygous *Sox11* mutants, the overall *Ret* expression pattern was unchanged, although it highlighted the second UB emerging slightly rostrally to the normal induction site (Figure 3b).

In contrast to the epithelial *Ret* expression, *Gdnf* is expressed in mesenchymal renal progenitor cells. In wild-type mice, low levels of *Gdnf* can be found as early as E9.5 along the entire length of the mesonephric mesenchyme, but by E10.75, expression becomes restricted to the MM at the caudal end of the nephrogenic cord (for a review, see Davis *et al.*⁵). Strikingly, homozygous mutants displayed a dramatic rostral extension of the *Gdnf* expression domain when compared with wild-type embryos of the same stage (Figure 3c and d and Supplementary Figure S4C and D). More anterior staining was also seen when using other MM-specific markers such as *Six2* (Figure 3e and f), indicating a rostral expansion of MM cells rather than a simple upregulation of *Gdnf* in *Sox11* mutant embryos. Taken together, these data show that SOX11 is required to restrict *Gdnf*-expressing cells to the caudal end of the nephrogenic cord.

SOX11 regulates the protocadherin β genes by directly binding to its cluster control region

SOX11 is foremost a transcriptional regulator, and loss of function is likely to affect the expression of downstream target genes. Formation of ectopic UBs has been reported previously in mouse mutants including *Gata3*,¹⁷ *Sprouty1*,¹⁸ *Bmp4*,¹⁹ *Foxc1/2*,⁷ *Robo2*, and its receptor *Slit*.⁶ ISH expression analysis showed no significant changes in these genes (Supplementary Figure S5 and data not shown), suggesting that SOX11 acts through independent molecular pathways.

To obtain an unbiased view on genes whose expression depends on SOX11, we performed microarray analysis on RNA isolated from the caudal region of E10.75 wild-type and mutant nephrogenic cords. A total of 281 probe sets presented statistically significant changes (76 up, 205 down; false discovery rate <0.1) with 68 of these (13 up and 55 down),

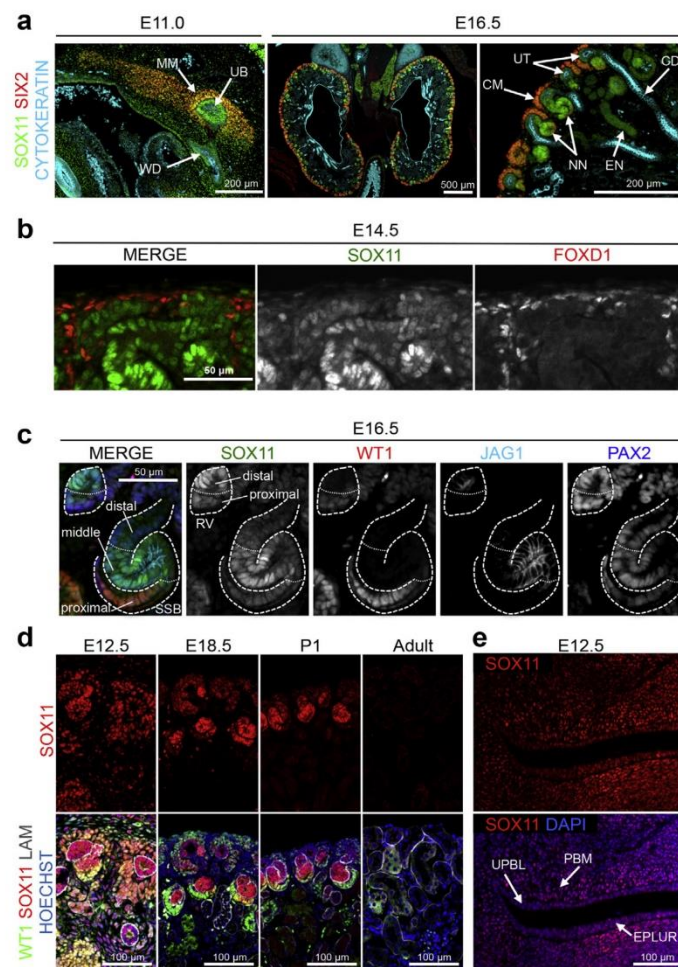


Figure 1 | Dynamic expression of SOX11 during kidney development. (a) Immunofluorescence analysis of wild-type embryos shows SOX11 expression in the metanephric mesenchyme (SIX2+) and Wolffian duct/ureteric bud (CYTOKERATIN+) at E11.0 (left panel). At embryonic day (E) 16.5, SOX11 expression is maintained at low levels in the Wolffian duct derivatives (ureteric tips and collecting ducts) and at high levels in the metanephric mesenchyme derivatives (cap mesenchyme and nascent nephrons) (middle and right panels). (b) High-power view showing that SOX11 is absent from FOXD1-positive stromal cells. (c) High magnification of a renal vesicle and S-shaped body of a wild-type E16.5 embryo showing SOX11 expression in the proximal (WT1+), middle (JAG1+), and distal (PAX2+ JAG1- WT1-) segments. Note the higher SOX11 expression in the distal renal vesicle and middle SSB segments. (d) Immunostaining of SOX11 at different stages of kidney development (E12.5, E18.5, postnatal day (P)1, and adult). Simultaneous staining with WT1 and laminin has been used to visualize the different renal structures. (e) SOX11 is expressed in the urethra of E12.5 embryos. CD, collecting duct; CM, cap mesenchyme; DAPI, 4',6-diamidino-2-phenylindole; EN, elongating nephron; EPLUR, epithelium of pelvic urethra; MM, metanephric mesenchyme; NN, nascent nephron; PBM, primitive bladder mesenchyme; RV, renal vesicle; SSB, S-shaped body; UB, ureteric bud; UPBL, urothelium of primitive bladder; UT, ureteric tip; WD, wolffian duct. Bars = 200 and 500 μ m (a), 50 μ m (b,c), 100 μ m (d,e). To optimize viewing of this image, please see the online version of this article at www.kidney-international.org.

showing >1.5 fold up-/downregulation (Supplementary Data 1). Expression of genes known to be involved in duplex kidney formation was not significantly changed in mutant mice, thus further corroborating our *in situ* hybridization analysis.

Bioinformatic analysis using the DAVID tool²⁰ revealed a 144-fold enrichment of the protocadherin β annotation cluster ($P = 6.3e-18$) (Supplementary Data 2) with 17 of 22 genes being downregulated in *Sox11* mutants (Figure 4a).

Protocadherin β genes are organized in a cluster on mouse chromosome 18,²¹ and mapping the fold-change of probe sets along the chromosome showed a compelling reduction of expression of the entire gene family (Figure 4b). Previous analysis had identified a cluster control region mapping 320 kb downstream of the protocadherin β locus that seems to be required for the expression of the 22 *Pcdhb* genes.²² To test whether SOX11 might directly bind the cluster control region, we performed chromatin immunoprecipitation quantitative

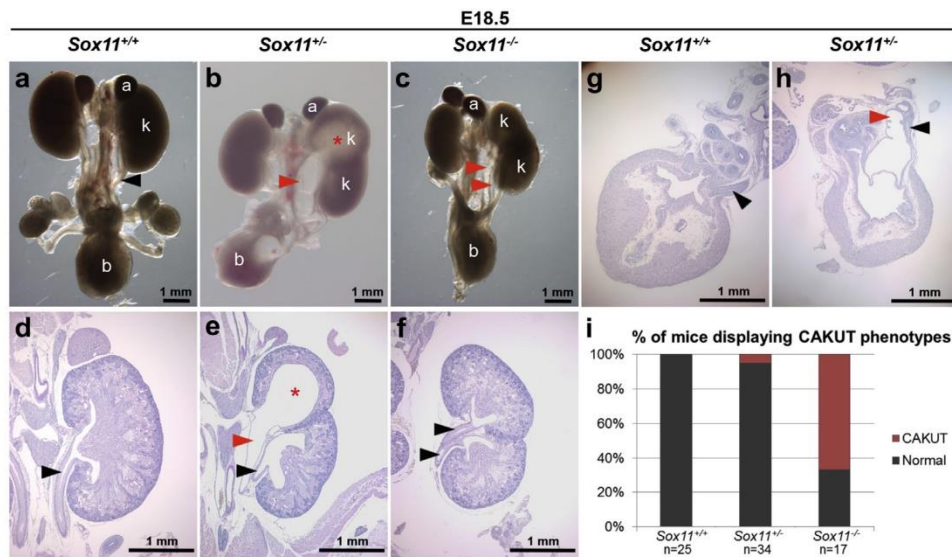


Figure 2 | Kidney and ureter abnormalities in *Sox11* knockout mice. Urinary tracts of embryonic day (E) 18.5 mice were processed as whole-mount (a–c) or with periodic acid–Schiff staining of tissue sections (d–h). Control *Sox11*^{+/+} embryos (a,d) showing normal kidneys (k), adrenal glands (a), ureters (black arrowhead), and bladder (b). *Sox11*^{+/-} (b,e,h) and *Sox11*^{-/-} (c,f) embryos showing duplex kidneys, hydronephrosis (*), and hydroureter (red arrowheads). (i) Frequency of congenital abnormalities of the kidney and urinary tract (CAKUT) phenotype in *Sox11*^{+/+}, *Sox11*^{+/-}, and *Sox11*^{-/-} embryos at postnatal day (P)0. Bar = 1 mm. To optimize viewing of this image, please see the online version of this article at www.kidney-international.org.

polymerase chain reaction experiments on E14.5 wild-type kidneys. Strikingly, an 8-fold enrichment of chromatin precipitated with SOX11 (over IgG) was found at hypersensitive site HS19-20 of the cluster control region (Figure 4c). No such enrichment could be detected with primers for a negative control region, located in the 3'UTR region of the *Cd24a* gene. We concluded that direct binding of SOX11 to the locus control region is essential to provide high levels of expression of the *Pcdhb* gene cluster.

Nephron segment defects in *Sox11* mutants

The dynamic expression pattern of *Sox11* during nephron formation prompted us to analyze a potential function of this gene at later stages of kidney development. Examination of E18.5 kidney sections revealed hypodysplastic kidneys with an apparent reduction of epithelial components and an increase of stromal tissue in the medulla (Figure 5a–b'). A proportion of mice also displayed mild proximal tubule dilation, but this phenotype was not 100% penetrant (data not shown). ISH experiments revealed persistent expression of proximal (*Slc5a2* and *Slc5a1*), distal, and connecting tubule (*Slc12a3* [*Ncc*]) markers, but dramatically shortened Henle's loops (*Slc12a1* [*Nkcc2*]) (Figure 5c–j), which was also reflected by reduced expression of *Irx1* and *Irx2* (Supplementary Figure S6A–D). To obtain a more quantitative evaluation of segment specific changes, we next counted the number of structures/cells highlighted by specific markers. Glomerular numbers, as defined by the expression of podocin (NPHS2), were unchanged in mutant kidneys,

indicating that loss of *Sox11* does not interfere with nephron induction and glomerular maturation (Figure 6a–c). Immunostaining with antibodies detecting lotus tetragonolobus lectin (LTL) (proximal tubule) showed a small decrease, which, however, did not reach statistical significance (Figure 6d–f). By contrast, the number of cells positive for markers identifying Henle's loops (Tamm-Horsfall protein) and, to a lesser extent, the distal convoluted tubule (NaCl cotransporter) were significantly reduced, indicating a particular need for SOX11 for these segments (Figure 6g–l). Interestingly, number of cells positive for Henle's loop and distal tubule markers was also reduced in *Sox11* heterozygous mutants, suggesting that SOX11 acts in a dose-sensitive manner also during nephron maturation. Analysis of early nephron patterning markers (WT1, PAX2, JAG1, HNF1β, BRN1, SOX9, and *Papss2*) revealed normal expression (Supplementary Figure S6E–H).

Previous studies have shown that elongation of Henle's loops depends on collecting duct–derived *Wnt7b* that induces canonical β-catenin signaling in surrounding stromal cells, resulting in the activation of *Lef1*.²³ qPCR analyses revealed a mild increase of the Wnt inhibitor *Dkk1* in *Sox11* mutant (Supplementary Figure S7C). However, ISH, immunofluorescence, and qPCR analyses did not reveal significant changes in *Wnt7b*, *Lef1*, and *Axin2* expression, thus ruling out regulation of this pathway by SOX11 (Supplementary Figure S7C and D). Moreover, mitotic figures (phosphohistone H3) revealed no significant changes in the proliferation rate of early nephron structures nor in elongating loops of

Table 1 | Sox11 is required to ensure proper kidney development

Genotype	N	Normal (%)	CAKUT (%)	Duplex kidney		Hydroureter	Hydronephrosis	Hypoplasia	
				Unilateral	Bilateral			Unilateral	Bilateral
Sox11 ^{+/+}	26	26 (100)	0 (0)						
Sox11 ^{+/-}	39	37 (94.9)	2 (5.1)	2		2	2		
Sox11 ^{-/-}	21	7 (33.3)	14 (66.7)	7	5	2	1	2	2

CAKUT, congenital abnormalities of the kidney and urinary tract.

Frequency and detailed kidney phenotypes of Sox11 knockout and Sox11^{+/-} mutant mice. Note that hydroureter and hydronephrosis defects were always found in association with duplex kidney.

Henle (Supplementary Figure S7A and B). Similarly, apoptotic figures were unchanged between wild type and controls (data not shown).

Analysis of SOX11 in a cohort of human CAKUT patients

Urogenital tract defects observed in Sox11 null mice are reminiscent of congenital abnormalities observed in human CAKUT patients. To determine whether SOX11 variants are associated with CAKUT, we screened the coding sequence of SOX11 (NM_003108.3) in a cohort of 560 patients (Supplementary Table S1). A total of 6 heterozygous variants were detected in 6 patients, including 2 silent point mutations, 3 missense point mutations, and 1 insertion of 12 nucleotides, resulting in an in-frame insertion of 4 amino acids (Figure 7). One patient (patient 5) with posterior urethral valves and kidney hypoplasia showed 2 SOX11 variants, including a 12-bp insertion and a missense mutation.

Comparison of our variants with online databases (1000 Genomes Project,²⁴ NCBI database of genetic variation dbSNP,²⁵ and ExAC Browser²⁶) revealed the presence of 4 variants (c.63G>T, c.257G>T, c.658G>A, and c.1131C>T [not validated]) in previously sequenced populations (Table 2). The other 2 variants (c.995C>T and c.1063_1064insAGCGG-CAGCAGC) were absent from public databases. Online mutation prediction using RegRNA 2.0 software²⁷ suggested that the silent C.1131C>T variant may introduce a novel splice donor site (Supplementary Data File 3). SIFT analysis (<http://sift.jcvi.org/>) did not reach a high enough score, but both PolyPhen-2 (genetics.bwh.harvard.edu/pph2) and Mutation tasting (<http://www.mutationtaster.org/>) considered several variants as damaging. Of particular interest is variant c.257G>T (p.R86L), as it affects the HMG box DNA binding domain, which has been highly conserved throughout evolution.

SoxC class proteins can act as classic transcription factors that bind to DNA and activate downstream target genes. To test whether the variants would interfere with transactivation, we recreated expression vectors and cotransfected them with a luciferase reporter plasmid of the Gdf5 promoter, a proposed downstream target of SOX11.²⁸ Most variants had no dramatic effect on reporter gene expression (Supplementary Figure S8). One exception was the insertion mutation c.1063_1064insAGCGG-CAGCAGC, which completely abrogated reporter plasmid activation.

DISCUSSION

Kidney development is a highly complex process that requires the orchestrated action of transcription factors to ensure proper induction, proliferation, and differentiation. SOX genes are one class of factors that have already previously been implicated in kidney development. Although SOX8 and SOX9 are required for ureter branching,¹¹ SOX4 has been

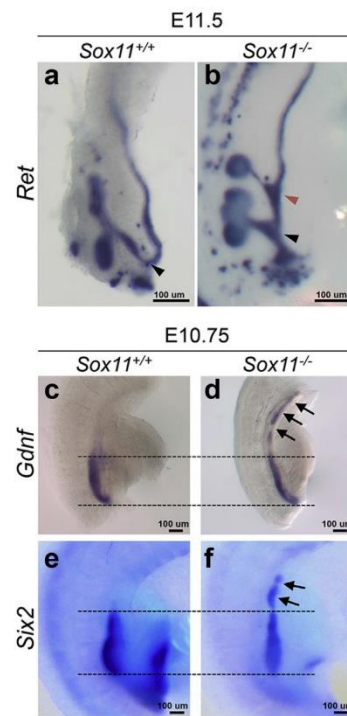


Figure 3 | Loss of Sox11 results in supernumerary ureteric buds and rostral extension of the Gdnf expression domain. (a,b) Dissected urogenital tracts of embryonic day (E)11.5 mutant embryos were processed for whole-mount *in situ* hybridization using a *Ret* probe. A single ureteric bud (black arrowhead) has emerged and branched in the Sox11^{+/+} embryo, whereas 2 ureteric buds (black and red arrowheads) had formed in the absence of Sox11. (c-f) Whole-mount *in situ* hybridization on urogenital tracts of E10.75 embryos using *Gdnf* and *Six2* probes shows a rostral extension of the *Gdnf* and *Six2* expression domain in Sox11^{-/-} (black arrows, right panel) compared with Sox11^{+/+} (left panel). Bar = 100 μm. To optimize viewing of this image, please see the online version of this article at www.kidney-international.org.

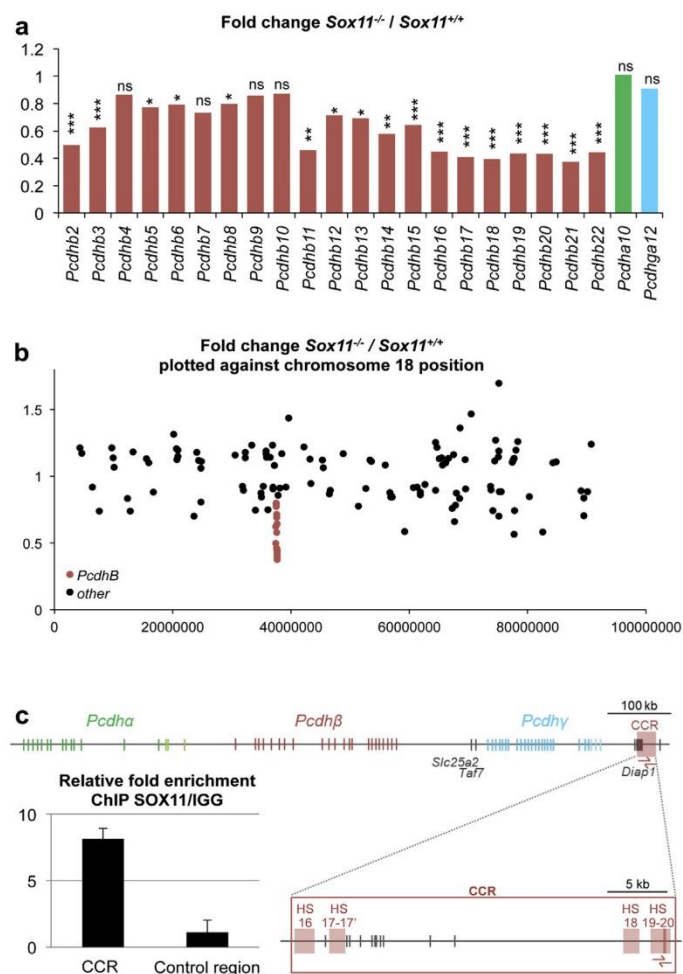


Figure 4 | Microarray and ChIP analysis identifies the protocadherin- β cluster as a direct target of SOX11. (a) Relative fold change in expression (*Sox11*^{-/-}/*Sox11*^{+/+}) of protocadherin genes obtained by microarray (* $P < 0.5$, ** $P < 0.01$, *** $P < 0.001$). (b) Relative fold change expression (*Sox11*^{-/-}/*Sox11*^{+/+}) of chromosome 18 genes obtained by microarray ($P < 0.05$), plotted against their chromosomal location. (c) Schematic representation of the *Pcdh*- α (green), - β (red), and - γ (blue) loci. The *Pcdh* β -cluster control region (CCR) is represented as a red box, containing 4 DNaseI hypersensitivity sites (HS16, 17-17', 18, and 19-20). Red arrows represent the primers used for ChIP analysis. ChIP-quantitative polymerase chain reaction analysis ($N = 2$) reveals an 8-fold enrichment of HS19-20 in SOX11-immunoprecipitated chromatin versus IgG-immunoprecipitated chromatin. No difference was seen on a control locus. ChIP, chromatin immunoprecipitation; HS, hypersensitivity site; ns, nonsignificant; *Pcdh*, protocadherin.

suggested to be required for nephron endowment.¹³ Here we identified SOX11 as a novel player in kidney formation that appears to act during metanephros induction and nephrogenesis.

The first step in kidney development involves specification of the MM within the nephrogenic cord, with *Gdnf* and *Six2* often being used as molecular markers for this compartment. Both of these genes are expressed in *Sox11* mutants, indicating that specification occurs normally in the absence of this gene. Ureter induction relies on GDNF/rearranged during transfection signaling, and alterations in this pathway can lead to renal agenesis or ectopic budding. Overall expression levels

of *Ret* and *Gdnf* appeared unaffected in mutants when analyzed by qPCR. ISH analysis, however, revealed a dramatic rostral extension of the *Gdnf* expression domain, which could be explained by several mechanisms: (i) A requirement for SOX11 to suppress *Gdnf* expression; this seems unlikely as SOX11 expression is also found in MM and thus overlaps with *Gdnf* and *Six2*; (ii) a lack of apoptosis in rostral domains; (iii) disrupted cell migration of rostrally located MM precursors toward the caudal end. Although directed migration of mesenchymal cells toward the caudal end of the intermediate mesoderm has not been demonstrated so far, 2 previous studies using *Wnt5a/Ror2* knockout mice have suggested that

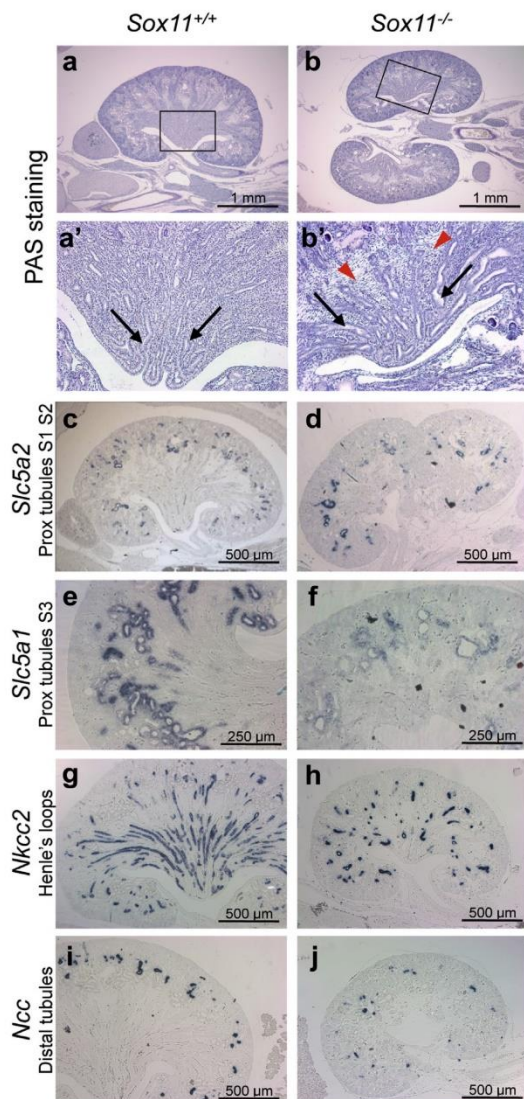


Figure 5 | Loss of *Sox11* causes changes in renal architecture. (a,b) Periodic acid–Schiff (PAS) staining of postnatal day (P0) kidneys from wild-type and *Sox11*^{-/-} animals. Closer views of the medullary zone (a',b') show a reduction of epithelial components and an increase of stromal tissue in *Sox11* mutant embryos compared with controls. Black arrows point to the collecting ducts and red arrowheads to stromal cells. (c–j) *In situ* hybridization analysis of nephron segments in embryonic day 18.5 *Sox11*^{+/+} (left panel) and *Sox11*^{-/-} (right panel) embryos. *Slc5a2* (solute carrier family 5, member 2), *Slc5a1* (solute carrier family 5, member 1), *Nkcc2* (solute carrier family 12, member 1), and *Ncc* (solute carrier family 12, member 3) riboprobes were used to visualize segments 1/2 of proximal (prox) tubules, segments S3 of proximal tubules, Henle's loops, and distal tubules, respectively. Bars = 1 mm (a,b), 250 μm (e,f), and 500 μm (c,d,g–j). To optimize viewing of this image, please see the online version of this article at www.kidney-international.org.

such a migration may occur.^{29,30} Several lines of evidence from our own studies further support this hypothesis. First, the extended expression domain in the rostral mesonephros is accompanied by a thinning of the *Gdnf*⁺ and *Six2*⁺ domain in the caudal region (Figure 3), an observation that is consistent with a disrupted migration of MM cells. Second, our microarray analysis in E10.75 *Sox11* mutants revealed a dramatic loss of molecules involved in cell adhesion and cell migration, such as the protocadherin-β cluster and members of the semaphorin signaling pathway (*Sema6C*, *Dpysl5*). Although duplex formation in mutant mice for these genes^{31,32} nor the *Pcdhb* locus control region²² has not been reported, mutations in the semaphorin family member *Sema3a* leads to increased ureter branching.³³ We therefore hypothesize that the combined reduction of these genes causes defects in cell adhesion and migration. A role for SOX11 as a regulator of cellular migration was previously shown in mesenchymal stem cells.³⁴ Further experiments will need to be performed to demonstrate active migration of *Gdnf*-positive mesenchymal cells toward the caudal end of the nephrogenic cord as a potential mechanism required for the formation of a bona fide metanephric mesenchyme. If our model turns out to be correct, mesenchymal cell migration would mirror the active migration of epithelial cells within the mesonephric duct that has been shown previously to be essential for proper kidney induction.^{35,36}

Although expression of SOX11 is maintained in the ureter and MM throughout development, deletion does not seem to affect ureter branching, and based on glomerular counts, *Sox11* mutants develop the normal number of nephrons. This finding is somewhat surprising given that previous studies have suggested an important function for SOX11 in regulating *Wnt4* during nephron formation at least in *Xenopus* embryos.³⁷ The persistent nephrogenesis could potentially be explained through functional redundancy with other members of the SOXC gene family (SOX4 and SOX12). By contrast, *Sox11* seems to have a unique role during nephron formation, and mutants display a dramatically shortened Henle's loop, whereas other segments were only mildly affected. Nephron patterning occurs at a very early stage during morphogenesis, and several key genes have been identified in recent years.^{38,39} Molecular analysis revealed the expression of all segment specific markers, indicating that initial patterning of the nephron occurs in *Sox11* mutant mice. Assignment of segment identity involves a careful balance between β-catenin, Notch, and BMP signaling, with distal/intermediate segments showing the highest β-catenin activity.³⁸ Because the proliferation rate in both S-shaped bodies and elongating Henle's loops was unchanged in mutants, we can speculate that the initial number of progenitors within the intermediate segments may be reduced. Proving this hypothesis would require a careful 3-dimensional analysis of a precisely defined nephron stage, which is difficult due to the highly dynamic nature of nephrogenesis.

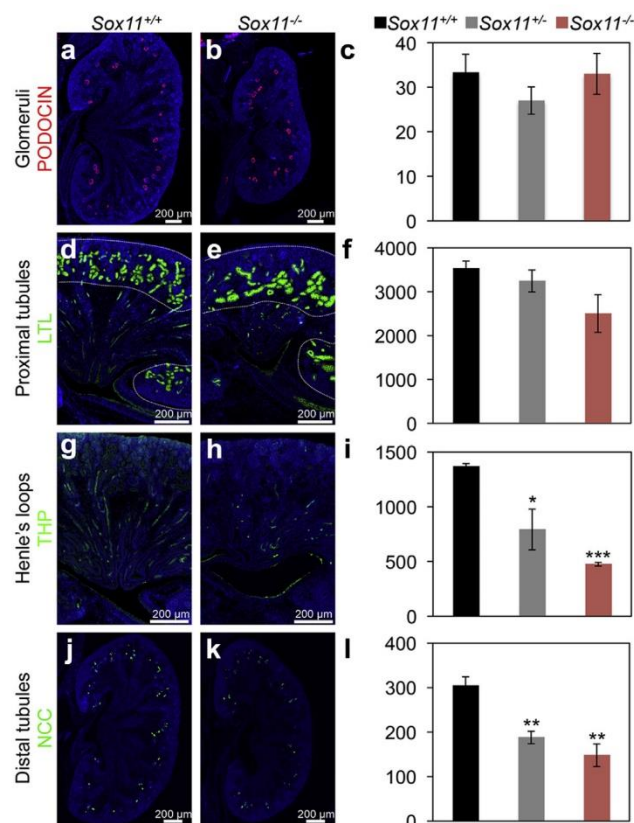


Figure 6 | Nephron segment defects in *Sox11* mutant mice. Immunofluorescence analysis of nephron segments in embryonic day (E) 17.5 *Sox11*^{+/+} (left panel) and *Sox11*^{-/-} (right panel) embryos. Podocin/NPHS2 (**a,b**), lotus tetragonolobus lectin (LTL) (**d,e**), Tamm-Horsfall protein (THP) (**g,h**), and NaCl cotransporter (NCC) (**j,k**) were used to visualize glomeruli, proximal tubules, Henle's loops and distal tubules, respectively. Dotted lines in **d** and **e** highlight the renal cortex containing the S1 and S2 segment of proximal tubules. (**c,f,i,l**) Quantification of glomeruli and cells in proximal (LTL+), Henle's loop (THP+) and distal (NCC+) tubules in *Sox11*^{+/+}, *Sox11*^{+/-}, and *Sox11*^{-/-} E17.5 embryos. Cells number is presented as the average with SEM of data obtained from 3 embryos of each genotype (**P* < 0.05, ***P* < 0.01, ****P* < 0.001). Bars = 200 μ m. To optimize viewing of this image, please see the online version of this article at www.kidney-international.org.

During fetal life, gonads are anchored in the abdominal wall by the cranial suspensory ligament and the gubernaculum, at their cranial and caudal poles, respectively. Sex dimorphic regression/development of both cranial suspensory ligament/gubernaculum causes testicular descent, whereas ovaries stay localized at the lower poles of the kidneys, processes controlled by testicular hormones.^{40–42} Given the fact that the position of both testes and ovaries is affected in *Sox11* mutant mice, the absence of male hormones appears unlikely to be the cause of these defects. Alternatively, *Sox11* may have a hormone-independent role within cranial suspensory ligament and/or gubernaculum to allow their proper morphogenesis. A third possible explanation involves interdependence of urinary and genital tract defects. Several reports have shown abnormal localization of the gonads in mouse mutants with ureter malformations^{7,18,43} with failure of gonadal duct/ureter separation due to common nephric duct persistence. Interestingly, ectopic testes in *Sox11*^{-/-} mice are associated with a hydroureter connecting to the vas

deferens (Supplementary Figure S2D'). Future work investigating the roles of *Sox11* in the development of gonads, cranial suspensory ligament/gubernaculum, and the common

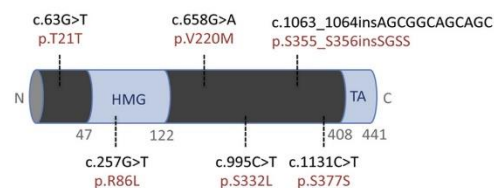


Figure 7 | Coding sequence variants of *SOX11* found in CAKUT patients. Linear representation of the human *SOX11* protein showing the location of the variants identified in the CAKUT cohort. The coding sequence variations (black) and the corresponding amino acid changes (red) are indicated. Functional domains previously reported are displayed in blue: high-mobility group (HMG) DNA-binding domain (HMG aa.47-122) and transactivation domain (TA; TA aa.408-441). Amino acid positions are displayed in gray. C, C terminus; CAKUT, congenital abnormalities of the kidney and urinary tract; N, N terminus.

Table 2 | Coding sequence variants of SOX11 found in CAKUT patients

Patient	1	2	3	4	5	6
Sex	Male	Male	Female	Male	Male	Male
Country	The Netherlands	The Netherlands	The Netherlands	Germany	Germany	The Netherlands
Ethnicity	Caucasian	Caucasian	Caucasian	Caucasian	Caucasian	Caucasian
Phenotype	Posterior urethral valves	Multicystic /kidney dysplasia (left)	Duplex collecting system (right) Ureteropelvic junction obstruction (right) Vesicoureteral reflux (right)	Posterior urethral valves Multicystic kidney dysplasia (bilateral) Hepatic fibrosis Retinal degeneration Skeletal abnormalities	Posterior urethral valves Kidney hypoplasia (bilateral)	Ureteropelvic junction obstruction (left) Maldescended testis (right) Urethral meatal stenosis Hearing loss Glaucoma (bilateral)
Position on chromosome 2 (GRCh38.p2)	5692784	5692978	5693716	5693784	5693784	5693379
Coding sequence change (NM_003108.3)	c.63G>T	c.257G>T	c.995C>T	c.1063insAGCGGCAGCAGC	c.1063insAGCGGCAGCAGC	c.658G>A
Type of mutation	Silent	Missense	Missense	Insertion	Insertion	Missense
Amino acid change (NP_003099.1)	p.T21T	p.R86L	p.S332L	p.355insSG55	p.355insSG55	p.V220M
Variant dbSNP ID	rs139885563	rs202211730	Novel	Novel	Novel	rs762687158 (not validated)
Allele frequency						
ExAC (non-Finnish Europeans)	0.001	—	—	—	—	0.0003
Our CAKUT cohort	0.0009	0.0009	0.0009	0.002	0.002	0.0009
PolyPhen-2 prediction	—	Probably damaging	Probably damaging	—	—	Probably damaging
Score	—	0.996	0.991	—	—	0.996
Sensitivity	—	0.55	0.71	—	—	0.55
Specificity	—	0.98	0.97	—	—	0.98
Mutation Taster						
Prediction	—	Disease causing	Disease causing	—	—	Disease causing
Prob	—	0.999	0.999	—	—	0.996
SIFT						
Prediction	—	Tolerated	Tolerated	—	—	Tolerated
score	—	0.46	0.14	—	—	0.11
RegRna prediction						
Motif type	Intron splicing enhancer	Functional RNA sequences	Functional RNA sequences	Transcriptional regulatory motif	Transcriptional regulatory motif	Human splicing sites
			Transcriptional regulatory motif	Transcriptional regulatory motif	Human splicing sites	Intron splicing enhancer
				Human splicing sites	Human splicing sites	Human splicing sites
				Transcriptional regulatory motif	Transcriptional regulatory motif	Intron splicing enhancer
				Intron splicing enhancer	Intron splicing enhancer	Intron splicing enhancer
				Human splicing sites	Human splicing sites	Human splicing sites
						Intron splicing enhancer (ISE)

Motif name	gh-1 intron 3	FR084090/ group I intron	FR012169/ Putative conserved_ noncoding_ region_(EvoFold)	HIC1	BEN	Donor	Acceptor	BEN	Amyloid precursor protein, exon 8	Donor	ighg2 cgamma2 (IgG heavy chain subclass g2 - cgamma2 gene) - intron 1	Additional
Change in variant versus wild type	Suppressed	Suppressed	Additional	Additional	Additional	Suppressed	Additional	Additional	Additional	Additional	Additional	Additional

SOX11 variants identified in CAKUT cohort, their associated phenotypes, frequency in our CAKUT cohort and the ExAC database, and *in silico* mutation prediction results. Patient phenotypes that were also displayed by the Sox11 knockout are shown in bold.

nephric duct will be needed to identify in which compartment this gene is required for proper genital tract development.

The incomplete penetrance of the phenotype is in line with observations made for CAKUT in humans. Indeed, disease-causing mutations are often transmitted from phenotypically normal parents to their children, thus highlighting the complexity of the genetics and a potential contribution of stochastic and environmental factors in complex diseases like CAKUT.⁴⁴ The fact that defects could be observed in a proportion of heterozygote mice supports gene dose sensitivity and is in line with the type of genetic alteration associated with CAKUT in human patients. The broad range of urogenital defects observed in *Sox11* mutant mice also corresponds to the observations of diverse phenotypes made in familial CAKUT.

SOX11 gene mutation analysis revealed a 12-bp insertion and 5 point mutations in a large cohort of CAKUT patients. These patients display different types of urogenital tract malformations that are recapitulated in the *Sox11* mouse model, namely, duplex kidneys, renal hypoplasia, testis, and ureteropelvic junction obstruction. Strikingly, 4 of the 5 male patients have ureter malformations. In mice, SOX11 is expressed in early urogenital sinus, which correlates with its potential role in ureteral development.

Although the pathogenic significance of the identified variants is uncertain at present, the complete absence or very low frequency of these genetic variants in public databases, further supported by *in silico* predictions, may suggest that at least some of them could be involved in the development of CAKUT. Functional analysis in transfection assays confirmed the disruptive nature of 1 variant for transcriptional activity of SOX11. Of interest, this variant has been recently identified in a patient with coloboma,⁴⁵ thus further implicating an important role for SOX11 disruption in human disease. It is challenging to determine *in vitro* whether the other variants identified in this study contribute to disease etiology. Modeling the mutations *in vivo* using CRISPR/Cas9 approaches may address this problem.

In conclusion, our study identified SOX11 as a crucial regulator of kidney development. SOX11 restricts *Gdnf*-expressing cells to the caudal part of the nephrogenic cord, controls single UB outgrowth, and is required for proper nephron formation. Although our study does not unequivocally prove an involvement of SOX11 in human CAKUT, the identification of rare variants in patients in combination with the phenotype observed in our mouse model makes it a strong candidate for human CAKUT disease.

MATERIALS AND METHODS

Mice

All animal work was conducted according to national and international guidelines and was approved by the local ethics committee (NCE/2011-19). The *Sox11* knockout mouse strain was described previously.¹⁴ *Sox11* knockout mice were maintained on a mixed B6D2F1 genetic background. All comparisons were done between

littermates of the same strains. Routine genotyping of mice was carried out by PCR, as previously described.¹¹

Glomeruli and cell number quantification

Paraffin sections of 6 independent E17.5 embryos for each condition (control, heterozygote, and *Sox11* knockout) were processed in immunofluorescence with antibodies against WT1 and podocin/NPHS2 or WT1 and Nephlin/NPHS1. For segment-specific cell number quantification, paraffin sections of 3 independent E17.5 embryos from the 3 different conditions were stained for LTL, Tamm-Horsfall protein, or NaCl cotransporter. Photographs were taken with an AxioCam Mrm camera (Carl Zeiss AC, Oberkochen, Germany) and processed with ImageJ. Glomeruli and cells were counted manually by a single blind operator. Statistical analysis was performed using Student *t* test.

Proliferation assay

For elongating Henle's loop analysis, mice were injected with bromodeoxyuridine i.p. on day 17.5 of pregnancy and killed 90 minutes later. Embryo sections were stained for bromodeoxyuridine, BRN1, LTL, and lectin Dolichos biflorus agglutinin (DBA), and cells were counted using the Cell Counter plugin in Fiji software. The total number of bromodeoxyuridine-positive/BRN1⁺/LTL⁻/DBA⁻ cells was normalized on the total number of BRN1⁺/LTL⁻/DBA⁻ cells and expressed as a percentage.

For early nephron analysis, E16.5 embryo sections were stained for pHH3 (cellular mitotic bodies), JAG1, and WT1. Transverse sections of renal vesicles, comma-shaped bodies, and S-shaped bodies were counted by a single blinded observer using the Cell Counter plugin in the Fiji software. A section of early nephron structure was considered positive if it contained ≥ 1 mitotic figures positive for pHH3. S-shaped bodies were divided into a medial segment (JAG1⁺) and a distal segment (JAG1⁻). The total number of positive early nephron sections was normalized on the total number of early nephron sections and expressed as a percentage.

Data were obtained from 3 biological replicates for each condition. *Sox11*^{+/-} and *Sox11*^{+/+} samples were considered as controls for this experiment. Statistical significance of the results was evaluated with the Student *t* test.

Microarray study and data processing

Total RNA was extracted in 4 independent replicates from a dissected caudal area of urogenital ridges of *Sox11* knockout and wild-type E10.75 embryos using the RNeasy MicroKit (Qiagen, Hilden, Germany) followed by column DNase digestion to remove any contaminating genomic DNA. RNA preparations from the 2 different conditions were processed and hybridized on the Mouse Gene Array (Thermo Fisher Scientific, Waltham, MA). Arrays were quantile normalized with respect to the probe GC content using the RMA algorithm. No or low expressed transcripts were removed by a maximum expression cutoff < 50 . The data filtering in 206768 of 234872 probe sets and 27478 metaprobe sets are defined in the full dataset. Differential expression of summarized gene level expression was calculated using the *f* test statistic followed by a false discovery rate multiple testing correction. Microarray data were deposited in Gene Expression Omnibus under accession number GSE105426.

Inclusion of CAKUT patients

Participants included 560 patients for DNA analysis derived from 3 cohorts: (i) A total of 461 patients derived from the Dutch AGORA (Aetiologic research into Genetic and Occupational/environmental

Risk factors for Anomalies in children) data- and biobank project, which comprises DNA as well as clinical and questionnaire data on lifestyle and environmental factors from patients diagnosed with congenital malformations or childhood cancers and their parents.⁴⁶ Patients were diagnosed with CAKUT at the Radboud University Medical Center, Amalia Children's Hospital, Nijmegen, The Netherlands. (ii) Eighty-three patients were derived from a duplex collecting system/vesicoureteral reflux patient cohort that was described previously,⁴⁷ and (iii) 16 children with CAKUT were selected for mutational analysis in a multicenter approach. The inclusion criteria comprised renal hypodysplasia, double kidneys, and/or anomalies of the ureter with renal hypodysplasia defined by the presence of small kidneys (lower than the third percentile), and/or maldeveloped renal tissue on renal ultrasound. Sonographic criteria of maldeveloped renal tissue included a lack of corticomedullary differentiation and optional proof of renal cysts. Clinical information from the family members was collected wherever possible.

The study was approved by the ethics committees in all participating centers, and informed assent and/or consent for genetic screening was obtained from patients and/or parents, as appropriate. Peripheral blood samples were obtained, and DNA was isolated from lymphocytes using standard procedures. The patients and their diagnoses are summarized in Supplementary Table S1.

Mutation analysis of the human SOX11 gene in CAKUT patients

The coding region and the intron-exon boundaries of the human *SOX11* gene (NM_003108.3) were analyzed by Sanger sequencing. Primers applied and PCR settings are available on request. In-house and the online available databases dbSNP, Ensembl genome browser, 1000 Genomes Project, and ExAC Browser were used to determine whether *SOX11* variants were detected previously. Evaluation of a functional effect of the variants was assessed using PolyPhen-2 (<http://genetics.bwh.harvard.edu/pph2/>), SIFT (<http://sift.jcvi.org/>) and mutation taster (<http://www.mutationtaster.org>).

Additional methods are provided in the Supplementary Material.

DISCLOSURE

All the authors declared no competing interests.

ACKNOWLEDGMENTS

We thank the team at the animal facility for their dedication. We are grateful to the patients, parents, and health care providers for participating in the collection of patient data. We are indebted to F. Costantini (New York) and S. Cereghini (Paris) for the *Gdnf* and *Paps2* ISH probes and to Valerie Vidal for help with ISH experiments. This work was supported by grants from ANR (ANR-09-GENO-027-01 & ANR-11-LABX-0028-01), ARC (SL22020605297), la Fondation de la Recherche Medicale (FRM, ING20160435020), and the EC (EUrenOmics Grant agreement 305608; RenaITract). KR and AMvE were funded by the Dutch Kidney Foundation (KSTP.10.004 and C02.2009).

SUPPLEMENTARY MATERIAL

Figure S1. SOX11 expression during kidney development.

Figure S2. Genital tract abnormalities are associated with duplex kidneys in *Sox11* knockout mice.

Figure S3. *Ex vivo* supernumerary bud formation in *Sox11* knockout embryos.

Figure S4. Rostral extension of the *Gdnf* expression domain in *Sox11* mutants.

Figure S5. Expression of genes known to be involved in ureteric bud outgrowth is not affected by the absence of Sox11.

Figure S6. Nephron patterning genes are expressed in Sox11 mutants.

Figure S7. Analysis of proliferation and the Wnt/ β -catenin pathway.

Figure S8. Effect of variants on SOX11 transactivation function in HEK293 cell line.

Table S1. Number of patients analyzed and phenotypic classification.

Table S2. List of antibodies and primers used in this study.

Supplementary Methods and Supplementary References.

Supplementary Data 1. Differentially expressed genes in Sox11 ko animals at E10.75.

Supplementary Data 2. Functional annotation chart.

Supplementary Data 3. RegRNA analysis.

Supplementary material is linked to the online version of the paper at www.kidney-international.org.

REFERENCES

- Schedl A. Renal abnormalities and their developmental origin. *Nat Rev Genet.* 2007;8:791–802.
- Nicolaou N, Renkema KY, Bongers EM, et al. Genetic, environmental, and epigenetic factors involved in CAKUT. *Nat Rev Nephrol.* 2015;11:720–731.
- Costantini F, Kopan R. Patterning a complex organ: branching morphogenesis and nephron segmentation in kidney development. *Dev Cell.* 2010;18:698–712.
- Lu BC, Cebrían C, Chi X, et al. Etv4 and Etv5 are required downstream of GDNF and Ret for kidney branching morphogenesis. *Nat Genet.* 2009;41:1295–1302.
- Davis TK, Hoshi M, Jain S. To bud or not to bud: the RET perspective in CAKUT. *Pediatr Nephrol.* 2014;29:597–608.
- Grieshammer U, Le M, Plump AS, Wang F, et al. SLIT2-mediated ROBO2 signaling restricts kidney induction to a single site. *Dev Cell.* 2004;6:709–717.
- Kume T, Deng K, Hogan BL. Murine forkhead/winged helix genes Foxc1 (Mf1) and Foxc2 (Mfh1) are required for the early organogenesis of the kidney and urinary tract. *Development.* 2000;127:1387–1395.
- Kopan R, Chen S, Little M. Nephron progenitor cells: shifting the balance of self-renewal and differentiation. *Curr Topics Dev Biol.* 2014;107:293–331.
- Lefebvre V, Dumitriu B, Penzo-Mendez A, et al. Control of cell fate and differentiation by Sry-related high-mobility-group box (Sox) transcription factors. *Int J Biochem Cell Biol.* 2007;39:2195–2214.
- Koopman P, Schepers G, Brenner S, Venkatesh B. Origin and diversity of the SOX transcription factor gene family: genome-wide analysis in Fugu rubripes. *Gene.* 2004;328:177–186.
- Reginensi A, Clarkson M, Neirijnck Y, et al. SOX9 controls epithelial branching by activating RET effector genes during kidney development. *Hum Mol Genet.* 2011;20:1143–1153.
- Kumar S, Liu J, Pang P, et al. Sox9 Activation Highlights a Cellular Pathway of Renal Repair in the Acutely Injured Mammalian Kidney. *Cell Rep.* 2015;12:1325–1338.
- Huang J, Arsenaault M, Kann M, et al. The transcription factor Sry-related HMG box-4 (SOX4) is required for normal renal development in vivo. *Dev Dyn.* 2013;242:790–799.
- Sock E, Rettig SD, Enderich J, et al. Gene targeting reveals a widespread role for the high-mobility-group transcription factor Sox11 in tissue remodeling. *Mol Cell Biol.* 2004;24:6635–6644.
- Wurm A, Sock E, Fuchshofer R, et al. Anterior segment dysgenesis in the eyes of mice deficient for the high-mobility-group transcription factor Sox11. *Exp Eye Res.* 2008;86:895–907.
- Hoser M, Potzner MR, Koch JM, et al. Sox12 deletion in the mouse reveals nonreciprocal redundancy with the related Sox4 and Sox11 transcription factors. *Mol Cell Biol.* 2008;28:4675–4687.
- Grote D, Boualia SK, Souabni A, et al. Gata3 acts downstream of beta-catenin signaling to prevent ectopic metanephric kidney induction. *PLoS Genet.* 2008;4:e1000316.
- Basson MA, Akbulut S, Watson-Johnson J, et al. Sprouty1 is a critical regulator of GDNF/RET-mediated kidney induction. *Dev Cell.* 2005;8:229–239.
- Miyazaki Y, Oshima K, Fogo A, et al. Bone morphogenetic protein 4 regulates the budding site and elongation of the mouse ureter. *J Clin Invest.* 2000;105:863–873.
- Huang da W, Sherman BT, Lempicki RA. Systematic and integrative analysis of large gene lists using DAVID bioinformatics resources. *Nat Protoc.* 2009;4:44–57.
- Hirayama T, Yagi T. Clustered protocadherins and neuronal diversity. *Prog Mol Biol Transl Sci.* 2013;116:145–167.
- Yokota S, Hirayama T, Hirano K, et al. Identification of the cluster control region for the protocadherin-beta genes located beyond the protocadherin-gamma cluster. *J Biol Chem.* 2011;286:31885–31895.
- Yu J, Carroll TJ, Rajagopal J, et al. A Wnt7b-dependent pathway regulates the orientation of epithelial cell division and establishes the cortico-medullary axis of the mammalian kidney. *Development.* 2009;136:161–171.
- 1000 Genomes Project Consortium, Abecasis GR, Auton A, et al. An integrated map of genetic variation from 1,092 human genomes. *Nature.* 2012;491:56–65.
- Sherry ST, Ward MH, Kholodov M, et al. dbSNP: the NCBI database of genetic variation. *Nucleic Acids Res.* 2001;29:308–311.
- Lek M, Karczewski K, Minikel E, et al. Analysis of protein-coding genetic variation in 60,706 humans. *bioRxiv.* 2015.
- Chang TH, Huang HY, Hsu JB, et al. An enhanced computational platform for investigating the roles of regulatory RNA and for identifying functional RNA motifs. *BMC Bioinform.* 2013;14(Suppl 2):S4.
- Kan A, Ikeda T, Fukai A, et al. SOX11 contributes to the regulation of GDF5 in joint maintenance. *BMC Dev Biol.* 2013;13:4.
- Nishita M, Qiao S, Miyamoto M, et al. Role of Wnt5a-Ror2 signaling in morphogenesis of the metanephric mesenchyme during ureteric budding. *Mol Cell Biol.* 2014;34:3096–3105.
- Yun K, Ajima R, Sharma N, et al. Non-canonical Wnt5a/Ror2 signaling regulates kidney morphogenesis by controlling intermediate mesoderm extension. *Hum Mol Genet.* 2014;23:6807–6814.
- Takamatsu H, Takegahara N, Nakagawa Y, et al. Semaphorins guide the entry of dendritic cells into the lymphatics by activating myosin II. *Nat Immunol.* 2010;11:594–600.
- Yamashita N, Mosinger B, Roy A, et al. CRMP5 (collapsin response mediator protein 5) regulates dendritic development and synaptic plasticity in the cerebellar Purkinje cells. *J Neurosci.* 2011;31:1773–1779.
- Tufro A, Teichman J, Woda C, Villegas G. Semaphorin3a inhibits ureteric bud branching morphogenesis. *Mech Dev.* 2008;125:558–568.
- Xu L, Huang S, Hou Y, et al. Sox11-modified mesenchymal stem cells (MSCs) accelerate bone fracture healing: Sox11 regulates differentiation and migration of MSCs. *FASEB J.* 2015;29:1143–1152.
- Chi X, Michos O, Shakya R, et al. Ret-dependent cell rearrangements in the Wolffian duct epithelium initiate ureteric bud morphogenesis. *Dev Cell.* 2009;17:199–209.
- Kuure S, Cebrían C, Machingo Q, et al. Actin depolymerizing factors cofilin1 and destrin are required for ureteric bud branching morphogenesis. *PLoS Genet.* 2010;6:e1001176.
- Murugan S, Shan J, Kuhl SJ, et al. WT1 and Sox11 regulate synergistically the promoter of the Wnt4 gene that encodes a critical signal for nephrogenesis. *Exp Cell Res.* 2012;318:1134–1145.
- Lindstrom NO, Lawrence ML, Burn SF, et al. Integrated beta-catenin, BMP, PTEN, and Notch signalling patterns the nephron. *eLife.* 2014;3:e04000.
- Desgrange A, Cereghini S. Nephron Patterning: Lessons from Xenopus, Zebrafish, and Mouse Studies. *Cells.* 2015;4:483–499.
- Zimmermann S, Steding G, Emmen JM, et al. Targeted disruption of the Insl3 gene causes bilateral cryptorchidism. *Mol Endocrinol.* 1999;13:681–691.
- Hutson JM, Hasthorpe S, Heyns CF. Anatomical and functional aspects of testicular descent and cryptorchidism. *Endocr Rev.* 1997;18:259–280.
- Nef S, Parada LF. Cryptorchidism in mice mutant for Insl3. *Nat Genet.* 1999;22:295–299.
- Jain S, Encinas M, Johnson EM Jr, Milbrandt J. Critical and distinct roles for key RET tyrosine docking sites in renal development. *Genes Dev.* 2006;20:321–333.
- Nicolaou N, Pulit SL, Nijman IJ, et al. Prioritization and burden analysis of rare variants in 208 candidate genes suggest they do not play a major role in CAKUT. *Kidney Int.* 2016;89:476–486.
- Pillai-Kastoori L, Wen W, Wilson SG, et al. Sox11 is required to maintain proper levels of Hedgehog signaling during vertebrate ocular morphogenesis. *PLoS Genet.* 2014;10:e1004491.
- van Rooij IA, van der Zanden LF, Bongers EM, et al. AGORA, a data- and biobank for birth defects and childhood cancer. *Birth Defects Res A Clin Mol Teratol.* 2016;106:675–684.
- van Eerde AM, Duran K, van Riel E, et al. Genes in the ureteric budding pathway: association study on vesico-ureteral reflux patients. *PLoS One.* 2012;7:e31327.

SUPPLEMENTARY INFORMATION INVENTORY

Figure S1: SOX11 expression during kidney development.

Figure S2: Genital tract abnormalities are associated with duplex kidneys in Sox11 knock-out mice.

Figure S3: Ex-vivo supernumerary bud formation in Sox11 knock-out embryos.

Figure S4: Rostral extension of the Gdnf expression domain in Sox11 mutants.

Figure S5: Expression of genes known to be involved in ureteric bud outgrowth is not affected by the absence of Sox11.

Figure S6: Nephron patterning genes are expressed in Sox11 mutants.

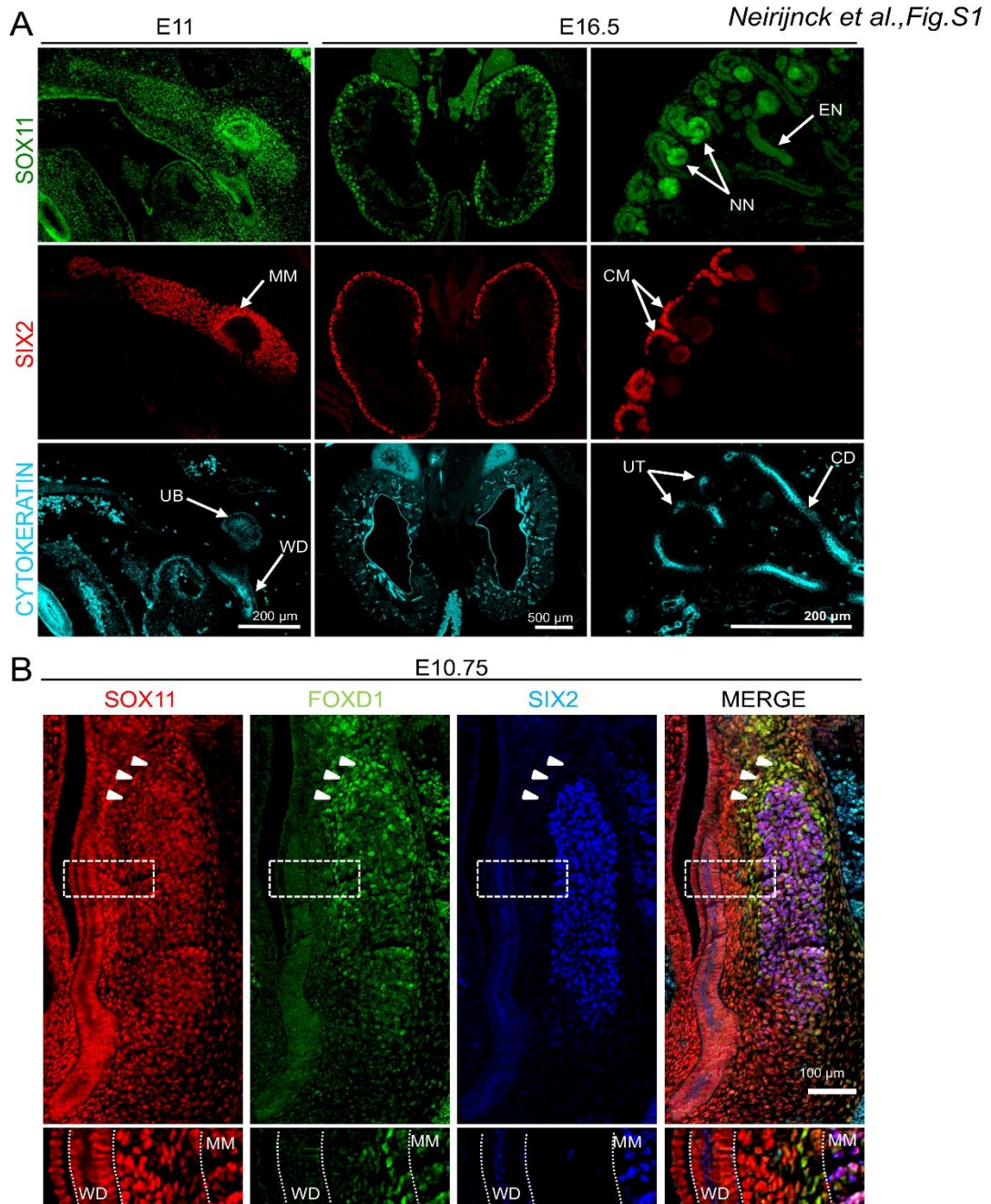
Figure S7: Analysis of proliferation and the Wnt/ β -catenin pathway.

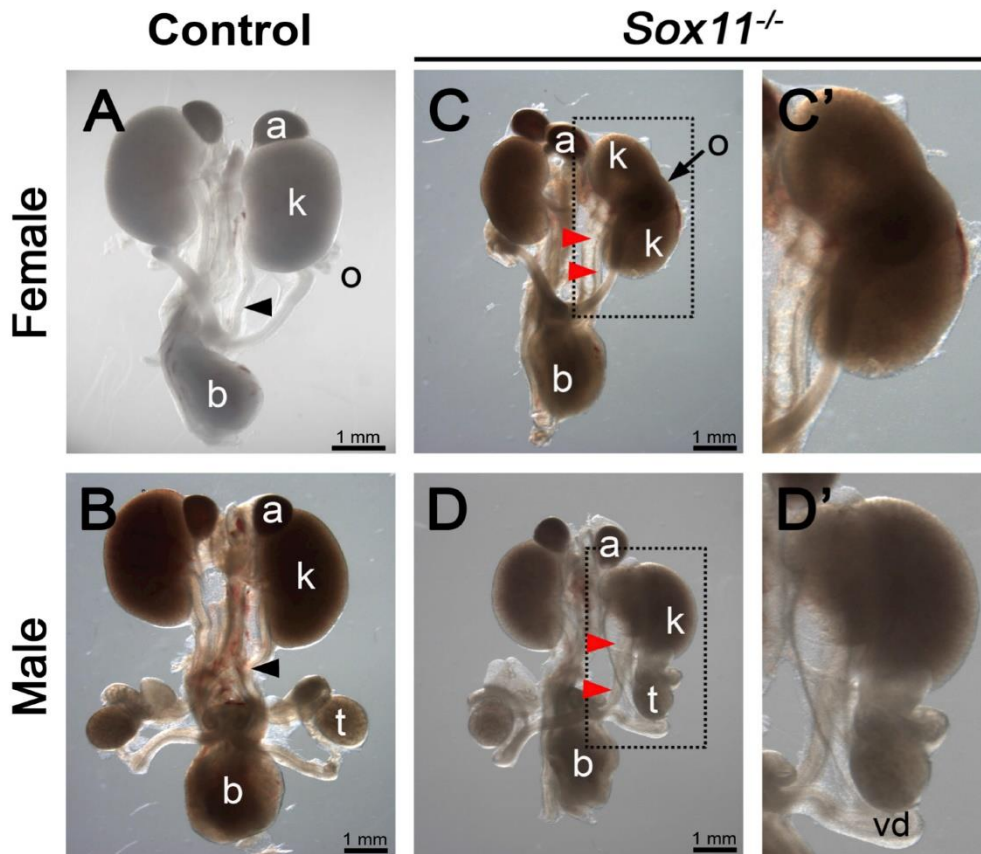
Table S1: Number of patients analysed and phenotypic classification

Table S2: List of antibodies and primers used in this study.

Supplementary methods

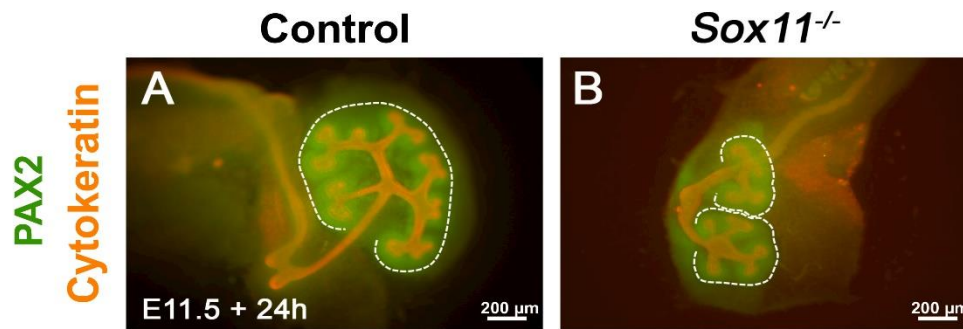
Supplementary references



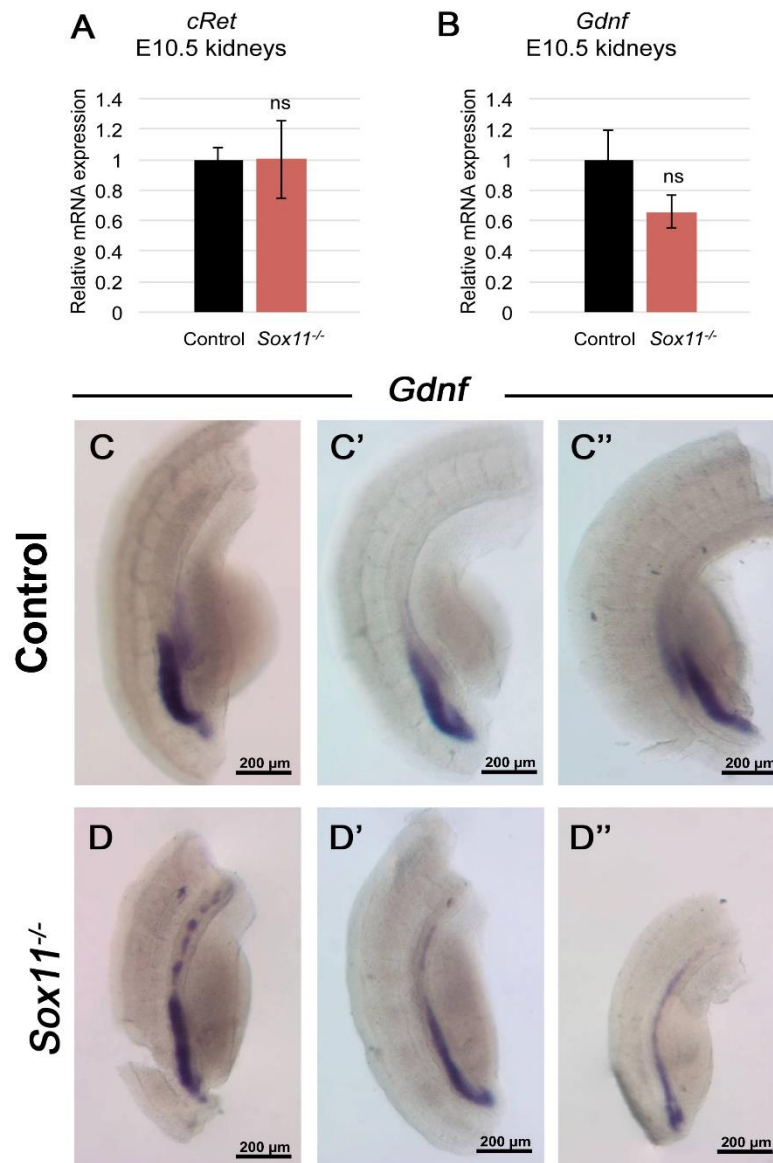


Supplementary Figure 2: Genital tract abnormalities are associated with duplex kidneys in Sox11 knock-out mice.

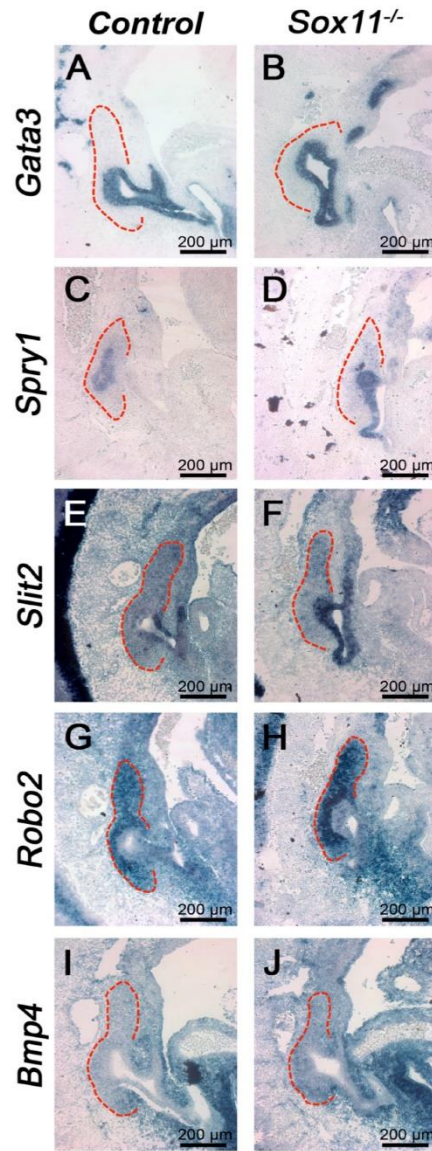
Urogenital tract of control (A,B) and Sox11 knock-out (C,D) E18.5 embryos. Control female (A) and male (B) urogenital tracts show normal kidneys (k), adrenal glands (a), ureters (black arrowhead), ovary (o) and testis (t). Sox11 knock-out female embryos (C) show duplex kidneys (k) and supernumerary ureters associated with ectopic ovary (o). Sox11 knock-out male embryos (D) show duplex kidneys associated with an hydroureter (red arrowheads) connecting to the vas deferens (vd) and undescended testis (t). Scale bars: 1 mm.



Supplementary Figure 3: Ex-vivo supernumerary bud formation in Sox11 knock-out embryos. Dissected urogenital ridges of E11.5 Sox11 mutant embryos were cultured for 24 hours and stained with PAX2 and Cytokeratin. A single ureteric bud has emerged and branched in Sox11^{+/+} embryos (A), whereas two ureteric buds had emerged from the Wolffian duct in the absence of Sox11 (B). Scale bars: 200μm.

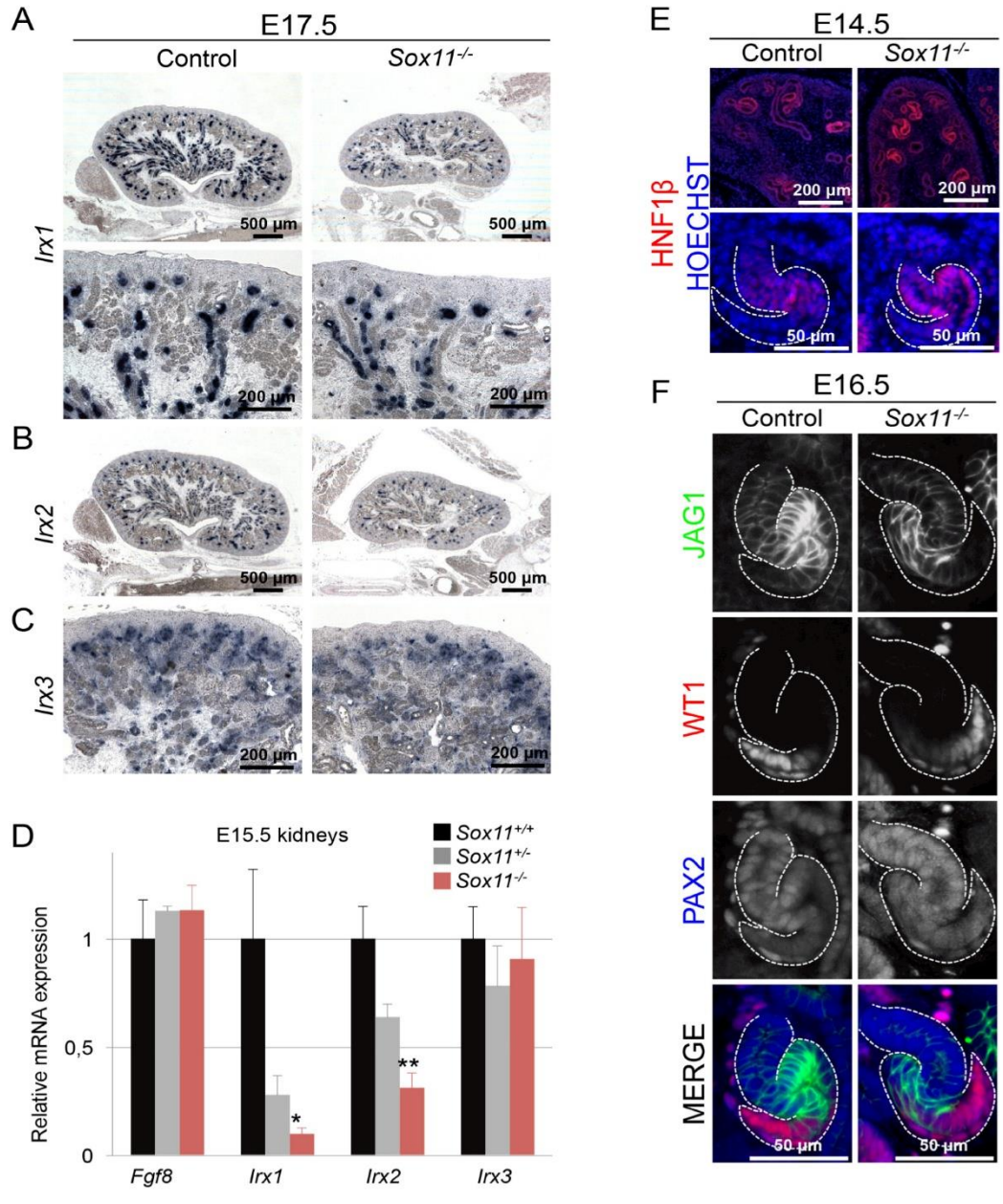


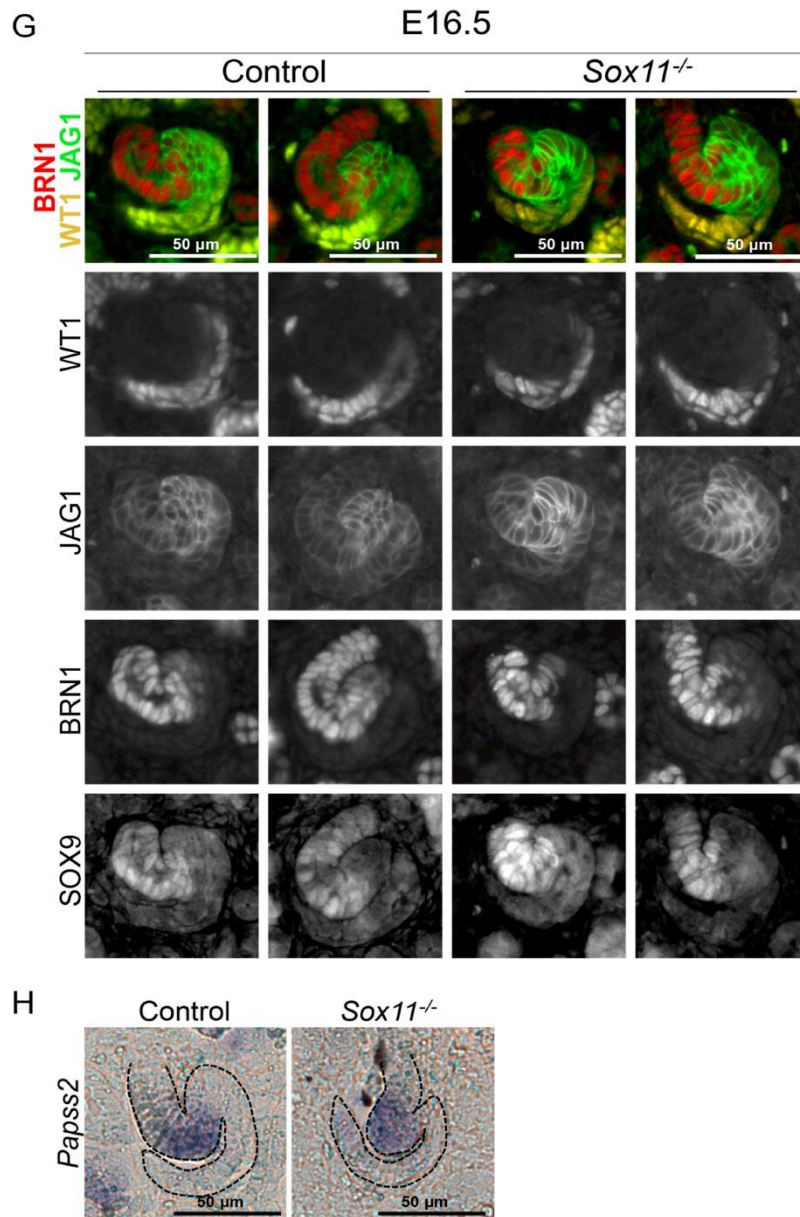
Supplementary Figure 4: Rostral extension of the Gdnf expression domain in Sox11 mutants.
 (A,B) *c-Ret* and *Gdnf* qPCR analysis shows no significant changes in E10.5 Sox11 mutant embryos compared to controls. Data are presented as the average with SEM (ns : non-significant). (C,D) Wholemount ISH on urogenital tracts of E10.75 embryos using *Gdnf* probe shows a rostral extension of the *Gdnf* expression domain in Sox11 knock-out embryos. C, C', C'' and D, D', D'' show different wildtype and Sox11 mutant embryos, respectively. Scale bars: 200μm.



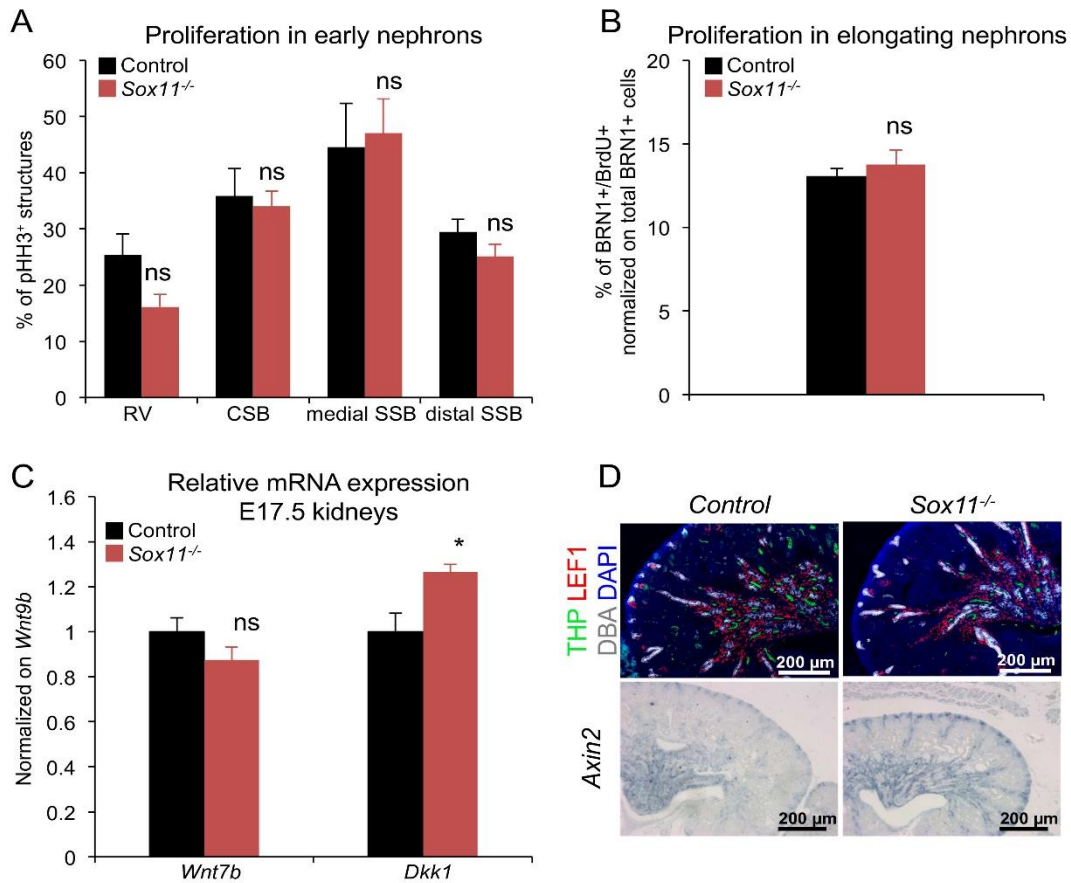
Supplementary Figure 5: Expression of genes known to be involved in ureteric bud outgrowth is not affected by the absence of Sox11.

In situ hybridization at E10.75 of control (A,C,E,G,I) and Sox11 knock-out (B,D,F,H,J) embryos. Gata3 (A,B), Sprouty1 (C,D), Slit2 (E,F), Robo2 (G,H) and Bmp4 (I,J) expression patterns are similar between control and Sox11 mutant. Dotted lines delineate the metanephric mesenchyme. Scale bars: 200µm.



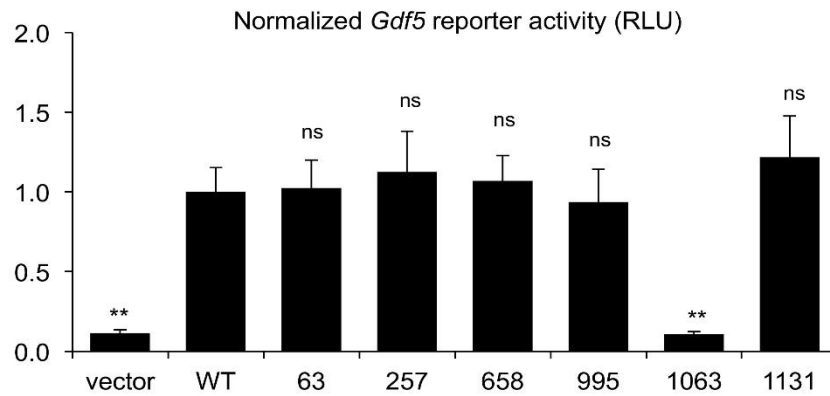


Supplementary Figure 6: Nephron patterning genes are expressed in *Sox11* mutants.
(A-C) Expression of *Irx1* (A), *Irx2* (B), *Irx3* (C) is maintained in nascent nephrons of *Sox11* mutant mice. **(D)** qPCR analysis on E15.5 kidneys shows decreased expression levels of *Irx1* and *Irx2* in *Sox11* mutants, highlighting the lack of elongated Henle's loop structures, while *Fgf8* and *Irx3* levels were unchanged. **(E-H)** Immunofluorescence and In situ hybridization analyses show that early nephron patterning is maintained in *Sox11* mutants.



Supplementary Figure 7: Analysis of proliferation and the Wnt/ β-catenin pathway.

(A,B) No significant change in proliferation rate using the pHH3 or BrdU markers were observed in the early nephron structures (renal vesicle (RV), comma (CSB) and S-shaped bodies (SSB)) nor in the elongating loop of Henle. (C,D) qPCR, immunostaining and in situ hybridization reveals no significant changes in Wnt7b, Dkk1, LEF1 and Axin2. Data are presented as the average with SEM (*p<0.05, ns : non-significant). Scale bars: 200μm.



Supplementary Figure 8: Effect of variants on SOX11 trans-activation function in HEK293 cell line.

Transient transfection of HEK293 cells with *Gdf5* reporter and expression vectors for wildtype *SOX11* (wt), *SOX11* variants (numbers corresponding to mutations in the coding sequence) or empty vector. Reporter activities (RLU, relative luciferase units) were normalized for transfection efficiency and on wt condition. Data are represented as the average \pm SEM of three experiments conducted in triplicate. ns: non-significant, **:p<0.01 versus wt (Student t-test).

Table S1: Number of patients analysed and phenotypic classification

CAKUT* phenotype	Number of patients
Pelvic kidney	2
Horseshoe kidney	3
Duplex collecting system	181
Renal agenesis	15
Kidney hypo/dysplasia	51
Multicystic dysplastic kidney	36
Vesicoureteral reflux	25
Ureteropelvic junction obstruction	136
Hydronephrosis	14
Obstructive megaureter	2
Posterior urethral valves	65
VACTERL* association with CAKUT	30
Total	560

*CAKUT, congenital anomalies of the kidney and urinary tract
VACTERL, Vertebral anomalies, Anal atresia, Cardiac defects,
Tracheoesophageal fistula and/or Esophageal atresia, Renal and Radial anomalies, and Limb defects.

Table S2 : Antibodies and primers used in this study.

Antibodies		
	Dilution	Producer
BRN1	1:1000	Michael Wegner Ref ¹
pan-Cytokeratin	1:500	Sigma, C2562,
Cytokeratin 18	1:500	Abcam, ab 52948
DBA	1:100	Sigma, L6533
FOXD1	1:100	Santa Cruz Biotechnology, sc47585
GFP	1:500	Abcam, AB290
phospho-Histone H3	1:300	Abcam, ab14955
JAG1	1:500	Santa Cruz Biotechnology, sc-6011
LEF1	1:200	Clinisciences
LTL	1:200	Abcys, B-1325
NCC	1:200	Millipore, AB3553
Nephrin/NPHS1	1:200	R&D Systems, AF3159
PAX2	1:200	Covance, PRB-276P
Podocin/NPHS2	1:250	Sigma, P0372
SIX2	1:200	Proteintech, 11562-1-AP
α -SMA Cy3-conjugated	1:1000	Sigma, C6198, 1/1000
SOX11	1:500	Michael Wegner Ref. ²
THP	1:500	AbD Serotec, 8595-0054
Uromodulin	1:500	Meridian
WT1	1:100	DAKO, M3561
qPCR primers		
Name	Forward	Reverse
<i>cRet</i>	TGGAGTTTAAGCGGAAGGAG	ACATCTGCATCGAACACCTG
<i>Dkk1</i>	CTGAAGATGAGGAGTGCGGCTC	GGCTGTGGTCAGAGGGCATG
<i>Fgf8</i>	TCCTGCCTAAAGTCACACAGC	TGAGCTGATCCGTCACCA
<i>Gdnf</i>	TCCAACCTGGGGTCTACG	GACATCCATAAATTCATCTTAGAGTC
<i>Irx1</i>	GCCCCACAACAGTAAAGTC	CCCCTTAATCAGGCAGACG
<i>Irx2</i>	GCATTCACCTGGCGTCCCACT	CACAGCCCTCACTGGTATCTT
<i>Irx3</i>	AGGAGGGCAATGCTTATGG	TGCTCTTTCCTCGTCTTCC
<i>Wnt7b</i>	ATGCGGTCTCCAGAACCT	TTCTCGTCGCTTTGTGGATG
<i>Wnt9b</i>	ATGCGGTCTCCAGAACCT	TTCTCGTCGCTTTGTGGATG

Mutagenesis primers	
Mut_SOX11_63_Fw	GGAGGCGCTGGACACTGAGGAGGGCGAATTCATGGC
Mut_SOX11_63_Rs	GCCATGAATTCGCCCTCCTCAGTGTCCAGCGCCTCC
MutSOX11_257_Fw	AGAGGCTGGGCAAGCTCTGGAAAATGCTGAAGG
MutSOX11_257_Rs	CCTTCAGCATTTTCCAGAGCTTGCCCAGCCTCT
Mut_SOX11_658_Fw	GACGGTCAAGTGCATGTTTCTGGATGAGG
Mut_SOX11_658_Rs	CCTCATCCAGAAACATGCACTTGACCGTC
MutSOX11_995_Fw	CGCAGCCCGCGCTGTTGCCCGCGTCCTCGCG
MutSOX11_995_Rs	CGCGAGGACGCGGGCAACAGCGCGGGCTGCG
MutSOX11_1131_Fw_nv2	CGCGCACAGCGCCAGTGAGCAGCAGCTGGGG
MutSOX11_1131_Rs_nv2	CCCCAGCTGCTGCTCACTGGCGCTGTGCGCG
ChIP-qPCR primers	
CCR_F	GCACATTTCTACCTCACTCG
CCR_R	CCCTTCTCCACCCTTTCCTG
Control_F	CCAGCATTGGGATGTGAAGACTG
Control_R	CGTGGCTATTCTGATCCACC

Supplementary Methods

ISH analysis

Embryos were fixed in 4% paraformaldehyde in PBS overnight at 4°C. ISH on section and wholemount ISH were carried out as previously described³. Riboprobes for *Ret*⁴, *Gata3* (kind gift from M. Bouchard), *Gdnf*, *Papss2* (kind gifts from F. Costantini and S. Cereghini)⁵, *Robo2* & *Slit2*⁶, *Bmp4*⁷, *Sprouty1*⁸ and *Ncc*, *Nkcc2*, *Slc5a1*, *Slc5a2*⁹, were synthesized as described previously¹⁰.

Histological and immunological analyses

Embryonic samples from timed matings (day of vaginal plug = E0.5) were collected, fixed in 4% paraformaldehyde *o/n* at 4°C, dehydrated and then embedded in paraffin. Microtome sections of 7 µm thickness were examined histologically after periodic acid-Schiff staining. For immunofluorescent analysis, dewaxed and re-hydrated sections were treated in 10 mM Na citrate (pH 6) for 2 min in a pressure cooker and incubated for 2 hours in 3% BSA, 10% normal donkey serum (Jackson Laboratories), 0.1% Tween20 in PBS). Primary antibodies (Suppl. Table 2) were diluted in 3% BSA, 3% normal donkey serum, 0.1% Tween20 in PBS and incubated overnight at 4°C. Relevant Cy2-, Cy3- or Cy5-conjugated secondary antibodies (Jackson Laboratories), or AlexaFluor 488-, 594- or 647-conjugated secondary antibodies (Invitrogen), or Biotin-conjugated antibody (Jackson Laboratories, 515-065-003, 1/500) followed by Streptavidin-Cy3 (Sigma, S6402, 1/1000) were used. After mounting (Hoechst, Invitrogen) images were taken on a Zeiss Axio ImagerZ1 (AxioCam MRM camera) and processed with Photoshop. Immunofluorescent analysis on organ cultures was carried out as described previously¹⁰.

RT-qPCR

Total RNA was extracted from the dissected caudal area of urogenital ridges of *Sox11* knockout and wildtype E10.75 embryos using the RNeasy MicroKit (Qiagen) followed by column DNase digestion to remove any contaminating genomic DNA. Samples (n=6) were reverse transcribed (M-MLV, Invitrogen) in combination with random primers. qPCR was performed using the TaqMan Master Kit (Roche) and a Light Cycler 1.5 (Roche). Expression levels were normalized for *Hprt*. Primers were designed on the Roche Universal ProbeLibrary website. Primer sequences are available as Supplementary Table 2.

ChIP-qPCR

Kidneys were isolated from E14.5 wild-type embryos (OF1, purchased from Charles River) in PBS and kept on ice until dissociation with trypsin (Gibco) at 37°C. Cells were 1% formaldehyde-fixed, washed, and nuclei released in lysis buffer (20 mM Tris pH8.0, 85mM KCl, 0,5% NP40, 0,5% SDS) using a 27G needle. Nuclei were collected by centrifugation, washed and re-suspended in sonication buffer (50 mM Hepes pH7.4, 140 mM NaCl, 1 mM Edta, 1% Triton, 0,1% NaDeoxycholate, 0.4% SDS, Protease inhibitor cocktail (Roche)). Chromatin was sheared to an average size of 300-700 nucleotides using a BioruptorPlus sonicator (Diagenode) for 25 × 30 s. Chromatin was immunoprecipitated with two different SOX11 antibodies (HPA000536, Sigma and kind gift from M.Wegner) or IgG, and protein-A sepharose beads (P3391, Sigma). After extensive washes and elution, chromatin was purified using the QIAquick PCR purification columns (Qiagen) and quantified using the Qubit dsDNA HS Assay Kit (Life technologies).

For qPCR reactions, same DNA quantities (25 pg) or same volumes (1/50 of the eluats) were amplified with Sybgreen (Roche) using primers located in the HS19-20 regulatory element of the protocadherin β cluster control region (CCR) or in the 3'UTR region of *Cd24a* gene as a negative control (Table S2). Fold enrichments were calculated using the standard curves method with normalization on IgG.

Reporter assays

pBluescript plasmid containing coding sequence (kind gift from P. Berta) were used for mutagenesis. Mutations were introduced by site-directed mutagenesis into full-length human *SOX11* plasmid using the QuickChange II XL Kit (Stratagene) and primers listed in Suppl, Table 2) and subcloned into pcDNA3.1 expression vector (Life Technologies). The expression vector for the 12 nucleotides insertion variant (mut1063) was a kind gift from A. Morris ¹¹.

For transient transfection, 12×10^4 HEK293 cells were plated per well of 24-well plates. Mixtures of 50 ng pCMV-Sport- β gal plasmid (Life Technologies), 50 ng pcDNA3.1-*Sox11* expression plasmid, 150 ng *Gdf5*-promoter reporter plasmid ¹² and 0.75 μ l FuGENE HD (Roche) were added to the cells 6 hours after plating. β -Galactosidase and luciferase activities were assayed after 24 h using the β -galactosidase Enzyme and Luciferase Assay System (Promega), respectively. Reporter activities were normalized for transfection efficiency.

Supplementary references:

1. Friedrich RP, Schlierf B, Tamm ER, Bosl MR, Wegner M. The class III POU domain protein Brn-1 can fully replace the related Oct-6 during schwann cell development and myelination. *Mol Cell Biol.* 2005;25(5):1821-1829.
2. Hoser M, Potzner MR, Koch JM, Bosl MR, Wegner M, Sock E. Sox12 deletion in the mouse reveals nonreciprocal redundancy with the related Sox4 and Sox11 transcription factors. *Mol Cell Biol.* 2008;28(15):4675-4687.
3. Acloque H, Wilkinson DG, Nieto MA. In situ hybridization analysis of chick embryos in whole-mount and tissue sections. *Methods in cell biology.* 2008;87:169-185.
4. Pachnis V, Mankoo B, Costantini F. Expression of the c-ret proto-oncogene during mouse embryogenesis. *Development.* 1993;119(4):1005-1017.
5. Heliot C, Desgrange A, Buisson I, et al. HNF1B controls proximal-intermediate nephron segment identity in vertebrates by regulating Notch signalling components and *lrx1/2*. *Development.* 2013;140(4):873-885.
6. Grieshammer U, Le M, Plump AS, Wang F, Tessier-Lavigne M, Martin GR. SLIT2-mediated ROBO2 signaling restricts kidney induction to a single site. *Dev Cell.* 2004;6(5):709-717.
7. Goncalves A, Zeller R. Genetic analysis reveals an unexpected role of BMP7 in initiation of ureteric bud outgrowth in mouse embryos. *PLoS One.* 2011;6(4):e19370.
8. Basson MA, Akbulut S, Watson-Johnson J, et al. Sprouty1 is a critical regulator of GDNF/RET-mediated kidney induction. *Dev Cell.* 2005;8(2):229-239.
9. Raciti D, Reggiani L, Geffers L, et al. Organization of the pronephric kidney revealed by large-scale gene expression mapping. *Genome Biol.* 2008;9(5):R84.
10. Reginensi A, Clarkson M, Neirijnck Y, et al. SOX9 controls epithelial branching by activating RET effector genes during kidney development. *Hum Mol Genet.* 2011;20(6):1143-1153.
11. Pillai-Kastoori L, Wen W, Wilson SG, et al. Sox11 is required to maintain proper levels of Hedgehog signaling during vertebrate ocular morphogenesis. *PLoS Genet.* 2014;10(7):e1004491.
12. Kan A, Ikeda T, Fukai A, et al. SOX11 contributes to the regulation of GDF5 in joint maintenance. *BMC developmental biology.* 2013;13:4.

Sox 11 role in MM domain specification

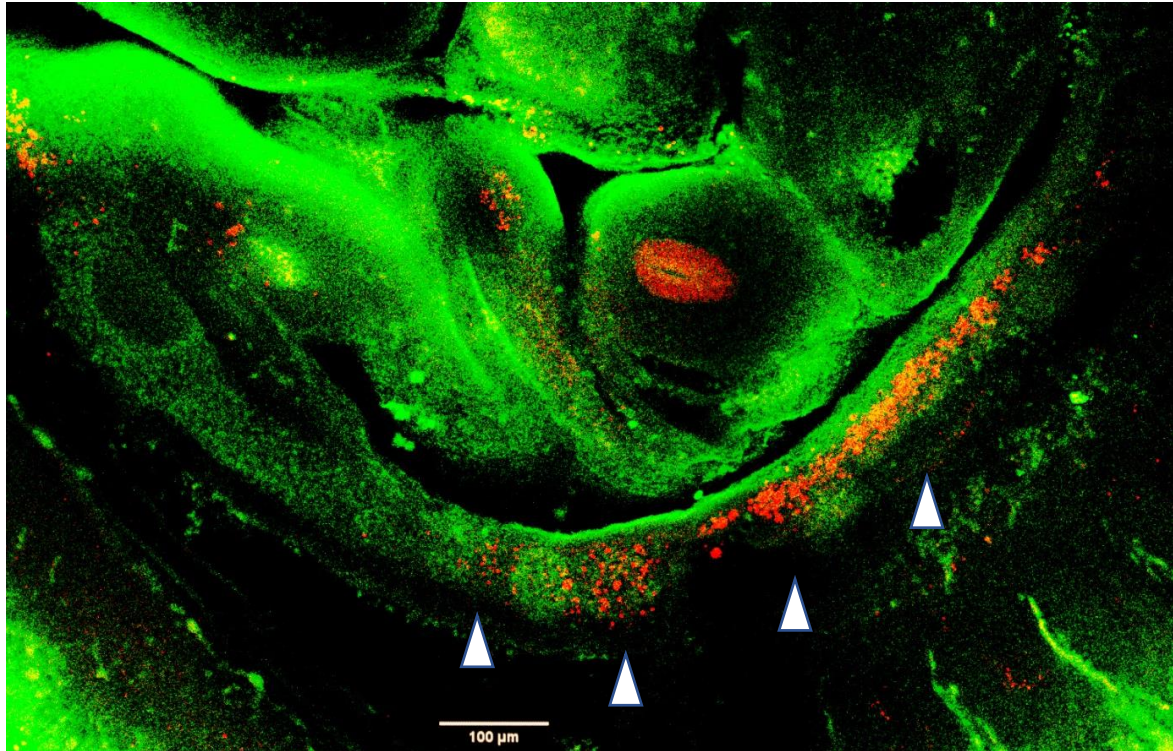
The above article demonstrated the duplex kidney phenotype of *Sox11*^{-/-} mutant mice stemming from the defect in MM domain specification and the subsequent ectopic UB formation. However, the mechanism of *Sox11* action in UB formation remained unclear.

We proposed three possible models for defective MM specification in *Sox11*^{-/-} mice (see also Figure 4 in the review Kozlov & Schedl):

- 1) Lack of apoptosis leading to abnormal survival of rostral MM cells
- 2) Defects in MM cell migration leading to mispositioning of the MM domain
- 3) Defects in NC cell differentiation leading to an imbalance in NC-derived cell lineages.

1. Effect of *Sox11* deletion in NC cells survival.

To test the process of apoptosis in the NC, 3D imaging of E10.5 mouse embryo was performed. The analysis revealed active apoptosis occurring in NC in the region rostral to the forming UB).



SIX2 LysoTracker Red

Figure 11: 2D slice of wholemount wildtype E10.5 embryo staining using antibody against SIX2 (green) and LysoTracker Red (red). Arrow indicates UB invading MM. Triangles indicate apoptosis in NC.

When compared against wildtype E10.5 embryos, the *Sox11*^{-/-} embryos do not display qualitative differences in apoptosis in IM. Both conditions reveal apoptosis occurring in IM rostrally to the UB (Figure 12). While this observation is limited by the resolution of confocal system, future improvements in the resolution of wide-angle confocal images could allow for quantification of apoptosis in IM. This quantitative approach would allow to conclusively reject the model where *Sox11* knockout leads to decrease in apoptosis and subsequent expansion of MM domain by finding the absence of effect of *Sox11* knockout on apoptosis.

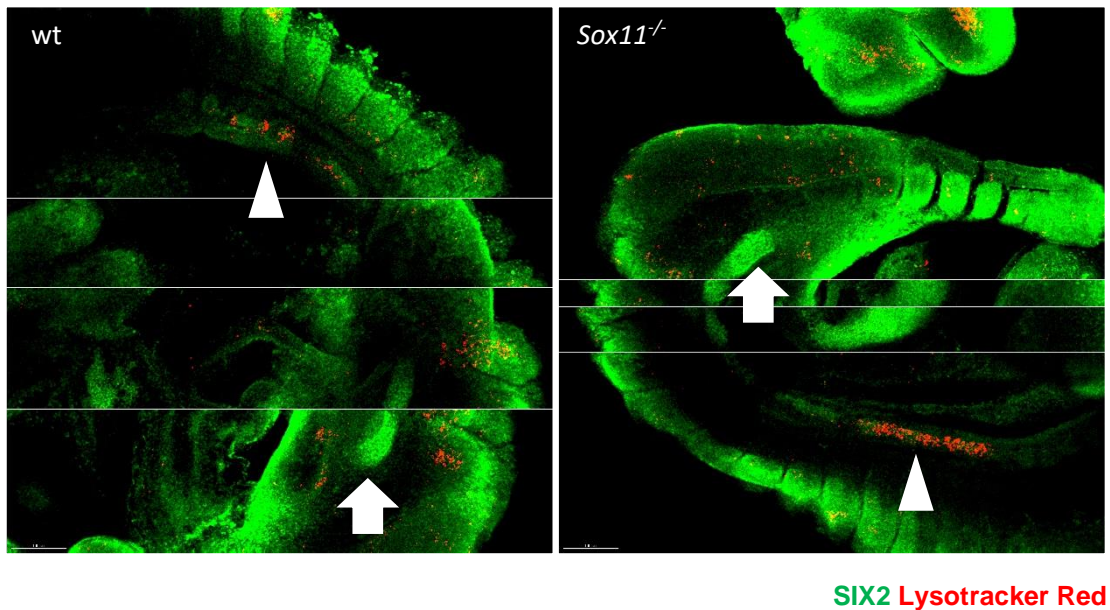


Figure 12: Comparison of wildtype (wt) and *Sox11*^{-/-} E10.5 embryos reveals that both conditions display apoptosis in the NC. White lines indicate transition to a different confocal slice. Arrows indicates U invading MM. Triangles indicate apoptosis in NC.

2. Effect of *SoxC* deletion on NPC migration.

Since apoptosis was found to occur both in wildtype and in *Sox11*^{-/-} nephrogenic cords, defective cell migration was tested as an alternative model for the rostral expansion of the MM domain in *Sox11*^{-/-} embryos. As *Sox4* and *Sox12* share molecular functions with *Sox11*, we decided to evaluate a potential effect on cell migration in cells that are defective (knockout) for all three *SoxC* genes.

To characterize the role of *SoxC* genes in cell migration and nephrogenesis, a conditional triple knockout mouse model was employed. The *CAG*^{CreERT2} line is a powerful system that allows timed deletion of *floxed* alleles through the simple addition of tamoxifen. The *CAG*^{CreERT2} *Sox4*^{flox/flox} *Sox11*^{flox/flox} *Sox12*^{-/-} mouse line was established, which is knockout on *Sox12* gene and has two other *SoxC* genes flanked by *flox* elements to achieve Tamoxifen-inducible conditional knockout (Figure 13). Renal progenitor cells were isolated from *CAG*^{CreERT2} *Sox4*^{flox/flox} *Sox11*^{flox/flox} *Sox12*^{-/-} mice by collagenase-pancreatin treatment, which releases the outer layer of kidney cells into the solution (Figure 14).

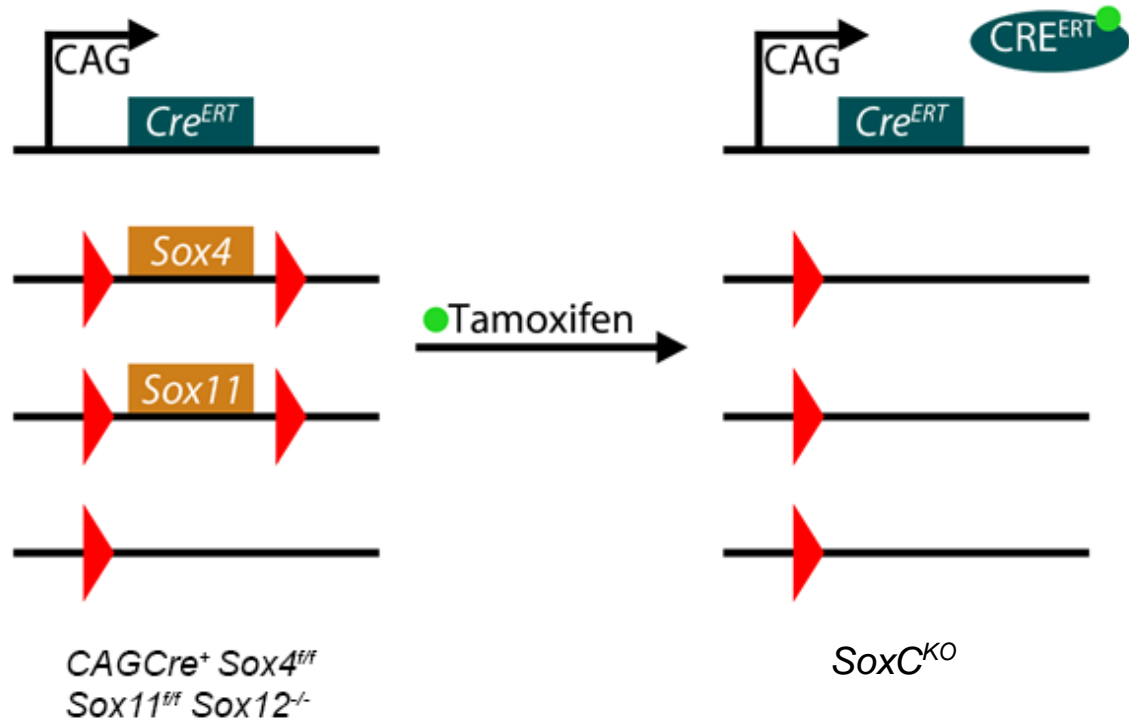
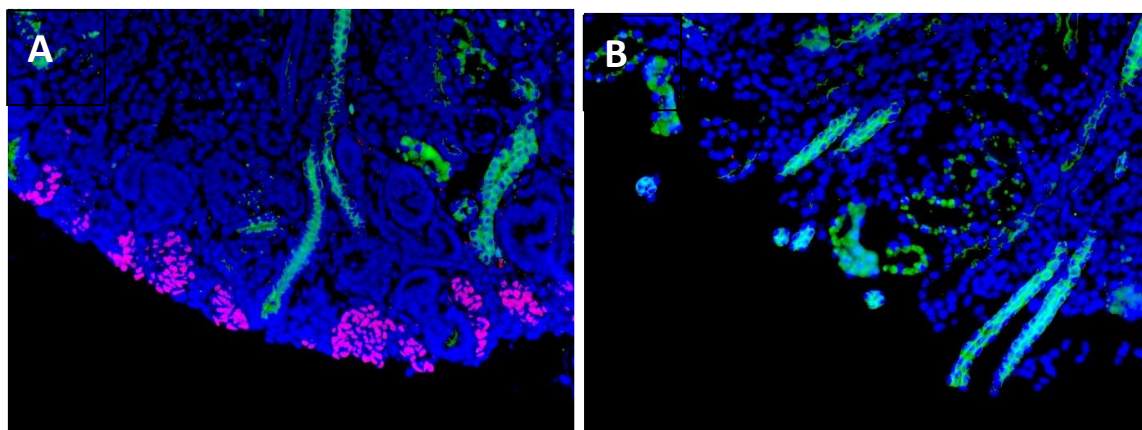


Figure 13: A transgenic mouse model was used to obtain a triple SoxC knockout in $CAGCre^+ Sox4^{f/f} Sox11^{f/f} Sox12^{-/-}$ NPC after the addition of 4OH-tamoxifen to the cell media.



SIX2 CYTOKERATIN DAPI

Figure 14: (A-B) The extent of kidney ablation before (A) and after (B) collagenase-pancreatin treatment. Note that all SIX2 positive cells were released during the mild treatment. Blue: DAPI; Green: Cytokeratin; Red: SIX2

After releasing kidney cells into the medium, a further selection is required to separate renal progenitor cells from other cell types in the embryonic kidney. For this purpose, the cell

suspension extracted from E16.5 embryonic kidneys were purified by magnetic-activated cell sorting (MACS) and cultured in medium that allows expansion of cells without losing their stem cell characteristics (Figure 15)

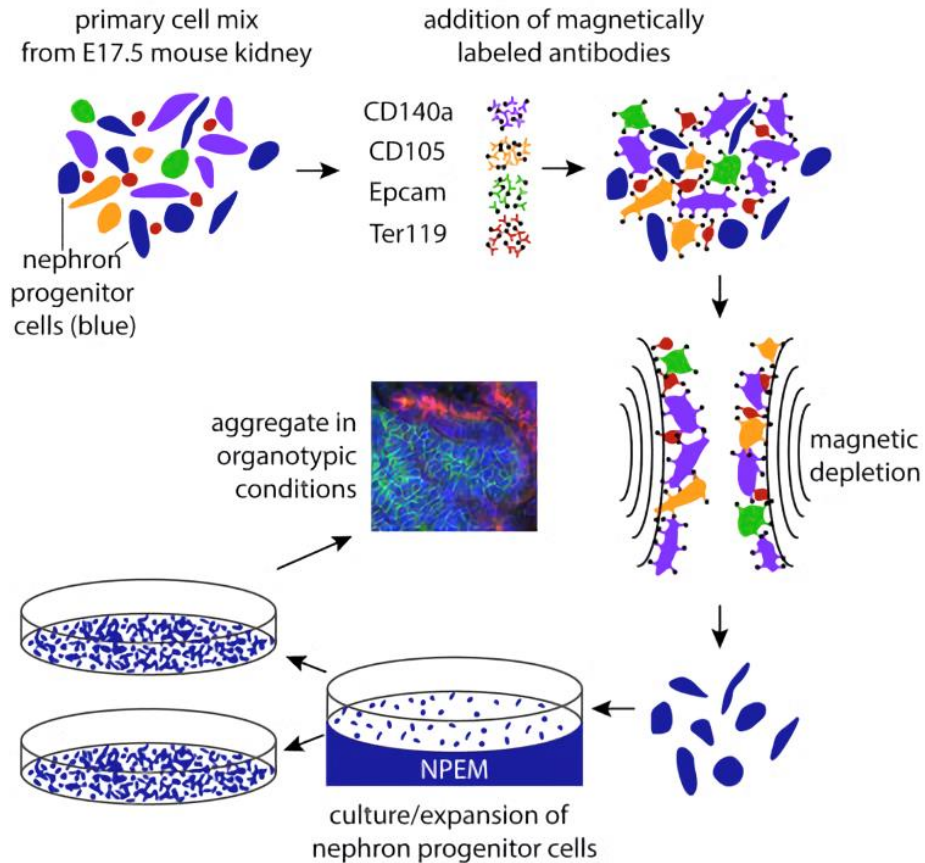


Figure 15: Isolation of NPC by MACS (Brown et al., 2015)

The NPC harvested in this fashion can be maintained in culture for several passages, maintaining their progenitor state as long as the cell density doesn't reach confluence (Figure 16). The addition of 4-OH-Tamoxifen to the medium results in subsequent deletion of *Sox4* and *Sox11* (Figure 20), effectively rendering the cells devoid of SOXC proteins.

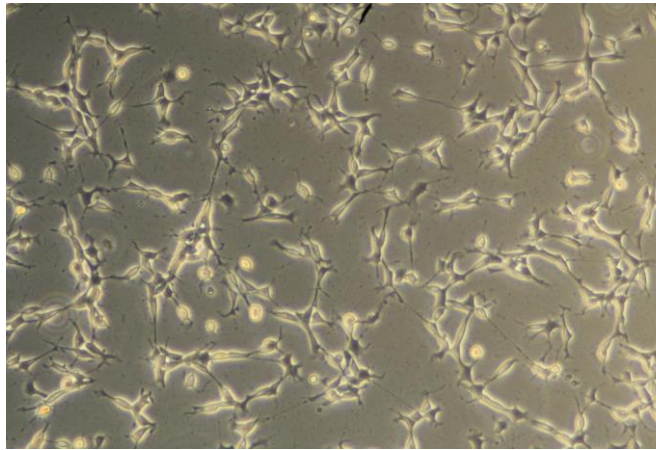


Figure 16: Isolated NPCs after 24h in culture.

To assess the impact of *SoxC* deletion on cell migration, an *in vitro* scratch wound assay was performed (Figure 17, Figure 18). *CAGCre⁺ Sox4^{ff} Sox11^{ff} Sox12^{-/-}* NPC demonstrate complete absence of migration compared to control *CAGCre⁻ Sox4^{ff} Sox11^{ff} Sox12^{-/-}* NPC.

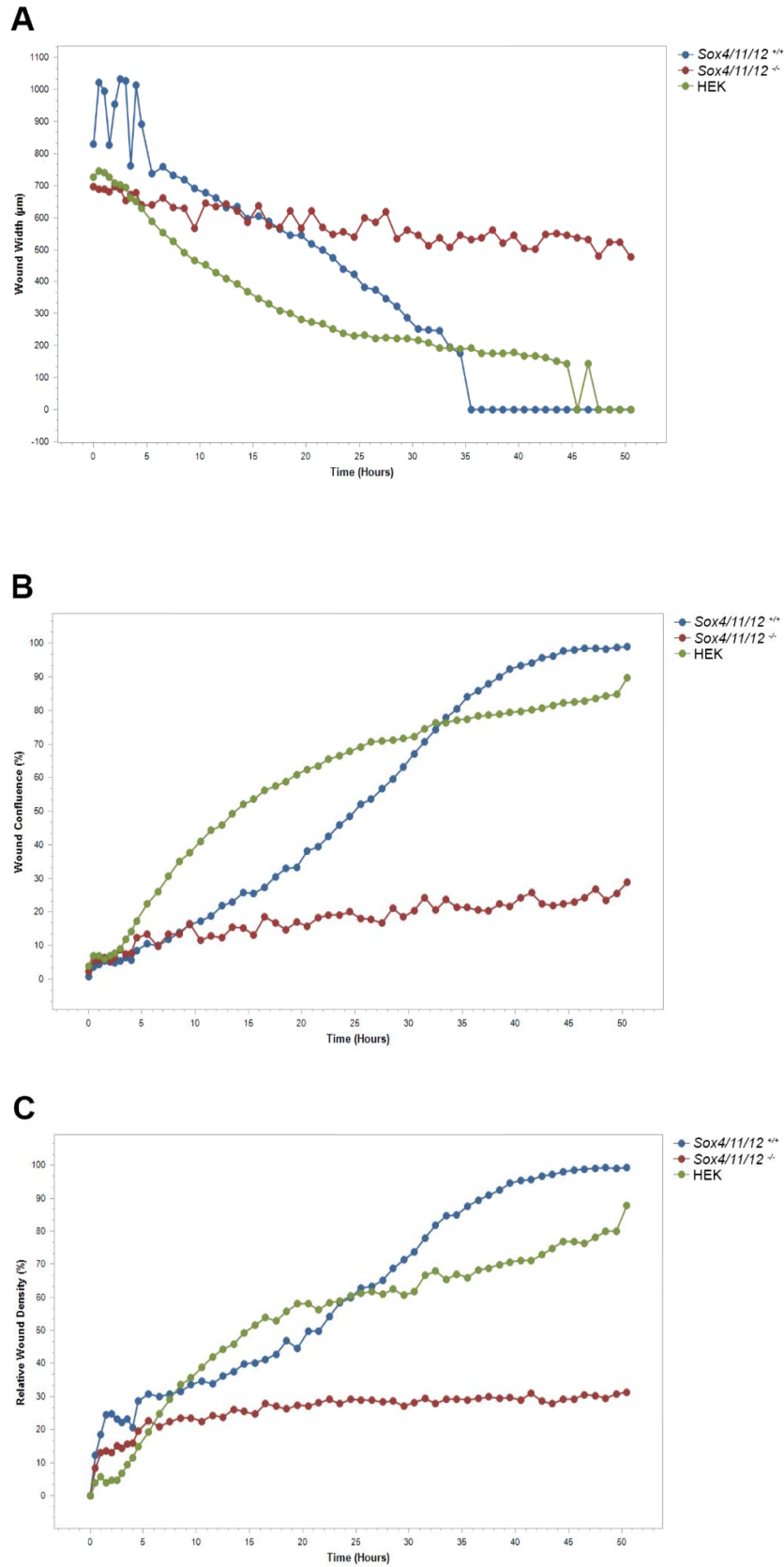


Figure 17: Dynamics of wound closure. (A) Wound width over time, (B) Wound confluence over time, (C) Relative wound density over time. Blue: SoxC⁺ NPC, Red: SoxC^{KO} NPC, Green: HEK cells.

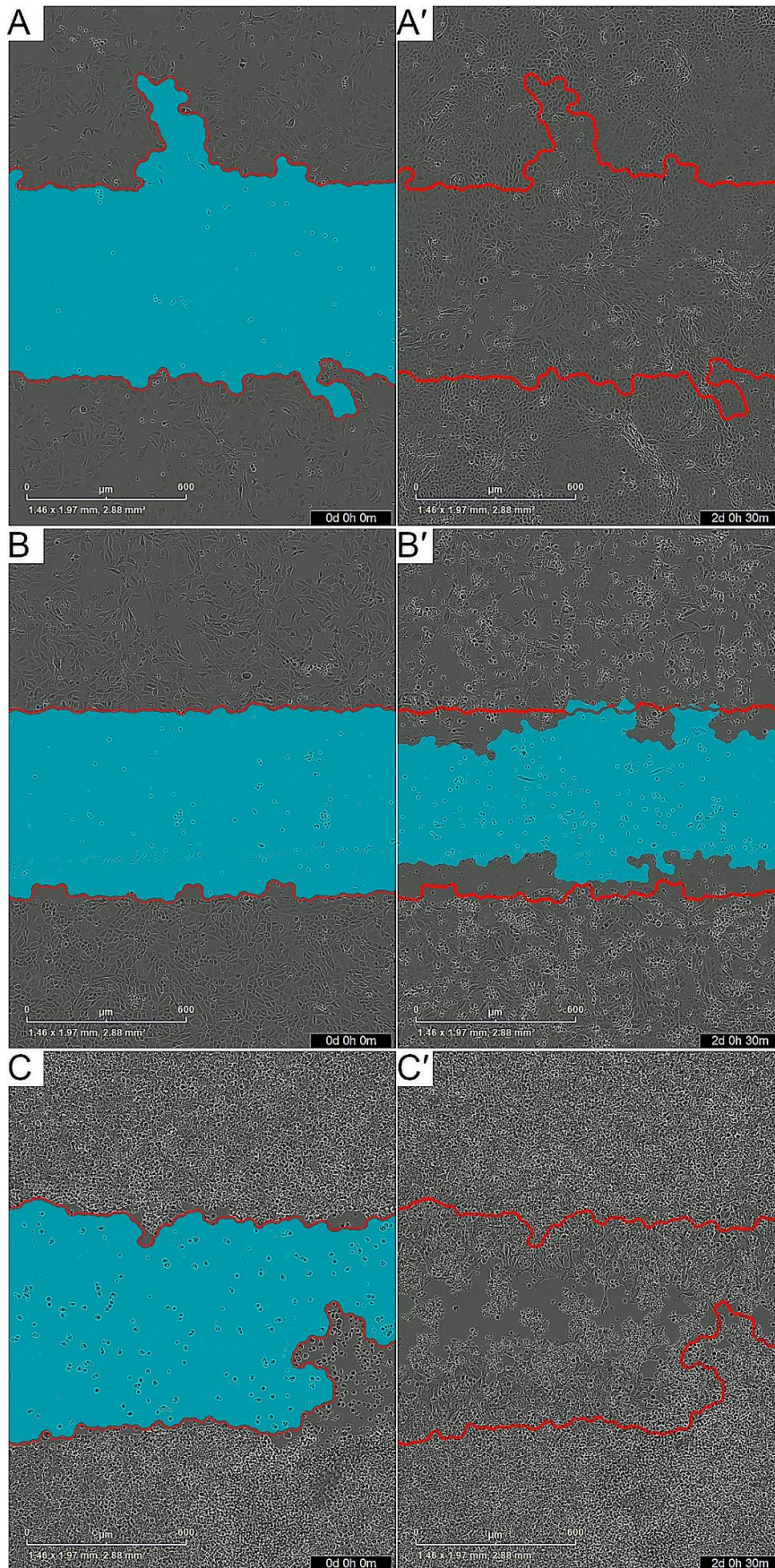


Figure 18: Progress of wound closure over 48h period. (A-A') SoxC⁺ NPC, (B-B') SoxC^{KO} NPC, (C-C') HEK cells.

The scratch wound assay provides evidence that *SoxC* genes are involved in the process of migration of NPCs *in vitro*. However further experiments will be required to conclusively show that *Sox11* deletion leads to migration defect in the early MM domain specification and resulting ectopic UB outgrowth.

3. Effect of *Sox11* deletion on cell fate

Another possibility for the role of *Sox11* in MM domain specification is the existence of the subset of rostral MM cells that undergo transdifferentiation into another cell type under the control of *Sox11*. In *Sox11*^{-/-} embryos, these cells would remain in the MM domain and induce ectopic UB formation. In addition, the impact of *Sox11* on possible transdifferentiation in the MM population, which wasn't assessed in this project, could be studied using the lineage tracing approach. Initial lineage tracing experiments using *Six2*CRE mouse lines established SIX2+ cells as self-renewing renal progenitor cells in cap mesenchyme (Kobayashi et al., 2008). A closely related type of cells is renal interstitium cells, sharing a common origin from intermediate mesoderm and forming FOXD1+ renal cortical stroma. Once nephron and renal interstitial progenitor cells are specified at the onset of kidney development, their descendants maintain distinct fates segregated by a lineage boundary. PAX2 maintains the boundary by repressing transdifferentiation of nephron progenitor cells into interstitium-like lineage. (Naiman et al., 2017) While rare double-expressing FOXD1+ SIX2+ cells were found, they were representing the cells of nephron progenitor lineage. (Kobayashi et al., 2014; Brunskill et al., 2014) Therefore, it is unlikely that transdifferentiation of SIX2+ cells occurs in normal early kidney development.

Role of *SoxC* in MET

SoxC genes were found to be important not only on the early stages of kidney development, but in the process of nephrogenesis as well. As known from prior experiments in the lab, simultaneous inactivation of *Sox4* and *Sox11* in renal progenitor cell population leads to severe anomalies of kidney development, including renal hypoplasia and strong reduction in nephron numbers (Figure 19, A). The persistence of mesenchymal SIX2+ cell population coupled with the reduction in the number of epithelialized renal vesicles (Figure 19, B) suggests that the effect of *SoxC* knockout is mediated through preventing cells from undergoing mesenchymal-to-epithelial transition (MET), which is a crucial step in early nephrogenesis. To uncover the molecular mechanism behind the *SoxC* action in MET, I employed the conditional *SoxC* knockout cell culture system described earlier (Figure 13).

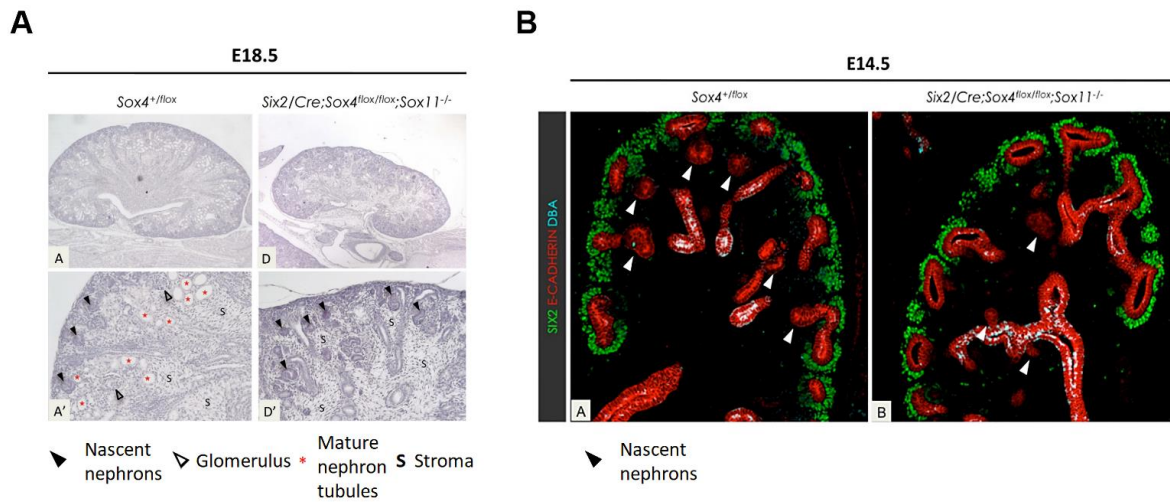
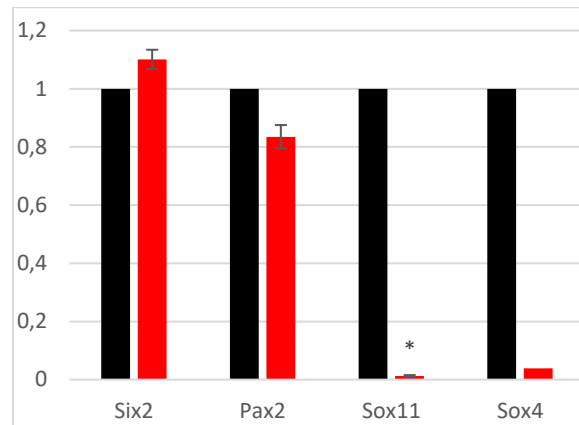


Figure 19: (A) Simultaneous inactivation of *Sox4* and *Sox11* leads to severe renal hypoplasia and a strong reduction in nephron numbers. (B) Immunofluorescence analysis at E14.5 confirmed a dramatic reduction in the number of nascent nephrons in *Six2^{CRE} Sox4^{flox/flox} Sox11^{-/-}* kidneys compared to controls. The defect does not result from a loss of renal progenitors, as strong *Six2* expression was still observed. (Data of Yasmine Neirijnck)

Effect of *SoxC* inactivation on NPC gene expression

qPCR analysis was performed on NPC after addition of 4-OH-tamoxifen to the culture medium (Figure 20). The analysis demonstrated maintenance of the progenitor markers *Six2* and *Pax2*, providing evidence that 4OH-tamoxifen does not interfere with the differentiation status of these cells. As expected, expression of *Sox4* and *Sox11* was entirely lost, thus confirming the suitability of the chosen approach. Moreover, the YAP/TAZ cofactor *Tead2*, a known target of SOX4, was significantly reduced in these cells, whereas the YAP/TAZ pathway targets *Serpine1* and *Cyr61* were increased. Thus, our data suggest that SOXC proteins regulate the YAP/TAZ pathway also within renal progenitors. However, since YAP/TAZ knockout mice do not show the same phenotype as *SoxC* knockout mice, additional levels of regulation must occur.



■ Control cells ■ *SoxC* knockout cells

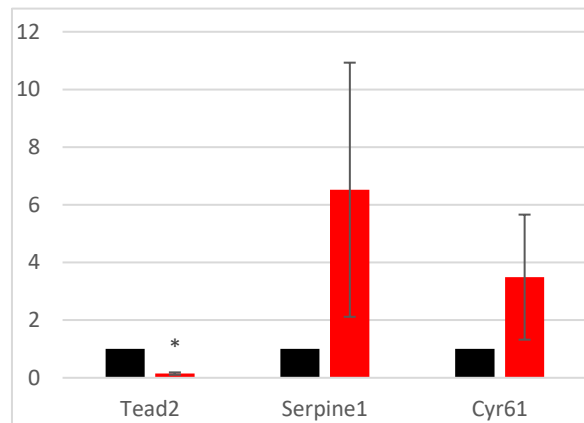


Figure 20: qPCR analysis of *CAGCre⁺ Sox4^{fl/fl} Sox11^{fl/fl} Sox12^{-/-}* NPC before and after 4OH-tamoxifen treatment. *Six2* and *Pax2* expression remains unchanged compared to control. *SoxC* genes and *SoxC* downstream target *Tead2* are downregulated. Genes downstream of *Tead2* show variable patterns of expression. Black: control, Red: treatment.

Organoid formation

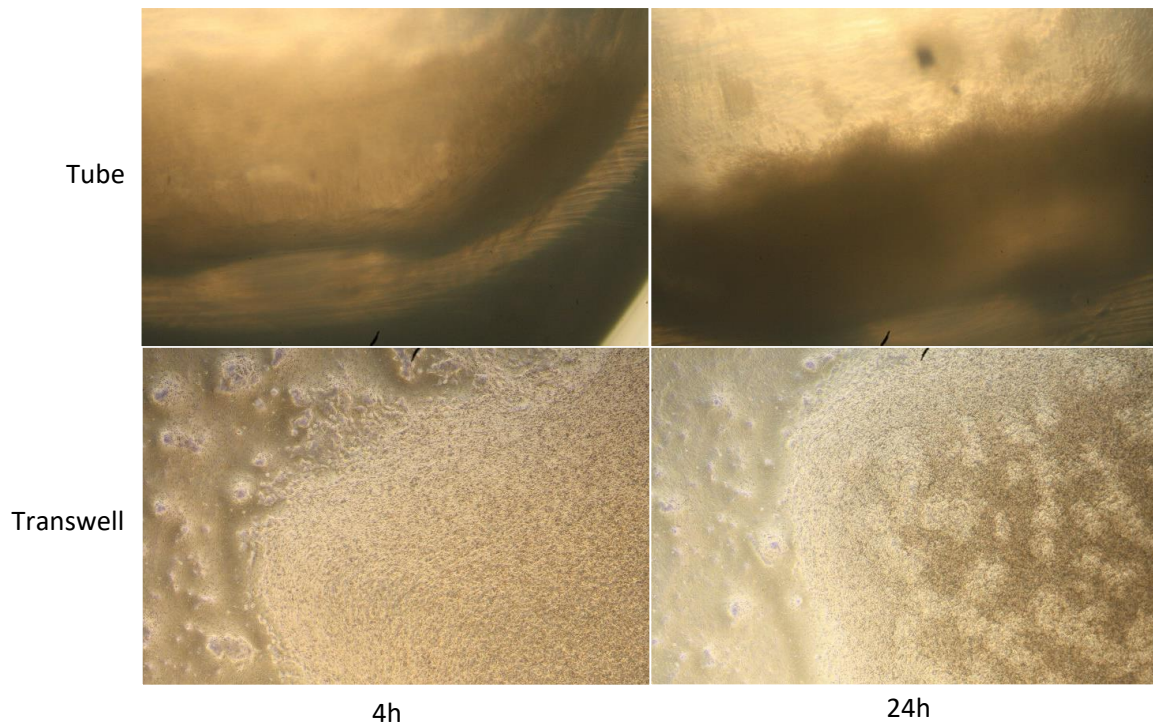


Figure 21: Images of organoid kidneys in tube and transwell before and after MET.

To analyse the MET dynamics *in vitro*, 3D organoid structures were employed as a better way to capture positional effects during nephrogenesis. Two different approaches were tested: tube organoids and transwell organoids (Figure 21). Tube organoid approach was ultimately selected as it requires lower cell numbers and therefore is more suitable for limited cell material split into multiple conditions.

Changes in NPC gene expression upon MET induction

Organoids were formed from NPCs and subjected to CHIR treatment to induce MET. To explore the dynamics of β -catenin signalling in the process of MET, two conditions of treatment were tested:

- Long CHIR treatment, where CHIR was added to the cell media for 48 hours,
- Pulse CHIR treatment, where CHIR was added to the cell media for 4 hours and then removed for 44 hours.

After the treatment, qPCR analysis indicated rise in E-cadherin expression in the condition of pulse CHIR treatment, when CHIR was added and removed; no rise on E-cadherin expression was observed in the condition where CHIR wasn't removed (Figure 22). As E-cadherin is a

marker of epithelialized cells, the condition where CHIR was added and removed represents normal nephrogenesis after successful MET. Additionally, *SoxC* knockout cells demonstrated the absence of E-cadherin expression after CHIR treatment, which indicates failure to undergo MET in the absence of SOXC.

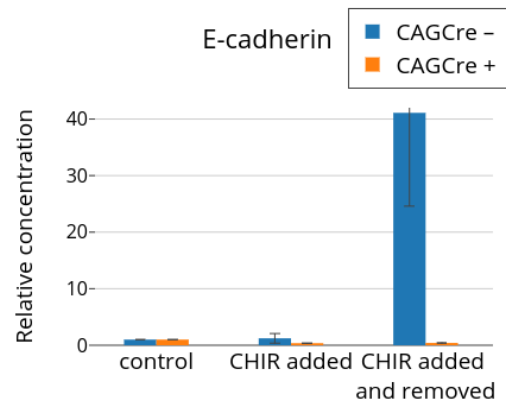


Figure 22: Rise of E-cadherin levels was observed in *Sox4^{fl/fl} Sox11^{fl/fl} Sox12^{-/-}* NPC after CHIR addition and removal; no rise was observed in *CAGCre⁺ Sox4^{fl/fl} Sox11^{fl/fl} Sox12^{-/-}* cells

Axin2 expression level, which serves as a proxy for β -catenin pathway activity, was found to be elevated after the addition of CHIR to the organoids (Figure 23). Interestingly, in the condition where MET was successful as indicated by E-cadherin expression, *Axin2* was no longer expressed. On the contrary, in *CAGCre⁺* cells, where *SoxC* genes were absent, *Axin2* levels were elevated as compared to control condition. These results suggest that in *SoxC^{KO}* cells undergoing MET, WNT/ β -catenin pathway activity is elevated compared to *SoxC⁺* cells. For MET to occur during nephrogenesis, transient elevation of β -catenin levels followed by reduction is required (Park et al., 2012), leading to the hypothesis that *SoxC* knockout prevents MET by keeping β -catenin levels abnormally high.

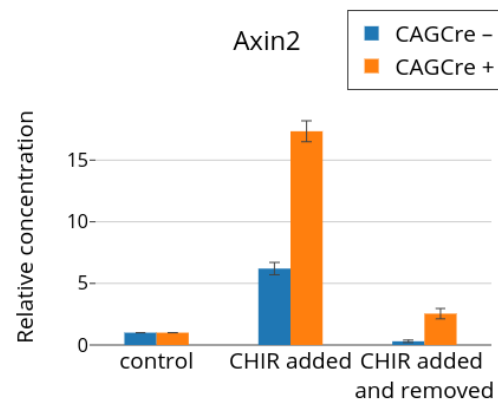


Figure 23: Rise of *Axin2* expression levels was observed in both in *Sox4^{fl/fl} Sox11^{fl/fl} Sox12^{-/-}* and *CAGCre⁺ Sox4^{fl/fl} Sox11^{fl/fl} Sox12^{-/-}* NPC after CHIR addition; however, *CAGCre⁺ Sox4^{fl/fl} Sox11^{fl/fl} Sox12^{-/-}* cells failed to suppress *Axin2* expression after CHIR removal

Comprehensive analysis of MET-related gene expression in the absence of *SoxC* genes

To provide more extensive and unbiased analysis of transcriptional dynamics in *SoxC^{-/-}* organoids, RNA-sequencing approach was employed. Two experimental conditions were analysed:

- **Baseline** NPC harvested immediately after MACS purification,
- **Pulse** NPC organoids that were treated with addition and removal of CHIR to induce MET, and then harvested,

Each experimental condition had three biological replicates.

The average RNA concentration yielded from 18 organoids was 56.6 ng/ μ L, and the average RNA integrity number (RIN) was 8.6 (Table 2).

Raw reads were filtered to remove reads containing adapters or reads of low quality, so that downstream analyses are based on clean reads. The filtering process was performed as follows:

- 1) Discard reads with adapter contamination
- 2) Discard reads when uncertain nucleotides constitute more than 10% of either read
- 3) Discard reads when low quality nucleotides (base quality less than 20) constitute more than 50% of the read

After performing quality control, an average of 49822310 reads were obtained from each sample. Overall, 94-97% of reads were mapped to the mouse genome. Among them, 89-92% of reads were uniquely mapped. (Figure 24)

Genotype	Condition and replicate	Raw data File size (GB)	Input Reads	Filtered reads	Overall Alignment rate (%)	Uniquely mapped reads (%)	RNA conc. (ng/ul)	RIN
<i>CAGCre⁻</i> <i>SoxC⁺</i>	Baseline 1	15.5	51642826	49949913	96.68	92.29	132	9.7
	Baseline 2	18.3	61081973	59266195	96.85	92.11	62	9.9
	Baseline 3	18	59922374	58230362	96.92	91.64	152	9.6
	Pulse 1	16.5	54926372	52866330	95.47	91.49	34	8.8
	Pulse 2	15.8	52832048	51539755	96.16	92.01	17	7.7
	Pulse 3	15.5	51828295	50494924	94.77	90.06	23	8.8
<i>CAGCre⁺</i> <i>SoxC^{KO}</i>	Baseline 1	13.2	43891081	42591876	96.19	91.53	76	9.6
	Baseline 2	17	56564478	54832394	97.34	92.49	268	9.8
	Baseline 3	15.3	51146701	49554363	97.03	92.34	61	9.9
	Pulse 1	13.9	46470154	45152031	96.31	92.01	21	9.9
	Pulse 2	12.7	42472803	41403910	96.95	92.83	26	9.0
	Pulse 3	15.3	50995213	49599943	96.06	91.68	30	9.5

Table 2. Overview of RNA-seq mapping

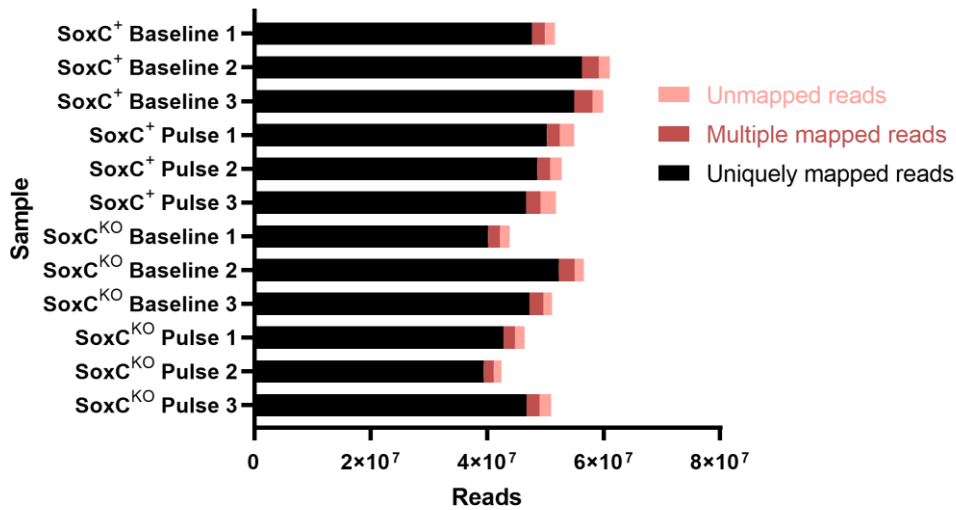


Figure 24: Overview of RNA-seq mapping

Reads were mapped on the mouse genome and classified as exonic, intergenic or intronic reads (Figure 25). In each sample, 85-94% of reads were classified as exonic reads, 3-12% of reads were classified as intronic reads, and 2-3% of reads were classified as intergenic reads.

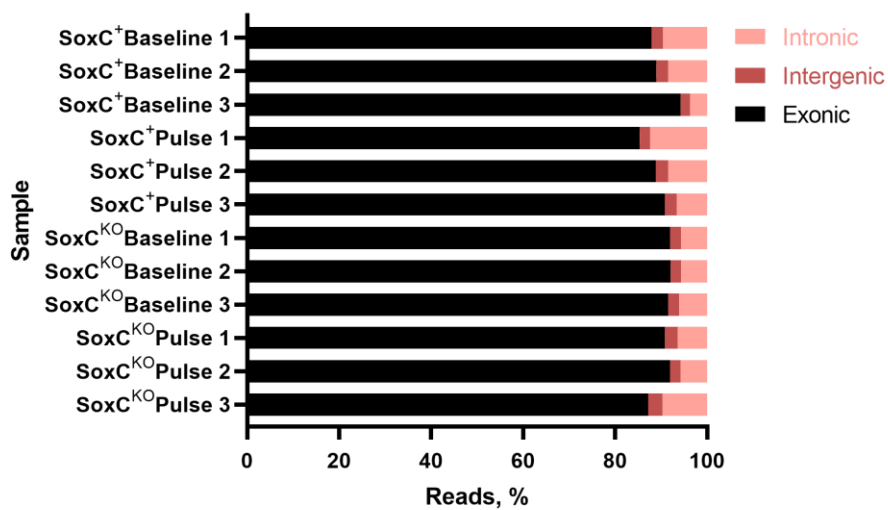


Figure 25: Mapping of reads by genomic region

Quantification was performed by normalizing the exonic read count to the gene length and sequencing depth using FPKM metric (Fragments per Kilobase of transcript sequence per Million base pairs sequenced).

Significantly expressed genes were screened with the threshold of FPKM set to 0.3. Coexpression analysis was performed on expressed genes across pairs of samples.

Phantasia analysis

The file with the filtered genes and normalized expression values was uploaded to Phantasia. Genes were annotated with ENSEMBL names from the AnnotationDB database for *Mus musculus* genes.

Each gene has 18 expression values, one per each sample replicate. To filter out non-relevant genes, a column with a mean expression value for each gene was created. From the total of 47,069 genes, only the top 10,000 genes by mean expression value were included in the analysis, with values ranging from 5.5 to 11296

To confirm that the conditional knockout in NPCs was successful, *Sox4* and *Sox11* mean expression values were inspected (Figure 26). As expected, *CAGCre⁻ Sox4^{fl/fl} Sox11^{fl/fl} Sox12^{-/-}* samples demonstrated high levels of *Sox4* and *Sox11* gene expression, while in *CAGCre⁺ Sox4^{fl/fl} Sox11^{fl/fl} Sox12^{-/-}* samples expression of *SoxC* genes was decreased. However, residual expression of *Sox4* was still observed after 4-OH-Tamoxifen-induced conditional knockout, which is a marked difference to earlier analysis of conditional knockout in cell culture (Figure 20). This discrepancy can be a factor leading to different outcomes in gene expression found between two experiments.

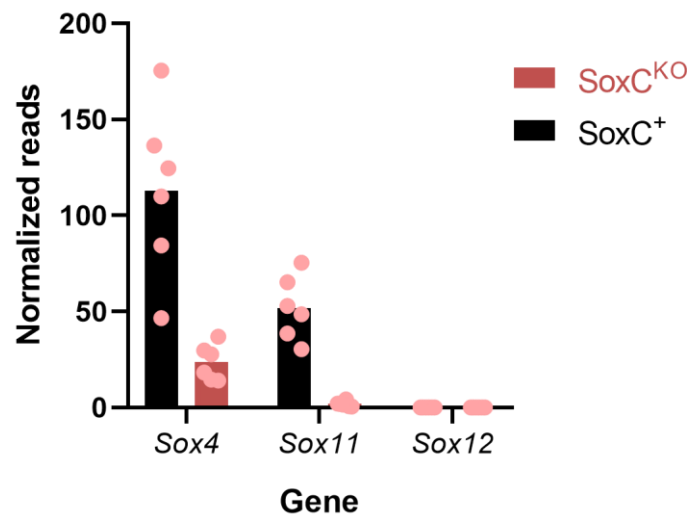


Figure 26: Mean expression of *SoxC* genes is decreased in *CAGCre⁺ Sox4^{fl/fl} Sox11^{fl/fl} Sox12^{-/-}* organoids (*SoxC^{KO}*).

Organoid samples used in RNA-seq analysis were obtained from littermates to limit the biological variation in the experiment. As a consequence, sex of the embryo can be a source of variation in gene expression, leading to artifacts in gene expression analysis. To analyse the

sex-specific transcription, Y-chromosome genes from ENSEMBL database were extracted from the reads table. Five of the genes were found to be expressed on a substantial level, displaying variability between replicates (Figure 27). Y-chromosome genes were expressed in *SoxC^{KO}* samples, marking them as male, and *SoxC⁺* samples as female. The exception is *Erdrl* gene, which is located in the pseudoautosomal regions of both X and Y chromosomes and is more highly expressed in females (Armoskus et al., 2015). To prevent variability of expression due to sex-specific genes, Y-chromosome genes were excluded from the further analysis.

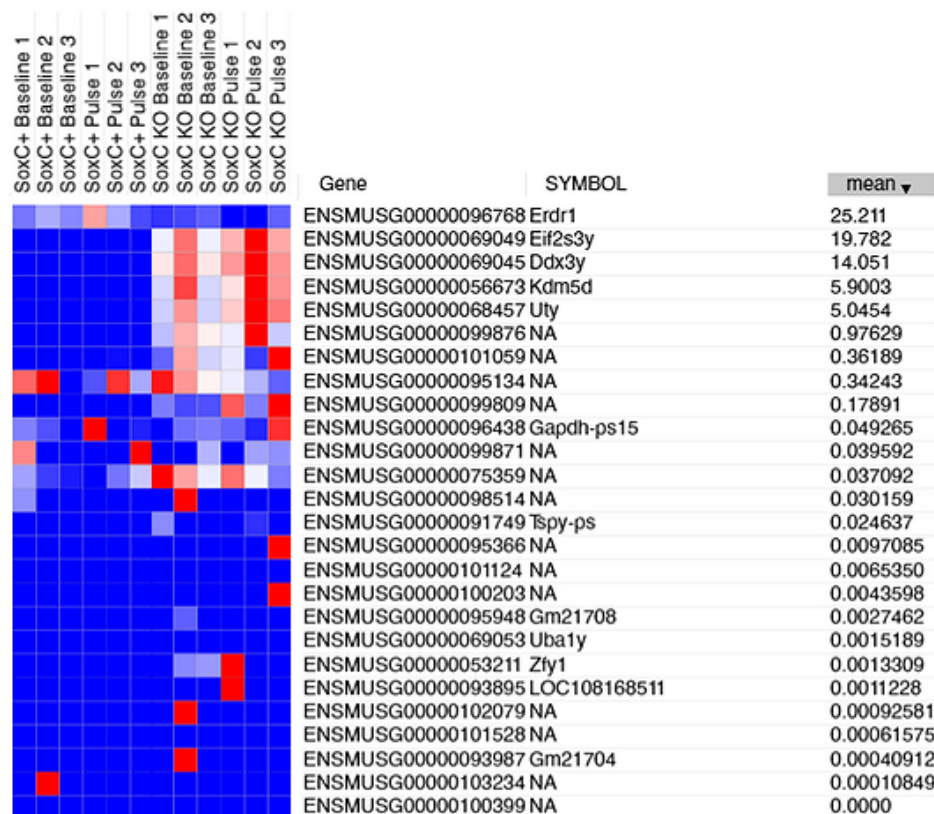


Figure 27: A heatmap of Y-chromosome specific gene expression sorted by mean expression levels. Five genes were found to be expressed on a substantial level.

Principal Component Analysis (PCA) on all samples was performed to determine whether samples in each group clustered with each other or with other groups. PCA plot of the samples was calculated using Phantasus web service (Figure 28).

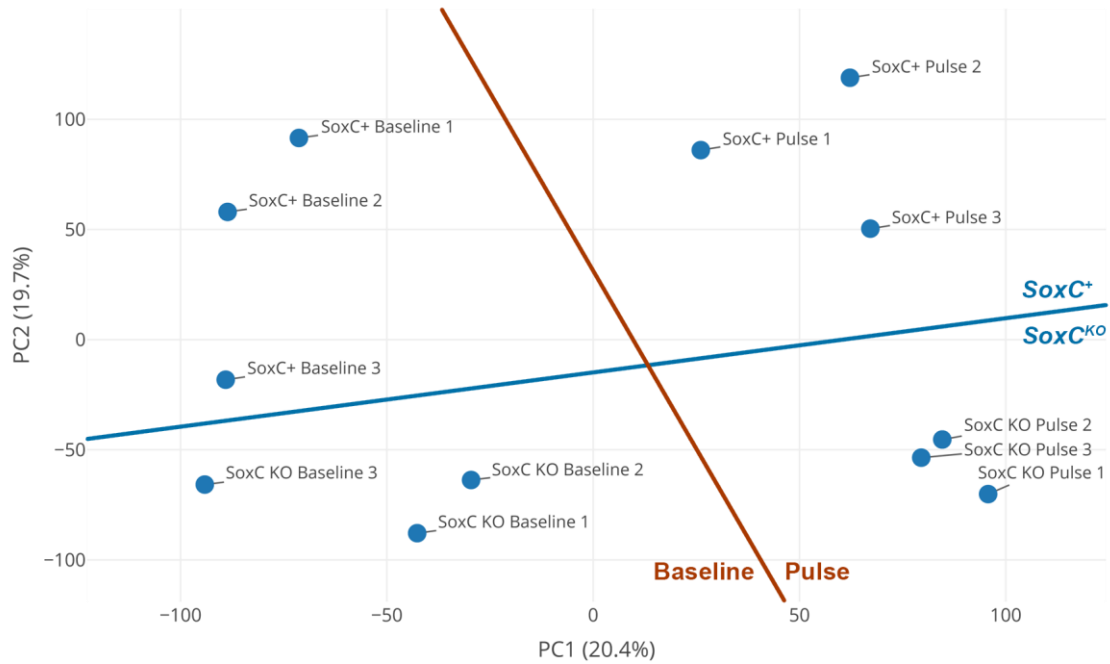


Figure 28: PCA plot of RNA-seq samples show distribution into four quadrants.

Here the PC2 component is responsible for the difference between *SoxC⁺* and *SoxC^{KO}* samples, and PC1 component reflects the effect of MET induction. As expected, samples separate into four groups corresponding to two genotypes and two experimental conditions.

Next, k-means clustering into 4 clusters was performed (Figure 29). The analysis revealed that genes expressed in *SoxC^{KO}* organoids in Pulse condition were clustering together, as did genes expressed in all six of the control samples. However, both of two other clusters include genes expressed in *SoxC⁺* organoids in Pulse condition. This observation can be explained by the difference in gene expression between two conditions being smaller than the difference in gene expression between three replicates of the same condition. It is possible that after the induction of MET, one of the replicates undergoes differentiation in a distinct manner from the other two replicates.

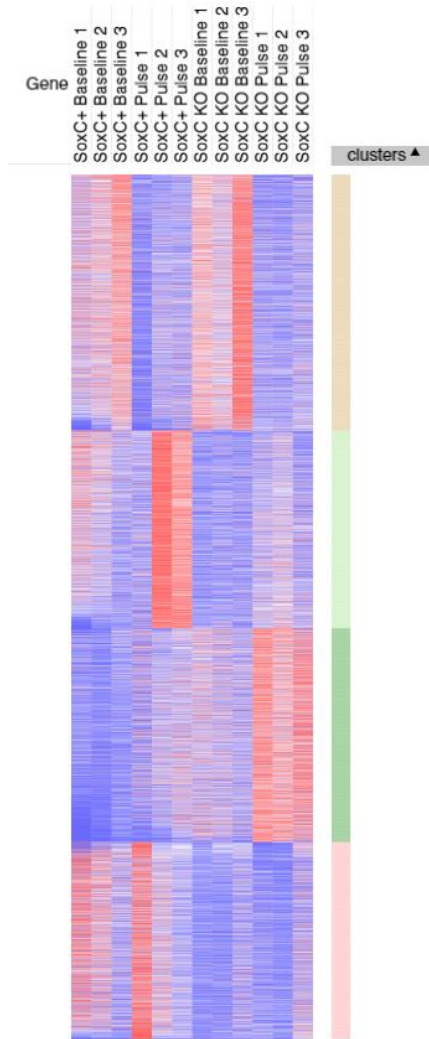


Figure 29: k-means clustering of expressed genes into 4 clusters reveals heterogeneity in SoxC⁺ samples.

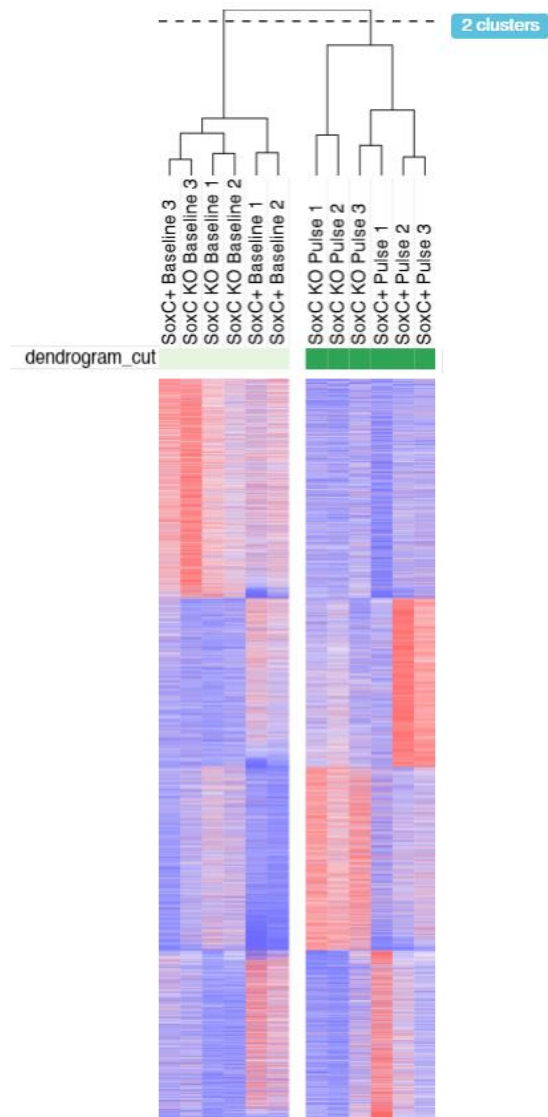


Figure 30: Hierarchical clustering of samples allows to divide them into two broad groups based on MET treatment.

Hierarchical clustering of samples was performed using Phantasus application (One minus Pearson correlation metric, Average linkage method). Hierarchical clustering splits samples in two broad groups based on the treatment method: Baseline samples cluster in one group, and Pulse samples cluster in another group (Figure 30).

A similar relationship between samples is revealed by the Pearson correlation diagram, demonstrating that SoxC^{KO} Pulse samples 2 and 3 don't correlate with each other, however they both correlate with SoxC^{KO} Pulse 1 sample (Figure 31). This observation could be a result of disturbed differentiation program leading to transcriptional heterogeneity after an attempt at

MET induction. Baseline samples were found to well correlate with each other, and to be distinct from Pulse samples.

Differential expression analysis

The input data for differential gene expression analysis is read counts from gene expression level analysis. The analysis provides normalized read counts, p-value, and q-value estimation of FDR (false discovery rate).

On average, 21800 genes were mapped by at least one read in each of the kidney organoid samples (Figure 32). Overall, from 4 to 6804 DEG (differentially expressed genes) were identified in 9 comparative analyses with the q-value threshold of $q < 0.05$.

SoxC⁺ Pulse vs. *SoxC*⁺ Baseline

Rationale: This comparison allows to identify genes whose regulation is affected during the normal course of MET.

Differentially expressed gene analysis revealed 2297 genes significantly upregulated or downregulated in *SoxC*⁺ Pulse condition compared to *SoxC*⁺ Baseline condition. Among the most significant of these genes are:

Rspo1, which is required for a BMP7-dependent activation of WNT/ β -catenin pathway leading to MET in NPC. (Vidal et al., 2019)

Rn7sk is a ncRNA implicated in transcription regulation during differentiation (Bazi et al., 2018)

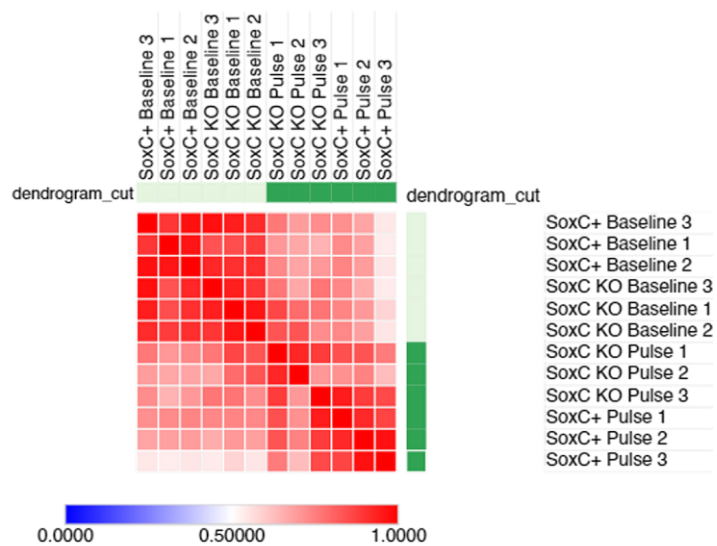


Figure 31: Pearson correlation between samples.

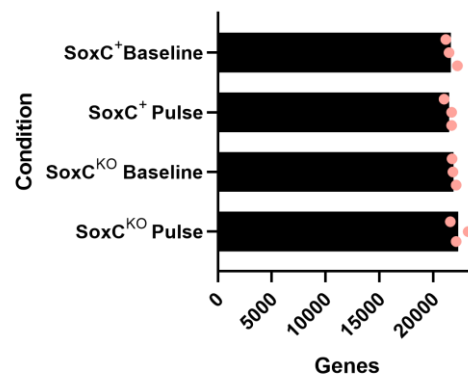


Figure 32: Number of genes mapped with at least one read. Replicates were grouped by condition.

Vstm5 is a cell adhesion-like transmembrane protein modulating cell membrane morphology and dynamics (Lee et al., 2016)

KEGG analysis on *SoxC*⁺ Pulse samples compared to *SoxC*⁺ Baseline samples yields high changes in Wnt and Hippo signalling pathways (Figure 33). This is expected since the induction of MET requires the coordinated activation of these pathways (McNeil and Reginensi, 2017). The high occurrence of cell cycle genes on the KEGG list conforms to the usual pattern of shifting cell cycle signatures during cell fate transitions (Li, Pei & Zheng, 2014) The appearance of cancer pathways on the KEGG list follows from shared pathway components between EMT, which is believed to confer invasive properties to metastatic cells, and MET, which was found to occur in metastasized cells that reverted back to the epithelial phenotype (Banyard and Bielenberg, 2015). DNA replication genes are known to be highly expressed during the kidney development (Stuart, Bush, Nigam, 2001)

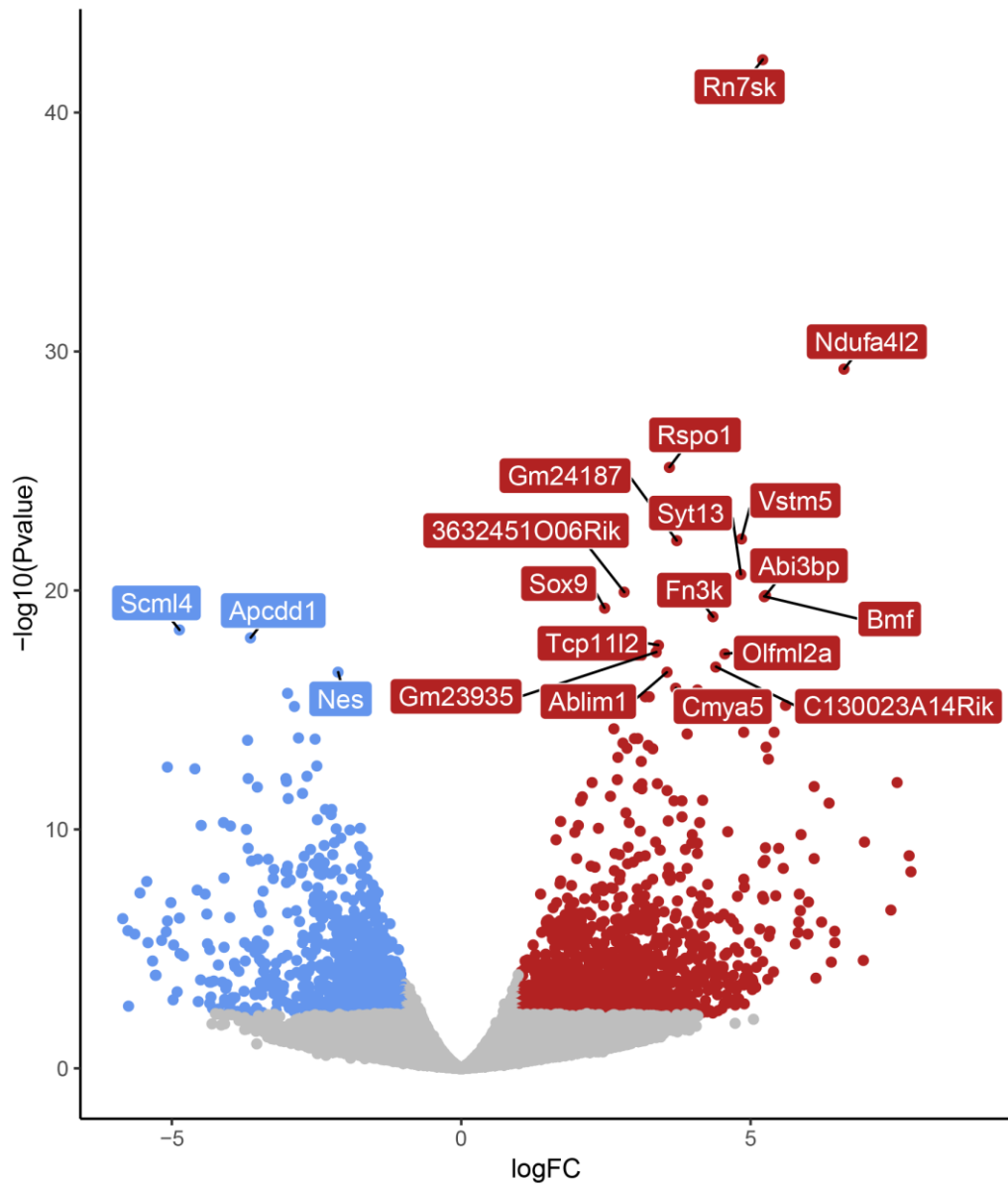


Figure 33: Volcano plot demonstrating difference in expression of genes in the samples of SoxC+ Pulse compared to SoxC+ Baseline: 1321 upregulated genes (red), 976 downregulated genes (blue).

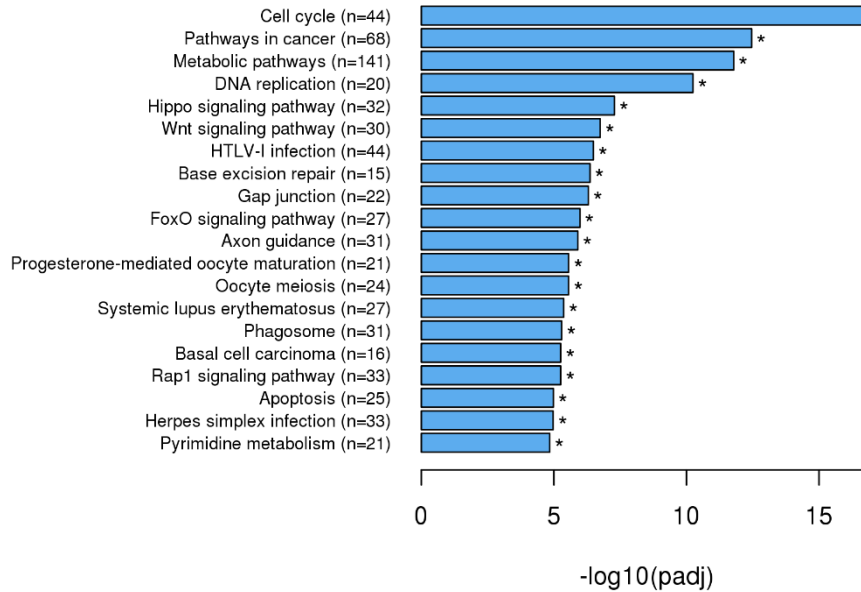


Figure 34: KEGG pathway enrichment in the samples of SoxC⁺ Pulse compared to SoxC⁺ Baseline

SoxC^{KO} Baseline vs. *SoxC⁺* Baseline

Rationale: This comparison allows to identify genes whose regulation is affected by the deletion of *SoxC* genes in cap mesenchyme population represented by the NPC.

The majority of the genes in *SoxC^{KO}* Baseline samples were found to be downregulated in comparison to *SoxC⁺* Baseline samples (Figure 35).

Podxl2 is involved in lumen formation during nephrogenesis (Yang et al., 2016)

Many genes earlier identified as transcriptional targets of *Sox11* regulation are present in the list of significantly downregulated genes, such as *Adssl1*, *Casp6*, *Cd24a*, *Dbn1*, *Hmgb3*, *Ick*, *Rnf122*, *Tfdp2*, *Tuba1a*, *Tubb3*, *Ypell* (Wang et al., 2010).

Sox4 targets in the list include *Pcdhb* genes (*Pcdhb1/2/3/5/6/7/9-22*), *Ccng2*, *Egr3*, *Mbtd1*, *Mllt3*, *Myb*, *Rbp1*, *Tead2*, *Tmeff1*, *Vash2*, *Zic3* and others, with many transcripts being highly specific to neural-derived tissues (Castillo et al., 2012)

KEGG pathway analysis indicates changes in expression of gene pathways known to be regulated by *SoxC* genes, such as axon guidance genes (Kuwajima et al., 2017) and cancer genes (Penzo-Méndez, 2010).

Rap1 signalling pathway appears to play a role in stabilizing β -catenin and enhancing β -catenin dependent transcription (Goto et al., 2010). Rap1 pathway components *Efna4* and *Efna2*, which are significantly downregulated in *SoxC^{KO}* Baseline samples, were found to promote MET through binding to EPHA receptors (Li, Chen & Chen, 2014). *Efna4* was previously identified as positively regulated by SOX4 (Moran et al., 2014)

KEGG analysis highlighted changes in expression linked with pathways regulating pluripotency genes (Table 3). Genes in this category include pluripotency genes themselves (*Sox2*), as well as genes in pathways such as Wnt pathway (*Wnt16*, *Wnt10*, *Zic3*, *Fzd3*, *Tcf3*, *Smarcad1*, *Rest*, *Dvl1*), BMP pathway (*Dlx5*, *Bmp4*), FGF pathway (*Fgfr2*), MAPK/ERK pathway (*Mapk11-13*), TGF-B pathway (*Acvr2b*, *Smad1*, *Smad4-5*, *Inhbb*), PI3K/AKT pathway (*Pik3cd*, *Pik3r3*, *Pik3ca*). The majority of genes in this group were found to be downregulated, reflecting loss of pluripotent cell identity in *SoxC^{KO}* kidney organoids. Due to possible heterogeneity of *SoxC^{KO}* cells after MET induction, further analysis, such as single-cell RNA sequencing, could be employed in the future to robustly determine the developmental trajectory of mutant cells.

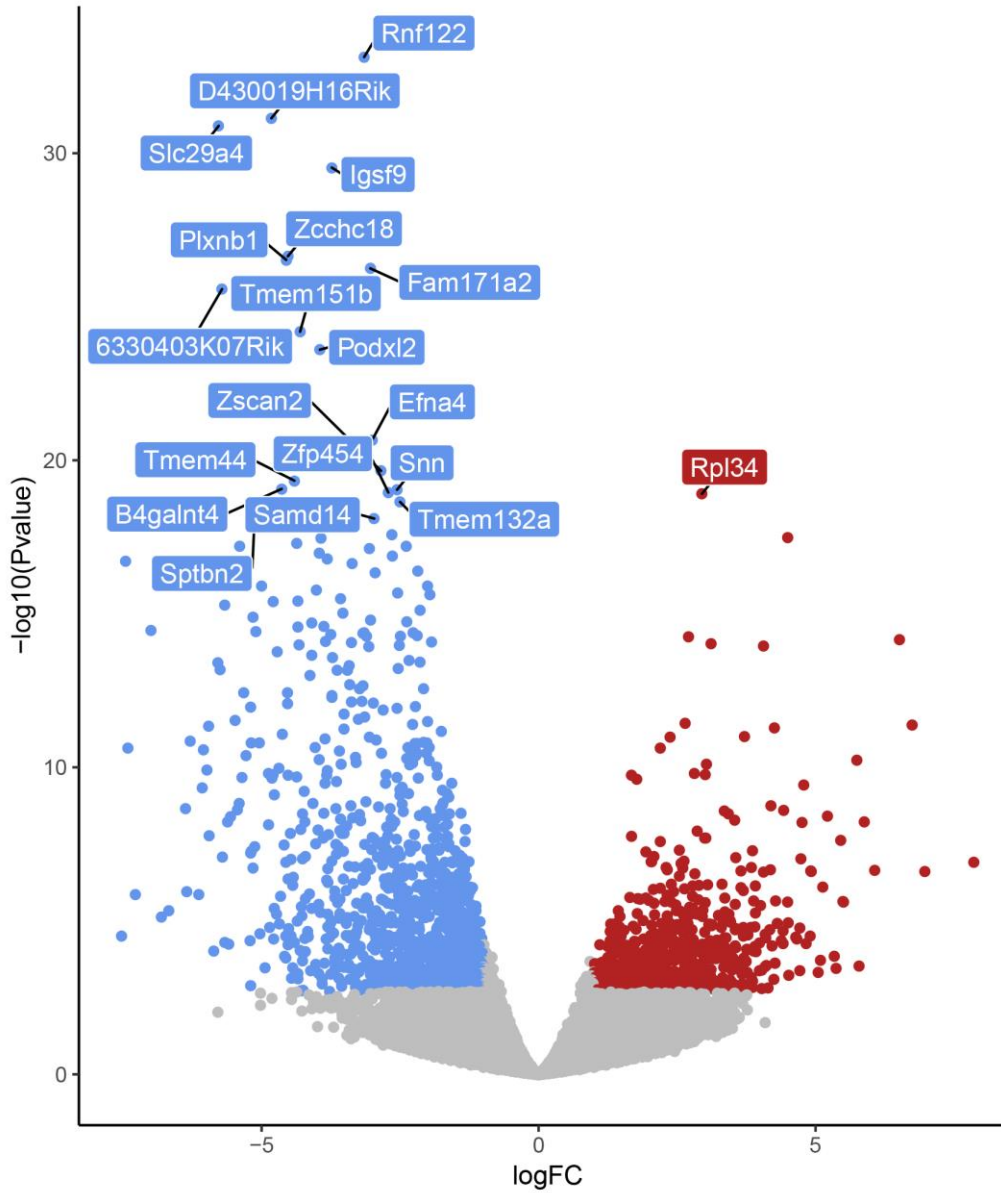


Figure 35: Volcano plot demonstrating difference in expression of genes in the samples of SoxC^{KO} Baseline compared to SoxC⁺ Baseline: 616 upregulated genes (red), 1273 downregulated genes (blue).

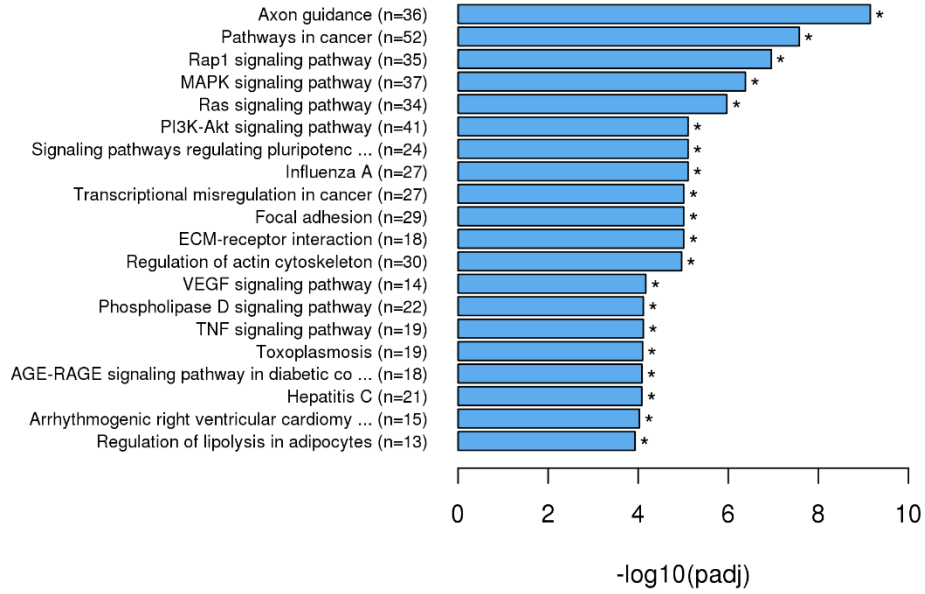


Figure 36: KEGG pathway enrichment in the samples of SoxC^{KO} Baseline compared to SoxC⁺ Baseline

Gene	SoxC ⁺ Baseline reads	SoxC ^{KO} Baseline reads	SoxC ^{KO} Baseline vs. SoxC ⁺ Baseline Log Fold Change	SoxC ^{KO} Baseline vs. SoxC ⁺ Baseline Adjusted p-value
<i>Sox2</i>	2.2941	0.0542	-5.4037	3.69E-07
<i>Zic3</i>	2.4167	0.0734	-5.0402	6.05E-09
<i>Dlx5</i>	2.4670	0.3353	-2.8791	0.0008
<i>Fzd3</i>	15.4081	3.2006	-2.2673	3.27E-12
<i>Pik3cd</i>	11.6713	3.0196	-1.9505	0.0034
<i>Bmp4</i>	685.9136	187.0719	-1.8744	0.0044
<i>Fgfr2</i>	71.8652	19.6142	-1.8734	0.0256
<i>Mapk11</i>	8.7142	2.4383	-1.8375	0.0012
<i>Acvr2b</i>	3.3787	1.0346	-1.7074	0.0090
<i>Tcf3</i>	173.2662	54.8139	-1.6604	5.17E-06
<i>Smad1</i>	81.3632	26.2277	-1.6333	0.0003
<i>Pik3r3</i>	36.5986	12.4194	-1.5592	0.0028
<i>Smad5</i>	149.7938	62.3997	-1.2634	0.0230
<i>Mapk12</i>	1.3332	0.5683	-1.2303	0.0025
<i>Smarcad1</i>	45.2322	22.2241	-1.0252	0.0106
<i>Rest</i>	25.1941	13.3559	-0.9156	0.0168
<i>Pcgf3</i>	67.4618	35.9096	-0.9097	0.0094
<i>Pik3ca</i>	15.3818	8.5524	-0.8468	0.0159
<i>Smad4</i>	79.8229	44.9456	-0.8286	0.0241
<i>Dvl1</i>	20.0312	33.8887	0.7586	0.0358
<i>Inhbb</i>	13.8026	54.7137	1.9870	0.0022
<i>Mapk13</i>	0.5925	2.3962	2.0159	0.0030
<i>Wnt16</i>	0.8512	3.5742	2.0700	0.0001
<i>Wnt10b</i>	0.1232	1.0981	3.1558	0.0075

Table 3. List of pluripotency-associated genes whose expression is affected in *SoxC^{KO}* Baseline samples compared to *SoxC⁺* Baseline samples.

***SoxC^{KO}* Pulse vs. *SoxC⁺* Pulse**

Rationale: This comparison allows to identify genes whose misregulation in *SOXC^{KO}* cells make it impossible for the organoids to undergo MET.

In the absence of *Sox4* and *Sox11*, a large number of genes appear to be regulated differently under the effect of CHIR99021 and DMH1.

Cdh16 is a cadherin normally present in ureter-derived epithelial cells in metanephric kidney in mice (Wertz, Herrmann, 1999).

Many genes, such as *Tubb3*, *Podxl2* and *Zcchc18*, also appear on the list of genes for *SoxC^{KO}* Baseline samples compared to *SoxC⁺* Baseline samples, which suggests that they represent targets of *SoxC* genes under both conditions.

KEGG pathway analysis reveals that significantly deregulated genes belong to PI3K/Akt, MAPK and HIF-1 signalling pathways, both of which are known to play role in EMT and MET.

As expected from previous research on *Sox4* role in EMT, multiple chromatin remodelling genes are downregulated after *SoxC* knockdown, including components of SWI/SNF chromatin remodelling complex (*Smarca1*, *Smarce1-ps1*, *Smarce1*, *Smarcc1*, *Smarcd1*, *Smarcd3*, *Smarca4*, *Smarcad1*).

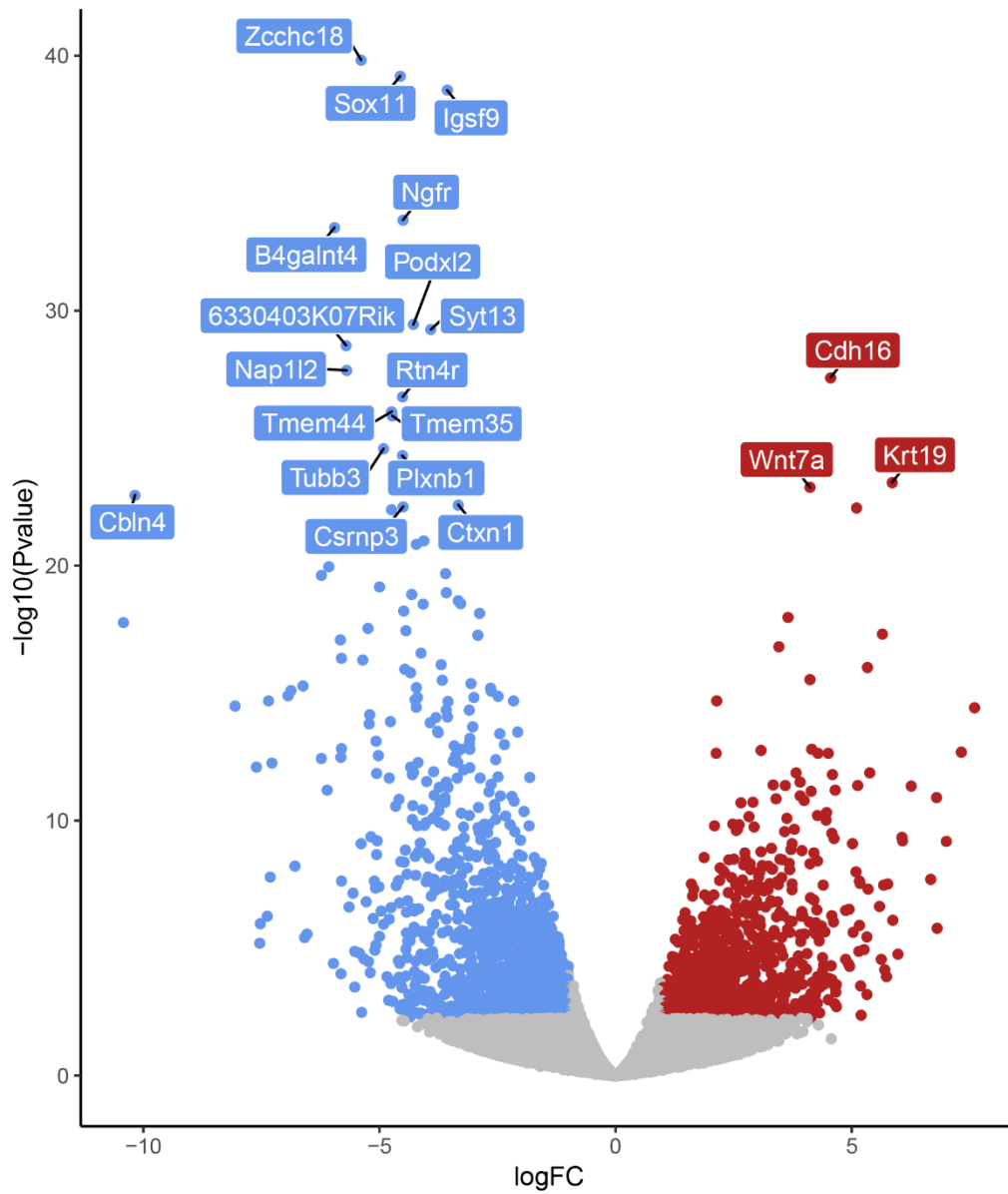


Figure 37: Volcano plot demonstrating difference in expression of genes in the samples of SoxC^{KO} Pulse compared to SoxC⁺ Pulse: 1009 upregulated genes (red), 1618 downregulated genes (blue)

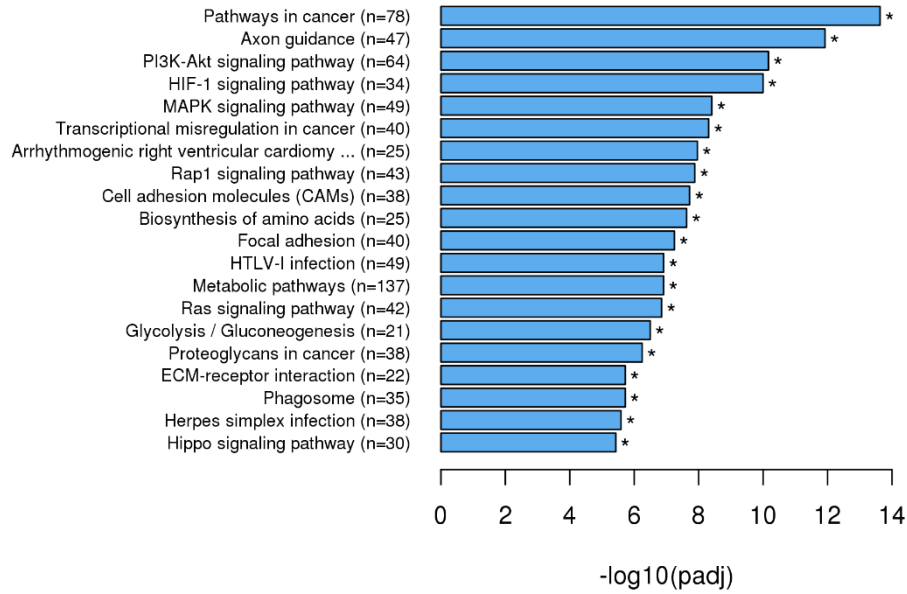


Figure 38: KEGG pathway enrichment in the samples of *SoxC^{KO}* Pulse compared to *SoxC⁺* Pulse

Overlap of DEG lists

Identification of MET genes influenced by *SoxC* deletion

To identify which of the genes regulated during the process of MET are affected in *CagCRE⁺ Sox4^{fl/fl} Sox11^{fl/fl} Sox12^{-/-}* kidney organoids, a chart showing the overlap between four lists of genes was constructed. DEG list in *SoxC^{KO}* Baseline vs. *SoxC⁺* Baseline comparison was compared to DEG list in *SoxC⁺* Pulse vs. *SoxC⁺* Baseline comparison. The genes in both lists were separated in the upregulated and downregulated groups. This allowed to identify 31 genes upregulated in *SoxC⁺* Pulse condition but downregulated in *SoxC^{KO}* Baseline condition (Table 3), as well as 15 genes downregulated in *SoxC⁺* Pulse condition but upregulated in *SoxC^{KO}* Baseline condition (Table 4), compared to *SoxC⁺* Baseline condition.

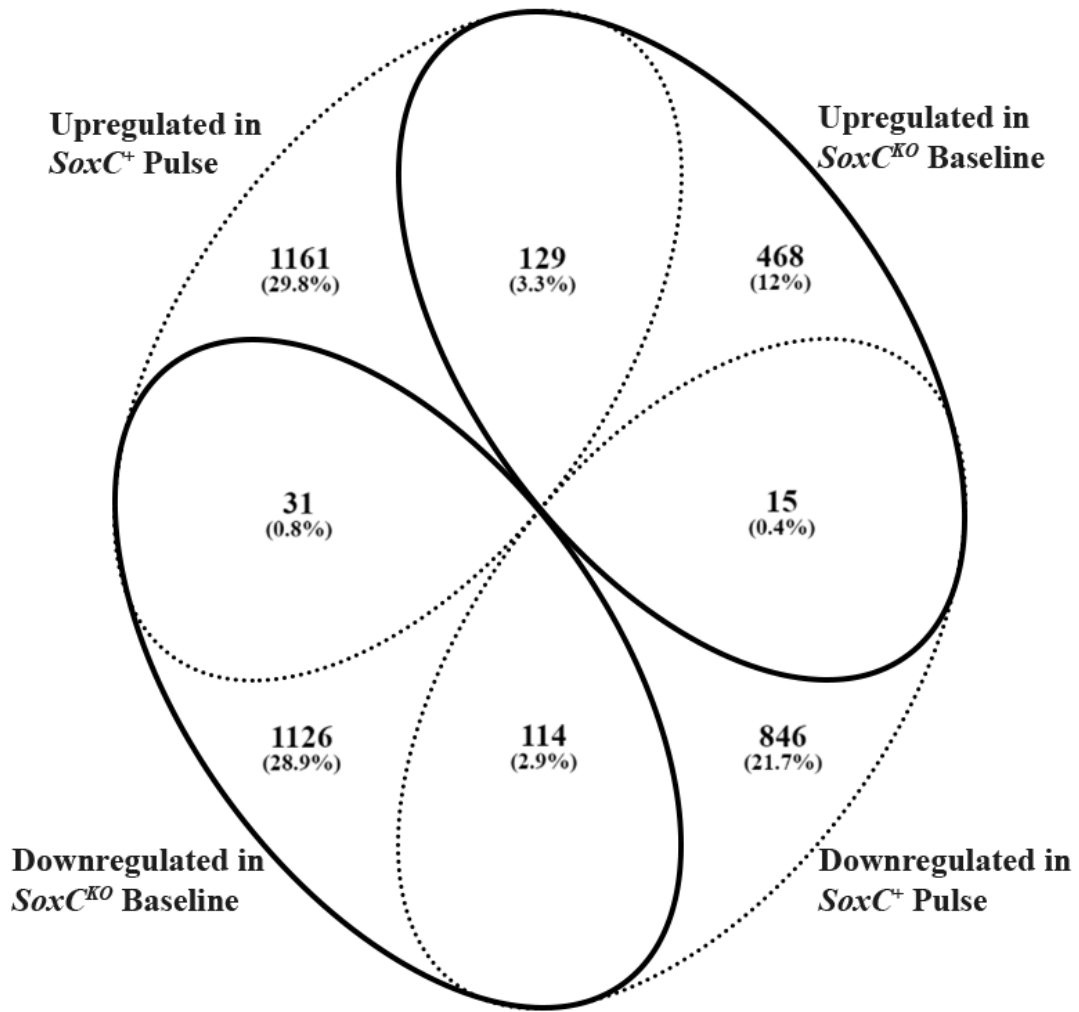


Figure 39: Overlap of differentially expressed genes between four lists: upregulated in *SoxC*^{KO} Baseline vs. *SoxC*⁺ Baseline (solid top area), downregulated in *SoxC*^{KO} Baseline vs. *SoxC*⁺ Baseline (solid bottom area), upregulated in *SoxC*⁺ Pulse vs. *SoxC*⁺ Baseline (dotted top area), downregulated in *SoxC*⁺ Pulse vs. *SoxC*⁺ Baseline (dotted bottom area).

Gene	SoxC ⁺ Baseline reads	SoxC ⁺ Pulse reads	SoxC ^{KO} Baseline reads	SoxC ⁺ Pulse vs. SoxC ⁺ Baseline Log Fold Change	SoxC ⁺ Pulse vs. SoxC ⁺ Baseline adj. p-value	SoxC ^{KO} Baseline vs. SoxC ⁺ Baseline Log Fold Change	SoxC ^{KO} Baseline vs. SoxC ⁺ Baseline adj. p-value	Log Fold Change difference
<i>Gm28512</i>	0.3303	2.8641	0.0163	3.1164	0.0023	-4.3458	0.0180	7.4622
<i>Lrrc4b</i>	0.1620	1.1138	0.0085	2.7818	8.24E-05	-4.2479	0.0055	7.0297
<i>Lin7b</i>	0.9908	10.9394	0.1625	3.4648	0.0043	-2.6088	0.0301	6.0736
<i>Cdkn1c</i>	107.3459	346.4548	7.4713	1.6904	0.0041	-3.8458	5.44E-12	5.5362
<i>Zkscan16</i>	0.3677	1.9845	0.0502	2.4323	0.0031	-2.8725	0.0005	5.3049
<i>Rnasel</i>	1.5637	12.4833	0.4728	2.9969	0.0002	-1.7268	0.0337	4.7237
<i>Efnb3</i>	4.5261	39.5323	1.5747	3.1267	7.74E-10	-1.5243	0.0042	4.6510
<i>Nacad</i>	0.5923	1.6331	0.0841	1.4632	0.0342	-2.8165	2.16E-05	4.2796
<i>H3f3aos</i>	0.7293	2.4038	0.1291	1.7207	0.0386	-2.4990	0.0132	4.2198
<i>Baiap3</i>	0.2885	1.8230	0.1012	2.6595	1.99E-07	-1.5119	0.0371	4.1714
<i>Kcnb1</i>	0.8259	2.8672	0.1698	1.7957	0.0065	-2.2834	0.0201	4.0790
<i>Klhl24</i>	4.6170	18.4452	1.1361	1.9982	2.97E-07	-2.0239	0.0005	4.0221
<i>Syt5</i>	2.0652	6.6354	0.4210	1.6839	0.0025	-2.2955	0.0095	3.9794
<i>Ccng2</i>	21.7735	66.2411	4.9915	1.6052	0.0128	-2.1261	2.35E-05	3.7312
<i>Zscan2</i>	13.9356	25.5828	1.9415	0.8764	0.0342	-2.8446	6.50E-17	3.7210
<i>Hif3a</i>	1.9230	6.6866	0.5108	1.7980	0.0125	-1.9135	0.0411	3.7114
<i>Olfm2</i>	1.9738	5.6923	0.4506	1.5280	0.0403	-2.1320	0.0047	3.6600
<i>Fcho1</i>	1.7611	5.7481	0.5004	1.7066	4.85E-05	-1.8163	0.0004	3.5229
<i>Hist3h2ba</i>	20.4803	72.9979	7.2890	1.8336	7.75E-05	-1.4915	0.0350	3.3251
<i>Armc2</i>	0.6857	1.7074	0.1785	1.3161	0.0345	-1.9425	0.0102	3.2586
<i>Cers1</i>	2.7861	8.8763	1.1042	1.6717	0.0003	-1.3364	0.0322	3.0081
<i>Ppp1r3d</i>	4.0751	10.8362	1.3939	1.4110	0.0218	-1.5488	0.0345	2.9597
<i>Zkscan4</i>	0.9626	2.4152	0.3251	1.3271	0.0402	-1.5670	0.0332	2.8941
<i>Pdgfra</i>	137.1945	319.9526	45.0468	1.2216	0.0462	-1.6078	0.0411	2.8294
<i>Calcoco1</i>	26.8048	71.2431	10.1820	1.4103	0.0090	-1.3975	0.0229	2.8078
<i>Slc9a3r2</i>	6.3955	14.9502	2.5557	1.2250	0.0249	-1.3244	0.0027	2.5494
<i>Serf1</i>	31.9018	68.0123	12.0684	1.0922	0.0067	-1.4035	0.0031	2.4956
<i>Kantr</i>	3.3912	6.9002	1.1545	1.0249	0.0355	-1.0979	0.0080	2.1228
<i>Vps37d</i>	7.6244	17.2547	4.0791	1.1783	0.0198	-0.9034	0.0301	2.0817
<i>H2afv</i>	34.7994	59.9097	15.1487	0.7837	0.0330	-1.2009	0.0068	1.9847
<i>Pafah1b3</i>	59.5025	109.2226	29.4646	0.8762	0.0156	-1.0150	0.0096	1.8913

Table 4. List of genes that are downregulated in SoxC^{KO} Baseline vs. SoxC⁺ Baseline DEG list and upregulated in SoxC⁺ Pulse vs. SoxC⁺ Baseline DEG list.

Gene	SoxC ⁺ Baseline reads	SoxC ⁺ Pulse reads	SoxC ^{KO} Baseline reads	SoxC ⁺ Pulse vs. SoxC ⁺ Baseline Log Fold Change	SoxC ⁺ Pulse vs. SoxC ⁺ Baseline adj. p-value	SoxC ^{KO} Baseline vs. SoxC ⁺ Baseline Log Fold Change	SoxC ^{KO} Baseline vs. SoxC ⁺ Baseline adj. p-value	Log Fold Change difference
<i>Ccl12</i>	14.4680	0.4296	114.1425	-5.0738	4.86E-05	2.9788	0.0090	8.0526
<i>Lypd2</i>	0.6985	0.0466	6.2815	-3.9069	0.0162	3.1678	0.0387	7.0747
<i>Slco4a1</i>	4.3785	0.3912	34.1935	-3.4844	0.0009	2.9642	0.0004	6.4486
<i>Esrp1</i>	0.0638	0.0043	0.3727	-3.8745	0.0420	2.5462	0.0060	6.4207
<i>Sox17</i>	0.3960	0.0168	1.3402	-4.5590	3.97E-06	1.7578	0.0028	6.3168
<i>Cdcp1</i>	0.0671	0.0039	0.3052	-4.0875	0.0239	2.1856	0.0256	6.2730
<i>Cdh16</i>	2.8760	0.2626	14.7743	-3.4532	0.0004	2.3599	0.0423	5.8131
<i>Cnpy1</i>	0.3955	0.0264	1.2382	-3.9069	0.0017	1.6453	0.0436	5.5522
<i>Fam196b</i>	0.0603	0.0056	0.2231	-3.4406	0.0132	1.8865	0.0121	5.3271
<i>Mal2</i>	0.2840	0.0327	1.0236	-3.1180	0.0105	1.8488	0.0494	4.9668

<i>Adgrg2</i>	1.4631	0.2419	7.3050	-2.5964	0.0007	2.3187	0.0006	4.9151
<i>Gcnt1</i>	1.0962	0.2435	5.0288	-2.1707	0.0006	2.1967	8.45E-09	4.3674
<i>Ptpn7</i>	0.4148	0.1300	1.5565	-1.6742	0.0228	1.9069	0.0091	3.5811
<i>Trabd2b</i>	1.2133	0.4315	3.4741	-1.4917	0.0122	1.5166	0.0104	3.0083
<i>Pcsk5</i>	8.6082	3.5010	15.3885	-1.2979	0.0002	0.8370	0.0333	2.1349

Table 5. List of genes that are upregulated in *SoxC^{KO}* Baseline vs. *SoxC⁺* Baseline DEG list and downregulated in *SoxC⁺* Pulse vs. *SoxC⁺* Baseline DEG list.

As seen in the Table 4, Hypoxia response related genes *Cdkn1c*, *Klhl24*, *Ccng2* are upregulated during the normal MET, and at the same time they are downregulated in *SoxC^{KO}* cells.

Cdkn1c is a CDK inhibitor regulated by both hypoxia and TGF- β pathways (Wierenga, Vellenga & Schuringa, 2014). *Cdkn1c* is expressed in developing kidney tubules and mutations in *Cdkn1c* are linked with renal anomalies in humans (Goldman et al., 2002)

Ccng2 is a cyclin gene regulating expression of fibrosis-related proteins in renal epithelium via canonical Wnt pathway (Zhao et al., 2020).

LRRC4, an AKT/GSK3 β / β -catenin pathway inhibitor (Zhao et al., 2020), was found to be a target gene of miR-381 (Tang et al., 2014), which also regulates *Sox4* expression (Zhang, Huang & Long, 2017).

CCL12 is a ligand to podocyte-specific receptor CCR2 and its upregulation was linked to diabetes (You et al., 2018).

Slco4a1 is a lncRNA gene which was found to promote EMT and inhibit degradation of β -catenin by the GSK3 β complex (Yu et al., 2018).

Identification of genes misregulated during MET in *SoxC^{KO}* Pulse condition.

To filter out the genes influenced in the control condition from genes influenced in the condition of interest, Venn diagrams were made using Venny showing overlap of differentially expressed genes (Figure 40) (Oliveros, 2007). After filtering for SOXC-dependent genes, 1617 genes were found to be misregulated in *SoxC^{KO}* Pulse condition compared to *SoxC⁺* Pulse condition, out of them 730 were upregulated and 887 were downregulated compared to the normal MET process in renal organoids.

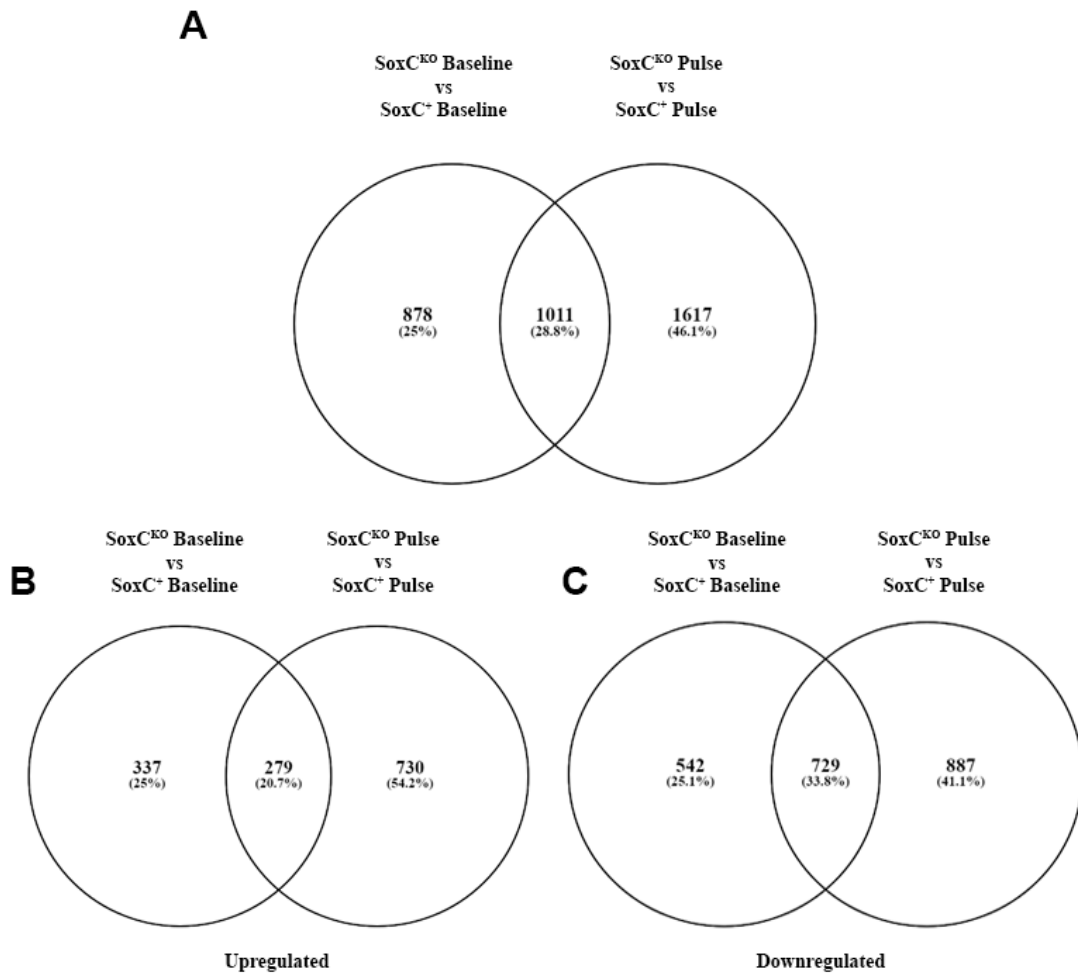


Figure 40: Overlap of differentially expressed genes between two lists: SoxC^{KO} Baseline vs SoxC⁺ Baseline, and SoxC^{KO} Pulse vs SoxC⁺ Pulse. (a) all genes, (b) only upregulated genes, (c) only downregulated genes

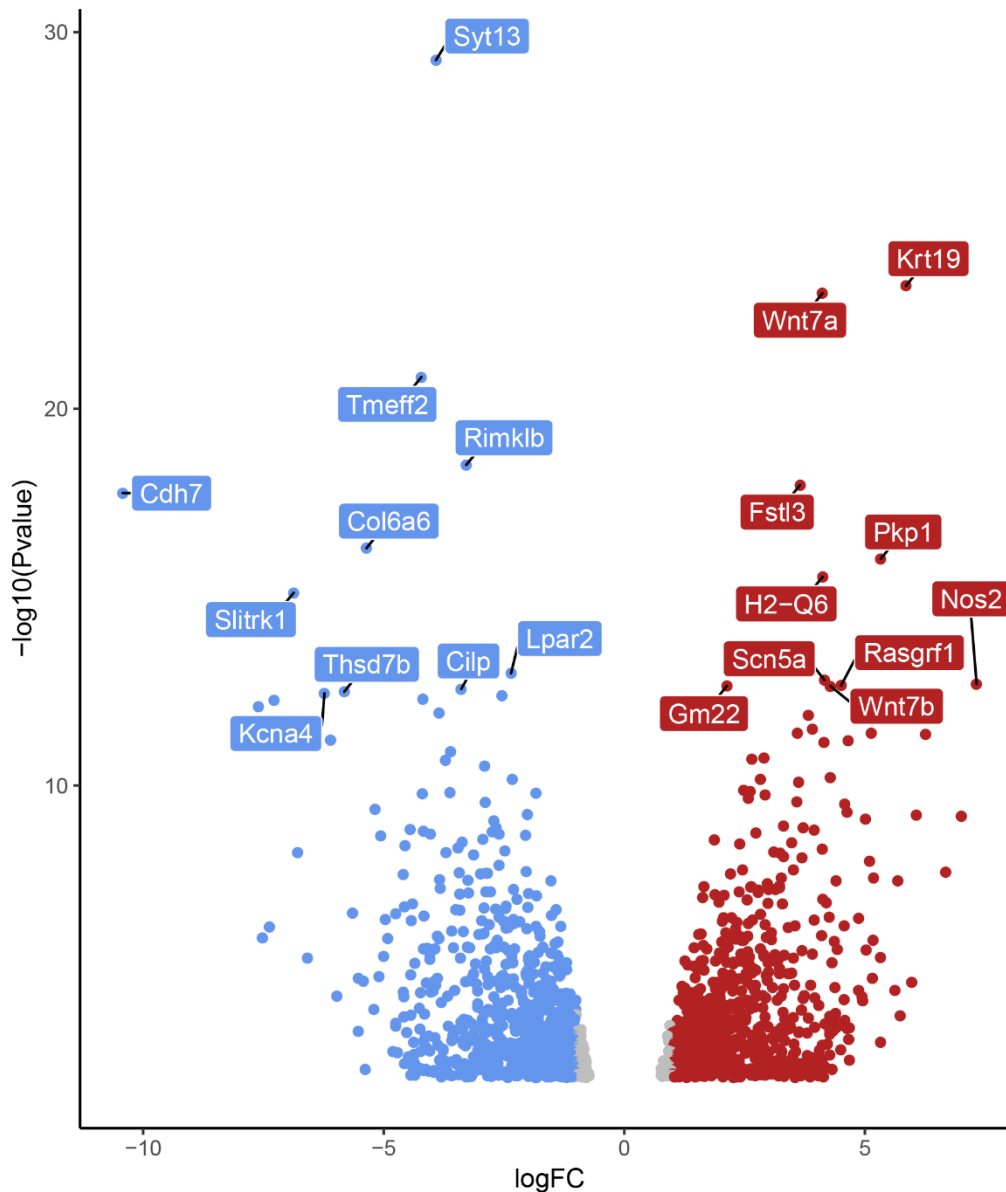


Figure 41: Genes appearing significant in the SoxC^{KO} Pulse vs. SoxC⁺ Pulse list, that do not appear significant in SoxC^{KO} Baseline vs. SoxC⁺ Baseline list. 730 upregulated genes (red), 887 downregulated genes (blue)

Among the most affected downregulated genes are:

Syt13, a factor associated with epithelial identity and acting through WT1 induction (Jahn and Coleman, 2006).

Tmeff2, a tumor suppressor mediating the process of EMT in carcinogenesis, inhibiting PI3K/Akt pathway (Gao et al., 2020).

Col6a6, a collagen gene found to induce EMT in cancer by inhibiting PI3K/Akt pathway (Chen, Cescon and Bonaldo, 2013; Long et al., 2019).

Cdh7 is a non-classical cadherin substituting N-cadherin during EMT process in select developmental processes. (Gheldof and Berx, 2013)

Lpar2 controls internalization of N-cadherin and is essential for neural crest cell migration. (Kuriyama, 2014)

Interestingly, abnormally downregulated genes include PI3K/Akt pathway inhibitors. PI3K/Akt inhibition was also shown to induce MET (Hong et al., 2009).

Upregulated genes include:

Wnt7a/b are nephrogenesis-inducing factors akin to Wnt4 (Kispert, Vainio, McMahon, 1998)

Krt19 is a marker of ureteric epithelia and, to a lesser degree, distal nephron (Combes et al., 2019)

Fstl3 is an EMT-associated gene coding a secreted glycoprotein (Reka et al., 2014)

Pkp3 is a gene which is repressed during EMT in metastatic cancer (Aigner et al., 2007).

Nos2 expression is elevated in mesenchymal tumor cells and it is associated with EMT induction through NF- κ B pathway activation (Kariche et al., 2019)

Rasgrf1 was identified as a bottleneck during the acquisition of metastatic identity by amniotic epithelial cells (Lollo et al., 2020)

Scn5a was found to be expressed after TGF- β 1 induction of EMT in cancer cells (Gradek et al., 2019).

The filtered list of misregulated genes was ranked according to their P-value multiplied by the sign of the fold change and subjected to FGSEA analysis using Galaxy software. Genes were ranked from 1 (most upregulated) to 1617 (most downregulated). The gene set was compared against mouse Hallmark genes dataset, taken from MSigDB database (Figure 42).

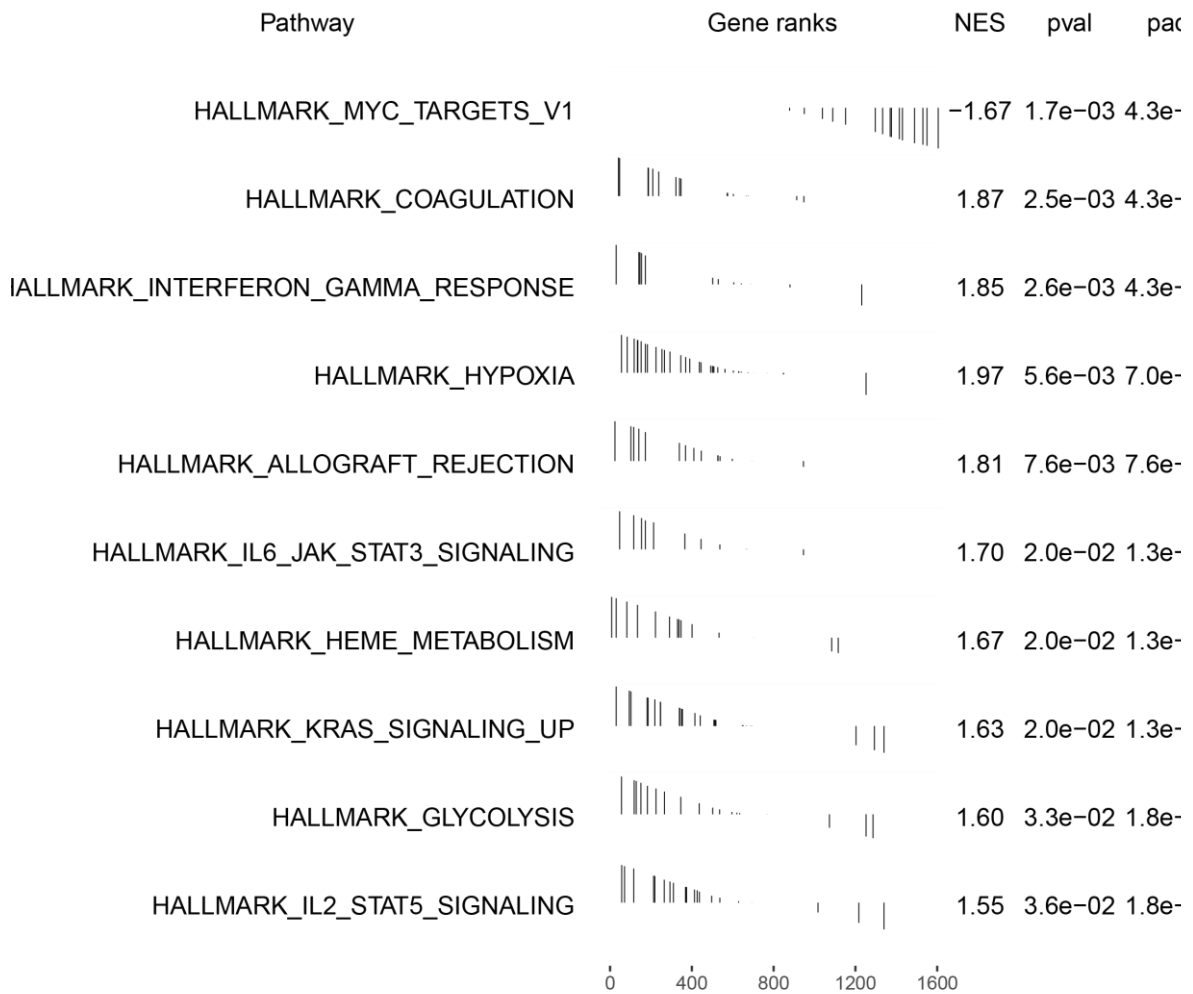


Figure 42: Summary of FGSEA analysis of a set of genes misregulated during MET induction in *SoxC^{KO}* organoids.

FGSEA analysis demonstrates upregulation of Hypoxia-related factors during MET induction in *SoxC^{KO}* organoids (Table 5).

Gene	<i>SoxC⁺</i> Pulse reads	<i>SoxC^{KO}</i> Pulse reads	<i>SoxC^{KO}</i> vs <i>SoxC⁺</i> Log Fold Change	<i>SoxC^{KO}</i> vs <i>SoxC⁺</i> Adjusted p-value
<i>Il6</i>	0.0468	0.3274	2.8074	0.0246
<i>Stc2</i>	10.9265	42.8374	1.9710	0.0419
<i>Fosl2</i>	20.5678	79.0091	1.9416	0.0059
<i>Lox</i>	17.8366	66.5195	1.8989	0.0311
<i>Gys1</i>	57.1209	206.6121	1.8548	0.0090
<i>Gcnt2</i>	0.7066	2.4661	1.8032	0.0289
<i>Selenbp1</i>	56.6999	179.5991	1.6634	0.0314
<i>Pam</i>	44.4509	120.1686	1.4348	0.0339
<i>Gck</i>	1.1857	3.1484	1.4089	0.0072
<i>Plin2</i>	159.8312	418.7651	1.3896	0.0131
<i>Myh9</i>	222.6768	532.1632	1.2569	0.0165

<i>Grhpr</i>	48.9447	112.4220	1.1997	0.0380
<i>Vldlr</i>	36.9156	80.3581	1.1222	0.0195
<i>Gpc1</i>	125.1565	247.3224	0.9827	0.0151
<i>Cited2</i>	45.4397	89.2885	0.9745	0.0238

Table 6. Hypoxia-related genes are upregulated in *SoxC*^{KO} Pulse samples.

Il6 induces EMT in multiple cell types (Zhou et al., 2017), possibly via JAK2/STAT3 pathway (Xiao et al., 2017). In FGSEA analysis, other upregulated genes in IL6/JAK2/STAT3 pathway were discovered, including *A2m*, *Ifngr1*, *Socs3*, *Il6*, *Map3k8* and *Il17ra*.

Stc2 promotes EMT via AKT-ERK signaling (Chen et al., 2016)

Fosl2 promotes the transcription of transcription factor *Snai2* which subsequently leads to EMT (Yin et al., 2019).

Lox is a regulator of EMT process, inhibition of LOX was found to result in MET (Wang et al., 2016). LOX is linked to several pathways including TGF- β , PI3K/Akt/mTOR and Notch (Tenti & Vannucci, 2019).

Gys1 is regulated during EMT as a component of PI3K and MAPK pathways (Mutlu et al., 2016)

Selenbp1 negatively regulates EMT via inhibition of TWIST, a HIF-1 target. (Ying et al., 2015).

Pam is a part of ubiquitin ligase complex which degrades EMT transcription factors (Xu et al., 2015)

Plin2 was found to influence MET via TGF- β 2 metabolism (Corbet et al., 2020).

Myh9 induces TGF- β mediated EMT (Li et al., 2018)

Grhpr and *Vldlr* are upregulated by HIF (Singh et al., 2018) (Shen et al., 2012).

Based on the RNA-seq exploratory analysis, the gene expression effect of *SoxC* conditional knockout seems to extend to multiple pathways regulating EMT-MET transition, such as HIF-1 signalling pathway, PI3K-Akt pathway, TGF- β pathway, MAPK pathway, JAK-STAT pathway, NF- κ B pathway. This provides evidence for the existence of WNT/ β -catenin independent mechanism of action of *SoxC* in nephrogenesis.

Select nephrogenic lineage markers were compared in *SoxC*⁺ and *SoxC*^{KO} cells in Baseline and Pulse experimental conditions. This includes markers for induced/differentiating cells (*Hes1*⁺, *Pax8*⁺), renal vesicles (*Cdh4*⁺), podocyte precursors and podocytes (*Mafb*⁺), proximal

precursors (*Jag1*⁺), distal precursors (*Sox9*⁺, *Gata3*⁺) and stromal cells (*Acta2*⁺) (Lindström et al., 2018).

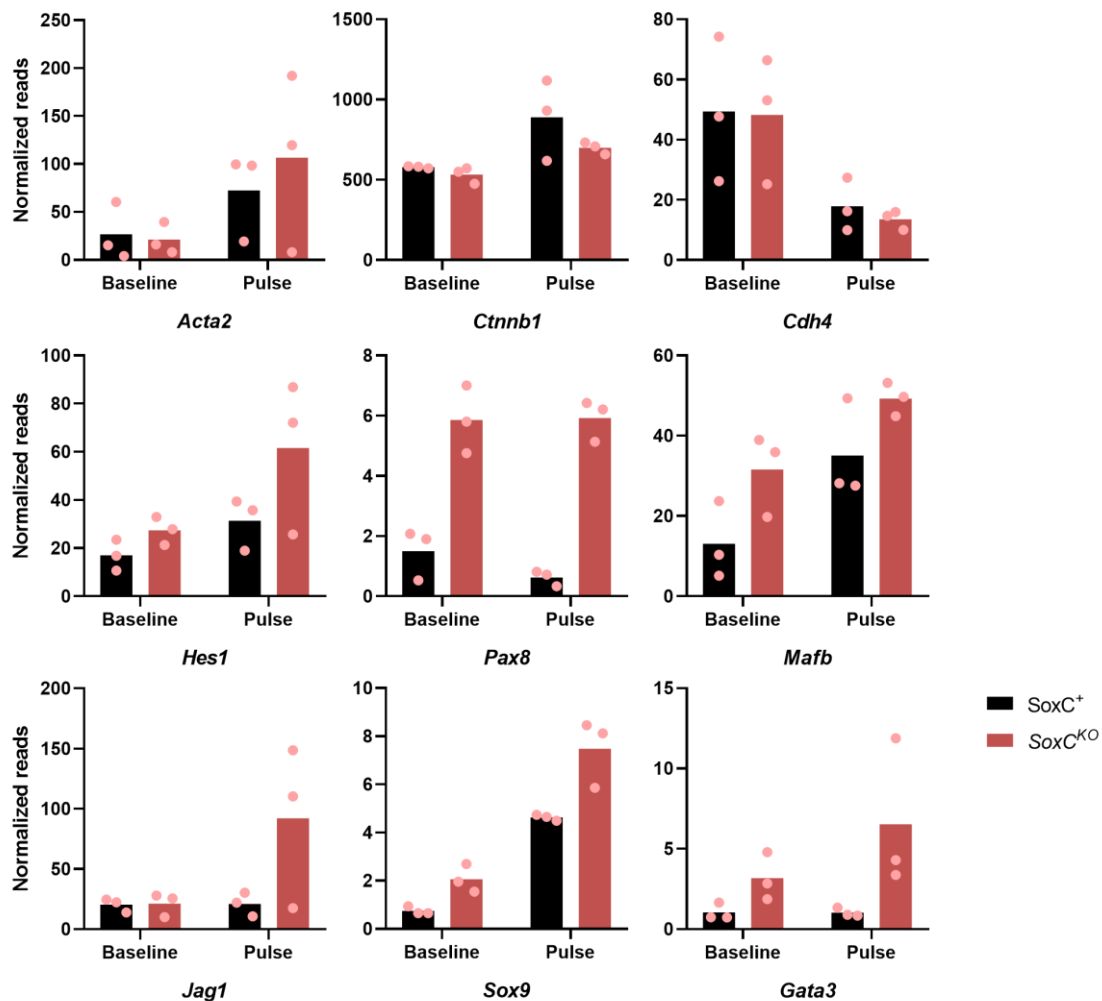


Figure 43: Metanephric lineage markers expression in different experimental conditions.

The markers of differentiated tissues were increased in Pulse conditions in *CagCRE*⁺ organoids compared to control *CagCRE*⁻ cells. However, no difference in β -catenin expression or E-cadherin expression could be found. This discrepancy with the result of qPCR data is likely stemming from the shorter time window of the RNA-seq analysis, where organoids were

harvested 24h after induction to capture the early stages of the transition, as opposed to 48h timepoint selected for qPCR analysis.

As known from previous research, *Sox4* silencing leads to downregulation of key *Sox4*-dependent EMT/MET factors. In this dataset, the downregulation of *Twist1* and *Sox2* was observed, which is consistent with other existing literature (Peng et al., 2018).

Interestingly, *Zeb1*, a transcription factor normally upregulated by *Sox4*, appeared to be upregulated in the absence of *Sox4* in the Pulse experimental condition (Figure 44). This discrepancy might reflect the role of *Zeb1* in MET regulation that is distinct from its role in EMT regulation.

Ezh2 is a known critical target gene of *Sox4* mediating its function in EMT through Polycomb repressive complex 2 (PRC2). *Ezh2* is downregulated in the absence of *SoxC* genes, reflecting the inability of *SoxC*^{KO} cells to undergo normal silencing of Polycomb-dependent genes in the process of MET. Interestingly, this reduction of *Ezh2* expression was balanced by comparable increase in expression of *Ezh1*, an alternative component of PRC2. PRC2 composition is changing in the process of development, with EZH2-PRC2 being associated with progenitor

cells, and EZH1-PRC2 being associated with adult differentiated cells (Xu et al., 2015; Kook, Seo & Jain, 2017)

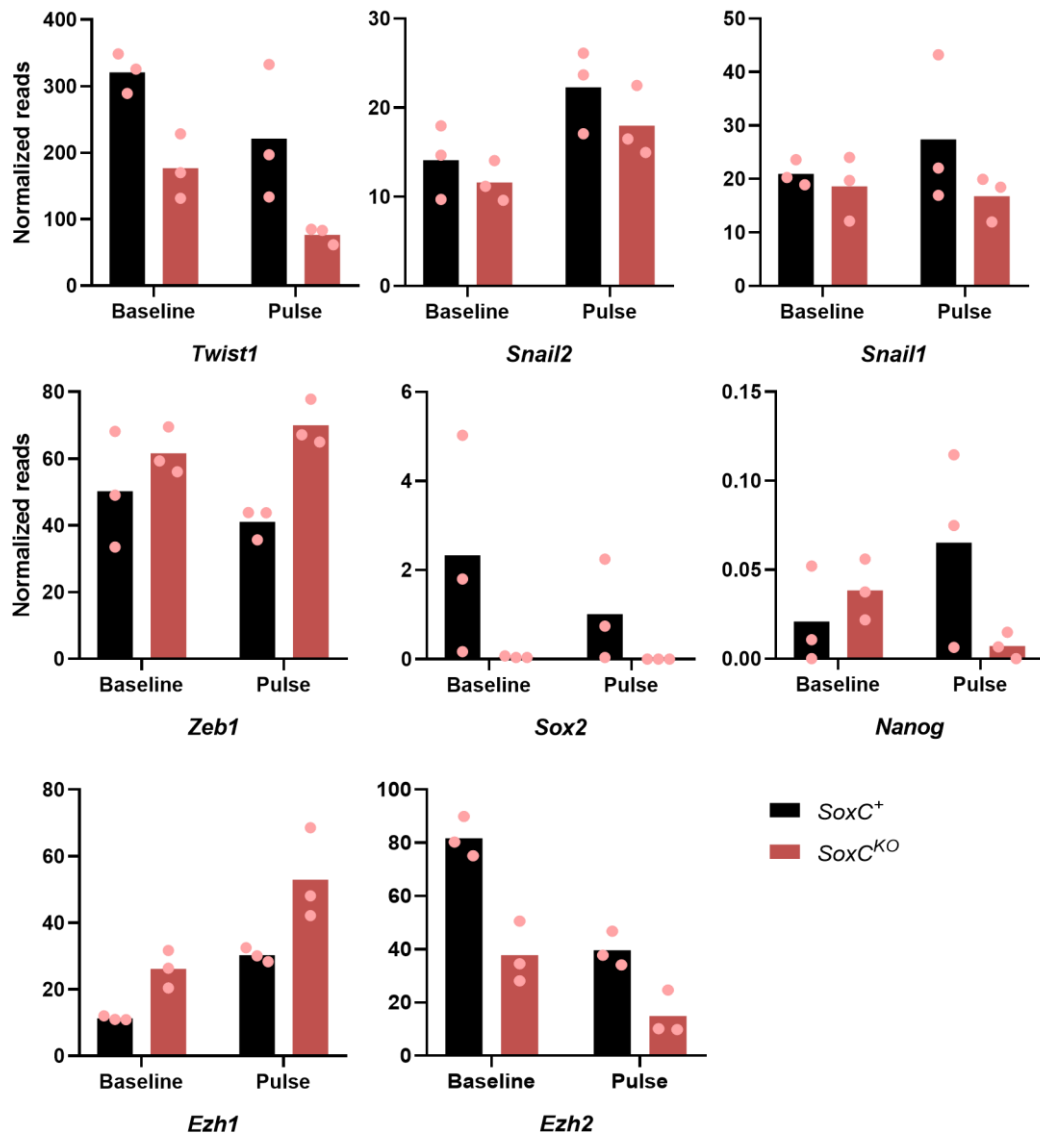


Figure 44: *Sox4*-dependent EMT factors expression in different experimental conditions.

Taking into consideration the above data, it's plausible that *SoxC* knockout causes the downregulation of *Ezh2* and upregulation of *Ezh1*, which affects PRC2 composition and leads

to misexpression of numerous PRC-dependent regulatory pathway genes, leading to the inability of *SoxC*^{KO} cells to undergo MET.

Conclusions and perspectives

SOX transcription factors are a protein family highly important in the process of development of multiple organs. Despite the abundance of studies on the role of *Sox* genes in development, little is known about their function during kidney morphogenesis. SOXC transcription factors were found to exhibit a multifaceted effect on kidney development, both on the early UB induction stage, and on the late nephrogenesis stage. The present work aimed to characterize the effect of *SoxC* genes on two stages of kidney development: the UB induction stage, and nephrogenesis stage.

Sox11 role during ureteric bud emergence

The phenotype of *Sox11*^{-/-} embryos features the duplication of the collecting system. The distinguishing feature of this phenotype is the emergence of only one ectopic UB, setting this phenotype apart from many other multiplex kidney mutations. The developmental mechanism behind this anomaly was the target of this research project. The *in situ* hybridization analysis revealed a rostral extension of *Gdnf* expression domain in the forming embryo. This observation can be explained with three different models of *Sox11* action: SOX11 is regulating either apoptosis, cell migration, or differentiation.

To narrow down the possible developmental mechanism, further experiments utilized wholemount confocal imaging to reveal regions of apoptosis in the forming IM. As apoptosis persisted in *Sox11*^{-/-} embryos, it was unlikely to influence early kidney development. Next, difference in cell migration was assessed *in vitro* using *SoxC* conditional knockout nephron progenitor cell line. *SoxC* knockout cells demonstrated absence of migration compared to controls, providing evidence in support of cell migration model of *Sox11* action in early kidney development.

To confirm the importance of cell migration in SOX11 action, further research would need to be performed *in vivo*. One possible experimental design would be to use time-lapse microscopy on *Six2-EGFP/cre* mouse embryos to track the movements of MM cells in *Sox11*^{+/+} and *Sox11*^{-/-} conditions. In addition, the role of differentiation in MM domain formation will need to be explored using lineage tracing tools to establish the fate of rostral MM cells.

SoxC genes in nephrogenesis

Sox11 mutant embryos were found to exhibit anomalies in their nephron patterning, such as shortened Henle's loops. Furthermore, conditional knockout of *SoxC* genes in CM resulted in drastically decreased nephron number due to the inability of progenitor cells to epithelialize. To gain further insight into the function of *SoxC* genes in nephrogenesis, *in vitro* approach was employed using nephron progenitor cells isolated from *SoxC* conditional knockout mouse embryos. After conditional deletion of *SoxC* using Cre-Lox recombination, cells were forced to undergo mesenchymal-to-epithelial transition and to organize into organoid structures. Molecular analysis was performed to uncover the changes in cellular differentiation brought by the absence of *SoxC*, which allowed to propose a model for their action in nephrogenesis.

To model MET in renal progenitor cells, cultured cells were treated with the β -catenin pathway inducer CHIR, and the resulting molecular changes analyzed via qPCR. After the addition of CHIR, renal progenitors showed *Axin2* (a downstream target and negative regulator of WNT/ β -catenin pathway) was upregulated. Short-term treatment of cultures with CHIR (pulse treatment) resulted in dramatic upregulation of *Cdh1* (a marker of epithelialized tissues) expression, while *Axin2* expression was downregulated. Therefore, we can conclude that addition of CHIR promotes β -catenin signalling, while following removal of CHIR allows for MET to conclude. In *CAG^{CreERT2} Sox4^{fllox/fllox} Sox11^{fllox/fllox} Sox12^{-/-}* cells, however, no upregulation of *Cdh1* was observed, and *Axin2* expression remained high after removal of CHIR. These data suggest that *SOXC* genes are important for downregulating the WNT/ β -catenin pathway activity during MET (Figure 45). This two-step protocol allows us to study MET at different timepoints, and coupled with tamoxifen-induced recombination, it constitutes a powerful system to analyse the role of *SOXC* proteins during MET

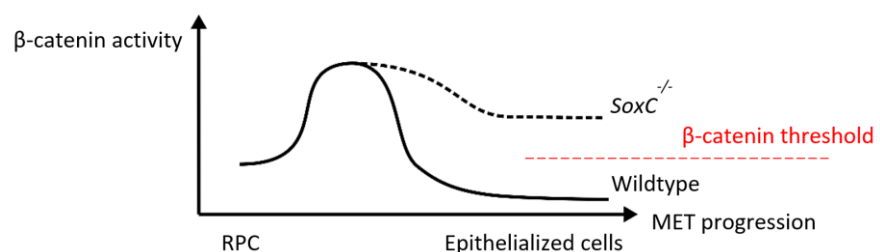


Figure 45: A model of direct interaction between *SOXC* and WNT/ β -catenin pathway. In wildtype renal progenitor cells, the rise and subsequent fall of β -catenin concentration leads to epithelialization of the cells. In *SoxC^{-/-}* cells, the fall of β -catenin concentration doesn't occur, preventing epithelialization.

RNA-seq analysis of control and *SoxC* knockout organoids undergoing MET allowed for screening of molecular pathways likely to mediate the effect of *SoxC* on epithelialization. After *SoxC* knockout, but before MET induction, a number of MET signaling pathways were found to be impacted, such as Wnt/ β -catenin pathway, FGF pathway, BMP pathway, HIF-1 pathway, PI3K-Akt pathway, TGF- β pathway, MAPK pathway, JAK-STAT pathway and NF- κ B pathway. It's probable that the difference in transcription activity of these pathways was brought by *SoxC* knockout and is responsible for inability of *SoxC^{KO}* cells to undergo MET. However, the mechanism of action of *SoxC* on these pathways needs to be explained.

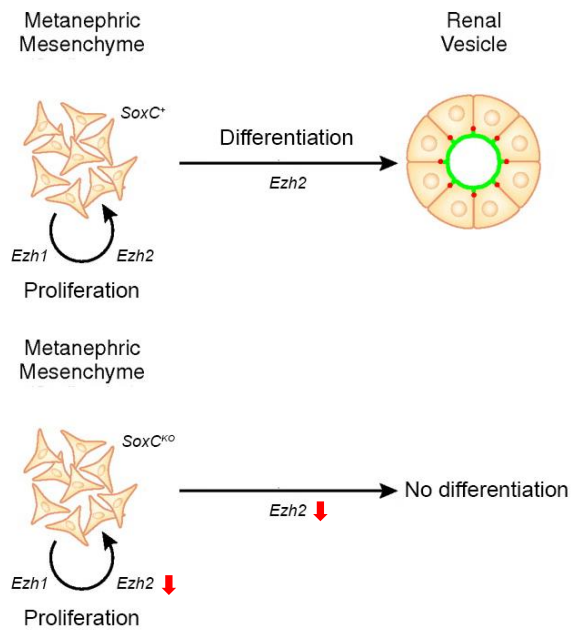


Figure 46: A model of indirect regulation of NPC differentiation by *SoxC* genes. In *SoxC⁺* renal progenitor cells, *Ezh1* and *Ezh2* are responsible for the maintenance of progenitor cell population, with *Ezh2* required for chromatin remodelling during differentiation into epithelialized renal vesicle. In *SoxC^{-/-}* cells, NPC cells lose their ability to epithelialize due to *Ezh2* downregulation, while maintaining progenitor cell population with the help of *Ezh1*.

In previous research, *Sox4* has been identified as a regulator of EMT and a factor associated with stemness (Tiwari et al., 2013). The mechanism of *Sox4* action was found to involve the regulation of *Ezh2* expression, with EZH2-PRC2 being responsible for H3K27me3 histone marks that are critical for transcriptomic reprogramming of cells undergoing EMT. In contrast, EZH1-PRC2, while targeting same genes as EZH2, appears to be associated with actively transcribed genes and promote mRNA transcription (Mousavi et al., 2012). While the role of EZH1 is safeguarding H3K27 methylation of EZH2-PRC2 have been established (Shen et al., 2008; Mu et al., 2017), there is no consensus on mechanism of action of EZH1-PRC2 on actively transcribed genes. *Ezh1* was found to be sufficient for maintenance of stemness and self-renewal in the absence of *Ezh2*, but not sufficient for successful differentiation (Bae et al., 2015; Bardot et al., 2013; Ezhkova et al., 2011; Mochizuki-Kashio et al., 2011). Similar observations were made in the experiments with *SoxC^{KO}* NPC, which lose their ability to epithelialize while maintaining the progenitor pool in CM. Depletion of *Ezh2* with continuing

expression of *Ezh1* is a possible mechanism explaining the inability of *SoxC^{KO}* NPC to epithelialize (Figure 46).

However, the RNA-seq approach was found to include some limitations, including:

- partial knockdown of *Sox4* expression instead of a full knockout,
- short timepoint of 24h which doesn't allow to observe MET long enough until E-cadherin expression becomes apparent, and
- sex difference between embryos of the same litter necessitating exclusion of sex-linked genes.

For this reason, direct investigation of the chromatin state of NPCs during MET will be required to observe the influence of *SoxC* genes on methylation of genes regulated by PRC2. In addition, PRC2 composition analysis will provide evidence for the shift from EZH2-PRC2 to EZH1-PRC2 in *SoxC^{KO}* NPCs.

In summary, the research presented in this manuscript identified potential mechanisms underlying the effect of *Sox11* and *SoxC* genes on early and late kidney development. Cell migration regulation was proposed as the potential mechanism responsible for the role of *Sox11* in MM domain specification in early kidney development. The developmental role of *Sox11* provides a parallel to its other functions as a wound repair gene enhancing epidermal cell migration (Miao et al., 2019) and as a migration regulator in mantle cell lymphoma (Balsas et al., 2017). The role of *SoxC* genes in nephrogenesis was linked to their effect on chromatin remodelling enzymes EZH1 and EZH2, which affect the process of MET in kidney development, leading to disruption in expression of WNT/ β -catenin genes and other molecular pathway genes. This function of *SoxC* genes during development is related to their role in esophageal cancer (Koumangoye et al., 2015), as well as in breast cancer and melanoma cells (Tiwari et al., 2013) where *Sox4* was found to directly interact with EZH2. Considering the shifting balance between EZH1 and EZH2 in the PRC2 complex between embryonic and adult tissues, developmental systems are likely to be a valuable experimental model for studying the effect of chromatin remodelling on development and disease.

Materials and methods

Mice

Animal experiments were conducted according to French and international guidelines. *Sox11* knockout mouse strain was previously obtained (Sock et al., 2004). Mice were maintained on a mixed B6D2F1 wildtype background. All comparisons were made between littermates of the same strain, therefore control and *Sox11* knockout embryos are named *Sox11*^{+/+} and *Sox11*^{-/-}, respectively. Genotyping of mice and embryos was carried out by PCR as previously described.

IF slides

Embryonic samples from timed matings were collected, where day of vaginal plug was equivalent to E0.5. Samples were fixed in 4% paraformaldehyde overnight at 4°C, serially dehydrated on a carousel and then embedded in paraffin. Embedded samples were sectioned on a microtome. Sections of 5 µm thickness were deposited on a glass slide.

For immunofluorescent analysis, paraffin sections were dewaxed and re-hydrated via incubation in diluted ethanol series. Epitope retrieval was performed in 10mM Sodium citrate (pH 6) at 2 min in a pressure cooker. Alternatively, Agilent PT Link was used for dewaxing and epitope retrieval, with a supplied pH 6 solution. Subsequently, sections were washed twice with PBS and incubated in blocking solution (PBS, 10% normal donkey serum) for 1 hour at room temperature. Blocking solution was replaced by a solution of corresponding mix of primary antibodies (see below) diluted in PBS with 1% normal donkey serum. Slides were incubated in wet chamber overnight at 4°C. Slides were washed twice with PBS, then incubated with a corresponding mix of secondary antibodies (see below) diluted in PBS containing Hoechst 1:15000. Slides were washed twice with PBS and mounted with Vectamount. Fluorescent images were taken on a ZEISS Apotome using Axiocam Mrm camera and processed with ImageJ.

Wholemout immunofluorescence

Lysotracker staining was performed on freshly dissected E10.5 embryos as described in (Fogel et al., 2012).

Embryos were fixed in 4% PFA overnight. Embryos were incubated with primary antibodies for 2 days at 37°C. Embryos were incubated with secondary antibodies for 2 days at 37°C. Embryos were clarified using BABB as described in (Yokomizo et al., 2013)

Embryos were imaged using confocal microscope and images were analysed using Imaris software.

Primary antibodies were diluted in PBS: Six2 (rabbit) 1:300, Pan-Cytokeratin (mouse) 1:500, Pax2 (rabbit) 1:200, DBA biotinylated 1:100, Sall1 (rabbit) 1:300

Protein extraction

Protein extraction buffer:

HEPES 10mM

KCl 10mM

EDTA 0.1 mM

EGTA 0.1 mM

cOmplete Protease Inhibitor (1X)

mQ H₂O

150 uL of protein extraction buffer was added to a cell pellet. Sample was vortexed for 20 seconds, incubated on ice for 15 minutes. 9,4 uL NP-40 (10%) were added to the sample. Sample was vortexed for 10 seconds and incubated on ice for 1 minute. Sample was centrifugated for 10 min on 3000g at 4°C. Cytoplasmic proteins in the supernatant were separated, and the pellet was washed with protein extraction buffer and centrifugated on 16000g for 1 minute at 4°C twice. Nuclear extraction buffer (20 mM Tris-Cl pH 8, 420mM NaCl, 1.5 mM MgCl₂, 0.2 mM EDTA) was added to the pellet and incubated on ice for 10 minutes with vortexing every 2 minutes. Samples were treated with ultrasound for 2 seconds. Samples were centrifugated on 16000g for 5 minutes at 4°C and supernatant with nuclear protein fraction was separated.

Western blotting

5x Laemmli buffer was added to the protein sample with 1M DTT. Proteins were denatured by heating the samples on 99°C for 5 minutes. Polyacrylamide resolving gel was cast in 1.5mm glass covers from 12% Acrylamide-Bis-acrylamide mix with Tris pH 8.8 (375mM), SDS (0,1%), Ammonium persulfate (0,1%) and TEMED (0,08%). Stacking gel was prepared from 5% Acrylamide-Bis-acrylamide mix with Tris pH 6.8 (130mM), SDS (0,1%), Ammonium persulfate (0,1%) and TEMED (0,08%). Gel was immersed in Tris-Glycine buffer (25mM Tris, 250mM Glycine, 0,1% SDS) at 100V of current until proteins reached the bottom of the gel.

Proteins were transferred from the gel to PVDF membrane. For this, they were assembled in a stack against each other in Tris-Glycine buffer with 10% methanol. Current of 100V was applied for 1 hour at 4°C with magnetic mixing.

qPCR

cDNA samples were diluted 1:10 with water, Samples were mixed together in 1:4 dilution and diluted 5-fold 4 times to obtain standards. Master mix was made of 2x SybrGreen, 10uM forward and reverse primers, and water. In 96-tube plastic plate, 9 uL of master mix and 1uL of cDNA sample were mixed. Plate was covered with film, briefly centrifugated and analysed on LightCycler 480.

qPCR parameters:

95°C 5 min activation

40 cycles:

95°C 10 sec denaturation

60°C 20 sec annealing

72°C 10 sec elongation

Melting curves were recorded at 95°C with continuous acquisition.

RPC isolation

Embryonic kidneys were isolated from E16.5 mouse embryos in cold PBS. The kidney capsule was removed without damaging the kidney surface. Kidneys were separated by genotype. Kidneys were treated with collagenase-pancreatin mix for 13 minutes at 37°C. RPC were centrifugated and transferred to AutoMACS buffer, run through a pre-separation filter. RPC were treated with antibodies anti-CD105-PE, anti-CD140-PE, anti-TER119-PE, anti-CD326-PE for 13 minutes, and then treated with anti-PE magnetic microbeads for 18 minutes. Cell suspension was then transferred to LD columns (Myltenyl Biotec) and run on a magnet. Eluted cells were centrifugated at 300g for 5 minutes and resuspended in RPC medium.

Cell culture

Isolated RPC cells were plated on a plastic cell culture plate of appropriate size corresponding to the cell density of 20000 cells per cm². Plate wells were coated by Geltrex diluted in cell media 1:100 for 30 minutes at 37°C. Cells were cultured using advanced RPMI medium at 37°C with 5% CO₂:

Advanced RPMI medium

Glutamax (1x)

Penstrep (1x)

FGF9 (200 ng/ml)

Y27632 (10 uM)

IGF1 (20 ng/ml)

IGF2 (2 ng/ml)

BMP4 (30 ng/ml)

BMP7 (30 ng/ml)

LDN-193189 (125 nM)

CHIR99021 (1.25 uM)

Heparin (1ug/ml)

Upon reaching 80% confluency, RPC were split using TrypLE for 1 minute at room temperature, and then centrifugated at 300g for 5 minutes

Organoid formation

RPC were detached using TrypLE for 1 minute at room temperature, and then centrifugated at 300g for 5 minutes. A portion of cells was set aside to be harvested as a “Baseline” condition. Cells were resuspended in RPMI media and transferred to 500ul plastic tubes. The lid of the tube was perforated with a needle to provide airflow. Tubes were centrifugated at 300g for 2 minutes. Tubes were incubated at 37°C with 5% CO₂.

Cell culture media were changed during the incubation to achieve MET. The media were based on Advanced RPMI with addition of Glutamax (1x), Penstrep (1x) and:

- 1) CHIR99021 5uM, DMH1 4uM
- 2) CHIR99021 3uM, DMH1 0.4uM, FGF9 10ng
- 3) FGF9 20ng

The cells under the “pulse” condition were incubated for 1 hour in medium 1, then for 3 hours in medium 2, then overnight in medium 3.

RNA-seq

RPC Organoids were harvested in RLT buffer after an overnight incubation and stored at -80°C. RNA was isolated using Qiagen RNeasy Mini Kit. RNA quality was analysed by Bioanalyzer Nano Chip. The RNA samples were analysed by Novogene using Illumina NovaSeq 6000 with paired-end read length of 150.

Volcano Plots

Data were plotted using Galaxy web service. LogFold Change cutoff of 1 corresponds to 2-fold difference in expression. Significance cutoff was set on $q < 0.05$.

Scratch wound assay

CAG^{CreERT2} Sox4^{fl/fl} Sox11^{fl/fl} Sox12^{-/-} RPC were grown to the confluency of 80%. Cells were treated with Tamoxifen for 1 day to achieve knockout of *Sox4* and *Sox11*. Cells were transferred to 96-well ImageLock plates and wounds were created by Woundmaker. Cells were incubated in IncuCyte at 37°C with 5% CO₂ until the closure of the wound. Images were taken every 60 minutes and analysed automatically by IncuCyte software.

Bibliography

- Aigner, K., Descovich, L., Mikula, M., Sultan, A., Dampier, B., Bonné, S., van Roy, F., Mikulits, W., Schreiber, M., Brabletz, T., Sommergruber, W., Schweifer, N., Wernitznig, A., Beug, H., Foisner, R., & Eger, A. (2007). The transcription factor ZEB1 (δ EF1) represses Plakophilin 3 during human cancer progression. *FEBS Letters*, *581*(8), 1617–1624. <https://doi.org/10.1016/j.febslet.2007.03.026>
- Airik, R., Trowe, M.-O., Foik, A., Farin, H. F., Petry, M., Schuster-Gossler, K., Schweizer, M., Scherer, G., Kist, R., & Kispert, A. (2010). Hydroureteronephrosis due to loss of Sox9-regulated smooth muscle cell differentiation of the ureteric mesenchyme. *Human Molecular Genetics*, *19*(24), 4918–4929. <https://doi.org/10.1093/hmg/ddq426>
- Aisa, M. C., Cappuccini, B., Barbati, A., Clerici, G., Torlone, E., Gerli, S., & Di Renzo, G. C. (2019). Renal Consequences of Gestational Diabetes Mellitus in Term Neonates: A Multidisciplinary Approach to the DOHaD Perspective in the Prevention and Early Recognition of Neonates of GDM Mothers at Risk of Hypertension and Chronic Renal Diseases in Later Life. *Journal of Clinical Medicine*, *8*(4). <https://doi.org/10.3390/jcm8040429>
- Akiyama, H., Lyons, J. P., Mori-Akiyama, Y., Yang, X., Zhang, R., Zhang, Z., Deng, J. M., Taketo, M. M., Nakamura, T., Behringer, R. R., McCrea, P. D., & de Crombrughe, B. (2004). Interactions between Sox9 and beta-catenin control chondrocyte differentiation. *Genes & Development*, *18*(9), 1072–1087. <https://doi.org/10.1101/gad.1171104>
- Armoskus, C., Moreira, D., Bollinger, K., Jimenez, O., Taniguchi, S., & Tsai, H.-W. (2014). Identification of sexually dimorphic genes in the neonatal mouse cortex and hippocampus. *Brain Research*, *1562*, 23–38. <https://doi.org/10.1016/j.brainres.2014.03.017>

- Balsas, P., Esteve-Arenys, A., Roldán, J., Jiménez, L., Rodríguez, V., Valero, J. G., Chamorro-Jorganes, A., de la Bellacasa, R. P., Teixidó, J., Matas-Céspedes, A., Moros, A., Martínez, A., Campo, E., Sáez-Borderías, A., Borrell, J. I., Pérez-Galán, P., Colomer, D., & Roué, G. (2017). Activity of the novel BCR kinase inhibitor IQS019 in preclinical models of B-cell non-Hodgkin lymphoma. *Journal of Hematology & Oncology*, *10*(1), 80. <https://doi.org/10.1186/s13045-017-0447-6>
- Banyard, J., & Bielenberg, D. R. (2015). The role of EMT and MET in cancer dissemination. *Connective Tissue Research*, *56*(5), 403–413. <https://doi.org/10.3109/03008207.2015.1060970>
- Barak, H., Huh, S.-H., Chen, S., Jeanpierre, C., Martinovic, J., Parisot, M., Bole-Feysot, C., Nitschké, P., Salomon, R., Antignac, C., Ornitz, D. M., & Kopan, R. (2012). FGF9 and FGF20 maintain the stemness of nephron progenitors in mice and man. *Developmental Cell*, *22*(6), 1191–1207. <https://doi.org/10.1016/j.devcel.2012.04.018>
- Barasch, J. (1999). FGF-2: Specific activity in kidney? *Kidney International*, *56*(3), 1156–1157. <https://doi.org/10.1046/j.1523-1755.1999.00649.x>
- Basta, J. M., Robbins, L., Denner, D. R., Kolar, G. R., & Rauchman, M. (2017). A Sall1-NuRD interaction regulates multipotent nephron progenitors and is required for loop of Henle formation. *Development*, *144*(17), 3080–3094. <https://doi.org/10.1242/dev.148692>
- Bazi, Z., Bertacchi, M., Abasi, M., Mohammadi-Yeganeh, S., Soleimani, M., Wagner, N., & Ghanbarian, H. (2018). Rn7SK small nuclear RNA is involved in neuronal differentiation. *Journal of Cellular Biochemistry*, *119*(4), 3174–3182. <https://doi.org/10.1002/jcb.26472>
- Bernard, P., Tang, P., Liu, S., Dewing, P., Harley, V. R., & Vilain, E. (2003). Dimerization of SOX9 is required for chondrogenesis, but not for sex determination. *Human Molecular Genetics*, *12*(14), 1755–1765. <https://doi.org/10.1093/hmg/ddg182>
- Berry, R. L., Ozdemir, D. D., Aronow, B., Lindström, N. O., Dudnakova, T., Thornburn, A., Perry, P., Baldock, R., Armit, C., Joshi, A., Jeanpierre, C., Shan, J., Vainio, S., Baily, J., Brownstein, D., Davies, J., Hastie, N. D., & Hohenstein, P. (2015). Deducing the stage of origin of Wilms' tumours from a developmental series of Wt1-mutant mice. *Disease Models & Mechanisms*, *8*(8), 903–917. <https://doi.org/10.1242/dmm.018523>
- Bianchi, M. E., Falciola, L., Ferrari, S., & Lilley, D. M. (1992). The DNA binding site of HMG1 protein is composed of two similar segments (HMG boxes), both of which have counterparts in other eukaryotic regulatory proteins. *The EMBO Journal*, *11*(3), 1055–1063. <https://doi.org/10.1002/j.1460-2075.1992.tb05144.x>
- Blake, J., & Rosenblum, N. D. (2014). Renal branching morphogenesis: Morphogenetic and signaling mechanisms. *Seminars in Cell & Developmental Biology*, *36*, 2–12. <https://doi.org/10.1016/j.semcdb.2014.07.011>
- Blank, U., Brown, A., Adams, D. C., Karolak, M. J., & Oxburgh, L. (2009). BMP7 promotes proliferation of nephron progenitor cells via a JNK-dependent mechanism. *Development (Cambridge, England)*, *136*(21), 3557–3566. <https://doi.org/10.1242/dev.036335>
- Boubred, F., Vendemmia, M., Garcia-Meric, P., Buffat, C., Millet, V., & Simeoni, U. (2006). Effects of maternally administered drugs on the fetal and neonatal kidney. *Drug Safety*, *29*(5), 397–419. <https://doi.org/10.2165/00002018-200629050-00004>
- Bouchard, M. (2002). Nephric lineage specification by Pax2 and Pax8. *Genes & Development*, *16*(22), 2958–2970. <https://doi.org/10.1101/gad.240102>
- Bouchard, M., Pfeffer, P., & Busslinger, M. (2000). Functional equivalence of the transcription factors Pax2 and Pax5 in mouse development. *Development*, *127*(17), 3703 LP – 3713.

<http://dev.biologists.org/content/127/17/3703.abstract>

- Boyle, S. C., Kim, M., Valerius, M. T., McMahon, A. P., & Kopan, R. (2011). Notch pathway activation can replace the requirement for Wnt4 and Wnt9b in mesenchymal-to-epithelial transition of nephron stem cells. *Development (Cambridge, England)*, *138*(19), 4245–4254. <https://doi.org/10.1242/dev.070433>
- Boyle, S., Misfeldt, A., Chandler, K. J., Deal, K. K., Southard-Smith, E. M., Mortlock, D. P., Baldwin, H. S., & de Caestecker, M. (2008). Fate mapping using Cited1-CreERT2 mice demonstrates that the cap mesenchyme contains self-renewing progenitor cells and gives rise exclusively to nephronic epithelia. *Developmental Biology*, *313*(1), 234–245. <https://doi.org/10.1016/j.ydbio.2007.10.014>
- Boyle, S., Shioda, T., Perantoni, A. O., & de Caestecker, M. (2007). Cited1 and Cited2 are differentially expressed in the developing kidney but are not required for nephrogenesis. *Developmental Dynamics*, *236*(8), 2321–2330. <https://doi.org/10.1002/dvdy.21242>
- Brändli AW. (1999). Towards a molecular anatomy of the Xenopus pronephric kidney. *Int J Dev Biol*, *43*(5), 381–395. <https://doi.org/https://doi.org/10.1387/ijdb.10535314>
- Brophy, P. D., Ostrom, L., Lang, K. M., & Dressler, G. R. (2001). Regulation of ureteric bud outgrowth by Pax2-dependent activation of the glial derived neurotrophic factor gene. *Development (Cambridge, England)*, *128*(23), 4747–4756. <http://www.ncbi.nlm.nih.gov/pubmed/11731455>
- Brown, A. C., Adams, D., de Caestecker, M., Yang, X., Friesel, R., & Oxburgh, L. (2011). FGF/EGF signaling regulates the renewal of early nephron progenitors during embryonic development. *Development*, *138*(23), 5099–5112. <https://doi.org/10.1242/dev.065995>
- Brown, A. C., Muthukrishnan, S. D., Guay, J. A., Adams, D. C., Schafer, D. A., Fetting, J. L., & Oxburgh, L. (2013). Role for compartmentalization in nephron progenitor differentiation. *Proceedings of the National Academy of Sciences*, *110*(12), 4640–4645. <https://doi.org/10.1073/pnas.1213971110>
- Brunskill, E. W., Park, J.-S., Chung, E., Chen, F., Magella, B., & Potter, S. S. (2014). Single cell dissection of early kidney development: multilineage priming. *Development*, *141*(15), 3093–3101. <https://doi.org/10.1242/dev.110601>
- Burn, S. F., Webb, A., Berry, R. L., Davies, J. A., Ferrer-Vaquer, A., Hadjantonakis, A. K., Hastie, N. D., & Hohenstein, P. (2011). Calcium/NFAT signalling promotes early nephrogenesis. *Developmental Biology*, *352*(2), 288–298. <https://doi.org/10.1016/j.ydbio.2011.01.033>
- Burns, R. K. (1955). Urogenital system. In *Willier, B.H., Weiss, P.A., Hamburger, V. (Eds.). Analysis of Development.*
- Carroll, T. J., Park, J.-S., Hayashi, S., Majumdar, A., & McMahon, A. P. (2005). Wnt9b plays a central role in the regulation of mesenchymal to epithelial transitions underlying organogenesis of the mammalian urogenital system. *Developmental Cell*, *9*(2), 283–292. <https://doi.org/10.1016/j.devcel.2005.05.016>
- Castillo, S. D., Matheu, A., Mariani, N., Carretero, J., Lopez-Rios, F., Lovell-Badge, R., & Sanchez-Cespedes, M. (2012). Novel Transcriptional Targets of the SRY-HMG Box Transcription Factor SOX4 Link Its Expression to the Development of Small Cell Lung Cancer. *Cancer Research*, *72*(1), 176–186. <https://doi.org/10.1158/0008-5472.CAN-11-3506>
- Celli, G., LaRochelle, W. J., Mackem, S., Sharp, R., & Merlino, G. (1998). Soluble dominant-negative receptor uncovers essential roles for fibroblast growth factors in multi-organ induction and patterning. *The EMBO Journal*, *17*(6), 1642–1655. <https://doi.org/10.1093/emboj/17.6.1642>

- Chen, B., Zeng, X., He, Y., Wang, X., Liang, Z., Liu, J., Zhang, P., Zhu, H., Xu, N., & Liang, S. (2016). STC2 promotes the epithelial-mesenchymal transition of colorectal cancer cells through AKT-ERK signaling pathways. *Oncotarget*, *7*(44), 71400–71416. <https://doi.org/10.18632/oncotarget.12147>
- Chen, P., Cescon, M., & Bonaldo, P. (2013). Collagen VI in cancer and its biological mechanisms. *Trends in Molecular Medicine*, *19*(7), 410–417. <https://doi.org/10.1016/j.molmed.2013.04.001>
- Cheng, H.-T., Kim, M., Valerius, M. T., Surendran, K., Schuster-Gossler, K., Gossler, A., McMahon, A. P., & Kopan, R. (2007). Notch2, but not Notch1, is required for proximal fate acquisition in the mammalian nephron. *Development*, *134*(4), 801–811. <https://doi.org/10.1242/dev.02773>
- Chung, E., Deacon, P., & Park, J.-S. (2017). Notch is required for the formation of all nephron segments and primes nephron progenitors for differentiation. *Development (Cambridge, England)*, *144*(24), 4530–4539. <https://doi.org/10.1242/dev.156661>
- Colvin, J. S., Green, R. P., Schmahl, J., Capel, B., & Ornitz, D. M. (2001). Male-to-female sex reversal in mice lacking fibroblast growth factor 9. *Cell*, *104*(6), 875–889. [https://doi.org/10.1016/s0092-8674\(01\)00284-7](https://doi.org/10.1016/s0092-8674(01)00284-7)
- Combes, A. N., Phipson, B., Lawlor, K. T., Dorison, A., Patrick, R., Zappia, L., Harvey, R. P., Oshlack, A., & Little, M. H. (2019). Single cell analysis of the developing mouse kidney provides deeper insight into marker gene expression and ligand-receptor crosstalk. *Development*, *146*(12), dev178673. <https://doi.org/10.1242/dev.178673>
- Connor, F., Cary, P. D., Read, C. M., Preston, N. S., Driscoll, P. C., Denny, P., Crane-Robinson, C., & Ashworth, A. (1994). DNA binding and bending properties of the postmeiotically expressed Sry-related protein Sox-5. *Nucleic Acids Research*, *22*(16), 3339–3346. <https://doi.org/10.1093/nar/22.16.3339>
- Corbet, C., Bastien, E., Santiago de Jesus, J. P., Dierge, E., Martherus, R., Vander Linden, C., Doix, B., Degavre, C., Guilbaud, C., Petit, L., Michiels, C., Dessy, C., Larondelle, Y., & Feron, O. (2020). TGFβ2-induced formation of lipid droplets supports acidosis-driven EMT and the metastatic spreading of cancer cells. *Nature Communications*, *11*(1), 454. <https://doi.org/10.1038/s41467-019-14262-3>
- Costantini, F. (2010). GDNF/Ret signaling and renal branching morphogenesis. *Organogenesis*, *6*(4), 252–262. <https://doi.org/10.4161/org.6.4.12680>
- Das, A., Tanigawa, S., Karner, C. M., Xin, M., Lum, L., Chen, C., Olson, E. N., Perantoni, A. O., & Carroll, T. J. (2013). Stromal–epithelial crosstalk regulates kidney progenitor cell differentiation. *Nature Cell Biology*, *15*(9), 1035–1044. <https://doi.org/10.1038/ncb2828>
- Davis, A. P., & Capecchi, M. R. (1994). Axial homeosis and appendicular skeleton defects in mice with a targeted disruption of hoxd-11. *Development*, *120*(8), 2187 LP – 2198. <http://dev.biologists.org/content/120/8/2187.abstract>
- Desgrange, A., & Cereghini, S. (2015). Nephron Patterning: Lessons from Xenopus, Zebrafish, and Mouse Studies. *Cells*, *4*(3), 483–499. <https://doi.org/10.3390/cells4030483>
- Di Lollo, V., Canciello, A., Orsini, M., Bernabò, N., Ancora, M., Di Federico, M., Curini, V., Mattioli, M., Russo, V., Mauro, A., Cammà, C., & Barboni, B. (2020). Transcriptomic and computational analysis identified LPA metabolism, KLHL14 and KCNE3 as novel regulators of Epithelial-Mesenchymal Transition. *Scientific Reports*, *10*(1), 4180. <https://doi.org/10.1038/s41598-020-61017-y>
- Dong, L., Pietsch, S., & Englert, C. (2015). Towards an understanding of kidney diseases associated

- with WT1 mutations. *Kidney International*, 88(4), 684–690. <https://doi.org/10.1038/ki.2015.198>
- Dono, R., Texido, G., Dussel, R., Ehmke, H., & Zeller, R. (1998). Impaired cerebral cortex development and blood pressure regulation in FGF-2-deficient mice. *The EMBO Journal*, 17(15), 4213–4225. <https://doi.org/10.1093/emboj/17.15.4213>
- Donovan, M. J., Natoli, T. A., Sainio, K., Amstutz, A., Jaenisch, R., Sariola, H., & Kreidberg, J. A. (1999). Initial differentiation of the metanephric mesenchyme is independent of WT1 and the ureteric bud. *Developmental Genetics*, 24(3–4), 252–262. [https://doi.org/10.1002/\(SICI\)1520-6408\(1999\)24:3/4<252::AID-DVG8>3.0.CO;2-K](https://doi.org/10.1002/(SICI)1520-6408(1999)24:3/4<252::AID-DVG8>3.0.CO;2-K)
- Drawbridge, J., Meighan, C. M., Lumpkins, R., & Kite, M. E. (2003). Pronephric duct extension in amphibian embryos: Migration and other mechanisms. *Developmental Dynamics*, 226(1), 1–11. <https://doi.org/10.1002/dvdy.10205>
- Dressler, G. R. (2009). Advances in early kidney specification, development and patterning. *Development*, 136(23), 3863–3874. <https://doi.org/10.1242/dev.034876>
- Dressler, G. R., Deutsch, U., Chowdhury, K., Nornes, H. O., & Gruss, P. (1990). Pax2, a new murine paired-box-containing gene and its expression in the developing excretory system. *Development*, 109(4), 787 LP – 795. <http://dev.biologists.org/content/109/4/787.abstract>
- Dressler, Gregory R. (2006). The Cellular Basis of Kidney Development. *Annual Review of Cell and Developmental Biology*, 22(1), 509–529. <https://doi.org/10.1146/annurev.cellbio.22.010305.104340>
- Dudley, A. T., Godin, R. E., & Robertson, E. J. (1999). Interaction between FGF and BMP signaling pathways regulates development of metanephric mesenchyme. *Genes & Development*, 13(12), 1601–1613. <https://doi.org/10.1101/gad.13.12.1601>
- Dudley, A. T., Lyons, K. M., & Robertson, E. J. (1995). A requirement for bone morphogenetic protein-7 during development of the mammalian kidney and eye. *Genes & Development*, 9(22), 2795–2807. <https://doi.org/10.1101/gad.9.22.2795>
- Dudley, A. T., & Robertson, E. J. (1997). Overlapping expression domains of bone morphogenetic protein family members potentially account for limited tissue defects in BMP7 deficient embryos. *Developmental Dynamics : An Official Publication of the American Association of Anatomists*, 208(3), 349–362. [https://doi.org/10.1002/\(SICI\)1097-0177\(199703\)208:3<349::AID-AJA6>3.0.CO;2-I](https://doi.org/10.1002/(SICI)1097-0177(199703)208:3<349::AID-AJA6>3.0.CO;2-I)
- Durbec, P., Marcos-Gutierrez, C. V., Kilkenny, C., Grigoriou, M., Wartiovaara, K., Suvanto, P., Smith, D., Ponder, B., Costantini, F., Saarma, M., Sariola, H., & Pachnis, V. (1996). GDNF signalling through the Ret receptor tyrosine kinase. *Nature*, 381(6585), 789–793. <https://doi.org/10.1038/381789a0>
- Essafi, A., Webb, A., Berry, R. L., Slight, J., Burn, S. F., Spraggon, L., Velecela, V., Martinez-Estrada, O. M., Wiltshire, J. H., Roberts, S. G. E., Brownstein, D., Davies, J. A., Hastie, N. D., & Hohenstein, P. (2011). A Wt1-Controlled Chromatin Switching Mechanism Underpins Tissue-Specific Wnt4 Activation and Repression. *Developmental Cell*, 21(3), 559–574. <https://doi.org/10.1016/j.devcel.2011.07.014>
- Fernández-Lloris, R., Osses, N., Jaffray, E., Shen, L. N., Vaughan, O. A., Girwood, D., Bartrons, R., Rosa, J. L., Hay, R. T., & Ventura, F. (2006). Repression of SOX6 transcriptional activity by SUMO modification. *FEBS Letters*, 580(5), 1215–1221. <https://doi.org/10.1016/j.febslet.2006.01.031>
- Fleming, B. M., Yelin, R., James, R. G., & Schultheiss, T. M. (2013). A role for Vg1/Nodal signaling in specification of the intermediate mesoderm. *Development*, 140(8), 1819–1829.

<https://doi.org/10.1242/dev.093740>

- Gao, L., Nie, X., Zheng, M., Li, X., Guo, Q., Liu, J., Liu, Q., Hao, Y., & Lin, B. (2020). TMEFF2 is a novel prognosis signature and target for endometrial carcinoma. *Life Sciences*, *243*, 116910. <https://doi.org/10.1016/j.lfs.2019.116910>
- Gheldof, A., & Berx, G. (2013). *Cadherins and Epithelial-to-Mesenchymal Transition* (pp. 317–336). <https://doi.org/10.1016/B978-0-12-394311-8.00014-5>
- Gimelli, S., Caridi, G., Beri, S., McCracken, K., Bocciardi, R., Zordan, P., Dagnino, M., Fiorio, P., Murer, L., Benetti, E., Zuffardi, O., Giorda, R., Wells, J. M., Gimelli, G., & Ghiggeri, G. M. (2010). Mutations in SOX17 are associated with congenital anomalies of the kidney and the urinary tract. *Human Mutation*, *31*(12), 1352–1359. <https://doi.org/10.1002/humu.21378>
- Girard, M., & Goossens, M. (2006). Sumoylation of the SOX10 transcription factor regulates its transcriptional activity. *FEBS Letters*, *580*(6), 1635–1641. <https://doi.org/10.1016/j.febslet.2006.02.011>
- Godin, R. E., Takaesu, N. T., Robertson, E. J., & Dudley, A. T. (1998). Regulation of BMP7 expression during kidney development. *Development (Cambridge, England)*, *125*(17), 3473–3482. <http://www.ncbi.nlm.nih.gov/pubmed/9693150>
- Goldman, M. (2002). Renal Abnormalities in Beckwith-Wiedemann Syndrome Are Associated with 11p15.5 Uniparental Disomy. *Journal of the American Society of Nephrology*, *13*(8), 2077–2084. <https://doi.org/10.1097/01.ASN.0000023431.16173.55>
- Goto, M., Mitra, R. S., Liu, M., Lee, J., Henson, B. S., Carey, T., Bradford, C., Prince, M., Wang, C.-Y., Fearon, E. R., & D'Silva, N. J. (2010). Rap1 Stabilizes -Catenin and Enhances -Catenin-Dependent Transcription and Invasion in Squamous Cell Carcinoma of the Head and Neck. *Clinical Cancer Research*, *16*(1), 65–76. <https://doi.org/10.1158/1078-0432.CCR-09-1122>
- Gradek, F., Lopez-Charcas, O., Chadet, S., Poisson, L., Ouldamer, L., Goupille, C., Jourdan, M.-L., Chevalier, S., Moussata, D., Besson, P., & Roger, S. (2019). Sodium Channel Nav1.5 Controls Epithelial-to-Mesenchymal Transition and Invasiveness in Breast Cancer Cells Through its Regulation by the Salt-Inducible Kinase-1. *Scientific Reports*, *9*(1), 18652. <https://doi.org/10.1038/s41598-019-55197-5>
- Grieshammer, U., Cebrián, C., Ilagan, R., Meyers, E., Herzlinger, D., & Martin, G. R. (2005). FGF8 is required for cell survival at distinct stages of nephrogenesis and for regulation of gene expression in nascent nephrons. *Development (Cambridge, England)*, *132*(17), 3847–3857. <https://doi.org/10.1242/dev.01944>
- Grobstein, C. (1953). Epithelio-mesenchymal specificity in the morphogenesis of mouse sub-mandibular rudiments in vitro. *Journal of Experimental Zoology*, *124*(2), 383–413. <https://doi.org/10.1002/jez.1401240211>
- Grobstein, C. (2008). *The Problem of the Chemical Nature of Embryonic Inducers*. 131–147. <https://doi.org/10.1002/9780470719589.ch9>
- Grote, D., Boualia, S. K., Souabni, A., Merkel, C., Chi, X., Costantini, F., Carroll, T., & Bouchard, M. (2008). Gata3 Acts Downstream of β -Catenin Signaling to Prevent Ectopic Metanephric Kidney Induction. *PLoS Genetics*, *4*(12), e1000316. <https://doi.org/10.1371/journal.pgen.1000316>
- Grote, D., Souabni, A., Busslinger, M., & Bouchard, M. (2006). Pax2/8-regulated Gata3 expression is necessary for morphogenesis and guidance of the nephric duct in the developing kidney. *Development*, *133*(1), 53 LP – 61. <https://doi.org/10.1242/dev.02184>

- Gubbay, J., Collignon, J., Koopman, P., Capel, B., Economou, A., Münsterberg, A., Vivian, N., Goodfellow, P., & Lovell-Badge, R. (1990). A gene mapping to the sex-determining region of the mouse Y chromosome is a member of a novel family of embryonically expressed genes. *Nature*, *346*(6281), 245–250. <https://doi.org/10.1038/346245a0>
- Harley, V. R., Lovell-Badge, R., & Goodfellow, P. N. (1994). Definition of a consensus DNA binding site for SRY. *Nucleic Acids Research*, *22*(8), 1500–1501. <https://doi.org/10.1093/nar/22.8.1500>
- Hartwig, S., Ho, J., Pandey, P., Macisaac, K., Taglienti, M., Xiang, M., Alterovitz, G., Ramoni, M., Fraenkel, E., & Kreidberg, J. A. (2010). Genomic characterization of Wilms' tumor suppressor 1 targets in nephron progenitor cells during kidney development. *Development (Cambridge, England)*, *137*(7), 1189–1203. <https://doi.org/10.1242/dev.045732>
- Hastie, N. D. (2017). Wilms' tumour 1 (WT1) in development, homeostasis and disease. *Development*, *144*(16), 2862–2872. <https://doi.org/10.1242/dev.153163>
- Hattori, T., Eberspaecher, H., Lu, J., Zhang, R., Nishida, T., Kahyo, T., Yasuda, H., & de Crombrughe, B. (2006). Interactions between PIAS proteins and SOX9 result in an increase in the cellular concentrations of SOX9. *The Journal of Biological Chemistry*, *281*(20), 14417–14428. <https://doi.org/10.1074/jbc.M511330200>
- Heliot, C., Desgrange, A., Buisson, I., Prunskaitė-Hyyryläinen, R., Shan, J., Vainio, S., Umbhauer, M., & Cereghini, S. (2013). HNF1B controls proximal-intermediate nephron segment identity in vertebrates by regulating Notch signalling components and *Irx1/2*. *Development*, *140*(4), 873–885. <https://doi.org/10.1242/dev.086538>
- Hong, K.-O., Kim, J.-H., Hong, J.-S., Yoon, H.-J., Lee, J.-I., Hong, S.-P., & Hong, S.-D. (2009). Inhibition of Akt activity induces the mesenchymal-to-epithelial reverting transition with restoring E-cadherin expression in KB and KOSCC-25B oral squamous cell carcinoma cells. *Journal of Experimental & Clinical Cancer Research*, *28*(1), 28. <https://doi.org/10.1186/1756-9966-28-28>
- Hoser, M., Potzner, M. R., Koch, J. M. C., Bösl, M. R., Wegner, M., & Sock, E. (2008). Sox12 deletion in the mouse reveals nonreciprocal redundancy with the related Sox4 and Sox11 transcription factors. *Molecular and Cellular Biology*, *28*(15), 4675–4687. <https://doi.org/10.1128/MCB.00338-08>
- Houston, C. S., Opitz, J. M., Spranger, J. W., Macpherson, R. I., Reed, M. H., Gilbert, E. F., Herrmann, J., & Schinzel, A. (1983). The campomelic syndrome: review, report of 17 cases, and follow-up on the currently 17-year-old boy first reported by Maroteaux et al in 1971. *American Journal of Medical Genetics*, *15*(1), 3–28. <https://doi.org/10.1002/ajmg.1320150103>
- Huang, J., Arsenault, M., Kann, M., Lopez-Mendez, C., Saleh, M., Wadowska, D., Taglienti, M., Ho, J., Miao, Y., Sims, D., Spears, J., Lopez, A., Wright, G., & Hartwig, S. (2013). The transcription factor sry-related HMG box-4 (SOX4) is required for normal renal development in vivo. *Developmental Dynamics*, *242*(6), 790–799. <https://doi.org/10.1002/dvdy.23971>
- Huang, W., Zhou, X., Lefebvre, V., & de Crombrughe, B. (2000). Phosphorylation of SOX9 by cyclic AMP-dependent protein kinase A enhances SOX9's ability to transactivate a Col2a1 chondrocyte-specific enhancer. *Molecular and Cellular Biology*, *20*(11), 4149–4158. <https://doi.org/10.1128/mcb.20.11.4149-4158.2000>
- Jahn, J. E., & Coleman, W. B. (2006). A potential role for synaptotagmin XIII (SYT13) in epithelial-mesenchymal transition. *Pathology (American Society for Investigative Pathology)*, *20*(4). <https://doi.org/10.1096/fasebj.20.4.A>
- James, R. G. (2006). Odd-skipped related 1 is required for development of the metanephric kidney

- and regulates formation and differentiation of kidney precursor cells. *Development*, 133(15), 2995–3004. <https://doi.org/10.1242/dev.02442>
- Jeong, C.-H., Cho, Y.-Y., Kim, M.-O., Kim, S.-H., Cho, E.-J., Lee, S.-Y., Jeon, Y.-J., Yeong Lee, K., Yao, K., Keum, Y.-S., Bode, A. M., & Dong, Z. (2010). Phosphorylation of Sox2 Cooperates in Reprogramming to Pluripotent Stem Cells. *STEM CELLS*, 28(12), 2141–2150. <https://doi.org/10.1002/stem.540>
- Jing, S., Wen, D., Yu, Y., Holst, P. L., Luo, Y., Fang, M., Tamir, R., Antonio, L., Hu, Z., Cupples, R., Louis, J.-C., Hu, S., Altmock, B. W., & Fox, G. M. (1996). GDNF-Induced Activation of the Ret Protein Tyrosine Kinase Is Mediated by GDNFR- α , a Novel Receptor for GDNF. *Cell*, 85(7), 1113–1124. [https://doi.org/10.1016/S0092-8674\(00\)81311-2](https://doi.org/10.1016/S0092-8674(00)81311-2)
- Kamachi, Y., Cheah, K. S., & Kondoh, H. (1999). Mechanism of regulatory target selection by the SOX high-mobility-group domain proteins as revealed by comparison of SOX1/2/3 and SOX9. *Molecular and Cellular Biology*, 19(1), 107–120. <https://doi.org/10.1128/mcb.19.1.107>
- Kanda, S., Tanigawa, S., Ohmori, T., Taguchi, A., Kudo, K., Suzuki, Y., Sato, Y., Hino, S., Sander, M., Perantoni, A. O., Sugano, S., Nakao, M., & Nishinakamura, R. (2014). Sall1 maintains nephron progenitors and nascent nephrons by acting as both an activator and a repressor. *Journal of the American Society of Nephrology : JASN*, 25(11), 2584–2595. <https://doi.org/10.1681/ASN.2013080896>
- Kann, M., Bae, E., Lenz, M. O., Li, L., Trannguyen, B., Schumacher, V. A., Taglienti, M. E., Bordeianou, L., Hartwig, S., Rinschen, M. M., Schermer, B., Benzing, T., Fan, C.-M., & Kreidberg, J. A. (2015). WT1 targets Gas1 to maintain nephron progenitor cells by modulating FGF signals. *Development (Cambridge, England)*, 142(7), 1254–1266. <https://doi.org/10.1242/dev.119735>
- Kariche, N., Moulai, N., Sellam, L.-S., Benyahia, S., Ouahioune, W., Djennaoui, D., Touil-Boukoffa, C., & Bourouba, M. (2019). Expression Analysis of the Mediators of Epithelial to Mesenchymal Transition and Early Risk Assessment of Therapeutic Failure in Laryngeal Carcinoma. *Journal of Oncology*, 2019, 1–15. <https://doi.org/10.1155/2019/5649846>
- Karner, C. M., Das, A., Ma, Z., Self, M., Chen, C., Lum, L., Oliver, G., & Carroll, T. J. (2011). Canonical Wnt9b signaling balances progenitor cell expansion and differentiation during kidney development. *Development (Cambridge, England)*, 138(7), 1247–1257. <https://doi.org/10.1242/dev.057646>
- Kent, J., Wheatley, S. C., Andrews, J. E., Sinclair, A. H., & Koopman, P. (1996). A male-specific role for SOX9 in vertebrate sex determination. *Development (Cambridge, England)*, 122(9), 2813–2822. <http://www.ncbi.nlm.nih.gov/pubmed/8787755>
- Kiefer, S. M., Robbins, L., Stumpff, K. M., Lin, C., Ma, L., & Rauchman, M. (2010). Sall1-dependent signals affect Wnt signaling and ureter tip fate to initiate kidney development. *Development*, 137(18), 3099–3106. <https://doi.org/10.1242/dev.037812>
- Kim, J., Lo, L., Dormand, E., & Anderson, D. J. (2003). SOX10 maintains multipotency and inhibits neuronal differentiation of neural crest stem cells. *Neuron*, 38(1), 17–31. [https://doi.org/10.1016/s0896-6273\(03\)00163-6](https://doi.org/10.1016/s0896-6273(03)00163-6)
- Kispert, A., Vainio, S., & McMahon, A. P. (1998). Wnt-4 is a mesenchymal signal for epithelial transformation of metanephric mesenchyme in the developing kidney. *Development*, 125(21), 4225 LP – 4234. <http://dev.biologists.org/content/125/21/4225.abstract>
- Kobayashi, A. (2005). Distinct and sequential tissue-specific activities of the LIM-class homeobox gene Lim1 for tubular morphogenesis during kidney development. *Development*, 132(12),

2809–2823. <https://doi.org/10.1242/dev.01858>

- Kobayashi, Akio, Mugford, J. W., Krautzberger, A. M., Naiman, N., Liao, J., & McMahon, A. P. (2014). Identification of a Multipotent Self-Renewing Stromal Progenitor Population during Mammalian Kidney Organogenesis. *Stem Cell Reports*, 3(4), 650–662. <https://doi.org/10.1016/j.stemcr.2014.08.008>
- Kobayashi, Akio, Valerius, M. T., Mugford, J. W., Carroll, T. J., Self, M., Oliver, G., & McMahon, A. P. (2008). Six2 defines and regulates a multipotent self-renewing nephron progenitor population throughout mammalian kidney development. *Cell Stem Cell*, 3(2), 169–181. <https://doi.org/10.1016/j.stem.2008.05.020>
- Kobayashi, H., Kawakami, K., Asashima, M., & Nishinakamura, R. (2007). Six1 and Six4 are essential for Gdnf expression in the metanephric mesenchyme and ureteric bud formation, while Six1 deficiency alone causes mesonephric-tubule defects. *Mechanisms of Development*, 124(4), 290–303. <https://doi.org/10.1016/j.mod.2007.01.002>
- Kook, H., Seo, S.-B., & Jain, R. (2017). EZ Switch From EZH2 to EZH1. *Circulation Research*, 121(2), 91–94. <https://doi.org/10.1161/CIRCRESAHA.117.311351>
- Kopan, R., Chen, S., & Liu, Z. (2014). Alagille, Notch, and robustness: why duplicating systems does not ensure redundancy. *Pediatric Nephrology*, 29(4), 651–657. <https://doi.org/10.1007/s00467-013-2661-y>
- Kormish, J. D., Sinner, D., & Zorn, A. M. (2010). Interactions between SOX factors and Wnt/beta-catenin signaling in development and disease. *Developmental Dynamics : An Official Publication of the American Association of Anatomists*, 239(1), 56–68. <https://doi.org/10.1002/dvdy.22046>
- Koumangoye, R. B., Andl, T., Taubenslag, K. J., Zilberman, S. T., Taylor, C. J., Loomans, H. A., & Andl, C. D. (2015). SOX4 interacts with EZH2 and HDAC3 to suppress microRNA-31 in invasive esophageal cancer cells. *Molecular Cancer*, 14(1), 24. <https://doi.org/10.1186/s12943-014-0284-y>
- Kreidberg, J. A., Sariola, H., Loring, J. M., Maeda, M., Pelletier, J., Housman, D., & Jaenisch, R. (1993). WT-1 is required for early kidney development. *Cell*, 74(4), 679–691. [https://doi.org/10.1016/0092-8674\(93\)90515-r](https://doi.org/10.1016/0092-8674(93)90515-r)
- Kume, T., Deng, K., & Hogan, B. L. (2000). Murine forkhead/winged helix genes Foxc1 (Mf1) and Foxc2 (Mfh1) are required for the early organogenesis of the kidney and urinary tract. *Development (Cambridge, England)*, 127(7), 1387–1395. <http://www.ncbi.nlm.nih.gov/pubmed/10704385>
- Kuriyama, S., Theveneau, E., Benedetto, A., Parsons, M., Tanaka, M., Charras, G., Kabla, A., & Mayor, R. (2014). In vivo collective cell migration requires an LPAR2-dependent increase in tissue fluidity. *Journal of Cell Biology*, 206(1), 113–127. <https://doi.org/10.1083/jcb.201402093>
- Kawahara, M., Yamashita, M., Shinoda, K., Tofukuji, S., Onodera, A., Shinnakasu, R., Motohashi, S., Hosokawa, H., Tumes, D., Iwamura, C., Lefebvre, V., & Nakayama, T. (2012). The transcription factor Sox4 is a downstream target of signaling by the cytokine TGF- β and suppresses T(H)2 differentiation. *Nature Immunology*, 13(8), 778–786. <https://doi.org/10.1038/ni.2362>
- Kuwajima, T., Soares, C. A., Sitko, A. A., Lefebvre, V., & Mason, C. (2017). SoxC Transcription Factors Promote Contralateral Retinal Ganglion Cell Differentiation and Axon Guidance in the Mouse Visual System. *Neuron*, 93(5), 1110–1125.e5. <https://doi.org/10.1016/j.neuron.2017.01.029>
- Lange, A. W., Keiser, A. R., Wells, J. M., Zorn, A. M., & Whitsett, J. A. (2009). Sox17 promotes cell cycle progression and inhibits TGF-beta/Smad3 signaling to initiate progenitor cell behavior in

- the respiratory epithelium. *PLoS One*, 4(5), e5711.
<https://doi.org/10.1371/journal.pone.0005711>
- Lawson, N. D., Scheer, N., Pham, V. N., Kim, C. H., Chitnis, A. B., Campos-Ortega, J. A., & Weinstein, B. M. (2001). Notch signaling is required for arterial-venous differentiation during embryonic vascular development. *Development (Cambridge, England)*, 128(19), 3675–3683.
<https://doi.org/11585794>
- Lee, A.-R., Ko, K. W., Lee, H., Yoon, Y.-S., Song, M.-R., & Park, C.-S. (2016). Putative Cell Adhesion Membrane Protein Vstm5 Regulates Neuronal Morphology and Migration in the Central Nervous System. *Journal of Neuroscience*, 36(39), 10181–10197.
<https://doi.org/10.1523/JNEUROSCI.0541-16.2016>
- Lee, Y. Q., Collins, C. E., Gordon, A., Rae, K. M., & Pringle, K. G. (2018). The Relationship between Maternal Nutrition during Pregnancy and Offspring Kidney Structure and Function in Humans: A Systematic Review. *Nutrients*, 10(2). <https://doi.org/10.3390/nu10020241>
- Lefebvre, V. (1998). A new long form of Sox5 (L-Sox5), Sox6 and Sox9 are coexpressed in chondrogenesis and cooperatively activate the type II collagen gene. *The EMBO Journal*, 17(19), 5718–5733. <https://doi.org/10.1093/emboj/17.19.5718>
- Lefebvre, Véronique, Dumitriu, B., Penzo-Méndez, A., Han, Y., & Pallavi, B. (2007). Control of cell fate and differentiation by Sry-related high-mobility-group box (Sox) transcription factors. *The International Journal of Biochemistry & Cell Biology*, 39(12), 2195–2214.
<https://doi.org/10.1016/j.biocel.2007.05.019>
- Li, F., Shi, J., Xu, Z., Yao, X., Mou, T., Yu, J., Liu, H., & Li, G. (2018). S100A4-MYH9 Axis Promote Migration and Invasion of Gastric Cancer Cells by Inducing TGF- β -Mediated Epithelial-Mesenchymal Transition. *Journal of Cancer*, 9(21), 3839–3849.
<https://doi.org/10.7150/jca.25469>
- Li, R.-X., Chen, Z.-H., & Chen, Z.-K. (2014). The role of EPH receptors in cancer-related epithelial-mesenchymal transition. *Chinese Journal of Cancer*, 33(5), 231–240.
<https://doi.org/10.5732/cjc.013.10108>
- Li, Xiang, Pei, D., & Zheng, H. (2014). Transitions between epithelial and mesenchymal states during cell fate conversions. *Protein & Cell*, 5(8), 580–591. <https://doi.org/10.1007/s13238-014-0064-x>
- Li, Xue, Ohgi, K. A., Zhang, J., Krones, A., Bush, K. T., Glass, C. K., Nigam, S. K., Aggarwal, A. K., Maas, R., Rose, D. W., & Rosenfeld, M. G. (2003). Eya protein phosphatase activity regulates Six1–Dach–Eya transcriptional effects in mammalian organogenesis. *Nature*, 426(6964), 247–254.
<https://doi.org/10.1038/nature02083>
- Lindström, N. O., De Sena Brandine, G., Tran, T., Ransick, A., Suh, G., Guo, J., Kim, A. D., Parvez, R. K., Ruffins, S. W., Rutledge, E. A., Thornton, M. E., Grubbs, B., McMahon, J. A., Smith, A. D., & McMahon, A. P. (2018). Progressive Recruitment of Mesenchymal Progenitors Reveals a Time-Dependent Process of Cell Fate Acquisition in Mouse and Human Nephrogenesis. *Developmental Cell*, 45(5), 651–660.e4. <https://doi.org/10.1016/j.devcel.2018.05.010>
- Little, M. H., & McMahon, A. P. (2012). Mammalian kidney development: principles, progress, and projections. *Cold Spring Harbor Perspectives in Biology*, 4(5).
<https://doi.org/10.1101/cshperspect.a008300>
- Liu, J. A. J., Wu, M.-H., Yan, C. H., Chau, B. K. H., So, H., Ng, A., Chan, A., Cheah, K. S. E., Briscoe, J., & Cheung, M. (2013). Phosphorylation of Sox9 is required for neural crest delamination and is regulated downstream of BMP and canonical Wnt signaling. *Proceedings of the National*

Academy of Sciences of the United States of America, 110(8), 2882–2887.
<https://doi.org/10.1073/pnas.1211747110>

- Long, R., Liu, Z., Li, J., & Yu, H. (2019). COL6A6 interacted with P4HA3 to suppress the growth and metastasis of pituitary adenoma via blocking PI3K-Akt pathway. *Aging*, 11(20), 8845–8859. <https://doi.org/10.18632/aging.102300>
- Lu, B. C., Cebrian, C., Chi, X., Kuure, S., Kuo, R., Bates, C. M., Arber, S., Hassell, J., MacNeil, L., Hoshi, M., Jain, S., Asai, N., Takahashi, M., Schmidt-Ott, K. M., Barasch, J., D'Agati, V., & Costantini, F. (2009). Etv4 and Etv5 are required downstream of GDNF and Ret for kidney branching morphogenesis. *Nature Genetics*, 41(12), 1295–1302. <https://doi.org/10.1038/ng.476>
- Luo, G., Hofmann, C., Bronckers, A. L., Sohocki, M., Bradley, A., & Karsenty, G. (1995). BMP-7 is an inducer of nephrogenesis, and is also required for eye development and skeletal patterning. *Genes & Development*, 9(22), 2808–2820. <https://doi.org/10.1101/gad.9.22.2808>
- Mackie, G. G., & Stephens, F. D. (1975). Duplex kidneys: a correlation of renal dysplasia with position of the ureteral orifice. *The Journal of Urology*, 114(2), 274–280. [https://doi.org/10.1016/s0022-5347\(17\)67007-1](https://doi.org/10.1016/s0022-5347(17)67007-1)
- Majumdar, A. (2003). Wnt11 and Ret/Gdnf pathways cooperate in regulating ureteric branching during metanephric kidney development. *Development*, 130(>14), 3175–3185. <https://doi.org/10.1242/dev.00520>
- Malki, S., Boizet-Bonhoure, B., & Poulat, F. (2010). Shuttling of SOX proteins. *The International Journal of Biochemistry & Cell Biology*, 42(3), 411–416. <https://doi.org/10.1016/j.biocel.2009.09.020>
- Mansouri, A., Chowdhury, K., & Gruss, P. (1998). Follicular cells of the thyroid gland require Pax8 gene function. *Nature Genetics*, 19(1), 87–90. <https://doi.org/10.1038/ng0598-87>
- Margueron, R., Li, G., Sarma, K., Blais, A., Zavadil, J., Woodcock, C. L., Dynlacht, B. D., & Reinberg, D. (2008). Ezh1 and Ezh2 Maintain Repressive Chromatin through Different Mechanisms. *Molecular Cell*, 32(4), 503–518. <https://doi.org/10.1016/j.molcel.2008.11.004>
- Martin, E., Caubit, X., Airik, R., Vola, C., Fatmi, A., Kispert, A., & Fasano, L. (2013). TSHZ3 and SOX9 Regulate the Timing of Smooth Muscle Cell Differentiation in the Ureter by Reducing Myocardin Activity. *PLoS ONE*, 8(5), e63721. <https://doi.org/10.1371/journal.pone.0063721>
- Massa, F., Garbay, S., Bouvier, R., Sugitani, Y., Noda, T., Gubler, M.-C., Heidet, L., Pontoglio, M., & Fischer, E. (2013). Hepatocyte nuclear factor 1 controls nephron tubular development. *Development*, 140(4), 886–896. <https://doi.org/10.1242/dev.086546>
- McNeill, H., & Reginensi, A. (2017). Lats1/2 Regulate Yap/Taz to Control Nephron Progenitor Epithelialization and Inhibit Myofibroblast Formation. *Journal of the American Society of Nephrology*, 28(3), 852–861. <https://doi.org/10.1681/ASN.2016060611>
- Mertin, S. (1999). The DNA-binding specificity of SOX9 and other SOX proteins. *Nucleic Acids Research*, 27(5), 1359–1364. <https://doi.org/10.1093/nar/27.5.1359>
- Miao, Q., Hill, M. C., Chen, F., Mo, Q., Ku, A. T., Ramos, C., Sock, E., Lefebvre, V., & Nguyen, H. (2019). SOX11 and SOX4 drive the reactivation of an embryonic gene program during murine wound repair. *Nature Communications*, 10(1), 4042. <https://doi.org/10.1038/s41467-019-11880-9>
- Michos, O., Gonçalves, A., Lopez-Rios, J., Tiecke, E., Naillat, F., Beier, K., Galli, A., Vainio, S., & Zeller, R. (2007). Reduction of BMP4 activity by gremlin 1 enables ureteric bud outgrowth and GDNF/WNT11 feedback signalling during kidney branching morphogenesis. *Development*

- (Cambridge, England), 134(13), 2397–2405. <https://doi.org/10.1242/dev.02861>
- Mizuseki, K., Kishi, M., Matsui, M., Nakanishi, S., & Sasai, Y. (1998). Xenopus Zic-related-1 and Sox-2, two factors induced by chordin, have distinct activities in the initiation of neural induction. *Development (Cambridge, England)*, 125(4), 579–587. <https://doi.org/9435279>
- Moore, M. W., Klein, R. D., Fariñas, I., Sauer, H., Armanini, M., Phillips, H., Reichardt, L. F., Ryan, A. M., Carver-Moore, K., & Rosenthal, A. (1996). Renal and neuronal abnormalities in mice lacking GDNF. *Nature*, 382(6586), 76–79. <https://doi.org/10.1038/382076a0>
- Moran, J., Kim, H., Li, Z., & Moreno, C. (2019). SOX4 regulates invasion of bladder cancer cells via repression of WNT5a. *International Journal of Oncology*. <https://doi.org/10.3892/ijo.2019.4832>
- Motamedi, F. J., Badro, D. A., Clarkson, M., Lecca, M. R., Bradford, S. T., Buske, F. A., Saar, K., Hübner, N., Brändli, A. W., & Schedl, A. (2014). WT1 controls antagonistic FGF and BMP-pSMAD pathways in early renal progenitors. *Nature Communications*, 5, 4444. <https://doi.org/10.1038/ncomms5444>
- Mousavi, K., Zare, H., Wang, A. H., & Sartorelli, V. (2012). Polycomb Protein Ezh1 Promotes RNA Polymerase II Elongation. *Molecular Cell*, 45(2), 255–262. <https://doi.org/10.1016/j.molcel.2011.11.019>
- Mu, W., Starmer, J., Shibata, Y., Yee, D., & Magnuson, T. (2017). EZH1 in germ cells safeguards the function of PRC2 during spermatogenesis. *Developmental Biology*, 424(2), 198–207. <https://doi.org/10.1016/j.ydbio.2017.02.017>
- Mugford, J. W., Sipilä, P., McMahon, J. A., & McMahon, A. P. (2008). Osr1 expression demarcates a multi-potent population of intermediate mesoderm that undergoes progressive restriction to an Osr1-dependent nephron progenitor compartment within the mammalian kidney. *Developmental Biology*, 324(1), 88–98. <https://doi.org/10.1016/j.ydbio.2008.09.010>
- Mugford, J. W., Yu, J., Kobayashi, A., & McMahon, A. P. (2009). High-resolution gene expression analysis of the developing mouse kidney defines novel cellular compartments within the nephron progenitor population. *Developmental Biology*, 333(2), 312–323. <https://doi.org/10.1016/j.ydbio.2009.06.043>
- Mukherjee, M., DeRiso, J., Otterpohl, K., Ratnayake, I., Kota, D., Ahrenkiel, P., Chandrasekar, I., & Surendran, K. (2019). Endogenous Notch Signaling in Adult Kidneys Maintains Segment-Specific Epithelial Cell Types of the Distal Tubules and Collecting Ducts to Ensure Water Homeostasis. *Journal of the American Society of Nephrology*, 30(1), 110–126. <https://doi.org/10.1681/ASN.2018040440>
- Munro, D. A. D., Hohenstein, P., & Davies, J. A. (2017). Cycles of vascular plexus formation within the nephrogenic zone of the developing mouse kidney. *Scientific Reports*, 7(1), 3273. <https://doi.org/10.1038/s41598-017-03808-4>
- Murakami, A., Ishida, S., Thurlow, J., Revest, J. M., & Dickson, C. (2001). SOX6 binds CtBP2 to repress transcription from the Fgf-3 promoter. *Nucleic Acids Research*, 29(16), 3347–3355. <https://doi.org/10.1093/nar/29.16.3347>
- Murawski, I. J., Maina, R. W., & Gupta, I. R. (2010). The relationship between nephron number, kidney size and body weight in two inbred mouse strains. *Organogenesis*, 6(3), 189–194. <https://doi.org/10.4161/org.6.3.12125>
- Murugan, S., Shan, J., Kühl, S. J., Tata, A., Pietilä, I., Kühl, M., & Vainio, S. J. (2012). WT1 and Sox11 regulate synergistically the promoter of the Wnt4 gene that encodes a critical signal for nephrogenesis. *Experimental Cell Research*, 318(10), 1134–1145.

<https://doi.org/10.1016/j.yexcr.2012.03.008>

- Mutlu, M., Saatci, Ö., Ansari, S. A., Yurdusev, E., Shehwana, H., Konu, Ö., Raza, U., & Şahin, Ö. (2016). miR-564 acts as a dual inhibitor of PI3K and MAPK signaling networks and inhibits proliferation and invasion in breast cancer. *Scientific Reports*, *6*(1), 32541. <https://doi.org/10.1038/srep32541>
- Muto, A., Iida, A., Satoh, S., & Watanabe, S. (2009). The group E Sox genes Sox8 and Sox9 are regulated by Notch signaling and are required for Müller glial cell development in mouse retina. *Experimental Eye Research*, *89*(4), 549–558. <https://doi.org/10.1016/j.exer.2009.05.006>
- Naiman, N., Fujioka, K., Fujino, M., Valerius, M. T., Potter, S. S., McMahon, A. P., & Kobayashi, A. (2017). Repression of Interstitial Identity in Nephron Progenitor Cells by Pax2 Establishes the Nephron-Interstitium Boundary during Kidney Development. *Developmental Cell*, *41*(4), 349–365.e3. <https://doi.org/10.1016/j.devcel.2017.04.022>
- Nakai, S., Sugitani, Y., Sato, H., Ito, S., Miura, Y., Ogawa, M., Nishi, M., Jishage, K., Minowa, O., & Noda, T. (2003). Crucial roles of Brn1 in distal tubule formation and function in mouse kidney. *Development*, *130*(19), 4751–4759. <https://doi.org/10.1242/dev.00666>
- Nakano, T., Niimura, F., Hohenfellner, K., Miyakita, E., & Ichikawa, I. (2003). Screening for mutations in BMP4 and FOXC1 genes in congenital anomalies of the kidney and urinary tract in humans. *The Tokai Journal of Experimental and Clinical Medicine*, *28*(3), 121–126. <http://www.ncbi.nlm.nih.gov/pubmed/15055404>
- Narlis, M., Grote, D., Gaitan, Y., Boualia, S. K., & Bouchard, M. (2007). Pax2 and Pax8 Regulate Branching Morphogenesis and Nephron Differentiation in the Developing Kidney. *Journal of the American Society of Nephrology*, *18*(4), 1121–1129. <https://doi.org/10.1681/ASN.2006070739>
- Nishinakamura, R., Matsumoto, Y., Nakao, K., Nakamura, K., Sato, A., Copeland, N. G., Gilbert, D. J., Jenkins, N. A., Scully, S., Lacey, D. L., Katsuki, M., Asashima, M., & Yokota, T. (2001). Murine homolog of SALL1 is essential for ureteric bud invasion in kidney development. *Development (Cambridge, England)*, *128*(16), 3105–3115. <http://www.ncbi.nlm.nih.gov/pubmed/11688560>
- O'Brien, L. L., Guo, Q., Lee, Y., Tran, T., Benazet, J.-D., Whitney, P. H., Valouev, A., & McMahon, A. P. (2016). Differential regulation of mouse and human nephron progenitors by the Six family of transcriptional regulators. *Development (Cambridge, England)*, *143*(4), 595–608. <https://doi.org/10.1242/dev.127175>
- Ohe, K., Lalli, E., & Sassone-Corsi, P. (2002). A direct role of SRY and SOX proteins in pre-mRNA splicing. *Proceedings of the National Academy of Sciences*, *99*(3), 1146–1151. <https://doi.org/10.1073/pnas.022645899>
- Oliveros, J. C. (2007). VENNY. An interactive tool for comparing lists with Venn Diagrams. <http://bioinfogp.cnb.csic.es/tools/venny/index.html>. <http://bioinfogp.cnb.csic.es/Tools/Venny/Index.Html>. <http://bioinfogp.cnnb.csic.es/tools/venny/index.html>
- Ortega, S., Ittmann, M., Tsang, S. H., Ehrlich, M., & Basilico, C. (1998). Neuronal defects and delayed wound healing in mice lacking fibroblast growth factor 2. *Proceedings of the National Academy of Sciences of the United States of America*, *95*(10), 5672–5677. <https://doi.org/10.1073/pnas.95.10.5672>
- Park, J.-S., Ma, W., O'Brien, L. L., Chung, E., Guo, J.-J., Cheng, J.-G., Valerius, M. T., McMahon, J. A., Wong, W. H., & McMahon, A. P. (2012). Six2 and Wnt regulate self-renewal and commitment of nephron progenitors through shared gene regulatory networks. *Developmental Cell*, *23*(3), 637–

651. <https://doi.org/10.1016/j.devcel.2012.07.008>

- Park, J.-S., Valerius, M. T., & McMahon, A. P. (2007). Wnt/beta-catenin signaling regulates nephron induction during mouse kidney development. *Development (Cambridge, England)*, *134*(13), 2533–2539. <https://doi.org/10.1242/dev.006155>
- Patel, K. M., Crisostomo, P., Lahm, T., Markel, T., Herring, C., Wang, M., Meldrum, K. K., Lillemo, K. D., & Meldrum, D. R. (2007). Mesenchymal Stem Cells Attenuate Hypoxic Pulmonary Vasoconstriction by a Paracrine Mechanism. *Journal of Surgical Research*, *143*(2), 281–285. <https://doi.org/https://doi.org/10.1016/j.jss.2006.11.006>
- Pedersen, A., Skjong, C., & Shawlot, W. (2005). Lim1 is required for nephric duct extension and ureteric bud morphogenesis. *Developmental Biology*, *288*(2), 571–581. <https://doi.org/10.1016/j.ydbio.2005.09.027>
- Peng, X., Liu, G., Peng, H., Chen, A., Zha, L., & Wang, Z. (2018). SOX4 contributes to TGF- β -induced epithelial–mesenchymal transition and stem cell characteristics of gastric cancer cells. *Genes & Diseases*, *5*(1), 49–61. <https://doi.org/10.1016/j.gendis.2017.12.005>
- Penzo-Méndez, A. I. (2010). Critical roles for SoxC transcription factors in development and cancer. *The International Journal of Biochemistry & Cell Biology*, *42*(3), 425–428. <https://doi.org/10.1016/j.biocel.2009.07.018>
- Perantoni, A O, Dove, L. F., & Karavanova, I. (1995). Basic fibroblast growth factor can mediate the early inductive events in renal development. *Proceedings of the National Academy of Sciences of the United States of America*, *92*(10), 4696–4700. <https://doi.org/10.1073/pnas.92.10.4696>
- Perantoni, Alan O, Timofeeva, O., Naillat, F., Richman, C., Pajni-Underwood, S., Wilson, C., Vainio, S., Dove, L. F., & Lewandoski, M. (2005). Inactivation of FGF8 in early mesoderm reveals an essential role in kidney development. *Development (Cambridge, England)*, *132*(17), 3859–3871. <https://doi.org/10.1242/dev.01945>
- Pichel, J. G., Shen, L., Sheng, H. Z., Granholm, A. C., Drago, J., Grinberg, A., Lee, E. J., Huang, S. P., Saarma, M., Hoffer, B. J., Sariola, H., & Westphal, H. (1996). Defects in enteric innervation and kidney development in mice lacking GDNF. *Nature*, *382*(6586), 73–76. <https://doi.org/10.1038/382073a0>
- Poladia, D. P., Kish, K., Kutay, B., Hains, D., Kegg, H., Zhao, H., & Bates, C. M. (2006). Role of fibroblast growth factor receptors 1 and 2 in the metanephric mesenchyme. *Developmental Biology*, *291*(2), 325–339. <https://doi.org/10.1016/j.ydbio.2005.12.034>
- Ranghini, E. J., & Dressler, G. R. (2015). Evidence for intermediate mesoderm and kidney progenitor cell specification by Pax2 and PTIP dependent mechanisms. *Developmental Biology*, *399*(2), 296–305. <https://doi.org/10.1016/j.ydbio.2015.01.005>
- Reginensi, A., Clarkson, M., Neirijnck, Y., Lu, B., Ohyama, T., Groves, A. K., Sock, E., Wegner, M., Costantini, F., Chaboissier, M.-C., & Schedl, A. (2011). SOX9 controls epithelial branching by activating RET effector genes during kidney development. *Human Molecular Genetics*, *20*(6), 1143–1153. <https://doi.org/10.1093/hmg/ddq558>
- Reginensi, A., Scott, R. P., Gregorieff, A., Bagherie-Lachidan, M., Chung, C., Lim, D.-S., Pawson, T., Wrana, J., & McNeill, H. (2013). Yap- and Cdc42-dependent nephrogenesis and morphogenesis during mouse kidney development. *PLoS Genetics*, *9*(3), e1003380. <https://doi.org/10.1371/journal.pgen.1003380>
- Reka, A. K., Chen, G., Jones, R. C., Amunugama, R., Kim, S., Karnovsky, A., Standiford, T. J., Beer, D. G., Omenn, G. S., & Keshamouni, V. G. (2014). Epithelial-mesenchymal transition-associated

- secretory phenotype predicts survival in lung cancer patients. *Carcinogenesis*, 35(6), 1292–1300. <https://doi.org/10.1093/carcin/bgu041>
- Rieger, A., Kemter, E., Kumar, S., Popper, B., Aigner, B., Wolf, E., Wanke, R., & Blutke, A. (2016). Missense Mutation of POU Domain Class 3 Transcription Factor 3 in Pou3f3L423P Mice Causes Reduced Nephron Number and Impaired Development of the Thick Ascending Limb of the Loop of Henle. *PLOS ONE*, 11(7), e0158977. <https://doi.org/10.1371/journal.pone.0158977>
- Rumballe, B. A., Georgas, K. M., Combes, A. N., Ju, A. L., Gilbert, T., & Little, M. H. (2011). Nephron formation adopts a novel spatial topology at cessation of nephrogenesis. *Developmental Biology*, 360(1), 110–122. <https://doi.org/10.1016/j.ydbio.2011.09.011>
- Sacilotto, N., Monteiro, R., Fritzsche, M., Becker, P. W., Sanchez-del-Campo, L., Liu, K., Pinheiro, P., Ratnayaka, I., Davies, B., Goding, C. R., Patient, R., Bou-Gharios, G., & De Val, S. (2013). Analysis of Dll4 regulation reveals a combinatorial role for Sox and Notch in arterial development. *Proceedings of the National Academy of Sciences*, 110(29), 11893–11898. <https://doi.org/10.1073/pnas.1300805110>
- Sainio, K., Hellstedt, P., Kreidberg, J. A., Saxén, L., & Sariola, H. (1997). Differential regulation of two sets of mesonephric tubules by WT-1. *Development (Cambridge, England)*, 124(7), 1293–1299. <http://www.ncbi.nlm.nih.gov/pubmed/9118800>
- Sajithlal, G., Zou, D., Silviu, D., & Xu, P.-X. (2005). Eya1 acts as a critical regulator for specifying the metanephric mesenchyme. *Developmental Biology*, 284(2), 323–336. <https://doi.org/10.1016/j.ydbio.2005.05.029>
- Sánchez, M. P., Silos-Santiago, I., Frisé, J., He, B., Lira, S. A., & Barbacid, M. (1996). Renal agenesis and the absence of enteric neurons in mice lacking GDNF. *Nature*, 382(6586), 70–73. <https://doi.org/10.1038/382070a0>
- Satko, S. G., & Freedman, B. I. (2005). The familial clustering of renal disease and related phenotypes. *The Medical Clinics of North America*, 89(3), 447–456. <https://doi.org/10.1016/j.mcna.2004.11.011>
- Savare, J., Bonneaud, N., & Girard, F. (2005). SUMO Represses Transcriptional Activity of the Drosophila SoxNeuro and Human Sox3 Central Nervous System-specific Transcription Factors. *Molecular Biology of the Cell*, 16(6), 2660–2669. <https://doi.org/10.1091/mbc.e04-12-1062>
- Saxén, L., & Sariola, H. (1987). Early organogenesis of the kidney. *Pediatric Nephrology*, 1(3), 385–392. <https://doi.org/10.1007/BF00849241>
- Scharer, C. D., McCabe, C. D., Ali-Seyed, M., Berger, M. F., Bulyk, M. L., & Moreno, C. S. (2009). Genome-Wide Promoter Analysis of the SOX4 Transcriptional Network in Prostate Cancer Cells. *Cancer Research*, 69(2), 709–717. <https://doi.org/10.1158/0008-5472.CAN-08-3415>
- Schedl, A. (2007). Renal abnormalities and their developmental origin. *Nature Reviews Genetics*, 8(10), 791–802. <https://doi.org/10.1038/nrg2205>
- Schepers, G. E. (2000). Cloning and characterisation of the Sry-related transcription factor gene Sox8. *Nucleic Acids Research*, 28(6), 1473–1480. <https://doi.org/10.1093/nar/28.6.1473>
- Schlierf, B. (2002). Cooperative binding of Sox10 to DNA: requirements and consequences. *Nucleic Acids Research*, 30(24), 5509–5516. <https://doi.org/10.1093/nar/gkf690>
- Schreiner, S., Cossais, F., Fischer, K., Scholz, S., Bösl, M. R., Holtmann, B., Sendtner, M., & Wegner, M. (2007). Hypomorphic Sox10 alleles reveal novel protein functions and unravel developmental differences in glial lineages. *Development (Cambridge, England)*, 134(18), 3271–3281.

<https://doi.org/10.1242/dev.003350>

- Scott, R. P., & Quaggin, S. E. (2015). The cell biology of renal filtration. *Journal of Cell Biology*, 209(2), 199–210. <https://doi.org/10.1083/jcb.201410017>
- Seikaly, M. G., Ho, P. L., Emmett, L., Fine, R. N., & Tejani, A. (2003). Chronic renal insufficiency in children: the 2001 Annual Report of the NAPRTCS. *Pediatric Nephrology (Berlin, Germany)*, 18(8), 796–804. <https://doi.org/10.1007/s00467-003-1158-5>
- Self, M., Lagutin, O. V., Bowling, B., Hendrix, J., Cai, Y., Dressler, G. R., & Oliver, G. (2006). Six2 is required for suppression of nephrogenesis and progenitor renewal in the developing kidney. *The EMBO Journal*, 25(21), 5214–5228. <https://doi.org/10.1038/sj.emboj.7601381>
- Shawlot, W., & Behringer, R. R. (1995). Requirement for Llm1 in head-organizer function. *Nature*, 374(6521), 425–430. <https://doi.org/10.1038/374425a0>
- Shen, G.-M., Zhao, Y.-Z., Chen, M.-T., Zhang, F.-L., Liu, X.-L., Wang, Y., Liu, C.-Z., Yu, J., & Zhang, J.-W. (2012). Hypoxia-inducible factor-1 (HIF-1) promotes LDL and VLDL uptake through inducing VLDLR under hypoxia. *Biochemical Journal*, 441(2), 675–683. <https://doi.org/10.1042/BJ20111377>
- Shen, X., Liu, Y., Hsu, Y.-J., Fujiwara, Y., Kim, J., Mao, X., Yuan, G.-C., & Orkin, S. H. (2008). EZH1 Mediates Methylation on Histone H3 Lysine 27 and Complements EZH2 in Maintaining Stem Cell Identity and Executing Pluripotency. *Molecular Cell*, 32(4), 491–502. <https://doi.org/10.1016/j.molcel.2008.10.016>
- Sinclair, A. H., Berta, P., Palmer, M. S., Hawkins, J. R., Griffiths, B. L., Smith, M. J., Foster, J. W., Frischauf, A.-M., Lovell-Badge, R., & Goodfellow, P. N. (1990). A gene from the human sex-determining region encodes a protein with homology to a conserved DNA-binding motif. *Nature*, 346(6281), 240–244. <https://doi.org/10.1038/346240a0>
- Singh, C., Sharma, A., Hoppe, G., Song, W., Bolok, Y., & Sears, J. E. (2018). 3-Hydroxypyruvate Destabilizes Hypoxia Inducible Factor and Induces Angiostasis. *Investigative Ophthalmology & Visual Science*, 59(8), 3440. <https://doi.org/10.1167/iovs.18-24120>
- Sinner, D., Kordich, J. J., Spence, J. R., Opoka, R., Rankin, S., Lin, S.-C. J., Jonatan, D., Zorn, A. M., & Wells, J. M. (2007). Sox17 and Sox4 differentially regulate beta-catenin/T-cell factor activity and proliferation of colon carcinoma cells. *Molecular and Cellular Biology*, 27(22), 7802–7815. <https://doi.org/10.1128/MCB.02179-06>
- Song, R., & Yosypiv, I. V. (2011). Genetics of congenital anomalies of the kidney and urinary tract. *Pediatric Nephrology (Berlin, Germany)*, 26(3), 353–364. <https://doi.org/10.1007/s00467-010-1629-4>
- Stark, K., Vainio, S., Vassileva, G., & McMahon, A. P. (1994). Epithelial transformation of metanephric mesenchyme in the developing kidney regulated by Wnt-4. *Nature*, 372(6507), 679–683. <https://doi.org/10.1038/372679a0>
- Stolt, C. C., Rehberg, S., Ader, M., Lommes, P., Riethmacher, D., Schachner, M., Bartsch, U., & Wegner, M. (2002). Terminal differentiation of myelin-forming oligodendrocytes depends on the transcription factor Sox10. *Genes & Development*, 16(2), 165–170. <https://doi.org/10.1101/gad.215802>
- Stolt, C. C., & Wegner, M. (2016). Schwann cells and their transcriptional network: Evolution of key regulators of peripheral myelination. *Brain Research*, 1641, 101–110. <https://doi.org/10.1016/j.brainres.2015.09.025>

- Stuart, R. O., Bush, K. T., & Nigam, S. K. (2001). Changes in global gene expression patterns during development and maturation of the rat kidney. *Proceedings of the National Academy of Sciences*, *98*(10), 5649–5654. <https://doi.org/10.1073/pnas.091110798>
- Taguchi, A., Kaku, Y., Ohmori, T., Sharmin, S., Ogawa, M., Sasaki, H., & Nishinakamura, R. (2014). Redefining the In Vivo Origin of Metanephric Nephron Progenitors Enables Generation of Complex Kidney Structures from Pluripotent Stem Cells. *Cell Stem Cell*, *14*(1), 53–67. <https://doi.org/10.1016/j.stem.2013.11.010>
- Tang, F., Richardson, N., Albina, A., Chaboissier, M.-C., & Perea-Gomez, A. (2020). Mouse Gonad Development in the Absence of the Pro-Ovary Factor WNT4 and the Pro-Testis Factor SOX9. *Cells*, *9*(5), 1103. <https://doi.org/10.3390/cells9051103>
- Tanigawa, S., Wang, H., Yang, Y., Sharma, N., Tarasova, N., Ajima, R., Yamaguchi, T. P., Rodriguez, L. G., & Perantoni, A. O. (2011). Wnt4 induces nephronic tubules in metanephric mesenchyme by a non-canonical mechanism. *Developmental Biology*, *352*(1), 58–69. <https://doi.org/10.1016/j.ydbio.2011.01.012>
- Tenti, P., & Vannucci, L. (2020). Lysyl oxidases: linking structures and immunity in the tumor microenvironment. *Cancer Immunology, Immunotherapy*, *69*(2), 223–235. <https://doi.org/10.1007/s00262-019-02404-x>
- Thevenet, L., Méjean, C., Moniot, B., Bonneaud, N., Galéotti, N., Aldrian-Herrada, G., Poulat, F., Berta, P., Benkirane, M., & Boizet-Bonhoure, B. (2004). Regulation of human SRY subcellular distribution by its acetylation/deacetylation. *The EMBO Journal*, *23*(16), 3336–3345. <https://doi.org/10.1038/sj.emboj.7600352>
- Tiwari, N., Tiwari, V. K., Waldmeier, L., Balwierz, P. J., Arnold, P., Pachkov, M., Meyer-Schaller, N., Schübeler, D., van Nimwegen, E., & Christofori, G. (2013). Sox4 Is a Master Regulator of Epithelial-Mesenchymal Transition by Controlling Ezh2 Expression and Epigenetic Reprogramming. *Cancer Cell*, *23*(6), 768–783. <https://doi.org/10.1016/j.ccr.2013.04.020>
- Tomita, M., Asada, M., Asada, N., Nakamura, J., Oguchi, A., Higashi, A. Y., Endo, S., Robertson, E., Kimura, T., Kita, T., Economides, A. N., Kreidberg, J., & Yanagita, M. (2013). Bmp7 maintains undifferentiated kidney progenitor population and determines nephron numbers at birth. *PLoS One*, *8*(8), e73554. <https://doi.org/10.1371/journal.pone.0073554>
- Torban, E., Dziarmaga, A., Iglesias, D., Chu, L. L., Vassilieva, T., Little, M., Eccles, M., Discenza, M., Pelletier, J., & Goodyer, P. (2006). PAX2 activates WNT4 expression during mammalian kidney development. *The Journal of Biological Chemistry*, *281*(18), 12705–12712. <https://doi.org/10.1074/jbc.M513181200>
- Torres, M., Gomez-Pardo, E., Dressler, G. R., & Gruss, P. (1995). Pax-2 controls multiple steps of urogenital development. *Development*, *121*(12), 4057 LP – 4065. <http://dev.biologists.org/content/121/12/4057.abstract>
- Tsang, T. E., Shawlot, W., Kinder, S. J., Kobayashi, A., Kwan, K. M., Schughart, K., Kania, A., Jessell, T. M., Behringer, R. R., & Tam, P. P. (2000). Lim1 Activity Is Required for Intermediate Mesoderm Differentiation in the Mouse Embryo. *Developmental Biology*, *223*(1), 77–90. <https://doi.org/10.1006/dbio.2000.9733>
- van der Ven, A. T., Vivante, A., & Hildebrandt, F. (2018). Novel Insights into the Pathogenesis of Monogenic Congenital Anomalies of the Kidney and Urinary Tract. *Journal of the American Society of Nephrology : JASN*, *29*(1), 36–50. <https://doi.org/10.1681/ASN.2017050561>
- Vidal, V. P. I., Gregoire, E., Szenker-Ravi, E., Leushacke, M., Reversade, B., Chaboissier, M. C., &

- Schedl, A. (2019). Paracrine and autocrine R-spondin signalling is essential for the maintenance and differentiation of renal stem cells. *BioRxiv*, 859959. <https://doi.org/10.1101/859959>
- Vize, P. D., Seufert, D. W., Carroll, T. J., & Wallingford, J. B. (1997). Model Systems for the Study of Kidney Development: Use of the Pronephros in the Analysis of Organ Induction and Patterning. *Developmental Biology*, 188(2), 189–204. <https://doi.org/10.1006/dbio.1997.8629>
- Wagner, N., Wagner, K.-D., Scholz, H., Kirschner, K. M., & Schedl, A. (2006). Intermediate filament protein nestin is expressed in developing kidney and heart and might be regulated by the Wilms' tumor suppressor Wt1. *American Journal of Physiology. Regulatory, Integrative and Comparative Physiology*, 291(3), R779-87. <https://doi.org/10.1152/ajpregu.00219.2006>
- Wang, J., Zhu, Y., Tan, J., Meng, X., Xie, H., & Wang, R. (2016). Lysyl oxidase promotes epithelial-to-mesenchymal transition during paraquat-induced pulmonary fibrosis. *Molecular BioSystems*, 12(2), 499–507. <https://doi.org/10.1039/C5MB00698H>
- Wang, X., Björklund, S., Wasik, A. M., Grandien, A., Andersson, P., Kimby, E., Dahlman-Wright, K., Zhao, C., Christensson, B., & Sander, B. (2010). Gene Expression Profiling and Chromatin Immunoprecipitation Identify DBN1, SETMAR and HIG2 as Direct Targets of SOX11 in Mantle Cell Lymphoma. *PLoS ONE*, 5(11), e14085. <https://doi.org/10.1371/journal.pone.0014085>
- Wegner, M. (1999). From head to toes: the multiple facets of Sox proteins. *Nucleic Acids Research*, 27(6), 1409–1420. <https://doi.org/10.1093/nar/27.6.1409>
- Wegner, Michael. (2010). All purpose Sox: The many roles of Sox proteins in gene expression. *The International Journal of Biochemistry & Cell Biology*, 42(3), 381–390. <https://doi.org/10.1016/j.biocel.2009.07.006>
- Wellik, D. M. (2002). Hox11 paralogous genes are essential for metanephric kidney induction. *Genes & Development*, 16(11), 1423–1432. <https://doi.org/10.1101/gad.993302>
- Wertz, K., & Herrmann, B. G. (1999). Kidney-specific cadherin (cdh16) is expressed in embryonic kidney, lung, and sex ducts. *Mechanisms of Development*, 84(1–2), 185–188. [https://doi.org/10.1016/S0925-4773\(99\)00074-X](https://doi.org/10.1016/S0925-4773(99)00074-X)
- Wierenga, A. T. J., Vellenga, E., & Schuringa, J. J. (2014). Convergence of Hypoxia and TGFβ Pathways on Cell Cycle Regulation in Human Hematopoietic Stem/Progenitor Cells. *PLoS ONE*, 9(3), e93494. <https://doi.org/10.1371/journal.pone.0093494>
- Xiao, J., Gong, Y., Chen, Y., Yu, D., Wang, X., Zhang, X., Dou, Y., Liu, D., Cheng, G., Lu, S., Yuan, W., Li, Y., & Zhao, Z. (2017). IL-6 promotes epithelial-to-mesenchymal transition of human peritoneal mesothelial cells possibly through the JAK2/STAT3 signaling pathway. *American Journal of Physiology-Renal Physiology*, 313(2), F310–F318. <https://doi.org/10.1152/ajprenal.00428.2016>
- Xu, Jian, Shao, Z., Li, D., Xie, H., Kim, W., Huang, J., Taylor, J. E., Pinello, L., Glass, K., Jaffe, J. D., Yuan, G.-C., & Orkin, S. H. (2015). Developmental Control of Polycomb Subunit Composition by GATA Factors Mediates a Switch to Non-Canonical Functions. *Molecular Cell*, 57(2), 304–316. <https://doi.org/10.1016/j.molcel.2014.12.009>
- Xu, Jingyue, Liu, H., Park, J.-S., Lan, Y., & Jiang, R. (2014). Osr1 acts downstream of and interacts synergistically with Six2 to maintain nephron progenitor cells during kidney organogenesis. *Development (Cambridge, England)*, 141(7), 1442–1452. <https://doi.org/10.1242/dev.103283>
- Xu, Jinshu, Wong, E. Y. M., Cheng, C., Li, J., Sharkar, M. T. K., Xu, C. Y., Chen, B., Sun, J., Jing, D., & Xu, P.-X. (2014). Eya1 interacts with Six2 and Myc to regulate expansion of the nephron progenitor pool during nephrogenesis. *Developmental Cell*, 31(4), 434–447. <https://doi.org/10.1016/j.devcel.2014.10.015>

- Xu, M., Zhu, C., Zhao, X., Chen, C., Zhang, H., Yuan, H., Deng, R., Dou, J., Wang, Y., Huang, J., Chen, Q., Jiang, B., & Yu, J. (2015). Atypical ubiquitin E3 ligase complex Skp1-Pam-Fbxo45 controls the core epithelial-to-mesenchymal transition-inducing transcription factors. *Oncotarget*, *6*(2), 979–994. <https://doi.org/10.18632/oncotarget.2825>
- Xu, P.-X. (2003). Six1 is required for the early organogenesis of mammalian kidney. *Development*, *130*(>14), 3085–3094. <https://doi.org/10.1242/dev.00536>
- Xu, P. X., Adams, J., Peters, H., Brown, M. C., Heaney, S., & Maas, R. (1999). Eya1-deficient mice lack ears and kidneys and show abnormal apoptosis of organ primordia. *Nature Genetics*, *23*(1), 113–117. <https://doi.org/10.1038/12722>
- Yang, Z., Zimmerman, S. E., Tsunazumi, J., Braitsch, C., Trent, C., Bryant, D. M., Cleaver, O., González-Manchón, C., & Marciano, D. K. (2016). Role of CD34 family members in lumen formation in the developing kidney. *Developmental Biology*, *418*(1), 66–74. <https://doi.org/10.1016/j.ydbio.2016.08.009>
- Yin, J., Hu, W., Fu, W., Dai, L., Jiang, Z., Zhong, S., Deng, B., & Zhao, J. (2019). HGF/MET Regulated Epithelial-Mesenchymal Transitions And Metastasis By FOSL2 In Non-Small Cell Lung Cancer. *OncoTargets and Therapy*, *Volume 12*, 9227–9237. <https://doi.org/10.2147/OTT.S217595>
- Ying, Q., Ansong, E., Diamond, A. M., Lu, Z., Yang, W., & Bie, X. (2015). Quantitative Proteomic Analysis Reveals That Anti-Cancer Effects of Selenium-Binding Protein 1 In Vivo Are Associated with Metabolic Pathways. *PLOS ONE*, *10*(5), e0126285. <https://doi.org/10.1371/journal.pone.0126285>
- Yosypiv, I. V. (2012). Congenital anomalies of the kidney and urinary tract: a genetic disorder? *International Journal of Nephrology*, *2012*, 909083. <https://doi.org/10.1155/2012/909083>
- You, H., Gao, T., Raup-Konsavage, W. M., Cooper, T. K., Bronson, S. K., Reeves, W. B., & Awad, A. S. (2017). Podocyte-specific chemokine (C-C motif) receptor 2 overexpression mediates diabetic renal injury in mice. *Kidney International*, *91*(3), 671–682. <https://doi.org/10.1016/j.kint.2016.09.042>
- Yu, J., Han, Z., Sun, Z., Wang, Y., Zheng, M., & Song, C. (2018). LncRNA SLCO4A1-AS1 facilitates growth and metastasis of colorectal cancer through β -catenin-dependent Wnt pathway. *Journal of Experimental & Clinical Cancer Research*, *37*(1), 222. <https://doi.org/10.1186/s13046-018-0896-y>
- Zhang, M., Huang, S., & Long, D. (2017). MiR-381 inhibits migration and invasion in human gastric carcinoma through downregulating SOX4. *Oncology Letters*, *14*(3), 3760–3766. <https://doi.org/10.3892/ol.2017.6637>
- Zhao, Chenyang, Gao, J., Li, S., Liu, Q., Hou, X., Xing, X., Wang, D., Sun, M., Wang, S., & Luo, Y. (2020). Cyclin G2 regulates canonical Wnt signalling via interaction with Dapper1 to attenuate tubulointerstitial fibrosis in diabetic nephropathy. *Journal of Cellular and Molecular Medicine*, *24*(5), 2749–2760. <https://doi.org/10.1111/jcmm.14946>
- Zhao, Chunhua, She, X., Zhang, Y., Liu, C., Li, P., Chen, S., Sai, B., Li, Y., Feng, J., Liu, J., Sun, Y., Xiao, S., Li, L., & Wu, M. (2020). LRRC4 Suppresses E-Cadherin-Dependent Collective Cell Invasion and Metastasis in Epithelial Ovarian Cancer. *Frontiers in Oncology*, *10*. <https://doi.org/10.3389/fonc.2020.00144>
- Zhou, M., Sutliff, R. L., Paul, R. J., Lorenz, J. N., Hoying, J. B., Haudenschild, C. C., Yin, M., Coffin, J. D., Kong, L., Kraniias, E. G., Luo, W., Boivin, G. P., Duffy, J. J., Pawlowski, S. A., & Doetschman, T. (1998). Fibroblast growth factor 2 control of vascular tone. *Nature Medicine*, *4*(2), 201–207.

<https://doi.org/10.1038/nm0298-201>

Zhou, P., Li, B., Liu, F., Zhang, M., Wang, Q., Liu, Y., Yao, Y., & Li, D. (2017). The epithelial to mesenchymal transition (EMT) and cancer stem cells: implication for treatment resistance in pancreatic cancer. *Molecular Cancer*, 16(1), 52. <https://doi.org/10.1186/s12943-017-0624-9>